
Electronic Thesis and Dissertation Repository

8-29-2019 10:30 AM

Synthesis and Characterization of Peptide Nucleic Acids Incorporating Modified Nucleobases

Ali Heidari
The University of Western Ontario

Supervisor
Hudson, Robert H. E.
The University of Western Ontario

Graduate Program in Chemistry
A thesis submitted in partial fulfillment of the requirements for the degree in Master of Science
© Ali Heidari 2019

Follow this and additional works at: <https://ir.lib.uwo.ca/etd>

 Part of the [Medicinal-Pharmaceutical Chemistry Commons](#), and the [Organic Chemistry Commons](#)

Recommended Citation

Heidari, Ali, "Synthesis and Characterization of Peptide Nucleic Acids Incorporating Modified Nucleobases" (2019). *Electronic Thesis and Dissertation Repository*. 6415.
<https://ir.lib.uwo.ca/etd/6415>

This Dissertation/Thesis is brought to you for free and open access by Scholarship@Western. It has been accepted for inclusion in Electronic Thesis and Dissertation Repository by an authorized administrator of Scholarship@Western. For more information, please contact wlsadmin@uwo.ca.

Abstract

Peptide Nucleic Acid (PNA), is a mimic of natural nucleic acids with exceptional binding properties. As such, numerous applications in biochemistry, medicine and biotechnology for PNA exist or have been proposed so far. Pseudo-complementary PNAs containing diaminopurine and thiouracil base pairs have been prepared and are shown to bind with high specificity and efficiency to complementary targets in double-stranded DNA by a mechanism termed “double duplex invasion” in which the duplex is unwound and both DNA strands are targeted simultaneously, each by one of the two pseudo-complementary PNAs. Chapter 2 describes a method for the preparation of modified nucleic acids and PNA oligomerization which can be used to study different pseudo-complementarity and base pairing and open up the possibility for the preparation of PNA oligomers with interesting new properties. Within the realm of PNA synthesis, we have examined different benzyl-type protections for the thiouracil nucleobase in PNA synthesis and oligomerization. We have also demonstrated for the first time that PNA oligomer synthesis can proceed without thiouracil protecting group on sulfur. Finally, the thermal stability of PNA bindings and pseudo-complementary PNA were studied.

As a part of the study of pseudo-complementary nucleobases, an optimized method of assaying DNA strand invasion by PNA was investigated. Traditional methods require time-consuming gel assays and lack an easily quantifiable marker. Instead, our method incorporates the fluorescent cytidine base analogue phenylpyrrolocytidine (PhpC) into a DNA strand such that upon invasion by PNA fluorescence increases when excited. We also synthesized pseudo-complementary PNA sequences that can undergo DNA invasion; no gels are required as all measurements are performed in solution. Nucleic acid detection takes place by changing either the reporter's fluorescence intensity or the colour of its fluorescence. The use of fluorescent probes for nucleic acid detection has attracted much attention due to its efficiency, the ease of synthesis and availability of commercial reporters that facilitate the probe synthesis.

Chapter 3 describes the synthesis of a novel quinazolinone-based uracil PNA monomers. Their photophysical properties were evaluated in different solvents and at varying temperatures. These luminescent PNA monomers show solvatochromism and solvent viscosity-dependent emission

which indicate that they have the potential to act fluorescent reporters of hybridization events once incorporated into PNA oligomers which will be done as future work for this study.

Keywords

Peptide nucleic acid, pseudo-complementary nucleic acid, nucleobase-modified PNA, solid-phase synthesis, thiouracil protecting groups, dihydroquinazolinone, quinazolinone, quinazolinone based nucleobase

Summary for Lay Audience

Peptide Nucleic Acid (PNA), is a mimic of natural nucleic acids, also known as the building blocks of DNA, with exceptional binding properties. As such, numerous applications in biochemistry, medicine and biotechnology for PNA exist or have been proposed so far. Pseudo-complementary PNAs containing diaminopurine and thiouracil base pairs have been prepared and are shown to bind with high specificity and efficiency to complementary targets in double-stranded DNA by a mechanism termed “double duplex invasion” in which the duplex is unwound and both DNA strands are targeted simultaneously, each by one of the two pseudo-complementary PNAs. The present work describes a method for the preparation of modified nucleic acids, and PNA oligomerization which can be used to study different pseudo-complementarity and base pairing and open up the possibility for the preparation of PNA oligomers with interesting new properties. Oligomerization is the process of making oligomers which are molecular complexes of chemicals that consist of repeating units. Within the realm of PNA synthesis, we have examined different acid-labile protections for the thiouracil nucleobase in PNA synthesis and oligomerization. We have also demonstrated for the first time that PNA oligomer synthesis can proceed without thiouracil protecting group on sulfur. Finally, the thermal stability of PNA bindings and pseudo-complementary PNA were studied. As a part of the study of pseudo-complementary nucleobases, an optimized method of assaying, or making, DNA strand invasion by PNA was investigated. Traditional methods require time consuming gel assays and lack an easily quantifiable marker. Instead, our method incorporates the fluorescent cytidine base analogue phenylpyrrolocytidine (PhpC) into a DNA strand such that upon invasion by PNA fluorescence increases when excited. We also synthesized pseudo-complementary PNA sequences that can undergo DNA invasion; no gels are required for this process, as all measurements are performed in solution.

Nucleic acid detection takes place by changing either the reporter's fluorescence intensity or the colour of its fluorescence. The use of fluorescent probes for nucleic acid detection has attracted much attention due to its efficiency, the ease of synthesis and availability of commercial reporters that facilitate the probe synthesis. Chapter 3 describes the synthesis of a novel quinazolinone-based uracil PNA monomers. The study of photophysical properties in different solvents and temperatures show that they can be good fluorescent reporters upon

hybridization with the complementary DNA sequence by incorporation of these PNA monomers into PNA oligomers as the future work for this study.

Co-Authorship Statement

Chapter 2 has been submitted as a manuscript to the Journal of Organic Chemistry as a research paper. Timothy Martin-Chan and I performed all the experimental work, the computational studies were done with the help of Dr. James A. Wisner, and I wrote the experimental and supplemental information and most of the figures for the manuscript and final revision and submission was done by Professor Hudson. Also, in this chapter all the DNA synthesis and purification and initial fluorescence studies were done with the help of Mr. Mason Hermann as a part of his fourth-year research project.

Chapter 3: Prof. Arash Ghorbani-Choghamarani synthesized the first dihydropyridine and unsubstituted dihydroquinazolinone uracil scaffolds. I prepared, functionalized and characterized all the other PNA monomers and oligomers; Also, I have prepared the experimental section and supplemental information for the manuscript in preparation.

Acknowledgements

Foremost, I would like to express my sincere gratitude to my chemistry father and my supervisor professor Robert H. E. Hudson for his faith, patience and amazing advice not only for my project but also for my life. I appreciate all his contributions of time, ideas and funding to make my experience at Western productive and joyful. His broad knowledge and enthusiasm of research on nucleic acids has been being contagious to me throughout the past two years and all that I have learnt from him will deeply influence my future career.

Next, I'd like to thank all the past and present members of Hudson group for teaching me the ways of organic synthesis, analytical techniques and working with PNA that have been immensely helpful to my study, research and personal life at Western. I would like to specifically acknowledge Gyeongsu (David) Park for putting up with my endless string of questions and Mason Hermann for his help during my research project. You guys have always been there and I'm happy to have such good labmates and friends.

I would like to acknowledge the hard work of Mathew Willans and Aneta Borecki in maintaining the NMR facilities which made the characterization of compounds possible. I would also like to thank Doug Hairsine for running mass spectrometry on my compounds.

Lastly and most importantly I'd like to thank my family. You have all been supportive of my academic choices. I am who I am today because of your effort, guidance, and support. I couldn't have done it without you. Words cannot express my gratitude for the support, encouragement and love I have received from my parents and from my girlfriend, Laura Cullen. I am grateful for their support and encouragement which has made this journey easier.

Table of Contents

ABSTRACT	II
SUMMARY FOR LAY AUDIENCE	IV
CO-AUTHORSHIP STATEMENT	VI
ACKNOWLEDGEMENTS	VII
TABLE OF CONTENTS	VIII
LIST OF FIGURES	XI
LIST OF SCHEMES	XIII
LIST OF TABLES	XIV
LIST OF ABBREVIATIONS	XV
CHAPTER 1	1
1. General Introduction to Pseudo-Complementary Nucleic Acids	1
1.2 Peptide Nucleic Acid Chemistry	2
1.3 Potential applications	4
1.3.1 Therapeutics	4
1.3.2 Applications in Biotechnology	4
1.4 Goals of this research	8
1.5 Introduction to Fluorescent nucleobases	9
1.5.1 Quinazolinone-based nucleobase scaffolds	12
1.5.2 Goal of this research	13
REFERENCES	14
CHAPTER 2	17

Highly acid-labile protecting group for thiouracil	17
2.1 Introduction	17
2.2 Results and discussions	19
2.2.1 Thiouracil protection with 4-methoxybenzyl and 2-methoxybenzyl group	19
2.2.2 Thiouracil PNA monomer	24
2.2.3 Tetrakis-Boc protected 2,6-diaminopurine PNA monomer	26
2.2.3.1 Coupling of Boc-protected acid 2,6-diaminopurine monomer to PNA backbone	27
2.2.4 Oligomerization of PNA Fmoc-based PNA monomers	28
2.2.5 Fluorescent studies	28
2.2.6 Thermal stability (T_m) analysis	30
2.2.7 Fluorescence analysis	32
2.3 Conclusion	34
2.4 Experimental Procedures	36
REFERENCES	50
CHAPTER 3	51
Modified fluorescent dihydroquinazolinone/quinazolinone heterocyclic frameworks based on uracil scaffold	51
3.1 Introduction	51
3.2 Synthesis of quinazolinone-based uracil scaffold as a PNA monomer	52
3.3 Approaches for the synthesis of quinazolinones	54
3.4 Photophysical properties	56
3.5 Conclusion	62
3.6 Future work	62
3.6 Experimental Procedure	63
REFERENCES	82
CHAPTER 4	83

Conclusion and Outlook	83
SUPPLEMENTAL INFORMATION	S1
General synthetic procedures	S2
Acidolysis studies and half-life calculations	S2
Time course studies on the acidolysis of thioesters	S4
Oligomer synthesis	S7
RP-HPLC conditions and chromatograms	S7
UV-vis absorbance and Beer-Lambert Plots	S22
Emission spectra	S28
NMR Spectra	S30
CURRICULUM VITAE	S31

List of Figures

Figure 1.1. Watson-Crick base pairing between nucleobases (A) thymine and adenine (B) cytosine and guanine	1
Figure 1.2. Chemical structure of peptide nucleic acid oligomer (PNA), deoxyribose nucleic acid oligomer (DNA), and amino acid oligomer (peptide).	3
Figure 1.3. Modes of hybridization between PNA oligomer and nucleic acid duplex.	5
Figure 1.4. Base pairing of natural and pseudo-complementary nucleobases A) adenine and thymine, B) diaminopurine and thymine, C) adenine and thiouracil, D) diaminopurine and thiouracil	6
Figure 1.5. Examples of pteridine derivatives	10
Figure 1.6. Examples of expanded nucleobases	10
Figure 1.7. Examples of hydrocarbons and heterocycle DNA base replacement	11
Figure 1.8. Examples of some conjugated base analogues	12
Figure 2.1. Possible structures of alkylation products of 10. Selected NOE correlations (double-headed arrows) and HMBC H-C correlations (single-headed arrows) of compounds 11a and 11b.	21
Figure 2.2. (a) Proposed stabilization of the protonated form of compound 14a by an intramolecular hydrogen bond with the 2-methoxybenzyl group. (b) Minimum energy structure for the protonated for model compound <i>S</i> -(2-methoxybenzyl)- <i>N1</i> -methylthiouracil. Arrowheads show the S→H distance (1.853 Å); O→N3 distance (2.854 Å).	23
Figure 2.3. 6-phenylpyrrolocytidine (PhpC)	29
Figure 2.4. DNA strand invasion by pseudocomplementary PNA (circle represents PhpC). The more stable PNA-DNA duplexes liberate the quenched PhpC base resulting in a turning-on of fluorescence.	30
Figure 2.5. Emission spectra of four target DNA (PhpC) samples upon excitation at 369 nm	32
Figure 2.6. Time-dependent (a-top) and Temperature-dependent (b-bottom) fluorescence spectra for pseudo-complementary H-Lys-G ^s UDGD ^s UCDCT-Lys-NH ₂ and H-Lys-DG ^s UGD ^s UC ^s UDC-Lys-NH ₂ PNA strands annealed with complementary 5' AGTGATCTACCT 3' and 5' AGTGATCTAC(PhpC)T 3' DNA strands. Strand concentration is 2 mM in a buffer containing NaCl (100 mM), EDTA (0.1 mM), and Na ₂ PO ₄ (10 mM, pH 7.0). Fluorescence excitation at λ=369 nm and integrated emission spectra from 400 nm to 580 nm were measured in triplicate.	34
Figure 3.1. 3D Molecular structure at minimum energy state ^a of modified dihydroquinazolinone (a) and quinazolinone (b) compounds.	58
Figure S2. ¹ H NMR spectra of ethyl 2-(2-(2-methoxybenzyl)thio)uracil-1-yl)acetate (14a) acidolysis in a solution of 2% TFA and 1% triethylsilane in CDCl ₃ . Benzylic methylene (*), N1- methylene (x).	S5

Figure S3. First order reaction curves for a) ethyl 2-(2-(S-(4 methoxybenzyl)thiouracil-1-yl)acetate, 12a, 17), and b) ethyl 2-(2-S-(2 methyl-4-methoxybenzyl)thiouracil-1-yl)acetate, 9 treated with 2% TFA, 1% TES in CDCl₃. S6

Figure S4. Emission at 446 nm of single stranded Target DNA (PhpC) upon excitation from 300 nm to 440 nm. S21

List of Schemes

Scheme 1.1. SPPS cycle for oligomerization with Fmoc/Bhoc based protecting group	8
Scheme 2.1 Retro-synthesis of thiouracil PNA monomer with different acid labile benzyl-type protection	17
Scheme 2.2. PNA monomer compatible with Boc-based peptide synthesis	18
Scheme 2.3 Different studied benzyl-type protection for thiouracil	19
Scheme 2.4. Synthesis of 2-methoxybenzyl protected thiouracil nucleobase	20
Scheme 2.5. Proposed mechanism of 2-methoxybenzyl thiol protecting group acidolysis.	22
Scheme 2.6. Synthesis of thiouracil PNA monomer	25
Scheme 2.7. Synthesis of protection-free thiouracil PNA monomer	26
Scheme 2.8. The synthesis of tetrakis-(Boc)-2,6-diaminopurine-9-yl acetic acid.	27
Scheme 2.9. The coupling of the Boc-protected acids to an Fmoc/Bn PNA backbone to form PNA monomer	27
Scheme 3.1. Retro-synthesis of quinazolinone uracil-based scaffolds	52
Scheme 3.2. Synthesis of modified quinazolinone based uracil scaffold tert-butyl- acetate	53
Scheme 3.3. CuCl/DABCO/TEMPO-catalyzed one-pot aerobic oxidative synthesis of modified quinazolinones	55
Scheme 3.4. Synthesis of quinazolinone based uracil scaffold PNA monomer	61

List of Tables

Table 2.1. The rate and half-life of acidolysis for different benzyl-type protections in the solution of 2% of trifluoroacetic acid condition.	23
Table 2.2. Thermal stabilities (T _m) of complexes	31
Table 3.1. Optimization on the Catalytic Aerobic Oxidative Synthesis of Quinazolinone	55
Table 3.2. Photophysical properties of dihydroquinazolinone compounds 31-35	56
Table 3.3. Photophysical properties of quinazolinone compounds 36-40	59
Table S1. Observed high-resolution mass of synthesized PNA oligomers	S20
Table S2. Calculated quantum yield values for reference standards in different solvents and temperatures	S20

List of Abbreviations

A	adenine
Aeg	<i>N</i> -(2-aminoethyl)glycine
aq.	aqueous
B	nucleobase
amu	atomic mass units
Bhoc	benzhydryloxycarbonyl
Boc	<i>tert</i> -butyloxycarbonyl
br	broad
Bz	benzoyl
C	cytosine
°C	degrees Celsius
calc.	calculated
cDNA	complementary deoxyribonucleic acid
cbz	carboxybenzyl
¹³ C NMR	carbon nuclear magnetic resonance
D	2,4-diaminopurine
DABCO	1,4-diazabicyclo[2.2.2]octane
d	doublet
DCC	<i>N,N'</i> -dicyclohexylcarbodiimide
DCM	dichloromethane
dd	doublet of doublets
DIPEA	diisopropylethylamine

DMF	<i>N,N</i> -dimethylformamide
DMSO- <i>d</i> ₆	deuterated dimethyl sulfoxide
DNA	deoxyribonucleic acid
EDC	<i>N</i> -(3-dimethylaminopropyl)- <i>N</i> -ethylcarbodiimide hydrochloride
EDTA	ethylenediaminetetraacetic acid
ESI	electrospray ionization
Et	ethyl
EtOH	ethanol
Fmoc	9-fluorenylmethyloxybarbonyl
g	grams
G	guanine
h	hours
HBTU	hexafluorophosphate benzotriazole tetramethyluronium
HMBC	heteronuclear multiple-bond correlation
¹ H NMR	proton nuclear magnetic resonance
HOBt	Hydroxybenzotriazole
HPLC	high-pressure liquid chromatography
HRMS	high-resolution mass spectrometry
Hz	hertz
K	lysine
μ	micro
MeOH	methanol

LRMS	low-resolution mass spectrometry
Me	methyl
min	minute
mRNA	messenger ribose nucleic acid
MW	molecular weight
NMP	<i>N</i> -methyl-2-pyrrolidone
NMR	nuclear magnetic resonance
pcPNA	pseudo-complementary peptide nucleic acid
PG	protecting group
PhpC	6-phenylpyrrolocytidine
PNA	peptide nucleic acid
ppm	parts per million
q	quartet
rt	room temperature
s	singlet
SPPS	solid-phase peptide synthesis
^s T	2-thiothymine
^s U	2-thiouracil
t	triplet
T	thymine
TES	triethylsilane
THF	tetrahydrofuran
TFA	trifluoroacetic acid

TFMSA	trifluoromethyl sulfonic acid
THF	tetrahydrofuran
TLC	thin-layer chromatography
T _m	thermal melt transition temperature (melting temperature for a nucleic acid complex)
UV	ultraviolet
vis	visible
v	volume
Φ	quantum yield

Chapter 1

1. General Introduction to Pseudo-Complementary Nucleic Acids

Nucleic acids are an essential component of all known life, with DNA containing the hereditary information for all eukaryotes and prokaryotes. DNA contains a sugar-phosphodiester backbone composed of β -2-deoxyribose sugars combined by phosphate at the 3-to-5-hydroxyl of sugars. Each sugar contains one of thymine, adenine, guanine, cytosine nucleobases attached to the C-1 position of the sugar. Nucleic acid strands can undergo hybridization between complementary base pairs cytosine and guanine, thymine and adenine to form a double-strand duplex¹. Adenine forming two hydrogen bonds with thymine and guanine forms three hydrogen bonds with cytosine and these bonding patterns between nucleobases provides specificity of base pairing (**Figure 1.1**). The duplex is not only stabilized due to hydrophilic interactions between the charged phosphate backbone and aqueous environment, but also by the hydrophobic interactions between the nucleobases. Hydrogen bonding between complementary nucleobases and π -stacking from the aromatic purine and pyrimidine nucleobases will also stabilize the duplex formation, while mismatched nucleobases destabilize the duplex.

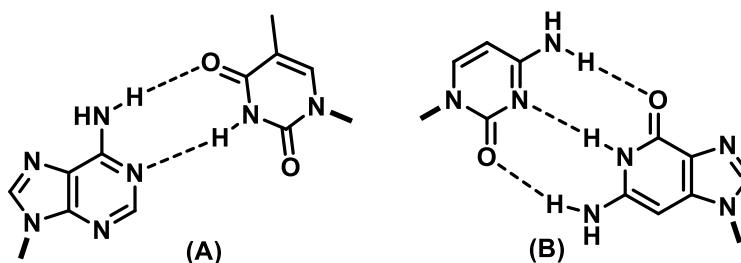


Figure 1.1 Watson-Crick base pairing between nucleobases (A) thymine and adenine (B) cytosine and guanine

Design of nucleic acid oligomers is approachable due to DNA synthetic methods and the specificity resulting from base complementary and allows chemists for reaching specific

hybridization with DNA or RNA targets, known as molecular probes. This specificity allows the design of nucleic acid probes for research and genetic screening, as well as potential design of nucleic acid-based therapeutic agents, which rely on highly specific targeting of a genetic sequence. Oligonucleotide sequences provide the required specificity through base pairing between complementary nucleobases and targeting of a specific genetic sequence can prevent undesired off-targeting effects.

One of the major limitations to oligodeoxynucleotides (ODNs) use in *in vivo* application results from the instability of nucleic acid strands. ODN strands are susceptible to hydrolysis by nucleases, enzymes responsible for cleaving phosphodiester bonds, preventing ODNs from reaching the desired target. Many chemical modifications have been developed to increase the stability of nucleic acid oligomers. Sugar-phosphodiester backbone modifications increase the stability *in vivo* as it prevents recognition and degradation by nucleases. Modification such as replacing the phosphate units with analogs like phosphothioates or phosphoborates or replacing the ribose sugar provide resistance to nucleases. However, these modifications often introduce chiral centers and reduce the binding affinity between the oligomer and the target DNA or RNA strand.

1.2 Peptide nucleic acid chemistry

Replacement of the sugar-phosphate backbone with an aminoethylglycine backbone with the nucleobases attached via a methylene carbonyl linker is one type of modification which forms a peptide nucleic acid (PNA). The modified backbone is oligomerized through peptide bonds between an N-terminal amine and a C-terminal carboxylic acid to form a PNA oligomer. Advantages of peptide nucleic acids include, the unnatural backbone is resistant to degradation from either nucleases or proteases, as the backbone is not recognized as either an oligonucleotide or a polypeptide for cleavage. In addition, the aminoethylglycine backbone maintains natural spacing observed with the sugar-phosphodiester backbone, allowing normal Watson-Crick base pairing with modified DNA, RNA, and PNA strands. The PNA oligomers can undergo more stable

hybridization with DNA and RNA than ODNs due to the neutral aminoethylglycine backbone, ODNs experience anionic repulsion due to the negatively charged phosphate groups present in the backbone. (**Figure 1.2**) Having high sequence specificity for hybridization, with a single base mismatch significantly destabilizing a PNA-DNA duplex, which is one of the PNA features. The aminoethyl glycine is achiral, allowing for the easy synthesis of PNA monomers without difficult purification, and the pseudo-peptide bonds allow for easy oligomerization using standard solid-phase peptide synthesis (SPPS) techniques.

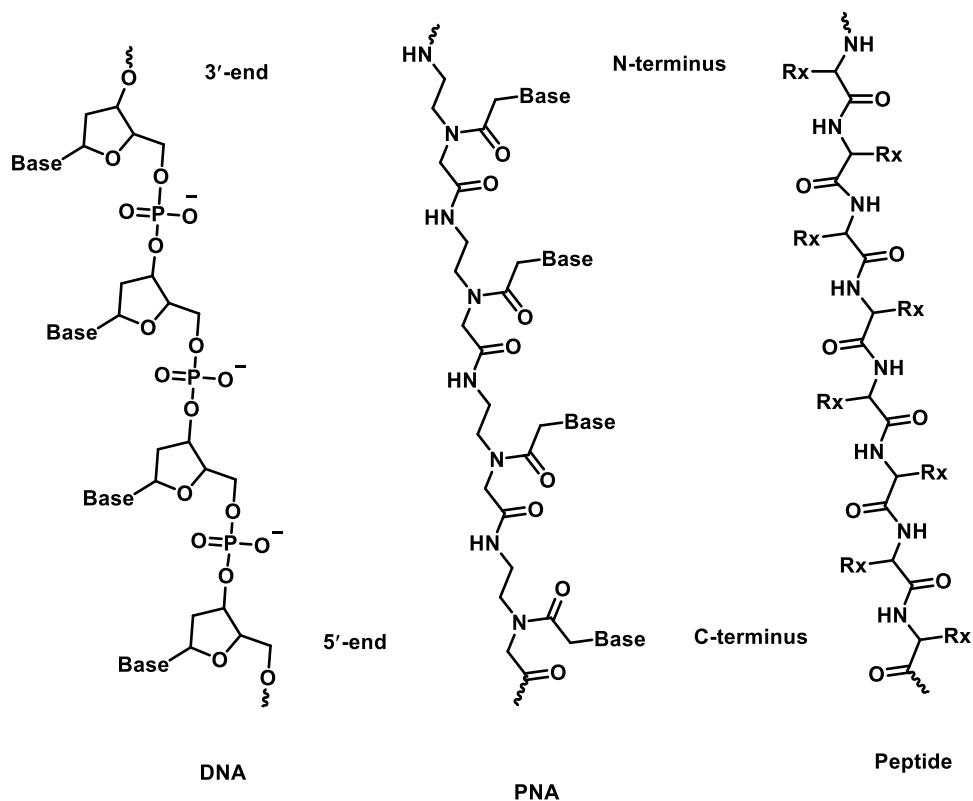


Figure 1.2 Chemical structure of peptide nucleic acid oligomer (PNA), deoxyribose nucleic acid oligomer (DNA), and amino acid oligomer (peptide).

1.3 Potential applications

1.3.1 Therapeutics

Potential therapeutic applications for PNA arise from their ability to selectively and strongly bind either DNA or RNA and inhibit biological processes. Although their poor cellular uptake is the main obstacle to their effective therapeutic use, enthusiasm for the use of PNA has been regained because of the discovery of a class of peptides with translocating properties and capable of carrying compounds across the plasma membrane.² Additionally, it was surprisingly found that PNA is able to enter the prokaryote *E. coli*.³

1.3.2 Applications in biotechnology

In particular, DNA targeting by triplex-forming oligonucleotides and helix-invading triplex-forming PNAs is still basically limited to homopurine targets because of the involvement of third-strand Hoogsteen recognition.⁴ However, general sequence recognition by the invasion of the DNA double helix exploiting just the Watson–Crick base pairing principle might be accomplished by helix invasion using duplex-forming PNAs. Unfortunately, mixed purine-pyrimidine sequence PNAs do not provide sufficient free energy upon hybridization for this mode of binding. However, the required free energy could be gained if both DNA strands were targeted simultaneously (**Figure 1.3**). Naturally, the two PNAs (or oligonucleotides) would be sequence complementary and if composed of the natural nucleobases A, C, G, and T would “quench” each other by forming a stable duplex. Thus, PNA oligomers do not undergo duplex invasion of a double-stranded DNA duplex, which is a major limitation of PNAs for many biological applications involving gene targeting. Hybridizing a complementary PNA oligomer to both strands of the complementary DNA duplex is one method to overcome this entropic restriction. However, the double duplex invasion using PNA oligomers is hindered by the strong hybridization of PNAs, which results in highly stable PNA-PNA hybridization, which is more favorable than PNA-DNA hybridization. As a result, the use of complementary PNA oligomers in a double duplex invasion instead of results in the formation of a stable PNA-PNA duplex leaving the target DNA duplex

intact.⁵ The design of unnatural nucleoside analogues is one of the main goals of medicinal chemistry, with different applications such as antiviral chemotherapeutics or in nucleic acid detection.

The unnatural nucleobase 2,6-diaminopurine (D) has found the interest for its strong and selective base pairing to uracil/thymine⁶. The placement of adenine with D in PNA is one of the simplest ways to increase the binding to a target nucleic acid. (**Figure 1.4.**)

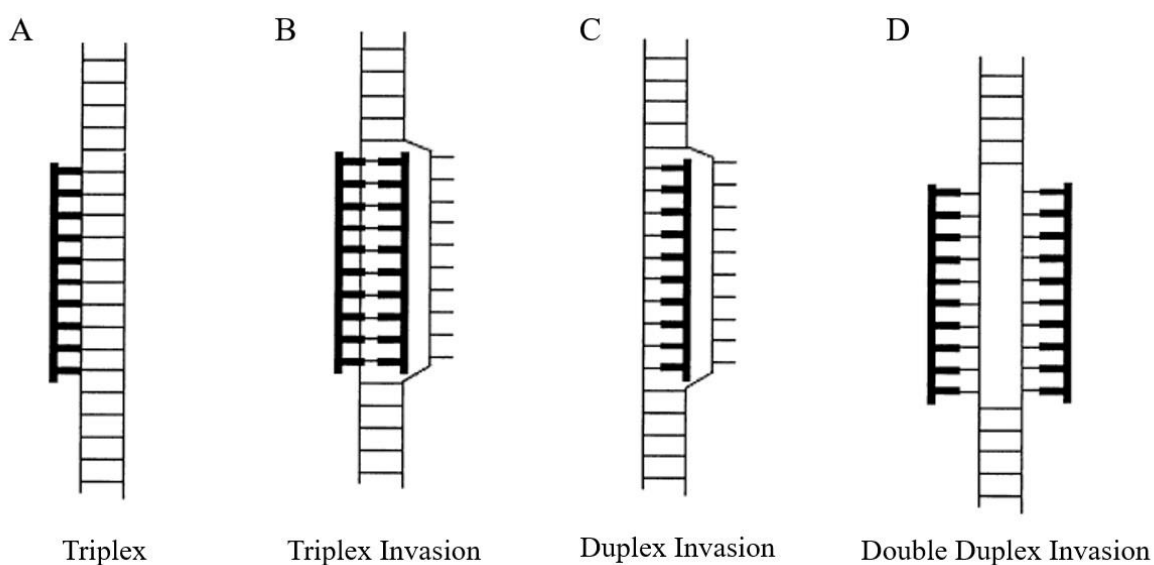


Figure 1.3. Modes of hybridization between PNA oligomer and nucleic acid duplex.

Pseudo-complementary nucleobases, first reported by Gamper et al. for DNA.⁷ In 1999, Nielsen et al.⁶ developed a method for destabilizing the PNA-PNA duplex, which utilized modified pseudo-complementary nucleobases to synthesize selectively binding oligomers, or pseudo-complementary PNAs (pcPNAs). The first synthesis of pcPNA oligomers using a Boc-based SPPS approach and demonstrating their ability to undergo a double duplex invasion of a target DNA duplex have been reported by Nielsen et al.⁶ (**Figure 1.4.**)

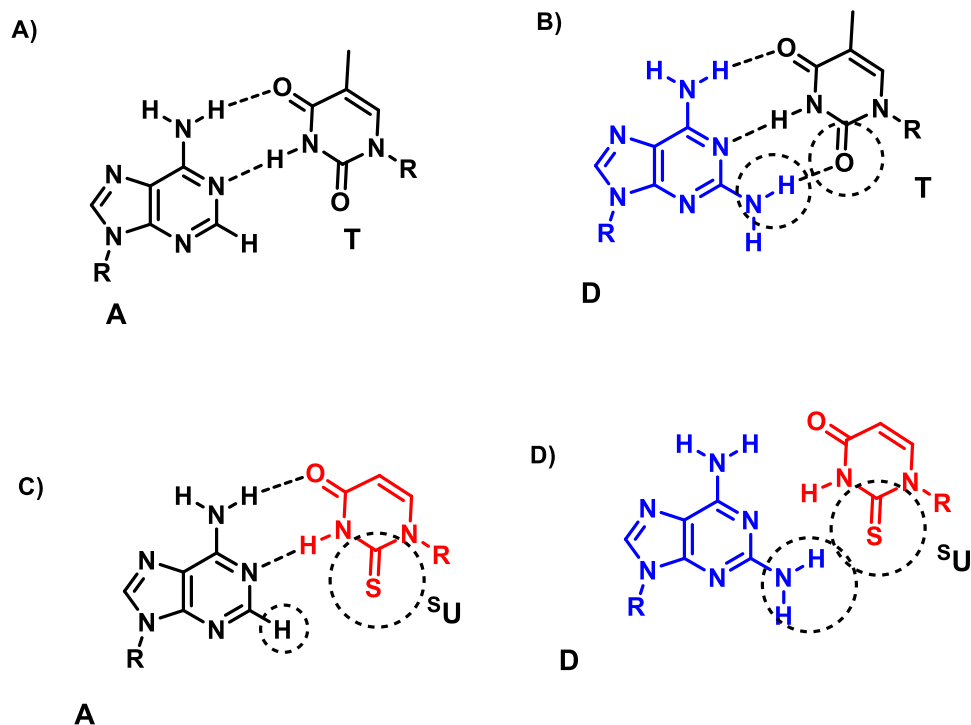


Figure 1.4. Base pairing of natural and pseudo-complementary nucleobases A) adenine and thymine, B) **diaminopurine and thymine, C) adenine and **thiouracil**, D) **diaminopurine** and **thiouracil****

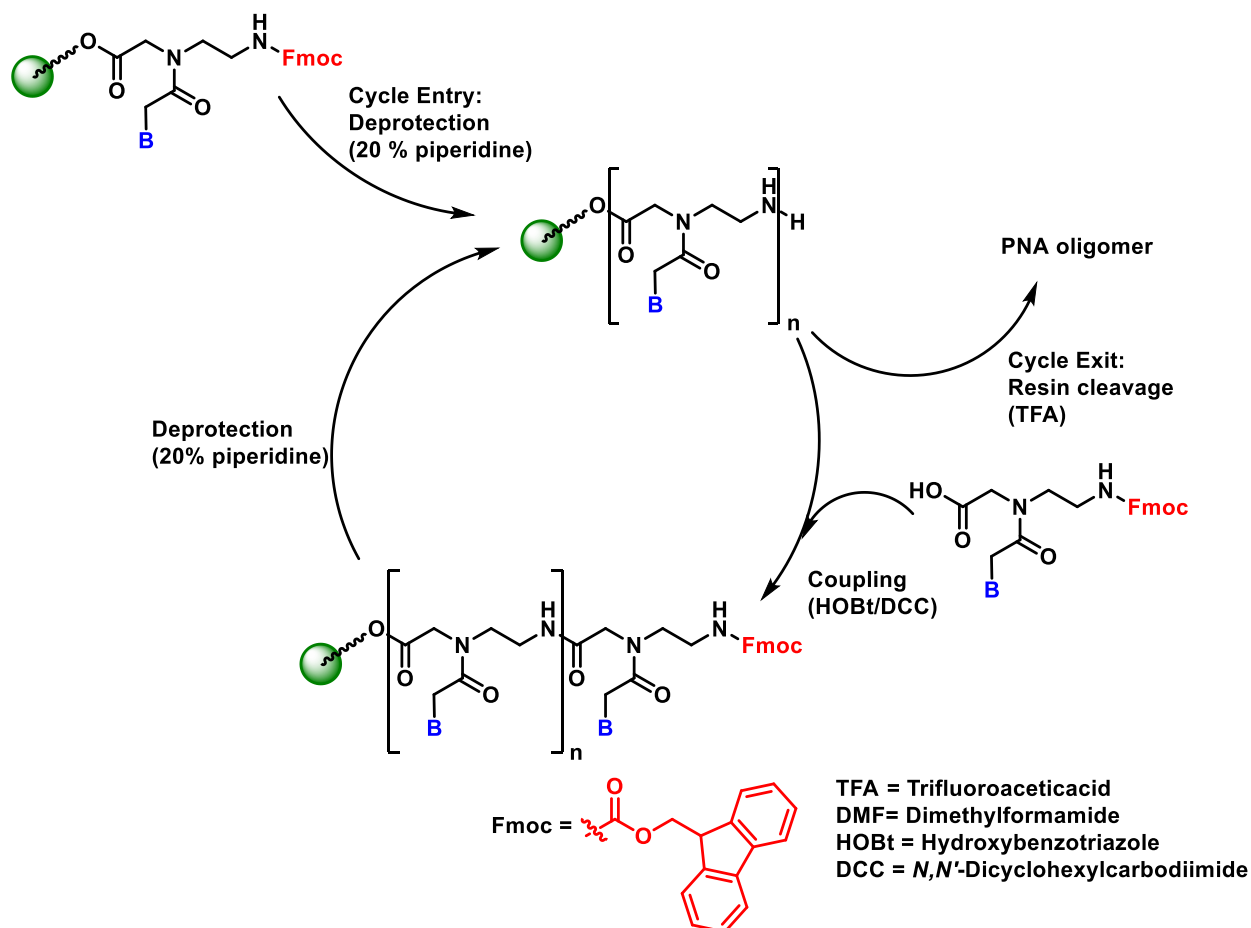
Basically, two SPPS methods have been used for chemical oligomerization in peptide synthesis, which primarily differs in the protecting group strategy. All amino acids contain both a carboxylic acid and an amine, which undergo a condensation reaction to form an amide linkage during oligomerization, which must be protected and require different deprotection conditions for control of sequence-specific oligomerization. Moreover, many amino acids contain reactive side chains, which require separate functional group protection. Similarly, PNAs contain both a carboxylic acid and a primary amine, which require separate protection and deprotection strategies, with most nucleobases requiring further protection during oligomerization.

Peptide synthesis was performed using gradient acidolysis protection strategies where N-terminal Boc deprotection occurred under relatively weaker acidic conditions, while C-terminal deprotection required stronger acidic conditions. Advances in chemical synthesis lead to the development of an orthogonal protection strategy with N-terminal Fmoc group for which deprotection occurred under weakly basic conditions and C-terminal deprotection occurring under

weakly acidic conditions. This strategy results in higher-yielding oligomerization, and as a result, can be used to synthesize longer peptide sequences. Both strategies have been modified for standard PNA oligomerization, with standard monomers commercially available for synthesis.

The original synthesis of PNA oligomers was reported by Egholm, Nielsen et al. in 1992⁶ which utilized the Boc-based technique developed by Merrifield for solid-phase peptide synthesis.⁸ This procedure uses a *tert*-butyloxycarbonyl protecting group on the terminal amine, while the C-terminal of the oligomer is attached to a solid support, typically a cross-linked polystyrene resin, by a 4-methyl benzhydrylamine linker. The nucleobases were protected using acid-labile protecting groups; so, oligomer deprotection can occur concurrently with resin cleavage under strongly acidic conditions.

A severe limitation of Boc-based peptide synthesis is the final deprotection and resin cleavage that requires strongly acidic treatment with hydrofluoric acid, which can damage the oligomer and the harsh reagents can be dangerous to work with. Orthogonal protection strategy which uses fluorenylmethyloxycarbonyl (Fmoc) protection on the terminal amine, which requires weakly basic conditions for deprotection can be used⁹. Normal deprotection conditions, which is a mixture of 20% v/v piperidine solution in dimethylformamide to remove the Fmoc protection, can be used for oligomerization on the N-terminal. By using Fmoc protection, more acid-labile protecting groups can be used for the C-terminal and nucleobase protection. An acid-labile linker is used to attach the polystyrene resin to the C-terminal of the oligomer. Nucleobase protection uses a more acid-labile Boc or benzhydryloxycarbonyl (Bhoc) group to protect the exocyclic amines on cytosine, adenine, and guanine allowing resin cleavage and the final deprotection of the oligomer to be performed using a solution of 95% v/v trifluoroacetic acid and 5% triethylsilane as a cation scavenger. This orthogonal protection strategy uses milder deprotection conditions and typically results in higher-yielding oligomerization compared to the Boc-based protection strategy. Due to these advantages, the Fmoc protection strategy has become the standard for the chemical synthesis of peptides and PNA oligomers.



Scheme 1.1. SPPS cycle for oligomerization with Fmoc/Bhoc based protecting group

1.4 Goals of this research

Until recently, the synthesis of pcPNA oligomers was carried out using Boc-based oligomerization strategy which has become unfavourable due to harsh deprotection conditions which result in lower-yielding reactions thus limiting oligomer length. Therefore, the primary aim of this work is to develop a highly acid-labile protecting group for thiouracil/thiothymine so that the PNA monomer is compatible with Fmoc-based PNA oligomerization (**Scheme 1.1**). The Fmoc-based thiouracil and diaminopurine PNA monomer were prepared and the binding study was done. Also, the need for keeping thiouracil protecting group during oligomerization, as well as the acid resistance of 2-methoxybenzyl protection was studied. And at the end, in our study toward the pseudo-complementary base pairs, we aimed to develop a more efficient method for detecting and quantifying duplex invasion by using fluorescent analysis.

1.5 Introduction to fluorescent nucleobases

Since the 1980s, much effort has been devoted to exploit using fluorescence techniques in the detection of nucleic acids. Aromatic-based amino acids (phenylalanine, tyrosine and/or tryptophan) are characterized by their intrinsic fluorescence that may be used in fluorescent studies; but natural nucleic acids are known to be nonfluorescent^{10,11}. Due to the promising results shown for the detection of nucleic acid using fluorescent probes, intensive research has been devoted to design and synthesize nucleobases possessing fluorescent properties. There is a great demand for such nucleobases, especially ones that are fluorescent while maintaining the hydrogen bonding ability to the complementary nucleobases.

Fluorescent nucleobases are classified by Tor¹² into five major families as 1) isomorphous base analogues, 2) pteridines, 3) expanded nucleobases, 4) chromophoric base analogues and 5) conjugated base analogues.

1) Isomorphous base analogues, heterocyclic compounds characterized by its similarity to the natural nucleobases in overall dimension and their ability to Watson-Crick base pairing. The most common example of this class is 2-aminopurine (2-AP). 2-AP is an analog of guanine and adenine and therefore it can pair with thymine and uracil obeying Watson-Crick base pairing.¹³ 2-AP is distinguished by its high fluorescence quantum yield ($\Phi_F = 0.68$ in aqueous solution) and high sensitivity to the local environment. Upon incorporation of 2-AP into a nucleic acid, the fluorescence intensity of 2-AP was drastically reduced ~ 100 times due to stacking interactions with nearest neighbor nucleobases. This reduction in 2-AP quantum yield is highly dependent on base sequence.¹³ Owing to 2-AP sensitivity to the microenvironment, it has been widely used in several studies of nucleic acid structure and dynamics within DNA and RNA.¹⁴

2) Pteridines, purine analogues, are bicyclic planar compounds formed from two condensed six-membered rings and are distinguished by their ability to form hydrogen bonds with complementary bases in addition to their intensive emission quantum yield ($\Phi_F = 0.77-0.88$ for adenosine analogues and $0.39-0.48$ for the guanosine)¹⁵ (**Figure 1.5**). Pteridines have been employed in numerous applications as hybridization probes which are used in measuring the cleavage activity of the retrovirally coded protein, human immunodeficiency virus-1 (HIV-1) integrase.¹⁶

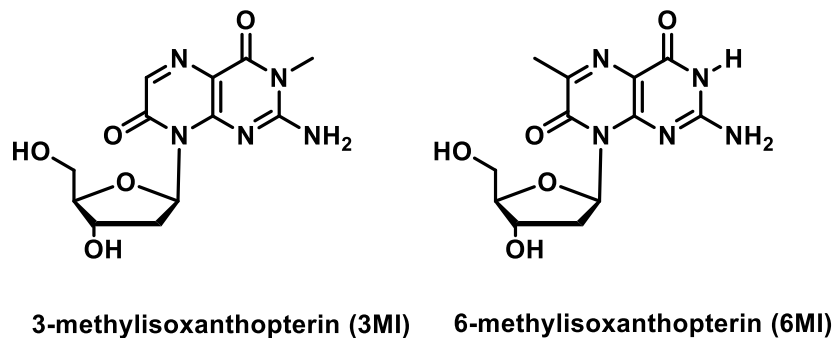


Figure 1.5 Examples of pteridine derivatives

3) Expanded nucleobases are natural nucleobases that have been extended with fused aromatic rings. Etheno-A,¹⁶ the simplest example of fluorescent extended nucleobases with quantum yield = 0.54 (in dioxane-H₂O 1:1), it was prepared by reaction of chloroacetaldehyde with adenosine. Despite the fluorescence property of Etheno-A, it cannot engage in hydrogen bonding. Much work has been done to extend the nucleobases structures while retaining their ability to hydrogen bond with complementary nucleobases (**Figure 1.6**).¹⁷

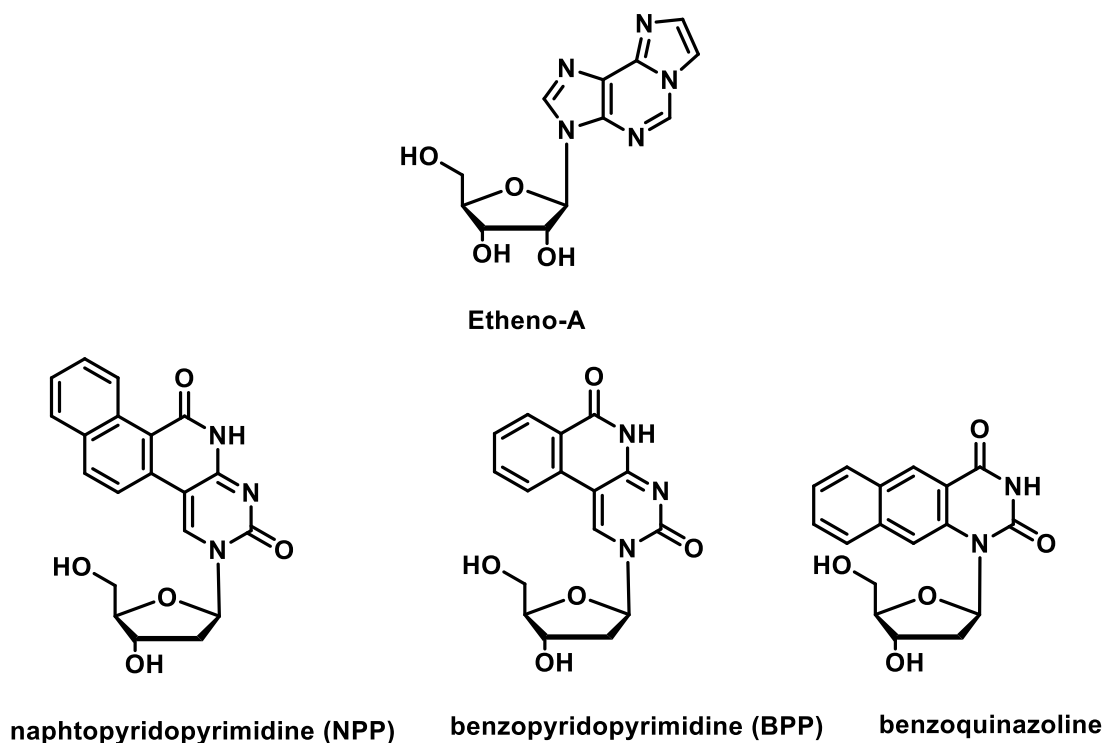


Figure 1.6 Examples of expanded nucleobases

4) Chromophoric base analogues, are produced when the natural nucleobases are replaced by hydrocarbons and heterocyclic residues that are characterized by their emission such as pyrene, phenanthrene, terphenyl, terthiophene, benzoterthiophene and coumarin (**Figure 1.7**).¹⁸ Using multiple dyes as replacement of DNA bases in adjacent position in DNA sequences can be used in the detection of a genetic sequence. For example, pyrene is a well-characterized excimer-forming fluorophore. When it is used alone it emits blue light while using two units of pyrene leads to emission of green light ascribed to the formation of an excimer complex through energy transfer from one pyrene unit to the other.

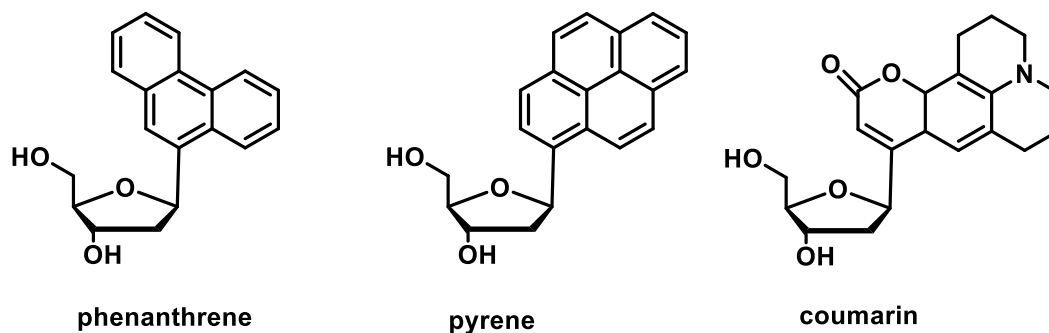


Figure 1.7 Examples of hydrocarbons and heterocycle DNA base replacement

5) Conjugated base analogues, are the fluorescent aromatic residues that are conjugated to the nucleobases via a linker. This class is characterized by introducing fluorescent property from the aromatic residue and maintaining the hydrogen bond ability with their complementary nucleobase. Numerous C5 or C6 modified pyrimidine nucleosides and C2 or C8 modified purine nucleosides have been synthesized in last 40 years employing the transition-metal assisted cross-coupling reactions^{19,20} Some of them show potent biological activity and/or are utilized as mechanistic or labelling probes (**Figure 1.8**). For example, the bicyclic furanopyrimidine-2-one nucleoside analogues bearing an aryl side chain display remarkable antiviral potency against the Varicella-Zoster virus. The 5-thienyl-deoxyuridines or 5-furyl-deoxyuridines were used as molecular beacons for oligonucleotide labeling.²¹

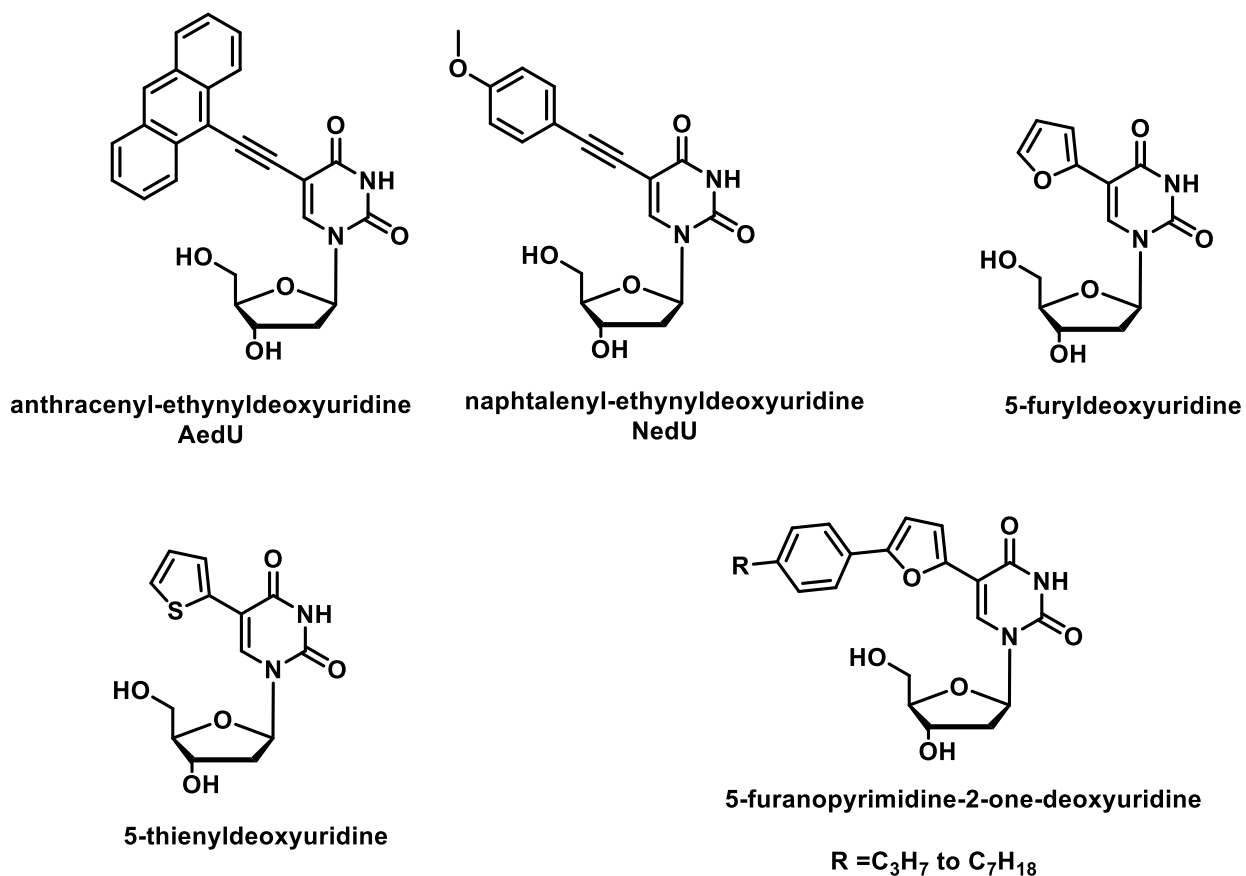


Figure 1.8 Examples of some conjugated base analogues

To date, different modified pyrimidines, extensively explored and utilized, contain a modification as a conjugated aromatic residue at 5-position. Herein we will discuss the preparation of emissive and highly responsive pyrimidines containing quinazolinone-based aromatic heterocycles that possess a molecular rotor element.

1.5.1 Quinazolinone-based nucleobase scaffolds

Many of the current treatment regimes for cancer utilize compounds which inhibit DNA synthesis. Such compounds are toxic to cells generally but their toxic effect on the rapidly dividing tumor cells can be beneficial. Alternative approaches to anti-cancer agents which act by

mechanisms other than the inhibition of DNA synthesis have the potential to display enhanced selectivity of action against cancer cells.

In recent years it has been discovered that a cell may become cancerous by virtue of the transformation of a portion of its DNA into an oncogene i.e. a gene which, on activation, leads to the formation of malignant tumor cells²⁸. Heterocycle moieties, such as quinazolinones, are present in natural products²¹ and synthetic pharmaceutical compounds²⁴. These compounds have been extensively studied for their biological and therapeutic activities.

Sequential recognition of metal ions and anions by a new fluorescent quinazolinone based probe has been achieved by previous studies^{23,30}. These probes exhibit highly selective and sensitive fluorescence “OFF-ON” recognition properties to metal ions and display high selectivity to anions through fluorescence relay enhancement²². It is well established that quinazolinone derivatives can show fluorescent properties, also the effect of adding electron donating and electron-withdrawing groups on the fluorescent intensity of some heterocyclic fluorophores have been studied³¹.

1.5.2 Goal of this research

Based on the aforementioned properties of either quinazolinone as a fluorogenic molecule or in peptide nucleic acid (PNA) as artificial nucleic acid analog with remarkable binding ability, we are interested in: first, the study of electron-withdrawing and electron-donating group effect on fluorescent properties of quinazolinone-based uracil scaffolds and second by investigating the photophysical properties of different functionalized quinazolinone-based uracil scaffold, and synthesis of PNA monomer possessing quinazolinone moiety. Incorporation of quinazolinone-based PNA monomer in PNA oligomer may be used as reporter probe for DNA detection in addition to its potential stabilization of the duplex structure by increased stacking interactions.

References

- (1) Watson, J. D.; Crick, F. H. C. Molecular Structure of Nucleic Acids. *Nature*. 1953, pp 737–738.
- (2) Derossi, D.; Chassaing, G.; Prochiantz, A. Trojan Peptides: The Penetration System for Intracellular Delivery. *Trends Cell Biol.* **1998**, 8 (2), 84–87.
- (3) Good, L.; Nielsen, P. E. Inhibition of Translation and Bacterial Growth by Peptide Nucleic Acid Targeted to Ribosomal RNA. *Biochemistry* **1998**, 95 (March), 2073–2076.
- (4) Frank-Kamenetskii, M. D.; Mirkin, S. M. Triplex DNA Structures. *Annu. Rev. Biochem.* **1995**, 64 (1), 65–95.
- (5) Marin, V. L.; Armitage, B. A. NIH Public Access. **2008**, 45 (6), 1745–1754.
- (6) Lohse, J.; Dahl, O.; Nielsen, P. E. Double Duplex Invasion by Peptide Nucleic Acid: A General Principle for Sequence-Specific Targeting of Double-Stranded DNA. *Proc. Natl. Acad. Sci. U. S. A.* **1999**, 96, 11804–11808.
- (7) Lahoud, G.; Timoshchuk, V.; Lebedev, A.; Arar, K.; Hou, Y. M.; Gamper, H. Properties of Pseudo-Complementary DNA Substituted with Weakly Pairing Analogs of Guanine or Cytosine. *Nucleic Acids Res.* **2008**, 36 (22), 6999–7008.
- (8) Merrifield, R. B. Solid Phase Peptide Synthesis. I. The Synthesis of a Tetrapeptide. *J. Am. Chem. Soc.* **1963**, 85 (14), 2149–2154.
- (9) Chandra, K. L.; Zhang, S.; Gorman, C. B. An Effective, Orthogonal Deprotection Strategy for Differentially Functionalized, Linear and Y-Shaped Oligo Phenylene Ethynylenes. *Tetrahedron* **2007**, 63 (30), 7120–7132.
- (10) Daniels, M.; Hauswirth, W. Fluorescence of the Purine and Pyrimidine Bases of the Nucleic Acids in Neutral Aqueous Solution at 300°K. *Science*. **1971**, 171 (3972), 675 LP-677.
- (11) Pecourt, J. L.; Peon, J.; Kohler, B.; June, R. V. Ultrafast Internal Conversion of Electronically Excited RNA and DNA Nucleosides in Water. *J. Am. Chem. Soc.* **2000**, 122 (5), 9348–9349.
- (12) Greco, N. J.; Tor, Y. Furan Decorated Nucleoside Analogues as Fluorescent Probes : Synthesis, Photophysical Evaluation, and Site-Specific Incorporation. *Tetrahedron*. **2007**, 63, 3515–3527.
- (13) Sowers, L. C.; Boulard, Y.; Fazakerley, G. V.; Cer, V.; Biochimie, D.; Moleculaire, D. G.; Biologie, D. De; October, R. V; Re, V.; Recei, M.; et al. Multiple Structures for the 2-Aminopurine - Cytosine Mispair. *Biochemistry*. **2000**, 39, 7613–7620.
- (14) Stivers JT. 2-Aminopurine fluorescence studies of base stacking interactions at abasic sites in DNA: metal-ion and base sequence effects. *Nucleic Acids Res.* **1998**, 26(16), 3837–3844.

- (15) Hawkins ME, Pfeleiderer W, Mazumder A, Pommier YG, Balis FM. Incorporation of a fluorescent guanosine analog into oligonucleotides and its application to a real-time assay for the HIV-1 integrase 3'-processing reaction. *Nucleic Acids Res.* **1995**, 23(15), 2872–2880.
- (16) Hawkins, M. E., Pfeleiderer, W., Balis, F. M., Porter, D. and Knutson, J. R. Fluorescence Properties of Pteridine Nucleoside Analogs as Monomers and Incorporated into Oligonucleotides. *Analytical Biochemistry.* **1997**, 244, 86–95
- (17) Liu, H.; Gao, J.; Lynch, S. R.; Saito, Y. D.; Maynard, L.; Kool, E. T. A Four-Base Paired Genetic Helix with Expanded Size. *Science.* **2003**, 302 (5646), 868 LP-871
- (18) Kool, E. T. Replacing the Nucleobases in DNA with Designer Molecules. *Acc. Chem. Res.* **2002**, 35 (11), 936–943
- (19) Greco, N. J.; Tor, Y. Simple Fluorescent Pyrimidine Analogues Detect the Presence of DNA Abasic Sites. *J. Am. Chem. Soc.* **2005**, 127 (31), 10784–10785.
- (20) Hudson, R. H. E.; Ghorbani-Choghamarani, A. Oligodeoxynucleotides Incorporating Structurally Simple 5-Alkynyl-2 - Deoxyuridines Fluorometrically Respond to Hybridization. *Org. Biomol. Chem.*, **2007**, 5, 1845-1848.
- (21) Yong L.; Stanislaw F. W. *Molecules*, **2015**, 20, 4874–4901
- (22) Michael, J. P. Quinoline, Quinazoline, and Acridone Alkaloids. *Nat. Prod. Rep.*, **1997**, 14, 605-618
- (23) Tang, L.; Zhou, P.; Zhong, K.; Hou, S. Sensors and Actuators B : Chemical Fluorescence Relay Enhancement Sequential Recognition of Cu ²⁺ and CN ⁻ by a New Quinazoline Derivative. *Sensors Actuators B. Chem.* **2013**, 182, 439–445.
- (24) Foster, B. A.; Coffey, H. A.; Morin, M. J.; Rastinejad, F. Pharmacological Rescue of Mutant P53 Conformation and Function. *Science.* **1999**, 286 (5449), 2507 -2510.
- (25) Da Silva, J. F. M.; Walters, M.; Al-Damluji, S.; Ganellin, C. R. Molecular Features of the Prazosin Molecule Required for Activation of Transport-P. *Bioorg. Med. Chem.* **2008**, 16 (15), 7254—7263.
- (26) Lapatinib, I. O Ncologist Dual Kinase Inhibition in the Treatment of Breast. **2004**, 9 (suppl 3), 10–15.
- (27) Girard, C.; Liu, S.; Cadepond, F.; Adams, D.; Lacroix, C.; Verleye, M.; Gillardin, J.-M.; Baulieu, E.-E.; Schumacher, M.; Schweizer-Groyer, G. Etifoxine Improves Peripheral Nerve Regeneration and Functional Recovery. *Proc. Natl. Acad. Sci.* **2008**, 105 (51), 20505–20510.
- (28) Lodish H, Berk A, Zipursky SL, et al. Molecular Cell Biology. 4th edition. New York: W. H. Freeman; **2000**. Section 24.2, Proto-Oncogenes and Tumor-Suppressor Genes.
- (29) Mohs, R. C.; Greig, N. H. Drug Discovery and Development : Role of Basic Biological Research. *Alzheimer's Dement. Transl. Res. Clin. Interv.* **2017**, 3 (4), 651–657.
- (30) Silva, A. P. De; Gunaratne, H. Q. N.; Gunnlaugsson, T.; Huxley, A. J. M.; Mccoy, C. P.;

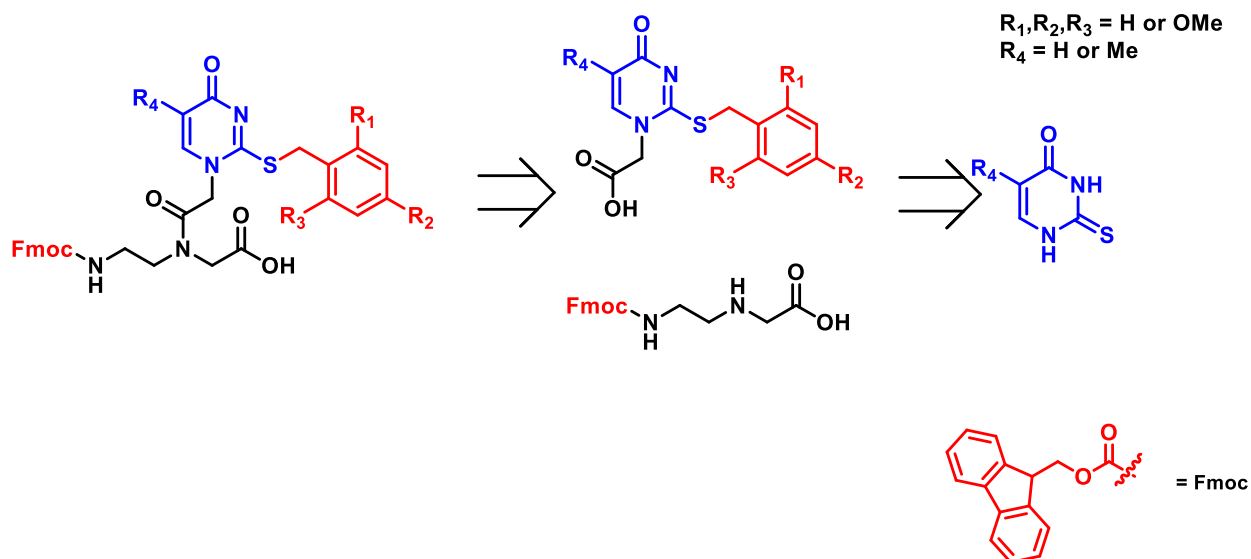
- Rademacher, J. T.; Rice, T. E. Signaling Recognition Events with Fluorescent Sensors and Switches. *Chem. Rev.* **1997**, 97(5) 1515-1566.
- (31) Dicesare, N.; Lakowicz, J. R. Spectral Properties of Fluorophores Combining the Boronic Acid Group with Electron Donor or Withdrawing Groups. Implication in the Development of Fluorescence Probes for Saccharides. *J. Phys. Chem. A.* **2001**, 105,28, 6834-6840.
- (32) Hamal, S.; Hlrayama, F. Actinometría Determination of Absolute Fluorescence Quantum Yields. *J. Phys. Chem.*, **1983**, 277 (9), 83–89.
- (33) Kirby, E. P.; Steiner, R. F.; Kirby, E. P.; Steiner, R. F. The Influence of Solvent and Temperature upon the Fluorescence of Indole Derivatives1 H. *J. Phys. Chem.*, **1970**, 74 (28), 4480–4490.

Chapter 2

Highly acid-labile protecting group for thiouracil

2.1 Introduction

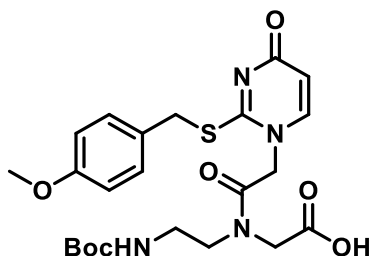
The normal oligomerization of peptide nucleic acids (PNAs) is based on peptide synthesis procedure.^{Bibliography}³¹ Although uracil and thymine nucleobase monomers normally do not require protection as they do not contain nucleophilic exocyclic amino groups, replacing the carbonyl group of T and U with a thionyl group at the 2-position of the nucleobase creates a nucleophilic site. Due to the greater nucleophilicity of sulfur compared to nitrogen, alkylation of the unprotected nucleobase with methylene carbonyl linker results in *S*-alkylation rather than the desired *N*-1-alkylation. Therefore, protection of the ^sU nucleobases is necessary due to the nucleophilicity of the thiol group.



Scheme 2.1 Retro-synthesis of thiouracil PNA monomer with different acid labile benzyl-type protection

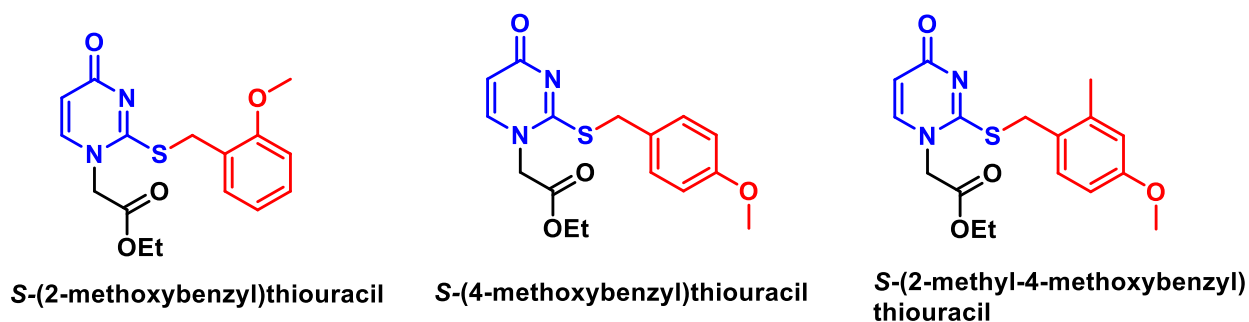
In 1999, Nielsen et al.⁶ developed the synthesis of a protected thiouracil (^sU) monomer compatible with PNA oligomerization under the SPPS condition. They used 4-methoxybenzyl protection on the 2-thiol position of the nucleobase, which can be removed under strongly acidic

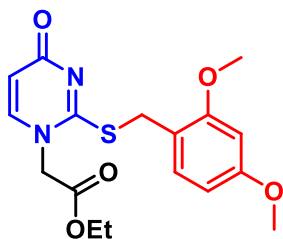
conditions used for global deprotection. The protected thiouracil nucleobase is then attached to the protected aminoethyl glycine backbone via a methylene carbonyl linker to yield the ^sU monomer for oligomerization (**Scheme 2.2**). The ^sU monomer is then incorporated into PNA oligomers using standard Boc-based SPPS procedures.



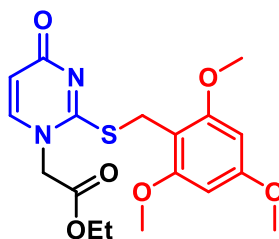
Scheme 2.2. PNA monomer compatible with Boc-based peptide synthesis⁶.

An orthogonal protection system, which removes protecting groups and cleaves the peptide from the solid support resin under acidic condition, is being used in modern SPPS technique. Due to the mild conditions used for global deprotection, this work aims to develop a more acid-labile protecting strategy for the ^sU monomer, which can be easily removed. The methoxy group can act as an electron donation group on the benzyl-type protection and helps stabilize the carbocation formed from acidolysis of the protecting group. We proposed increasing the electron donation into the benzylic position would increase the stability of the transition state (**Scheme 2.3**). The stabilization of the cationic product can be reached by using a more acid-labile protecting group, which can be removed under milder acidolysis conditions. However, we found that 2-methoxybenzyl protection is surprisingly very acid resistant and cannot be used for Fmoc-based synthesis in PNA synthesis procedure.





S-(2,4-dimethoxybenzyl)thiouracil



S-(2,4,6-trimethoxybenzyl)thiouracil

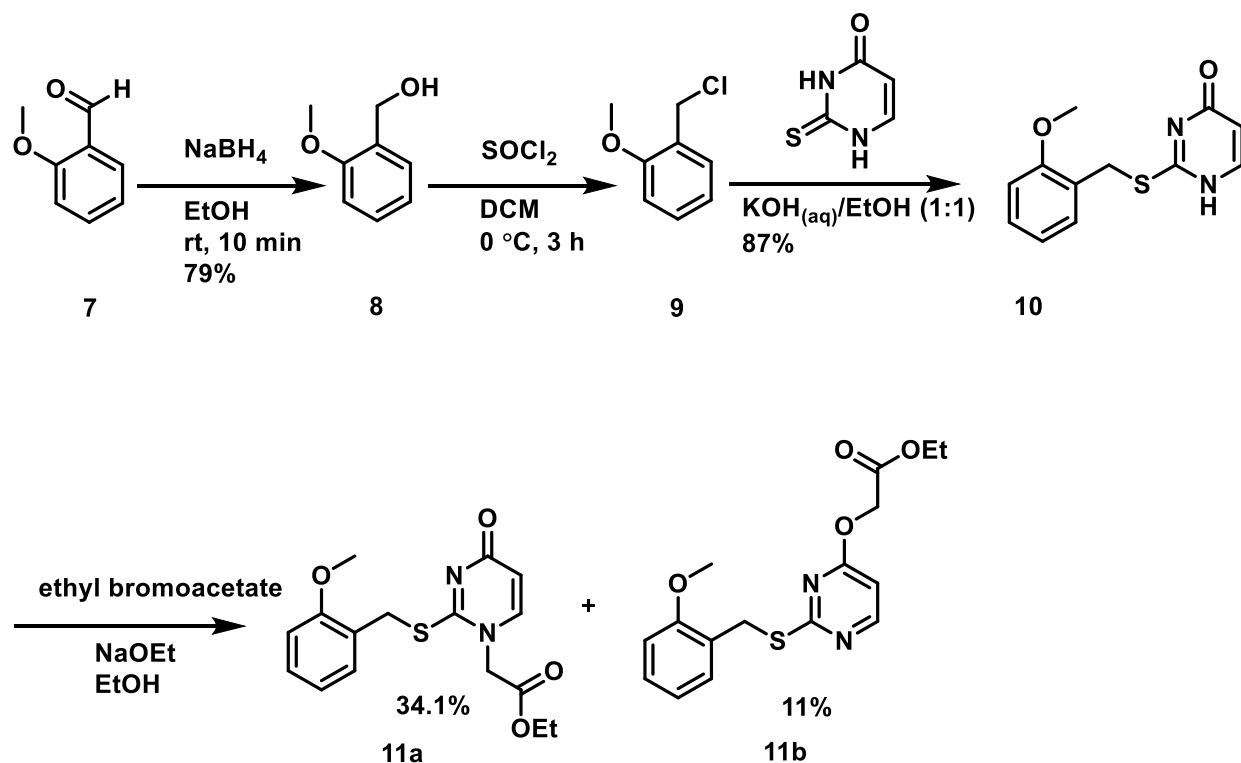
Scheme 2.3 Different studied benzyl-type protection for thiouracil

2.2 Results and discussions

2.2.1 Thiouracil protection with 4-methoxybenzyl and 2-methoxybenzyl group

In order to study the effects of the addition of methoxy substituent to the ortho- and para-positions of the benzene ring on the rate of the acidolysis of the benzyl protecting group from the thiol of the thiouracil nucleobase, the 4-methoxybenzyl (**5**) protected and 2-methoxybenzyl protected (**11a**) thiouracil were synthesized. The 4-methoxybenzyl thiouracil (**5**) has been used in the original synthesis of the thiouracil monomer for Boc-based oligomerization and it was synthesized as a comparison for the more acid-labile thiol protecting groups. The 2,4,6-trimethoxybenzyl and 2,4-dimethoxybenzyl thiouracil protection have been synthesized in Dr. Hudson's research group previously by Timothy Martin-Chan. In this work, a 2-methoxybenzyl protecting group was studied as the sulfur protection. The 2-methoxybenzaldehyde was reduced using sodium borohydride (**Scheme 2.4**), to yield 2-methoxybenzyl alcohol as the product. Then benzyl alcohol was halogenated using thionyl chloride to replace the hydroxyl group with a good leaving group for addition onto the thiouracil nucleobase. The 2-methoxybenzyl chloride was extracted in ether to yield the compound as a clear colourless oil. The 2-methoxybenzyl group was added to thiouracil using potassium hydroxide as the base, which yielded the 2-(2-methoxybenzyl)thiouracil as a white solid. The protected thiouracil was then alkylated using ethyl bromoacetate in a solution of sodium ethoxide, which yielded a mixture containing both *N*-1-

alkylation and *O*-4-alkylation of the nucleobase, which can be separated by column chromatography. The 34% yield was reached for *N*-1-alkylated product, while the *O*-4-alkylated product resulted in 11% yield. Although the reaction progressed in low yield, the unreacted *S*-(2-methoxybenzyl)thiouracil was easily separated by column chromatography and reacted with ethyl bromoacetate and sodium ethoxide in a second alkylation reaction to increase the yield of the desired *N*-1-alkylated product (**Scheme 2.4**).



Scheme 2.4. Synthesis of 2-methoxybenzyl protected thiouracil nucleobase

The purified product (**11a**) was characterized by 2D NMR analysis to determine the exact structure of the synthesized compound. Three possible alkylations of the protected ^8U nucleobase could be formed. *N*-1 position or *N*-3 position common with alkylation of uracil and *O*-alkylation of the carbonyl at the 4-position also possible. Analysis of the ^1H NMR, ^{13}C NMR, COSY, HSQC, and HMBC have been done and HMBC spectra looks at the interactions between the methylene protons with the carbon atoms of the thiouracil ring. It is expected that for the desired *N*-1 alkylation, the interaction would be observed with the *C*-2 and *C*-6 atoms while *N*-3 alkylation

would result in interaction between the methylene carbonyl protons and the C-2 and C-4 atoms. Just the first outcome is observed in the HMBC spectra. Also, interactions between the methylene carbonyl protons and the C-4 and C-5 atoms indicating *O*-alkylation of thiouracil nucleobase (Figure 2.1.).

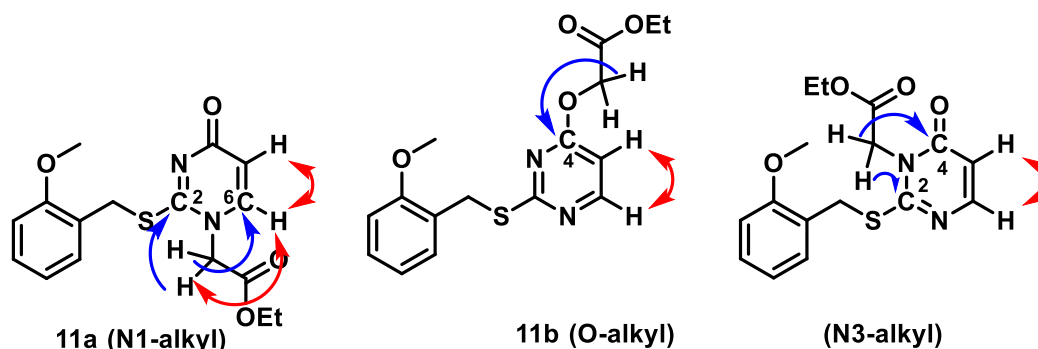
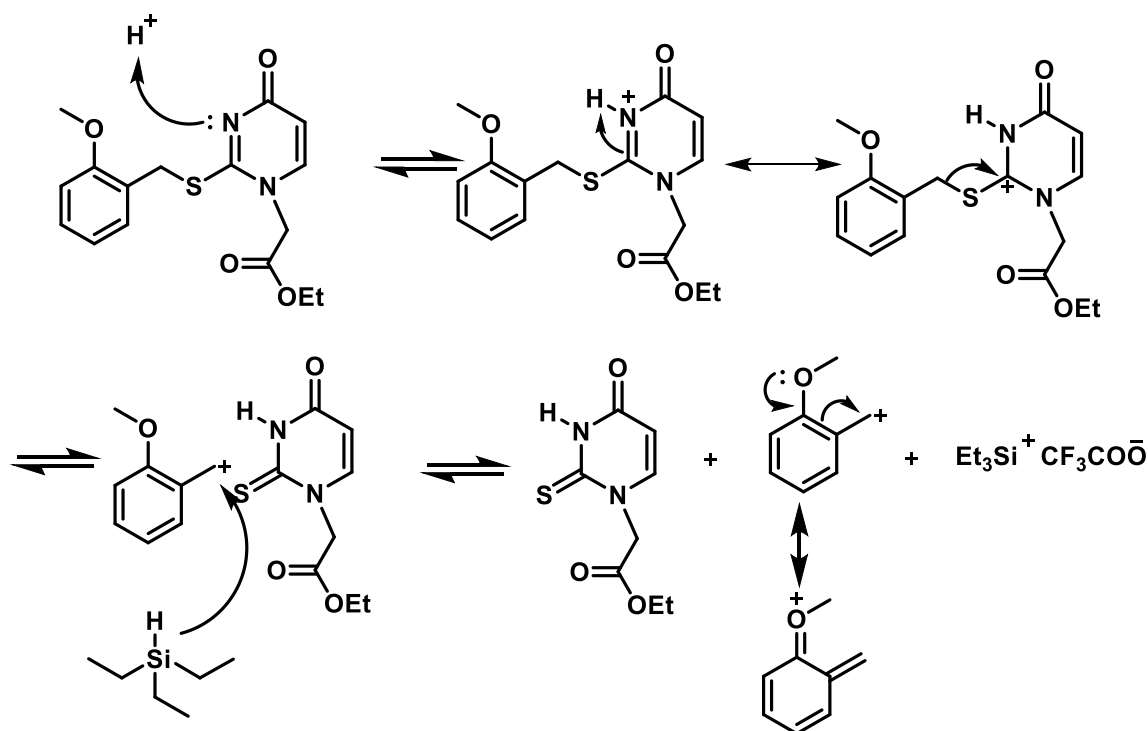


Figure 2.1. Possible structures of alkylation products of 10. Selected NOE correlations (double-headed arrows) and HMBC H-C correlations (single-headed arrows) of compounds 11a and 11b.

The ESI-MS data of compound **11a** with a molecular mass of $([M+H]^+ 214.04121$ found 214.04042) was collected. Based on the mass of the synthesized compound and its 2D NMR data suggest that there are two different final products. The *N*-1-alkylated compound (**11a**) subjected to the acidolysis analysis and the data was compared to other methoxybenzyl-type protected thiouracil nucleobases (Table 1.1.). The acid cleavage of the thiol-protecting group was confirmed under standard deprotection conditions used for global deprotection of PNA oligomers synthesized using Fmoc-based oligomerization.

The *N*-1-alkylated *S*-(4-methoxybenzyl)thiouracil was mixed with a solution of 2% trifluoroacetic acid in 0.5 mL of deuterated chloroform and 1 drop of triethylsilane in order to monitor the deprotection of benzyl-type protection. The ^1H NMR spectra of the obtained product show the removal of the thiol protecting group under these conditions (Figure S1). The absence of the aromatic benzyl protons and the benzylic protons in the NMR spectra proved the removal of the 4-methoxybenzyl group. This test confirmed the acid lability of the sulfur protecting group under standard deprotection conditions suggesting that once used into PNA oligomerization, using Fmoc-based chemistry, the thiouracil nucleobases could be easily deprotected during the global deprotection and resin cleavage of the PNA oligomer.

The *N*-1-alkylated *S*-(2-methoxybenzyl)thiouracil was mixed with a solution of 2% trifluoroacetic acid in 0.5 mL of deuterated chloroform and 1 drop of triethylsilane and the progression of acidolysis was monitored by ^1H NMR. Surprisingly, 2-methoxybenzyl protected thiouracil showed strong acid resistance in 2% and 10% trifluoroacetic acid, which cannot be explained by the proposed deprotection mechanism (**Scheme 2.5**). So, a more concentrated solution was prepared by using 95% of trifluoroacetic acid and it took 50 minutes to fully deprotect the thiol position and remove the 2-methoxybenzyl group (**Table 2.1**).



Scheme 2.5. Proposed mechanism of 2-methoxybenzyl thiol protecting group acidolysis.

Protecting group	Nucleobase	Rate constant (k)	Half-life ($t_{1/2}$) (min)
4-methoxybenzyl	^5U	0.0111	62
4-methoxybenzyl ^a	^5T	0.0070	99
2-methyl-4-methoxybenzyl ^a	^5U	0.0527	13
2,4-dimethoxybenzyl ^a	^5U	-	<1
2-methoxybenzyl	^5U	-	-
2,4,6-trimethoxybenzyl ^a	-	-	-

^a Studied by Timothy Martin-Chan from Hudson Group

Table 2.1 The rate and half-life of acidolysis for different benzyl-type protections in the solution of 2% of trifluoroacetic acid condition.

In order to elucidate the strong acidolysis resistance mechanism of S-(2-methoxybenzyl)thiouracil, the minimum energy structure for the S-(2-methoxybenzyl)thiouracil has been studied (**Figure 2.2**).

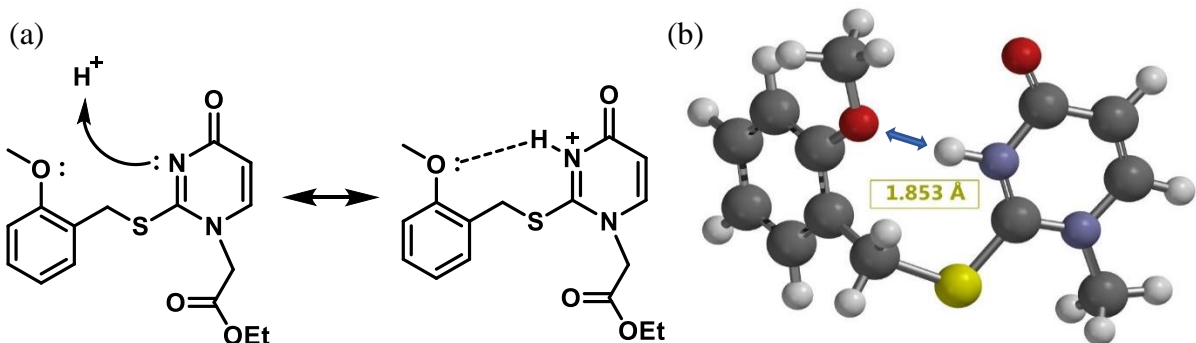


Figure 2.2. (a) Proposed stabilization of the protonated form of compound 14a by an intramolecular hydrogen bond with the 2-methoxybenzyl group. (b) Minimum energy structure for the protonated model compound S-(2-methoxybenzyl)-*N*1-methylthiouracil. Arrowheads show the S→H distance (1.853 Å); O→N3 distance (2.854 Å).

According to the Hammett equation³², there is a linear free-energy relationship relating reaction rates and equilibrium constants for many reactions involving benzoic acid derivatives with meta- and para-substituents to each other with just two parameters: a substituent constant and a reaction constant. However, in the case of ortho substituents, the Hammett equation is not valid because of the steric hindrance effects. The hydrogen bonds with donor-acceptor distances in the range of 2.2 to 2.5 Å considered as strong, 2.5 to 3.2 Å considered as moderate, and 3.2-4.0 Å is considered as a weak bond³². In this molecule, as it is shown in (**Figure 2.2**) the distance between oxygen atom in methoxy group and a hydrogen atom attached to N-3 position is 1.853 Å, which is suitable for forming a strong hydrogen bond. Therefore, forming a hydrogen bond with the proton on the N-3 position stabilizes the intermediate and prevents the normal deprotection mechanism to occur.

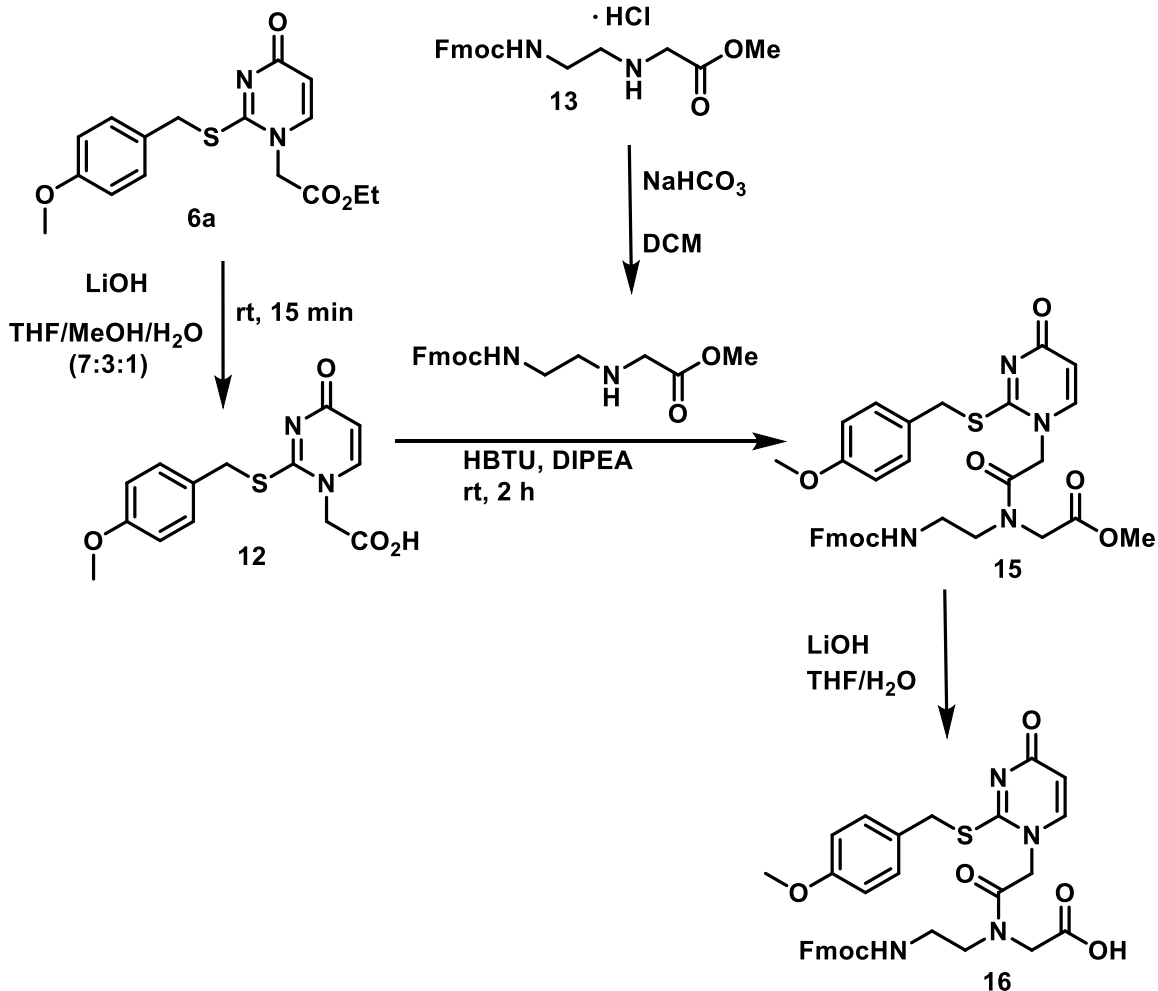
As it is shown in (**Figure 2.2**), the hydrogen bond formed will stabilize the lone pairs on oxygen in the methoxy group attached to the benzyl ring and it reduces its ability to act as an electron-donating group; so the deprotection needs stronger acid concentration to go to completion.

2.2.2 Thiouracil PNA monomer

The Fmoc-based aminoethylglycine backbone was synthesized as a hydrochloride salt in our research group previously by following literature procedures^{33,34}. The hydrochloride salt backbone was extracted in chloroform to yield the compound as a clear and colourless oil (**13**).

The alkylacetate of the protected nucleobase was hydrolyzed using a solution of aqueous lithium hydroxide, to obtain the carboxylic acid functional group for attachment to the aminoethylglycine backbone. The protected nucleobase was then reacted with a solution of hexafluorophosphate benzotriazole tetramethyl uronium (HBTU), which acts as the coupling agent, and diisopropylethylamine (DIPEA) which acts as the base. The activated nucleobase is then reacted with the protected aminoethylglycine (**14**) backbone to form the PNA monomer. The methyl ester protecting the C-terminus of the PNA monomer is then hydrolyzed using aqueous lithium hydroxide solution to form the C- terminus carboxylic acid. Because of the kinetics of the reactivity of the C-terminus protecting group compared to the N-terminus protecting group under aqueous alkali conditions favours hydrolysis of the methyl ester instead of removal of the Fmoc group, which can give the selective deprotection of the PNA backbone (**Scheme 2.6**).

Basic conditions to remove the Fmoc protecting group uses a solution of 20% piperidine ($pK_a=11$). Amine bases are effective in the removal of the Fmoc group since removing the Fmoc group results in the formation of highly reactive dibenzofulvene as a byproduct of the reaction, which is trapped by the amine base. Amine bases such as piperidine effectively trap the dibenzofulvene intermediate which drives the deprotection reaction to completion.^{35,36}

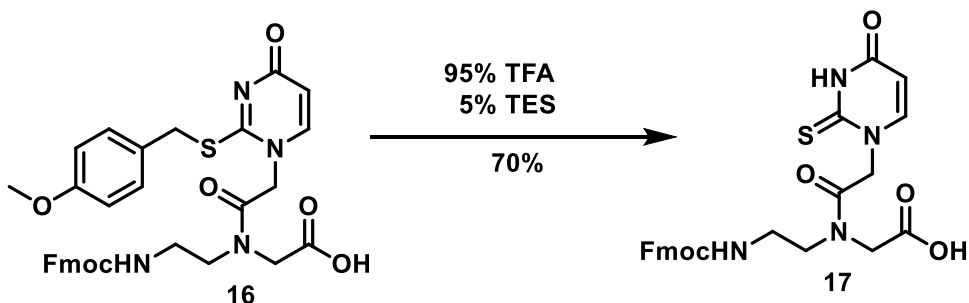


Scheme 2.6. Synthesis of thiouracil PNA monomer

After C-terminus methyl ester hydrolysis, which gives desired PNA monomer, the oligomerization can be done. The monomers were characterized using ^1H NMR and ^{13}C NMR spectroscopy as well as high-resolution mass spectrometry (HRMS). ^1H NMR spectra show the presence of rotameric structures which caused by amide bond formed between the methylene carbonyl linker and the aminoethylglycine backbone and resulting from the carbamate from Fmoc protection on the N-terminus.

After the successful PNA monomer and oligomer synthesis with protected nucleobases, it has been not stated using thiouracil monomers with protecting groups during the oligomerization is necessary. As stated above, the protecting group on the thio position is necessary in order to get the desired *N*-1-alkylation. So, the thiouracil PNA monomer was synthesized without methoxy

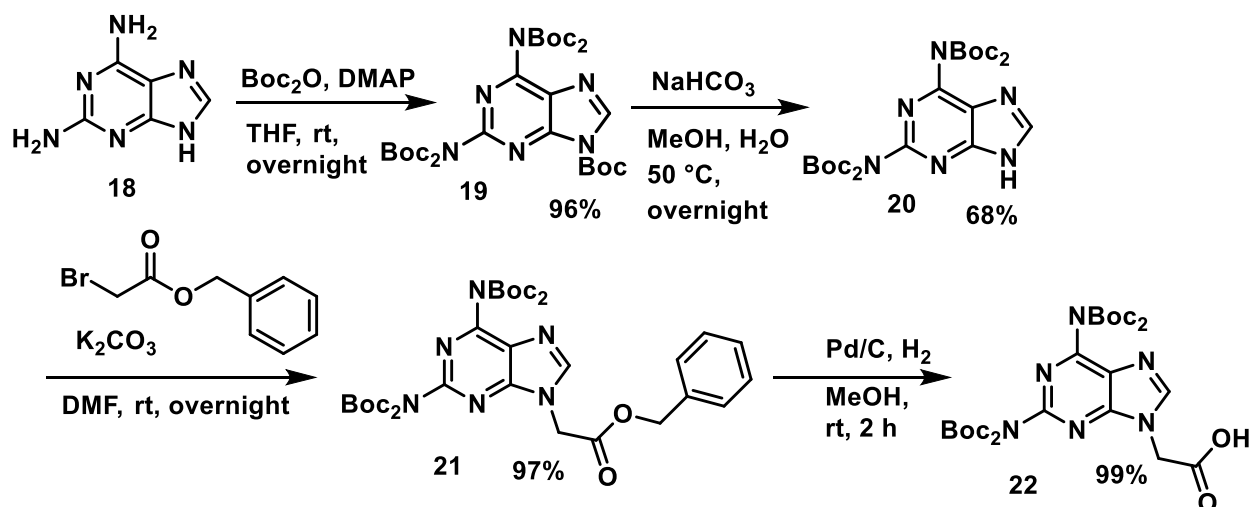
benzyl type protections. PNA monomer (**16**) added to a solution of 95% trifluoroacetic acid and 5% triethylsilane and it was stirred for 30 min. The solvent was then evaporated under a nitrogen stream and the resulting residue was washed twice with toluene to remove the protecting group from the nucleobase and give protection free-PNA monomer (**17**) (**Scheme 2.7**)



Scheme 2.7. Synthesis of protection-free thiouracil PNA monomer

2.2.3 Tetrakis-Boc protected 2,6-diaminopurine PNA monomer

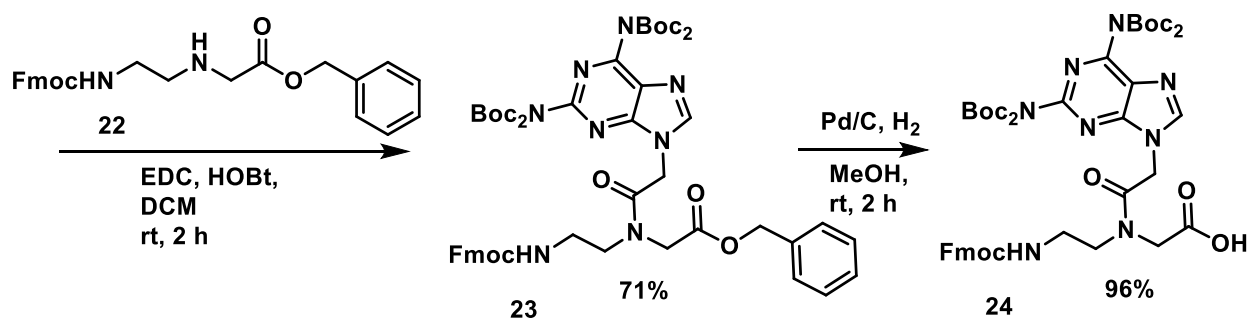
The synthesis of tetrakis-Boc protected 2,6-diaminopurine was done by penta-Boc protection of the commercially available 2,6-diaminopurine to form **19**, which proceeded in high yield (**Scheme 2.7**) 2,6-diaminopurine is insoluble in THF, and as it reacts the product becomes fully soluble. After that, the mono-deprotection using NaHCO_3 in MeOH gives **20**. The tetrakis-Boc protected nucleobase was subjected to an alkylation using benzyl bromoacetate, and the bulky protecting group directed the alkylation to *N*-9 position. The hydrogenation of the benzyl ester **21** gave the final tetra-Boc protected nucleobase acid **22** in high yield, before the coupling step.³⁷



Scheme 2.8. The synthesis of tetrakis-(Boc)-2,6-diaminopurine-9-yl acetic acid.

2.2.3.1 Coupling of Boc-protected acid 2,6-diaminopurine monomer to PNA backbone

The coupling of the Boc-protected acids to the previously synthesized Fmoc/Bn PNA backbone in our lab was done using standard EDC/HOBt coupling reagents in DCM and proceeded in typical coupling yield. (**Scheme 2.8**) The hydrogenation of the benzyl protecting group with Pd/C and hydrogen gas in methanol affords the PNA monomer ready for oligomerization in high yield (96%).



Scheme 2.9. The coupling of the Boc-protected acids to an Fmoc/Bn PNA backbone to form PNA monomer

2.2.4 Oligomerization of PNA Fmoc-based PNA monomers

The peptide synthesis was carried out using the thiothymine, thiouracil (with and without protecting group) and 2,6-diaminopurine PNA monomers, in order to show that the Fmoc/Boc protection strategy was effective for the synthesis of PNA and also the protection for sulfur is not necessary during the oligomerization and 4-methoxybenzyl type protection is labile enough for thiouracil.

The mass spectroscopy results and HPLC traces of crude and pure thiouracil PNA oligomers (with and without protection) showed comparable purity coupling yields to previous PNA syntheses in our laboratory. Melting temperature determination of the PNAs with their PNA and DNA complements was performed (**Table 2.2.**) to measure the effect of pseudo-complementarity and nucleobase mismatches on PNA and DNA duplex stability.

A DNA oligomer with an analogue of cytidine, phenylpyrrolocytidine (PhpC) insert has the advantage of being fluorescent and an experiment was done to see if this property could be exploited to see the effect of pseudo-complementary nucleobases on fluorescent intensity upon hybridization since PhpC introduced a mild stabilizing effect of ~ 2.5 °C as consistent with reported literature.³⁸ Also, ^SU bases were found to be slightly greater at destabilizing the duplex than the ^ST bases.

2.2.5 Fluorescent studies

Naturally, a method is required to visualize DNA strand invasion and the effect of pseudo-complementarity, and in our study toward the pseudo-complementary base pairs, we aimed to develop a more efficient method for detecting and quantifying duplex invasion. The current method of gel separation, while effective, is time-consuming. Gel separation is based upon charge to mass ratio; if DNA and PNA of identical sequences are run on the gel, a DNA duplex travels furthest, PNA duplex the least distance, and if hybridization has occurred, a DNA-PNA duplex will show on the gel at an intermediate distance³⁹. One major issue with this method is due to the uncharged PNA; it often does not migrate on the gel and thus, it cannot be visualized.

Our proposed method aims to move away from gel separation and instead adopt a novel fluorophore design incorporated into the strands. In our proof of concept study, we aim to incorporate a fluorescent base, 6-phenylpyrrolocytidine (PhpC) (**Figure 2.3.**), near the end of a synthesized DNA strand. When in duplex form, this modified cytidine will have low fluorescence as it is quenched by local base stacking and its pairing to the complementary strand³⁸. Upon duplex invasion by complementary PNA strands at the sequence adjacent to the PhpC site (i.e. they are a few bases shorter than the DNA strand length), the PhpC site will be freed from its base-pairing interactions and become a short overhang region. Upon excitation at 364 nm, fluorescence at 446 nm³⁸ will be used to monitor invasion of the DNA duplex by the pseudo-complementary PNA.

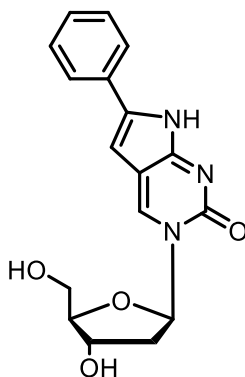


Figure 2.3. 6-phenylpyrrolocytidine (PhpC)

This method is inherently attractive due to the simplicity of fluorescence measurement, and the subsequent ability to not only qualitatively monitor strand invasion, but also qualitatively measure its extent and the dynamics (rate) of the process.

We previously synthesized pseudo-complementary PNA strands, and for this reason, we decided to incorporate the PhpC into the DNA strand; in future studies, this base could be alternatively incorporated into the PNA strand. Primarily, we will synthesize the complementary DNA strands to the PNAs including both unmodified DNA strands and the PhpC substituted strands.

Fluorescent studies will then be performed using the PNAs and either the control DNA or the PhpC sequences (in solution), which will show a turning-on of fluorescence when a PNA strand invades our PhpC modified DNA sequence (**Figure 2.4**).

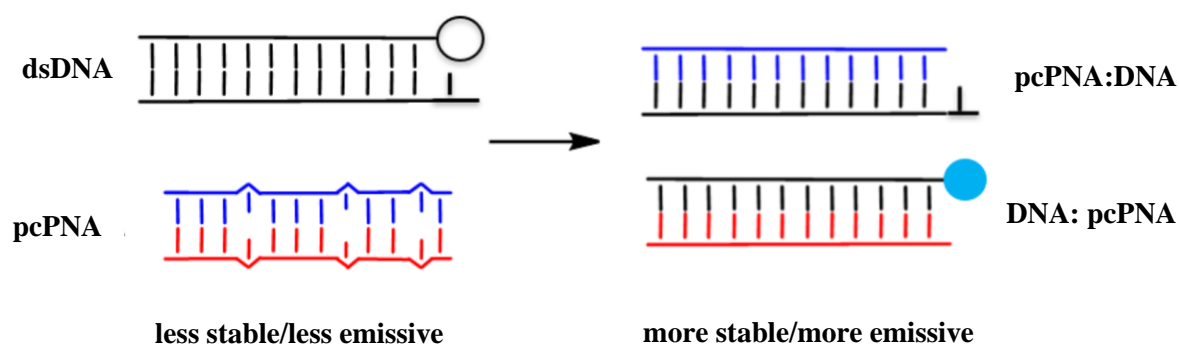


Figure 2.4. DNA strand invasion by pseudo-complementary PNA (circle represents PhpC). The more stable PNA-DNA duplexes liberate the quenched PhpC base resulting in a turning-on of fluorescence.

Overall, this design aims to be more efficient, precise and versatile than the previous methods; the ability to synthesize fluorescent molecules in exact locations greatly increases the specificity of the method. Future applications could eventually include simpler detection of specific genetic markers by *in vitro* hybridization studies involving on-off fluorescent switches or even *in vivo* gene silencing using PNAs that visually report their binding to the target. Our goal is to lay the foundation for this potentially significant advancement in invasion detection and to design a simple protocol for its use *in vitro*.

2.2.6 Thermal stability (T_m) analysis

PNA oligomers were purified by high-pressure liquid chromatography (HPLC). They were homogeneous by HPLC analysis and exhibited one major peak at the expected mass as analyzed by high-resolution mass spectrometry (HRMS) (**Table S1.**). Thermal stability analyses (T_m) were measured in 10 mM sodium hydrogen phosphate/ 100 mM NaCl / 0.1 mM EDTA, pH=7.0 at a heating rate of 0.7 °C/min (15-90 °C, for PNA-PNA duplexes), (15-85 °C, for PNA-DNA duplexes) and (10-70 °C for DNA-DNA duplexes). The thermal stability analyses have been done in order to study binding interaction between target vs. control and target vs. modified PNA and DNA strands using Varian 300 Bio UV-Vis Spectrometer at the wavelength of 260 nm and the resulting data are shown below (**Table 2.2.**).

Sequence (N→C)	vs. DNA [*]		vs. PNA [†]	
	T _m (°C)	ΔT _m	T _m (°C)	ΔT _m
H-Lys-GTAGATCACT-Lys-NH ₂	54.5		67.5	
H-Lys-G ^S TAGA ^S TCAC ^S T-Lys-NH ₂	62.0 (66.5) ^{**}	+7.5 (+12.0) ^{**}	64.5	-3.0
H-Lys-G ^S UAGA ^S UCAC ^S U-Lys-NH ₂	57.0 (64.0) ^{**}	+2.5(+9.5) ^{**}	68.5	+1.0
H-Lys-G ^S UDGD ^S UCDCT-Lys-NH ₂	66.0 (70.5) ^{**}	+11.5(+16.0) ^{**}	79.5 (40.5) [§] (49.0) [‡]	+12 (-27.0) [§] (-18.5) [‡]
H-Lys-AGTGATCTAC-Lys-NH ₂	54.5		67.5	
H-Lys-AG ^S UGA ^S UC ^S UAC-Lys-NH ₂	45.0	-9.5	69.0	+1.5
H-Lys-DG ^S UGD ^S UC ^S UDC-Lys-NH ₂	59.0	+4.5	74.5	+7.0
5' AGTGATCTACCT 3'	46.0 (48.5) ^{**}		54.5	

PNA oligomers are listed from the pseudo 5' terminus to the pseudo 3'-end. **Lys** = D-lysine, ^S**T** = 2-thiothymine
^S**U** = 2-thiouracil **D** = 2,6-diaminopurine PNA residues;

^{*}The complementary DNA oligonucleotides 5' AGTGATCTACCT 3' and 5' AGGTAGATCACT 3' were used.

^{**}Measured vs. 5' AGTGATCTAC(PhpC)T 3'. **PhpC** = 6-Phenylpyrrolocytidine

[†]The complementary PNA oligomers H-Lys-AGTGATCTAC-Lys-NH₂ or H-Lys-GTAGATCACT-Lys-NH₂ were used.

Temperature-dependent UV spectra of PNA-PNA duplexes at 2 μM strand concentration each in 100 mM sodium phosphate buffer, pH = 7.0.

[‡]Measured vs. H-Lys-AG^SUGA^SUC^SUAC-Lys-NH₂.

[§]Measured vs. H-Lys-DG^SUGD^SUC^SUDC-Lys-NH₂.

Table 2.2. Thermal stabilities (T_m) of complexes

2.2.7 Fluorescence analysis

The same samples prepared for the melting studies were used (2.0 μ M of each strand in buffer). A suitable excitation wavelength was measured first by observing emission at 446 nm; 369 nm resulted in the highest counts per second. Subsequently, the four samples measured for fluorescence were excited at this wavelength and emission values recorded from 400-580 nm. Excitation maximum of the PhpC base in the target DNA (PhpC) oligo was determined to be 369 nm by measuring emission at 446 nm (**Figure S4**) which is consistent with previously reported values.⁴⁰ This excitation wavelength was used for subsequent measurement of the emission spectra from 400 nm to 580 nm for each of four different target DNA (PhpC) containing samples (**Figure 2.5**).

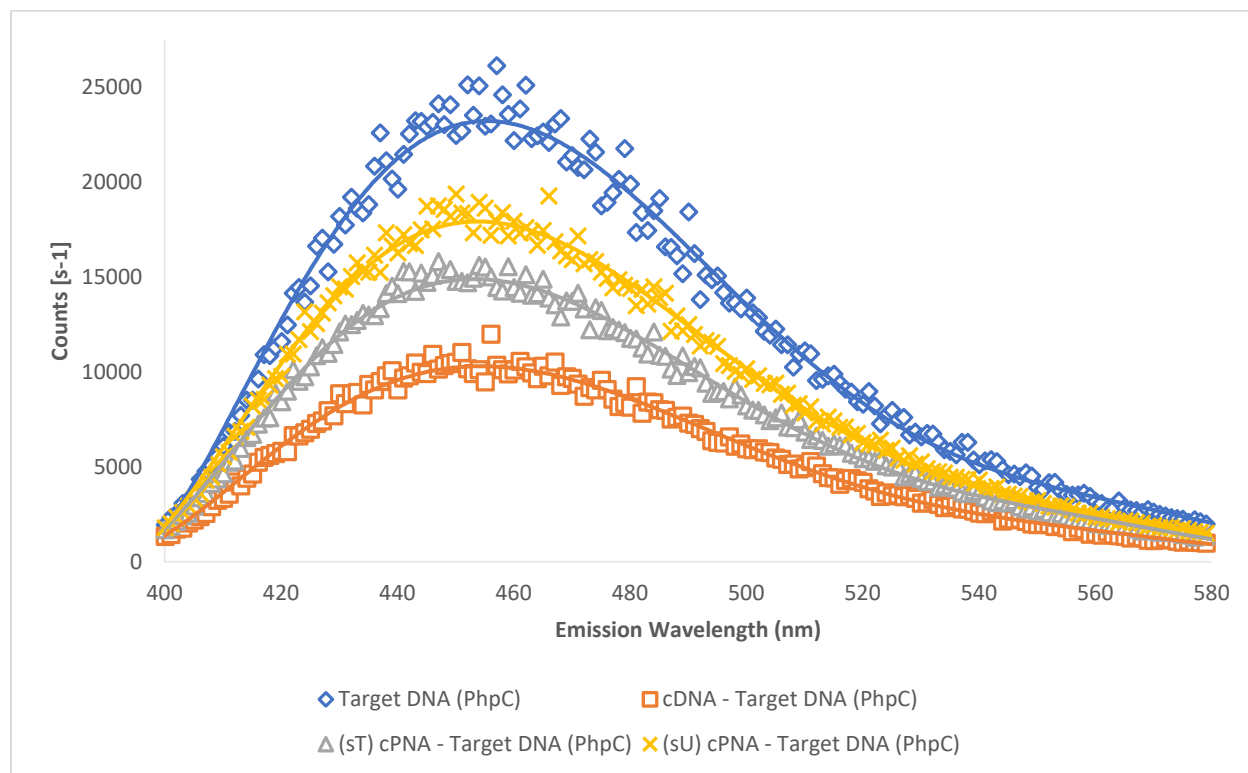
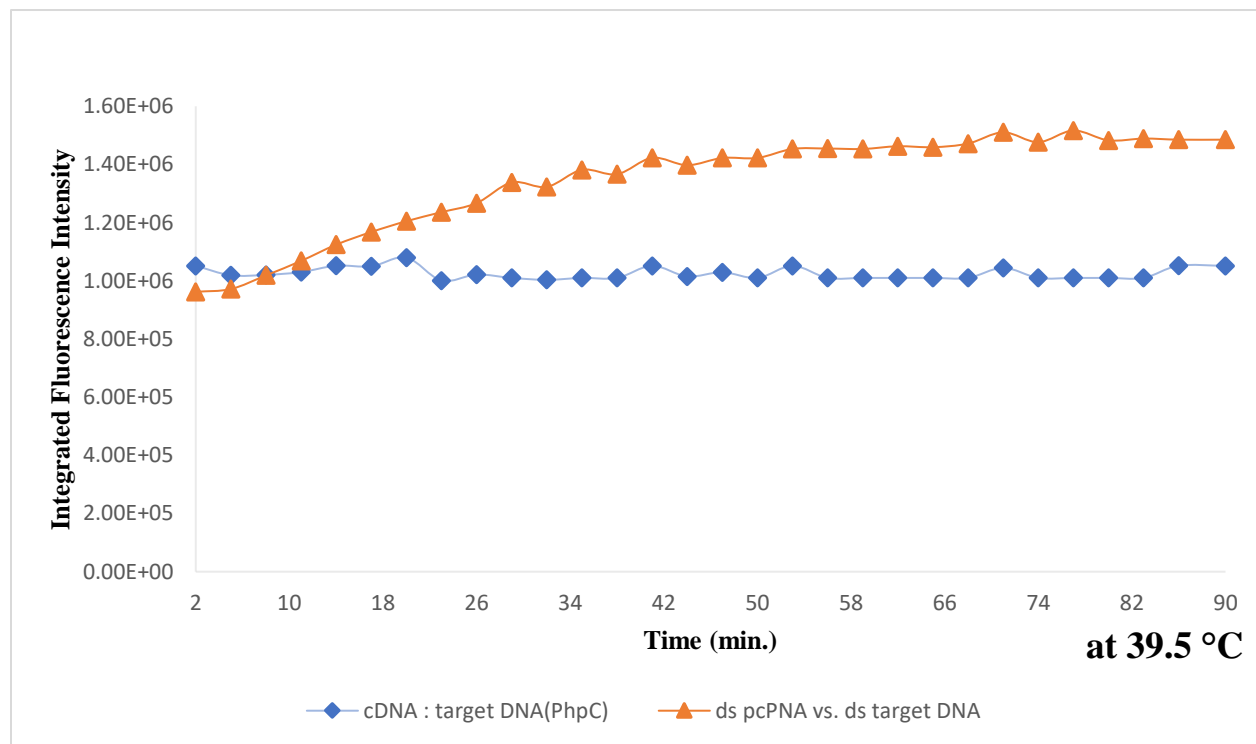


Figure 2.5. Emission spectra of four target DNA (PhpC) samples upon excitation at 369 nm.

A maximal emission was ~23000 counts per second for the single-stranded target DNA (PhpC); this was deemed as the “ON” state. The “OFF” state was determined to be ~10000 counts

per second as measured for the cDNA - Target DNA (PhpC) duplex. Integration of the emission curves was consistent with an approximate doubling in overall fluorescence between the “ON” and “OFF” states. Intermediate values were observed for the two alternate “ON” duplex states with the cPNA (^SU) - Target DNA (PhpC) measuring ~18000 counts per second and ~15000 for the cPNA (^ST) - Target DNA (PhpC).

Upon hybridization of dsPNA with dsDNA fluorescence intensity will increase over time showing the spontaneous dsDNA invasion with ds pcPNA taking place completely after ~45 min at 39.5 °C (**Figure 2.6a**). Using pcPNA and complementary DNA strands with PhpC insert, duplex denaturation was also examined by variable temperature fluorescence studies (**Figure 2.6b**). The results are comparable to those obtained by temperature-dependent UV-vis spectroscopy and showing fluorescence “OFF” and “ON” states upon hybridization to complementary oligomer and dissociation.



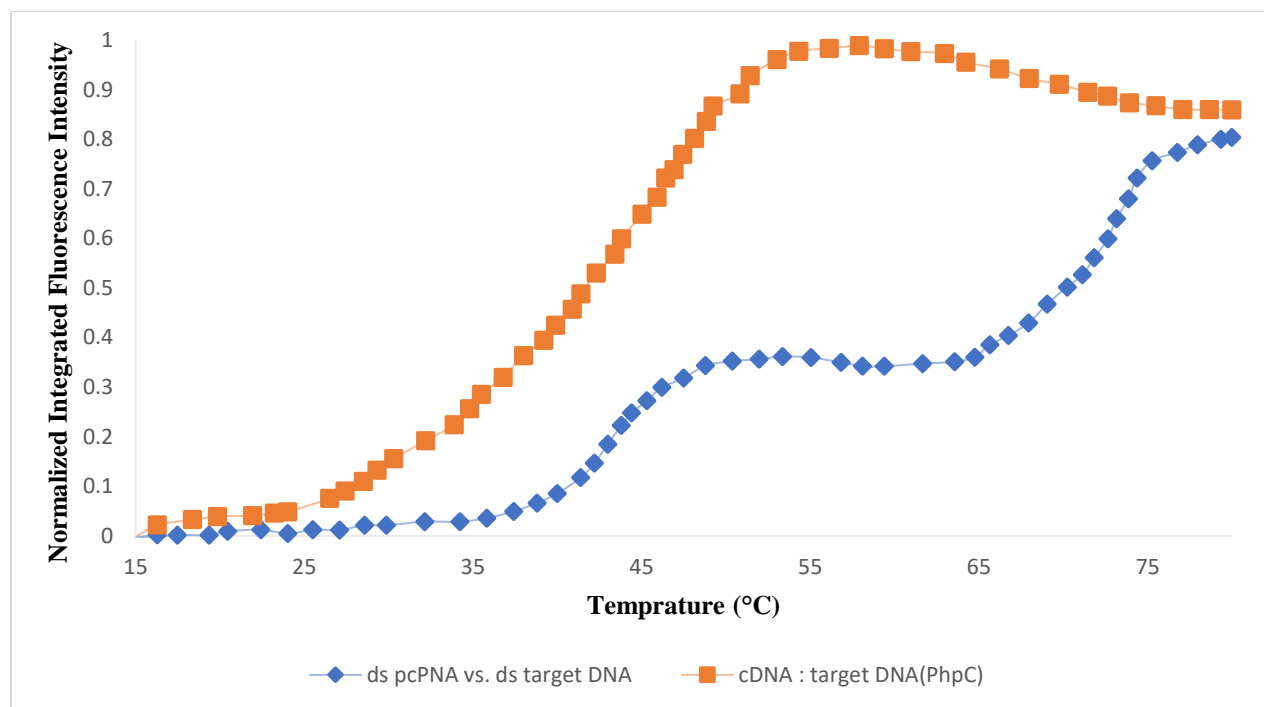


Figure 2.6. Time-dependent (a-top) and Temperature-dependent (b-bottom) fluorescence spectra for pseudo-complementary H-Lys-G^sUDGD^sUCDCT-Lys-NH₂ and H-Lys-DG^sUGD^sUC^sUDC-Lys-NH₂ PNA strands annealed with complementary 5' AGTGATCTACCT 3' and 5' AGTGATCTAC(PhpC)T 3' DNA strands. Strand concentration is 2 mM in a buffer containing NaCl (100 mM), EDTA (0.1 mM), and Na₂PO₄ (10 mM, pH 7.0). Fluorescence excitation at $\lambda=369$ nm and integrated emission spectra from 400 nm to 580 nm were measured in triplicate.

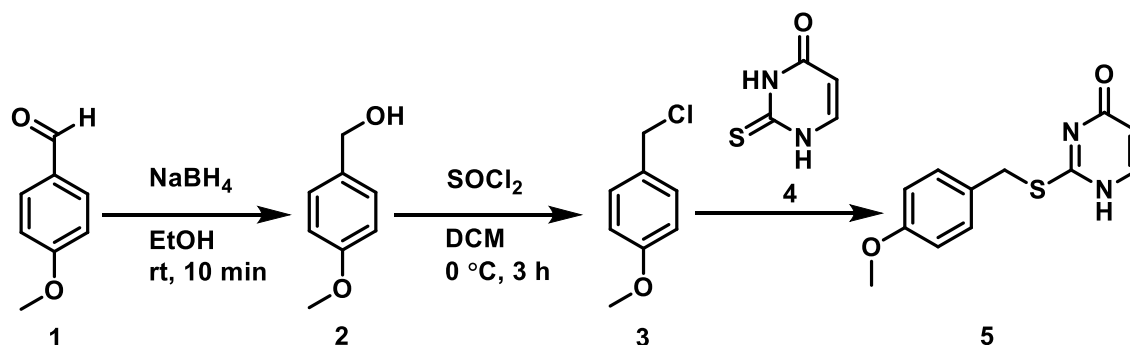
2.3 Conclusion

In summary, this study has shown that the 4-methoxybenzyl protection that has been used for Boc-based peptide synthesis containing thiouracil residues is also suitable for Fmoc-based oligomerization. Given that the 4-methoxybenzyl protecting group is removed rapidly under the same deprotection conditions as the *N*-Boc protecting group, the thiouracil protection most likely does not persist for Boc-based oligomer synthesis. This observation prompted us to examine the oligomerization of thiouracil PNA without nucleobase protection, which was successful. It is noteworthy that the solubility of the unprotected thiouracil PNA monomer is suitable for

oligomerization chemistry; thus, it appears that only role the protecting groups serves is to allow regioselective alkylation of *NI* during monomer synthesis. A method to achieve regioselective *NI* alkylation in the absence of 2-thiocarbonyl protection would be a significant benefit to monomer preparation. Although the 4-methoxybenzyl protecting group is suitable for Fmoc-based synthesis, milder cleavage conditions are achieved with Kittaka's 2-methyl-4-methoxybenzyl group. In comparison, the 2-methoxybenzyl protecting group was surprisingly robust and may find use in combination with highly acid labile resins (such as trityl-based) for the preparation of oligomers retaining the *S*-protecting group for further, post oligomerization chemistry. The origin of the resistance to acidolysis for the 2-methoxy group appears to be intramolecular stabilization of the protonated species and cannot be expected without this particular structural feature. Analysis of the results from melting curves suggests several general trends. Replacement of a C base with PhpC resulted in an increase in melting temperature; a stabilizing effect must be occurring. This could be due to PhpC engaging in greater π - π stacking interactions compared to unmodified cytidine. Secondly, as expected, a general increase in melting temperature was observed between DNA-PNA heteroduplexes. Even though the PNA sequences were two base pairs shorter than their DNA partner, the decrease in repulsion due to the neutrality of the PNA backbone resulted in increased T_m values. Finally, it appears that with regards to DNA-PNA bonding, ^ST in PNA has a slightly stronger bonding interaction with DNA than does a ^SU base. This was consistent across all cases when bonding to either the target DNA or target DNA (PhpC). Interestingly, when bonding to complementary PNA this phenomenon is reversed; PNA with ^SU has the higher T_m . In the sequence context examined, the ^ST insert resulted in a mild destabilization ($\Delta T_m = -1.0/\text{insert}$) relative to T, whereas ^SU had a slight stabilizing effect ($\Delta T_m = +0.3/\text{insert}$). This phenomenon requires further investigation but likely is a result of the different conformation of PNA-DNA versus PNA-PNA duplexes. The ^SU and D monomer incorporation into a PNA shows that and its melting temperature against PNA and DNA shows that the synthesis of PNA sequences containing additional pseudo-complementary bases can destabilize the PNA-PNA duplex while the DNA-PNA duplex is more stable. Fluorescence measurements were highly successful and were supportive of the original hypothesis. The target DNA (PhpC) baseline was initially compared to the target DNA (PhpC) paired to cDNA. The change between the "ON" and "OFF" states respectively was clearly evident as an overall change in fluorescence was approximately two-fold. Also, as expected, the fluorescence of the DNA-PNA hybrids in the "ON" state was intermediate

between the free Target DNA (PhpC) strand and its “OFF” partner. These results are encouraging because it is evident that a simple change in a binding partner can be used to induce a measurable change in fluorescence corresponding to its identity. Interestingly, using the cPNA strand with ^SU resulted in slightly higher fluorescence than its ^ST counterpart. This may be explained by the slightly weaker bonding interaction of the ^SU resulting in a more “open” duplex and thus less quenching of the PhpC base.

2.4 Experimental Procedures



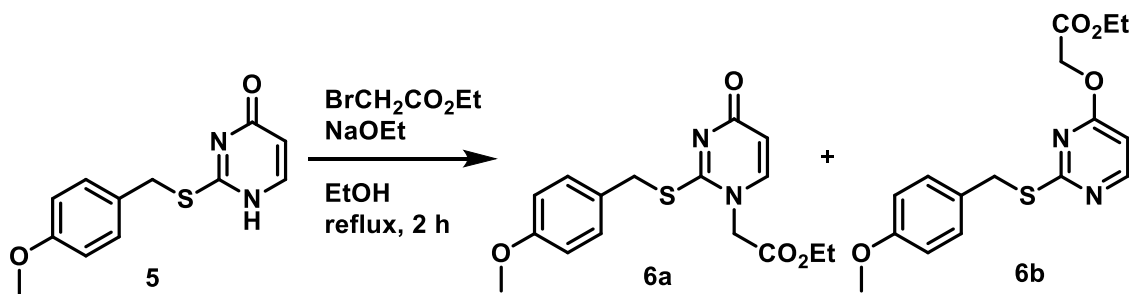
Synthesis of 2-((4-methoxybenzyl)thio)pyrimidin-4(1H)-one

4-methoxybenzyl alcohol (2)

To a solution of 4-methoxybenzaldehyde **1** (10 g, 95% purity, 73 mmol) in EtOH (40 mL) was added NaBH₄ (3.0 g, 80 mmol) portion-wise and the mixture was stirred at room temperature for 10 min. After the addition of H₂O (300 mL), the reaction mixture was acidified until pH=4 with 4 M HCl and extracted with Et₂O (80 mL ×3). The combined organic layers were washed with H₂O, brine, dried over anhydrous sodium sulfate, and the solvent evaporated *in vacuo* after filtration to give alcohol **2** (9.2 g, 66.6 mmol, 91%) as a clear colorless oil. ¹H NMR (400 MHz, CDCl₃) δ 7.27 (d, *J* = 8.4 Hz, 2H), 6.86 (d, *J* = 8.4 Hz, 2H), 4.58 (s, 2H), 3.77 (s, 3H), 1.61 (br s, 1H). This closely corresponded to the ¹H NMR spectrum previously reported in the literature.⁶

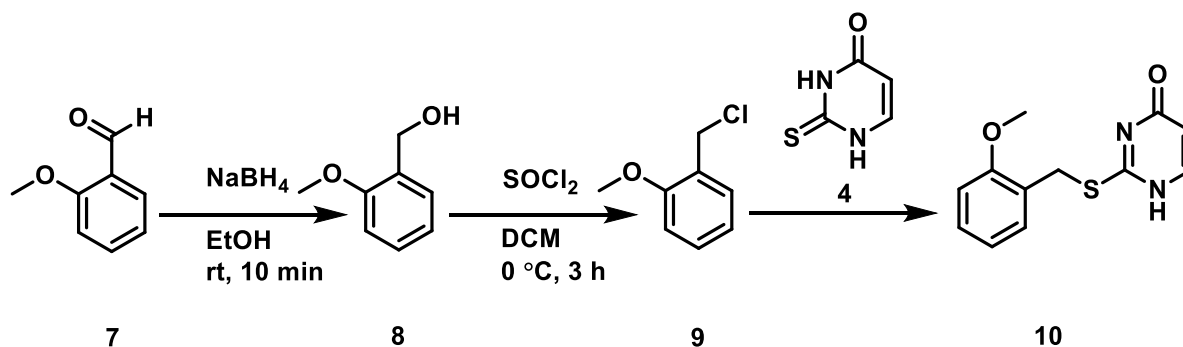
2-(4-methoxybenzyl)thiouracil (**5**)

To a solution of **2** (9.2 g, 66.6 mmol) in CH₂Cl₂ (200 mL) was added SOCl₂ (5.4 mL, 74.2 mmol) dropwise at 0 °C. After stirring at the same temperature for 20 min, the reaction mixture was poured into saturated aqueous NaHCO₃ (250 mL) with crushed ice. The resulting mixture was extracted with Et₂O (100 mL ×3). The combined organic layers were washed with H₂O, brine, dried over anhydrous sodium sulfate, and the solvent evaporated *in vacuo* after filtration. Crude chloride **3** (9.7 g, 8.46 mL, 62 mmol) was subjected to the next reaction without further purification. To a suspension of 2-thiouracil **4** (5 g, 39 mmol) in EtOH (50 mL) was added aqueous KOH solution (2.8 g KOH in 20 mL H₂O, 50.7 mmol) and the mixture was warmed to 45 °C to completely dissolve 2-thiouracil. After cooling to room temperature, crude chloride **3** (62 mmol) in EtOH (10 mL) was added to the solution and the reaction mixture was stirred at room temperature overnight. The mixture was evaporated to dryness and the crude product was suspended in saturated aqueous NaHCO₃ (50 mL). The resulting precipitate was collected by filtration and washed with H₂O, EtOH, EtOAc, and Et₂O to give **5** (8.4 g, 33.9 mmol, 87%) as a white solid. The ¹H NMR and ¹³C NMR spectra of the product is matched the literature spectra reported by Nielsen et. al.³¹ ¹H NMR (400 MHz, Chloroform-*d*) δ 7.89 (d, *J* = 6.6 Hz, 1H), 7.36 – 7.30 (m, 2H), 6.87 (d, *J* = 2.1 Hz, 2H), 6.23 (d, *J* = 6.6 Hz, 1H), 4.42 (s, 2H), 3.81 (s, 3H). ¹³C{¹H} NMR (101 MHz, DMSO-*d*₆) δ 176.6, 161.5, 159.0, 142.6, 130.7, 129.2, 114.4, 105.7, 55.5, 33.7.



Synthesis of *N*-1-(Ethoxycarbonylmethyl)-*S*-(4-methoxybenzyl)-2-thiouracil (**6a**)

Under the nitrogen atmosphere, sodium (620 mg, 27 mmol) was dissolved in refluxing absolute EtOH (40 ml) and was added to a suspension of **5** (6.4 g, 26 mmol) in EtOH (30 mL) and heated to reflux. To the reaction mixture was added ethyl bromoacetate (1.26 mL, 11.4 mmol) and reflux was continued for 2 h. Ethyl bromoacetate (4.7 g, 3.1 mL, 27 mmol) was added and reflux was continued for 3 h. The resulting mixture was cooled to room temperature and EtOH was removed under reduced pressure. Water (15 mL) was added, and the mixture was extracted with CH₂Cl₂/MeOH (3:1, 60mL) twice. The organic phase was evaporated to dryness, taken up in ethyl acetate/hexane, and again evaporated. The residue was triturated in cold ethyl acetate (10 ml), whereby the product precipitated. It was filtered off and washed with cold ethyl acetate to afford **6a** as a white solid. Yield: 2.7 g (2.7 g, 8 mmol, 30.7%). The ¹H NMR and ¹³C NMR spectra of the product is matched the literature spectra reported by Nielsen et. al.³¹ ¹H NMR (600 MHz, DMSO-*d*₆) δ 7.64 (d, *J* = 7.6 Hz, 1H), 7.31 (d, *J* = 8.7 Hz, 2H), 6.85 (d, *J* = 8.7 Hz, 2H), 5.91 (d, *J* = 7.5 Hz, 1H), 4.76 (s, 2H), 4.33 (s, 2H), 4.13 (q, *J* = 7.1 Hz, 2H), 3.70 (s, 3H), 1.15 (t, *J* = 7.1 Hz, 3H); ¹³C {¹H} NMR (101 MHz, DMSO-*d*₆) δ 167.5, 166.88, 162.8, 159.2, 146.1, 130.9, 128.4, 114.4, 109.1, 62.2, 55.5, 52.4, 40.6, 40.4, 40.2, 40.0, 39.7, 39.6, 39.4, 34.8, 14.4.

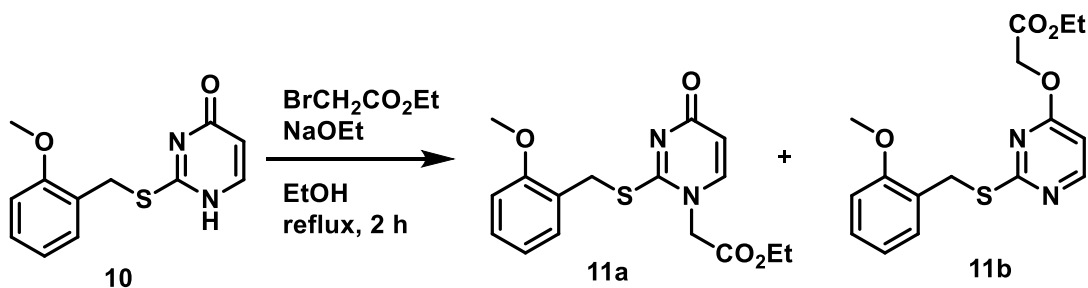


Synthesis of 2-((2-methoxybenzyl)thio)pyrimidin-4(1H)-one

2-(2-methoxybenzyl) thiouracil (10)

To a solution of 2-methoxybenzaldehyde **7** (5.0 g, 95% purity, 36.5 mmol) in EtOH (20 mL) was added NaBH₄ (1.5 g, 40 mmol) portion-wise and the mixture was stirred at room

temperature for 10 min. After the addition of H₂O (150 mL), the reaction mixture was acidified until pH=4 with 4 M HCl and extracted with Et₂O (40 mL × 3). The combined organic layers were washed with H₂O, brine, dried over anhydrous sodium sulfate, and the solvent evaporated *in vacuo* after filtration to give alcohol **8** (4 g, 28.9 mmol, 79%) as a clear yellow oil. Then, to a solution of **8** (4 g, 28.9 mmol) in CH₂Cl₂ (100 mL) was added SOCl₂ (5.4 mL, 32.0 mmol) dropwise at 0 °C. After stirring at the same temperature for 20 min, the reaction mixture was poured into saturated aqueous NaHCO₃ (150 mL) with crushed ice. The resulting mixture was extracted with Et₂O (100 mL × 3). The combined organic layers were washed with H₂O, brine, dried over anhydrous sodium sulfate, and the solvent evaporated *in vacuo* after filtration. Crude chloride **9** (4.7 g, 4.1 mL, 30 mmol) was subjected to the next reaction without further purification. To a suspension of 2-thiouracil **4** (2.4 g, 19 mmol) in EtOH (25 mL) was added aqueous KOH solution (1.4 g KOH in 10 mL H₂O, 25.3 mmol) and the mixture was warmed to 45 °C to completely dissolve 2-thiouracil. After cooling to room temperature, crude chloride **9** (30 mmol) in EtOH (5 mL) was added to the solution and the reaction mixture was stirred at room temperature overnight. The mixture was evaporated to dryness and the crude product was suspended in saturated aqueous NaHCO₃ (50 mL). The resulting precipitate was collected by filtration and washed with H₂O, EtOH, EtOAc, and Et₂O to give **10** (5.4 g, 21.9 mmol, 87%) as a white solid. ¹H NMR (400 MHz, DMSO-*d*₆) δ 7.90 (d, *J* = 6.5 Hz, 1H), 7.37 (dd, *J* = 7.4, 1.8 Hz, 1H), 7.28 (ddd, *J* = 8.2, 7.4, 1.8 Hz, 1H), 7.02 (dd, *J* = 8.3, 1.1 Hz, 1H), 6.89 (td, *J* = 7.4, 1.1 Hz, 1H), 6.09 (d, *J* = 6.5 Hz, 1H), 4.34 (s, 2H), 3.83 (s, 3H); ¹³C{¹H} NMR (101 MHz, DMSO-*d*₆) δ 174.6, 157.6, 130.8, 129.5, 124.9, 120.7, 111.4, 56.0, 29.3. HRMS (ESI/Q-TOF) *m/z*: [M+H]⁺ Calcd for C₁₂H₁₂N₂O₂S 248.0618; Found 248.0620.

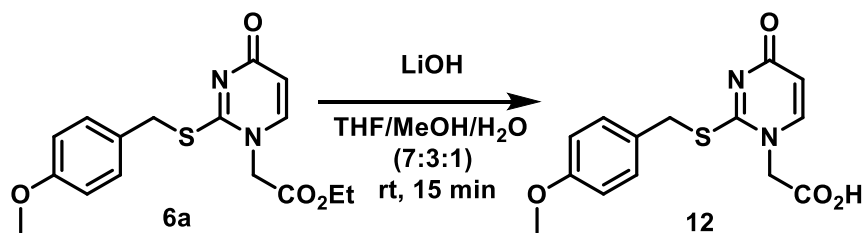


Synthesis of N-1-(Ethoxycarbonylmethyl)-S-(2-methoxybenzyl)-2-thiouracil (**11a**)

Under the nitrogen atmosphere, sodium (528 mg, 23 mmol) was added to refluxing absolute EtOH (40 ml) and was added to a suspension of **10** (5.4 g, 21.9 mmol) in EtOH (25 mL) and heated to reflux. To the reaction mixture was added ethyl bromoacetate (1.21 mL, 11.4 mmol) and reflux was continued for 2 h. Ethyl bromoacetate (4 g, 2.6 mL, 23 mmol) was added and reflux was continued for 4 h. The resulting mixture was cooled to room temperature and EtOH was removed under reduced pressure. Water (15 mL) was added, and the mixture was extracted with CH₂Cl₂ –MeOH (3:1, 60mL) twice. The combined organic layers were dried over anhydrous sodium sulfate and concentrated *in vacuo* after filtration. The residue was purified by column chromatography on silica gel (for **11b** hexane-EtOAc = 5:1 to 1:1; for **11a**, EtOAc to EtOAc-MeOH = 9:1) to afford **11a** (2.5 g, 7.4 mmol, 34.1%) as a white solid, **11b** (810 mg, 2.42 mmol, 11%) as an oil. ¹H NMR (599 MHz, Chloroform-*d*) δ 7.43 (d, *J* = 7.6 Hz, 1H), 7.26 – 7.19 (m, 1H), 7.11 (d, *J* = 7.6 Hz, 1H), 6.89 – 6.80 (m, 2H), 6.03 (dd, *J* = 7.5, 1.7 Hz, 1H), 4.51 (d, *J* = 1.7 Hz, 2H), 4.48 (d, *J* = 1.7 Hz, 2H), 4.20 (q, *J* = 7.1 Hz, 2H), 3.81 (s, 3H), 1.22 (t, *J* = 7.1 Hz, 3H); ¹³C {¹H} NMR (151 MHz, Chloroform-*d*) δ 167.8, 165.9, 163.6, 157.6, 143.81, 131.2, 129.3, 123.7, 120.6, 110.4, 109.9, 62.5, 55.4, 52.7, 31.3, 13.9. HRMS (ESI/Q-TOF) *m/z*: [M+H]⁺ Calcd for C₁₆H₁₈N₂O₄S 334.0987; Found 334.0990.

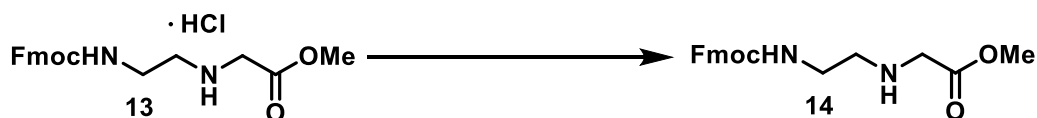
Acidolysis studies of thioesters

A solution of 0.02 mL trifluoroacetic acid, 0.02 mL triethylsilane and 0.96 mL deuterated chloroform were added to 3 mg of protected thiouracil (**6a**, **11a**) and the reaction was monitored by ¹H NMR at 2 min intervals until the reaction was completed (See **supporting information**). Integration of benzylic protons was monitored to determine the rate of deprotection. In order to confirm that acidolysis was complete ESI-MS data was collected. HRMS (ESI/Q-TOF) *m/z*: [M+H]⁺ Calcd for C₈H₁₀N₂O₃S [M+H]⁺ 214.0412 found 214.0404.



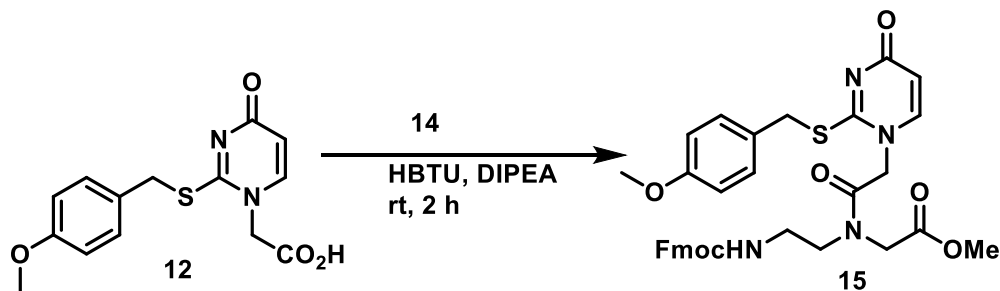
Synthesis of 2-(2-((4-methoxybenzyl)thio)-4-oxopyrimidin-1(4H)-yl)acetic acid (12)

To a solution of **6a** (1.7 mg, 5 mmol) in a mixture of methanol (10 mL) and tetrahydrofuran (20 mL) was added 2 M lithium hydroxide (4.3 mL, 8.7 mmol) at room temperature. After stirring at the same temperature for 30 min, the solvent was removed *in vacuo*. The residue was dissolved in 5 mL water and the solution was acidified with 2 M hydrochloric acid. The resulting precipitate was filtered and washed with cold ethyl acetate and diethyl ether and then dried under a high vacuum to give **12** (1.25g, 4.1 mmol, 82%) as a white solid. The ^1H NMR and ^{13}C NMR spectra of the product is matched the literature spectra reported by Nielsen et. al.³¹ ^1H NMR (400 MHz, DMSO- d_6) δ 7.51 (d, J = 7.5 Hz, 1H), 7.34 (d, J = 8.6 Hz, 2H), 6.87 (d, J = 8.7 Hz, 2H), 5.79 (d, J = 7.4 Hz, 1H), 4.29 (s, 2H), 4.04 (s, 2H), 3.73 (s, 3H); ^{13}C $\{^1\text{H}\}$ NMR (101 MHz, DMSO- d_6) δ 168.9, 168.0, 161.6, 159.1, 142.3, 130.9, 128.7, 117.5, 114.4, 55.6, 52.9, 40.6, 40.4, 40.2, 40.0, 39.8, 39.6, 39.4, 34.8.



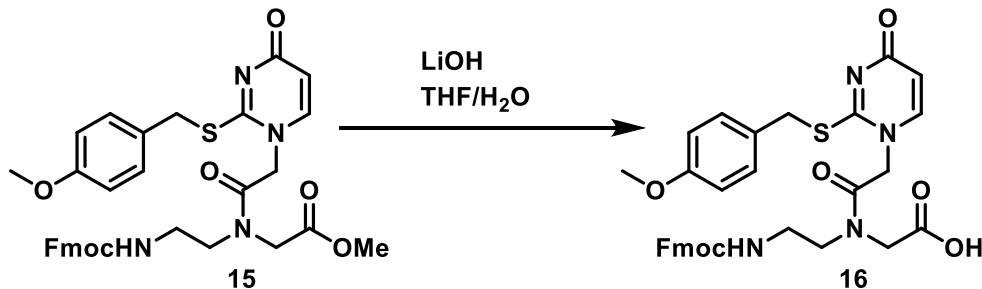
Synthesis of methyl (2-((((9H-fluoren-9-yl)methoxy)carbonyl)amino)ethyl)glycinate (14)

To liberate the free base of **13** the above HCl salt was dissolved in CHCl_3 , washed with saturated aqueous NaHCO_3 , dried (Na_2SO_4) and concentrated *in vacuo*, to give the free base of **14** as a colourless oil. ^1H NMR (400 MHz, DMSO- d_6) δ 9.07 (brs, 1H), 7.91 (d, J = 7.5 Hz, 2H), 7.69 (d, J = 7.5 Hz, 2H), 7.43 (t, J = 7.5 Hz, 2H), 7.35 (t, J = 7.4 Hz, 2H), 4.37 (d, J = 6.7 Hz, 2H), 4.24 (t, J = 6.7 Hz, 1H), 4.01 (s, 2H), 3.76 (s, 3H), 3.57 (s, 3H), 3.02 (t, J = 6.4 Hz, 2H). ^{13}C $\{^1\text{H}\}$ NMR (100 MHz, DMSO- d_6) δ 167.9, 156.7, 144.3, 141.2, 128.1, 127.7, 125.6, 120.6, 66.1, 55.4, 53.0, 47.3, 47.1, 47.1, 40.6, 40.4, 40.2, 40.0, 39.8, 39.6, 39.4, 37.3.



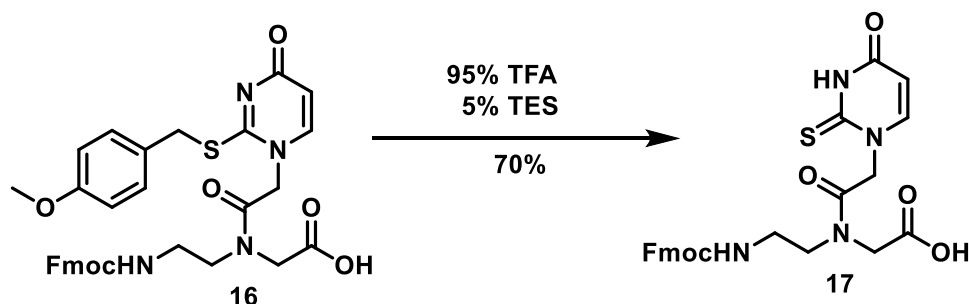
Synthesis of methyl N-(2-(((9H-fluoren-9-yl)methoxy)carbonyl)amino)ethyl)-N-(2-(2-((4-methoxybenzyl)thio)-4-oxopyrimidin-1(4H)-yl)acetyl)glycinate (**15**)

To a solution of **12** (700 mg, 2.28 mmol) in DMF (10 mL) were added HBTU (872 mg, 2.3 mmol) and DIPEA (674 mL, 3.96 mmol) at 0 °C. After stirring for 10 min, **14** (744.2 mg, 2.1 mmol) was added at the same temperature. The resulting mixture was allowed to warm to room temperature and stirred for 4 h. The reaction mixture was diluted with EtOAc, poured into water, and extracted with EtOAc three times. The combined organic layers were washed with 5% sat. citric acid/H₂O (20 mL), saturated aqueous NaHCO₃, brine, dried over anhydrous sodium sulfate, and concentrated *in vacuo* after filtration. The residue was purified by column chromatography on silica gel (CH₂Cl₂-MeOH = 30:1 to 19:1) to afford **15** (912 mg, 1.41 mmol, 69%) as an amorphous solid. ¹H NMR (400 MHz, CDCl₃) δ 7.83 – 7.33 (m, 5H), 7.22 – 6.98 (m, 1H), 6.94 – 6.73 (m, 2H), 6.14 – 6.00 (m, 1H), 5.72 (s, 1H), 5.32 (s, 2H), 4.82 – 4.22 (m, 6H), 4.26 – 4.00 (m, 3H), 3.86 – 3.31 (m, 7H); ¹³C{¹H} NMR (101 MHz, CDCl₃) δ 19.5, 29.7, 34.96, 35.04, 38.6, 38.8, 39.1, 47.1, 47.2, 47.8, 48.6, 48.9, 49.2, 50.3, 52.2, 55.07, 55.1, 55.8, 66.6, 66.7, 67.5, 68.0, 109.5, 111.2, 111.3, 116.2, 119.9, 120.0, 127.8, 128.3, 128.6, 128.6, 128.7, 128.8, 129.0, 131.8, 134.4, 134.8, 138.9, 141.3, 143.5, 143.8, 144.7, 156.6, 159.4, 163.5, 165.6, 168.3, 168.6, 169.2; HRMS (ESI/Q-TOF) m/z: [M+Na]⁺ Calcd for C₃₃H₃₂N₄O₇SNa 665.2046; Found 665.2050.



Synthesis of N-(2-((((9H-fluoren-9-yl)methoxy)carbonyl)amino)ethyl)-N-(2-(2-((4-methoxybenzyl)thio)-4-oxopyrimidin-1(4H)-yl)acetyl)glycine (**16**)

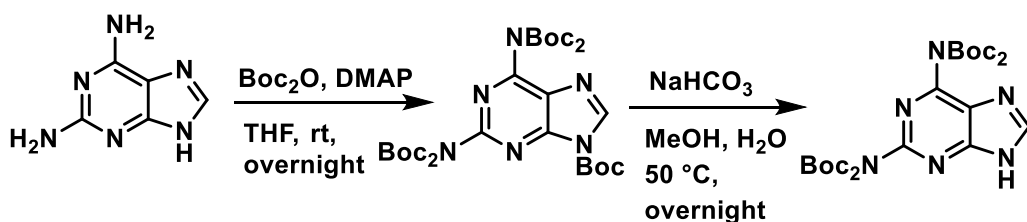
To a solution of **15** (570 mg, 0.87 mmol) in 15 mL tetrahydrofuran at 0 °C was added 10 mL 2M lithium hydroxide and solution was stirred for 30 min. The reaction was neutralized with 2 M hydrochloric acid then the solvent was evaporated under reduced pressure. The residue was suspended in 10 mL cold water with crushed ice and the solid was collected by filtration. The solid was suspended in cold dichloromethane and produce was collected by filtration, yielding the PNA monomer (**16**) as a pure white solid (220 mg, 0.34 mmol, 39%). The ¹H NMR and ¹³C NMR spectra of the product is matched the literature spectra reported by by Kittaka et al.⁴¹ ¹H NMR (600 MHz, Methanol-*d*₄) δ 7.78 (t, *J* = 6.9 Hz, 2H), 7.62 (d, *J* = 7.4 Hz, 1H), 7.59 – 7.54 (m, 1H), 7.37 (t, *J* = 7.4 Hz, 2H), 7.29 (t, *J* = 7.4 Hz, 2H), 7.22 (d, *J* = 8.2 Hz, 1H), 7.13 (d, *J* = 8.3 Hz, 1H), 6.71 (d, *J* = 8.2 Hz, 1H), 6.57 (d, *J* = 8.2 Hz, 1H), 4.48 – 4.05 (m, 5H), 3.94 (d, *J* = 12.9 Hz, 2H), 3.66 (s, 2H), 3.56 – 3.51 (m, 2H), 3.47 (qd, *J* = 9.1, 8.1, 3.8 Hz, 4H), 3.36 – 3.32 (m, 2H). ¹³C {¹H} NMR (100 MHz, DMSO-*d*₆) δ 170.1, 168.1, 166.8, 162.01, 159.0, 156.5, 144.4, 142.5, 141.1, 130.8, 129.4, 128.8, 128.0, 127.7, 127.6, 125.9, 121.9, 120.5, 117.1, 114.3, 66.0, 55.5, 53.5, 53.0, 48.4, 47.1, 40.6, 40.4, 40.2, 40.0, 39.8, 39.6, 39.4, 38.3, 34.9.; HRMS (ESI/Q-TOF) *m/z*: [M+Na]⁺ Calcd for C₃₃H₃₂N₄O₇SNa 651.1889; Found 651.1909.



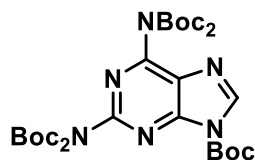
Synthesis of N-(2-((((9H-fluoren-9-yl)methoxy)carbonyl)amino)ethyl)-N-(2-(4-oxo-2-thioxo-3,4-dihydropyrimidin-1(2H)-yl)acetyl)glycine (**17**)

A solution of **16** (120 mg, 0.18 mmol) in 15 mL trifluoroacetic acid and 0.75 mL triethylsilane was prepared and it was stirred for 30 min. The solvent was then evaporated under a nitrogen stream and the resulting residue was washed twice with toluene to remove the protecting

group from the nucleobase, yielding the PNA monomer (**17**) as a pure white solid (70 mg, 0.38 mmol, 78%). ¹H NMR (400 MHz, DMSO-*d*₆) δ 8.1 (m, 1H), 7.89 (d, *J* = 7.4, 2H), 7.67 (m, 2H), 7.43-7.27 (m, 6H), 4.31 (s, 2H), 4.22 (s, 2H), 3.64 (s, 2H), 3.59 (s, 1H), 3.38 (m, 2H), 3.15 (m, 2H). ¹³C{¹H} NMR (400 MHz, DMSO) δ 170.2, 168.2, 166.8, 162.0, 156.5, 144.4, 142.5, 141.1, 130.8, 129.4, 128.8, 128.1, 127.8, 127.6, 125.9, 121.9, 120.5, 117.1, 66.0, 53.4, 53.1, 47.2, 38.4, 35.1. HRMS (ESI/Q-TOF) *m/z*: [M+Na]⁺ Calcd C₂₅H₂₄N₄O₆Na 531.1317; Found 531.1323.

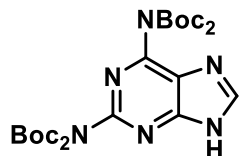


tert-butyl 2,6-bis(bis(tert-butoxycarbonyl)amino)-9H-purine-9-carboxylate (19**)**

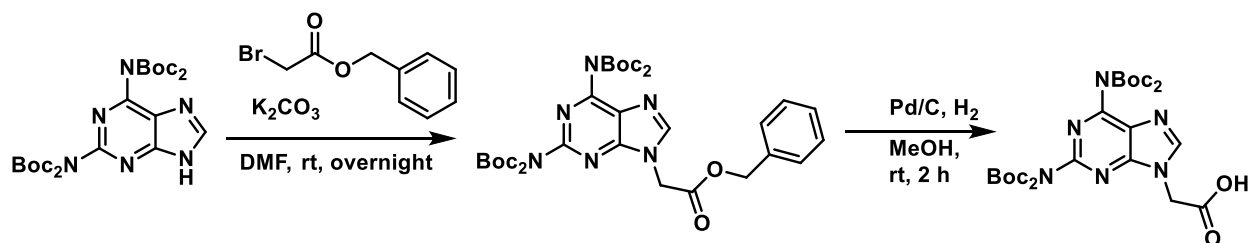


2,6-Diaminopurine (2 g, 13.32 mmol), Boc₂O (19 g, 80 mmol), and DMAP (0.2 g, 2 mmol) were added to THF (100 mL) at 0 °C. The solution was stirred for 10 min then warmed to room temperature. After 18 h the solvent was removed. The residue was dissolved in DCM (200 mL) and washed with H₂O (150 mL). The organic layer was dried over Na₂SO₄ and the solvent was removed. The residue was purified by column chromatography (EtOAc : Hexanes = 1 : 2) to yield **5** (8.02 g, 96%) as a white foam. Spectroscopic analysis conformed to previous reports⁴². ¹H NMR (400 MHz, Methylene Chloride-*d*₂) δ 8.60 (s, 1H), 1.73 (s, 9H), 1.48 (s, 18H), 1.45 (s, 18H). ¹³C{¹H} NMR (101 MHz, CD₂Cl₂) δ 153.7, 153.1, 151.6, 150.8, 149.7, 145.6, 144.3, 127.8, 87.3, 83.9, 83.3, 53.9, 53.7, 53.4, 53.1, 52.8, 27.5, 27.6, 27.4.

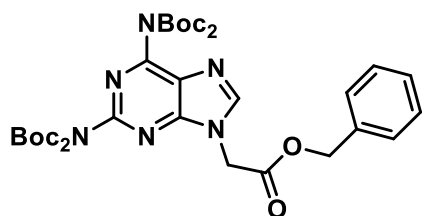
di-tert-butyl (9H-purine-2,6-diyl)bis((tert-butoxycarbonyl)carbamate) (20**)**



5 (7.9 g, 14.7 mmol) was suspended in a mixture of MeOH (50 mL) and saturated NaHCO₃ solution (25 mL). The turbid solution was heated to 50 °C for 1 h and then cooled to room temperature. After 18 h the MeOH was removed by rotary evaporation and the solution was diluted with H₂O (100 mL) and extracted with DCM (2 × 100 mL). The combined organic layers were dried over Na₂SO₄ and the solvent was removed to yield **6** (5.55 g, 10 mmol, 68% yield) as a white foam. Spectroscopic analysis conformed to previous reports⁴². ¹H NMR (400 MHz, Methylene Chloride-*d*₂) δ 8.55 (s, 1H), 1.47 (s, 18H), 1.46 (s, 19H). ¹³C NMR (101 MHz, CD₂Cl₂) δ 151.3, 151.0, 150.3, 144.3, 84.4, 83.3, 53.9, 53.6, 53.4, 53.1, 52.9, 27.6, 27.4.



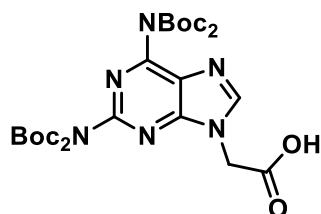
benzyl 2-(2,6-bis(bis(tert-butoxycarbonyl)amino)-9H-purin-9-yl)acetate (**21**)



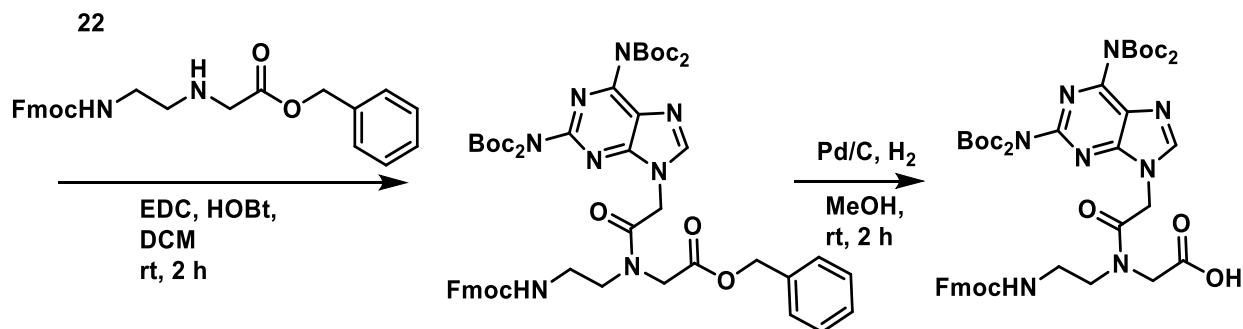
6 (5.35 g, 9.7 mmol) and K₂CO₃ (1.46 g, 10 mmol) were added to DMF (15 mL) at 0 °C. Benzyl bromoacetate (1.69 mL, 10 mmol) was added dropwise over 10 min. The solution was stirred for 15 min then warmed to room temperature. After 18 h the reaction mixture was diluted with H₂O (150 mL) and extracted with ether (2 × 100 mL). The organic layers were combined, washed with water (100 mL), dried over Na₂SO₄, and the solvent removed to yield **6** (6.5 g, 9.4 mmol 97% yield) as a white foam. Spectroscopic analysis conformed to previous reports⁴². ¹H NMR (400 MHz, Methylene Chloride-*d*₂) δ 8.23 (s, 1H), 7.41 (dd, *J* = 2.5, 0.9 Hz, 5H), 5.27 (s, 2H), 5.13 (s,

2H), 1.45 (s, 18H), 1.44 (s, 18H). $^{13}\text{C}\{^1\text{H}\}$ NMR (101 MHz, CD_2Cl_2) δ 166.7, 154.3, 152.3, 150.8, 150.1, 150.0, 145.9, 128.7, 128.4, 126.6, 83.7, 83.1, 67.9, 44.4, 27.5, 27.4.

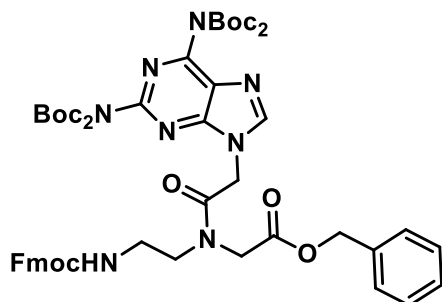
2-(2,6-bis(bis(tert-butoxycarbonyl)amino)-9H-purin-9-yl)acetic acid (22)



7 (5.65 g, 8.10 mmol) was dissolved in MeOH (10 mL). Pd/C (100 mg) was added and the reaction vessel was placed under an atmosphere of H_2 . The suspension was stirred for 2 h at room temperature. The suspension was filtered through Celite with MeOH (100 mL) and the solvent removed to yield **8** (4.9 g, 8.01 mmol, 99% yield) as a glassy grey solid. Spectroscopic analysis conformed to previous reports⁴². ^1H NMR (400 MHz, $\text{DMSO}-d_6$) δ 8.66 (s, 1H), 5.14 (s, 2H), 1.37 (s, 18H), 1.35 (s, 18H). $^{13}\text{C}\{^1\text{H}\}$ NMR (101 MHz, $\text{DMSO}-d_6$) δ 169.2, 154.6, 151.6, 150.7, 150.1, 148.9, 83.9, 83.4, 40.6, 40.4, 40.2, 39.9, 39.8, 39.5, 39.3, 27.7, 27.6.

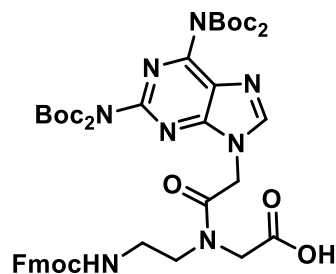


benzyl N-(2-(((9H-fluoren-9-yl)methoxy)carbonyl)amino)ethyl)-N-(2-(2,6-bis(bis(tert-butoxycarbonyl)amino)-9H-purin-9-yl)acetyl)glycinate (23)



Fmoc/Bn PNA backbone (1.03 g, 2.39 mmol), **8** (2.78 g, 4.50 mmol), EDC (0.95 g, 6.12 mmol) and HOBt (0.1 g, 0.67 mmol) were added to DCM (20 mL) at 0 °C. The solution stirred for 20 min then warmed to room temperature. The reaction was monitored by TLC. Upon completion, the reaction mixture was diluted with DCM (100 mL) and washed against a mixture of a saturated NaHCO₃ solution (50 mL) and brine (100 mL). The organic layer was dried over Na₂SO₄, and the solvent removed. The residue was subjected to FCC (EtOAc : hexane = 2 : 1 to 1 : 0) to yield **9** (1.72 g, 1.69 mmol 71% yield) as a white powder. Spectroscopic analysis conformed to previous reports⁴². ¹H NMR (400 MHz, DMSO-*d*₆) δ 7.93 – 7.85 (m, 2H), 7.65 (m, *J* = 16.5, 7.4, 4.5, 2.6 Hz, 2H), 7.44 – 7.24 (m, 9H), 5.42 – 5.11 (m, 3H), 4.36 – 4.16 (m, 3H), 3.72 (s, 1H), 3.62 – 3.57 (m, 1H), 2.39 – 2.09 (m, 2H), 1.43 – 1.33 (m, 36H). ¹³C{¹H} NMR (101 MHz, DMSO-*d*₆) δ 168.4, 167.8, 154.5, 151.6, 150.7, 150.1, 150.0, 148.7, 144.3, 141.2, 128.9, 128.8, 128.3, 128.3, 128.0, 127.5, 126.4, 125.6, 125.5, 120.5, 84.0, 83.4, 67.3, 65.8, 53.0, 47.1, 46.9, 44.9, 40.6, 40.4, 40.2, 40.0, 39.7, 39.5, 39.3, 32.7, 27.6, 27.5, 20.3.

N-(2-(((9H-fluoren-9-yl)methoxy)carbonyl)amino)ethyl)-N-(2-(2,6-bis(bis(tert-butoxycarbonyl)amino)-9H-purin-9-yl)acetyl)glycine (24**)**



9 (1.71 g, 1.67 mmol) was dissolved in MeOH (20 mL) and Pd/C (70 mg) was added. The reaction vessel was placed under an atmosphere of H₂. The suspension was stirred for 3 h at room temperature. The reaction was filtered through Celite with MeOH (100 mL) and the solvent removed to yield **10** (1.52 g, 1.61 mmol, 96% yield) as a flaky white solid. Spectroscopic analysis conformed to previous reports⁴². ¹H NMR (400 MHz, Methanol-*d*₄) δ 8.55 (s, 1H), 7.75 (dd, *J* = 16.7, 7.6 Hz, 2H), 7.64 (q, *J* = 7.3, 5.4 Hz, 2H), 7.47 – 7.21 (m, 4H), 5.36 (s, 1H), 5.22 (s, 1H), 4.87 (s, 2H), 4.60 – 4.09 (m, 3H), 3.77 (s, 1H), 3.67 – 3.44 (m, 2H), 3.31 (d, *J* = 6.6 Hz, 1H), 1.42

(d, $J = 6.6$ Hz, 36H). $^{13}\text{C}\{^1\text{H}\}$ NMR (101 MHz, Methanol- d_4) δ 171.1, 169.1, 167.7, 157.3, 154.5, 151.8, 150.8, 150.3, 150.0, 148.1, 143.8, 141.2, 128.3, 128.3, 127.5, 126.9, 124.9, 124.8, 119.7, 84.0, 83.5, 66.3, 52.1, 48.6, 48.4, 48.2, 48.0, 44.4, 44.1, 26.8, 26.7.

General procedure for acidolysis studies of thioesters. To a solution of 0.02 mL trifluoroacetic acid, 0.02 mL triethylsilane and 0.96 mL deuterated chloroform was added to 3 mg of protected thiouracil compound and the reaction was monitored by ^1H NMR at 2 min. intervals until the reaction was completed. The reaction was carried out at 25 °C and monitored for 2 h, or until reaction had gone to completion. Integration of benzylic protons was monitored to determine the rate of deprotection.

Oligomer synthesis. PNA oligomers were synthesized using the ABI 433A peptide synthesizer using manufacturer supplied “Fastmoc” cycles. Oligomerization was carried out using newly synthesized ^3U or ^3T monomers and commercially available Fmoc-A(Bhoc)-AEG-OH, Fmoc-G(Bhoc)-AEG-OH, and Fmoc-C(Bhoc)-AEG-OH, Fmoc-T(Bhoc)-AEG-OH (purchased from PolyOrg, Inc.), and $N\alpha$ -Fmoc- $N\epsilon$ -Boc-L-lysine (Chem-Impex International Inc.). FmocRAM-PS was used as a solid support resin preloaded with L-lysine at 0.057 mmol/g. The synthesis was carried out on a 5.0 μmol scale. The synthesis cycle was only modified by using 20% 4-methylpiperidine in dimethylformamide for Fmoc deprotection.²⁹ Following automated synthesis, the resin was treated with a solution of 95% trifluoroacetic acid and 5% triethylsilane to cleave the oligomer from the resin and remove the protecting group from the nucleobases (Bhoc) and amino group (Boc). The solvent was then evaporated under a nitrogen stream, the resulting residue was washed twice with cold ether, dissolved in a solution of 0.05% trifluoroacetic acid in water then purified by reverse-phase HPLC. Reverse-phase HPLC was performed on an Agilent MicrosorbMV 100-5 C18 250 \times 4.6 mm column heated to 50 °C. The purified PNA oligomer was eluted using a gradient (water/0.1% trifluoroacetic acid to acetonitrile/0.1% trifluoroacetic acid) over 60 min.

Thermal stability analysis. Thermal stabilities (T_m) of complexes were measured in solutions of 100 mM NaCl, 10 mM sodium hydrogen phosphate, 0.1 mM EDTA, pH=7.0 with individual PNA strand concentrations of 2 μ M. Absorbance at $\lambda = 260$ nm was measured at 0.5 $^{\circ}$ C intervals while the temperature was changed at a rate of 0.7 $^{\circ}$ C/min between 15-90 $^{\circ}$ C. T_m values were measured in triplicate and determined by the first derivative method applied through the manufacturer supplied Varian WinUV Bio software.

Computations. Structures were constructed and minimized in Spartan '14 using a desktop computer at the Hartree Fock 6-31G* level. A computational search for low energy conformers was performed using the same basis set. A variety of trials were run wherein the initial dihedral angle of C2-S-CH₂-Ph bond was set to avoid starting with the 2-methoxy group interacting with the protonated N3. The model nucleobase protected with 3-methoxybenzyl- or 4 methoxybenzyl protecting groups were similarly modeled and subjected to equilibrium conformer search for comparison.

References

- (1) Hyrup, B.; Nielsen, P. E. Peptide Nucleic Acids (PNA): Synthesis, Properties and Potential Applications. *Bioorganic Med. Chem.* **1996**, *4* (1), 5–23.
- (2) Lohse, J.; Dahl, O.; Nielsen, P. E. Double Duplex Invasion by Peptide Nucleic Acid: A General Principle for Sequence-Specific Targeting of Double-Stranded DNA. *Proc. Natl. Acad. Sci.* **1999**, *96*, 11804–11808.
- (3) Hepler, L. G. Effects of Substituents on Acidities of Organic Acids in Water: Thermodynamic Theory of the Hammett Equation. *J. Am. Chem. Soc.* **1963**, *85* (20), 3089–3092.
- (4) Bialy, L.; Díaz-Mochón, J. J.; Specker, E.; Keinicke, L.; Bradley, M. Dde-Protected PNA Monomers, Orthogonal to Fmoc, for the Synthesis of PNA-Peptide Conjugates. *Tetrahedron*, **2005**, *61* (34), 8295–8305.
- (5) Giorgio, C. Di; Palrot, S.; Schwergold, C.; Patino, N.; Condom, R.; Giorgio, A. F.; Guedj, R. O. *Tetrahedron* **1999**, *55*, 1937–1958.
- (6) Zinieris, N.; Leondiadis, L.; Ferderigos, N. N^{??}-Fmoc Removal from Resin-Bound Amino Acids by 5% Piperidine Solution. *J. Comb. Chem.* **2005**, *7* (1), 4–6.
- (7) Hachmann, J.; Lebl, M. Alternative to Piperidine in Fmoc Solid-Phase Synthesis. *J. Comb. Chem.* **2006**, *8* (2), 149.
- (8) St. Amant, A. H.; Hudson, R. H. E. Synthesis and Oligomerization of Fmoc/Boc-Protected PNA Monomers of 2,6-Diaminopurine, 2-Aminopurine and Thymine. *Org. Biomol. Chem.* **2012**, *10* (4), 876–881.
- (9) Rouhi, Atefeh, "Synthesis and Photophysical Studies of Pyrrolocytosine Derivatives" (**2017**). *Electronic Thesis and Dissertation Repository*. 5020.
- (10) Jansen, K.; Richelson, E. Detection of Peptide Nucleic Acids in Tissue Extracts of Treated Animals by Gel Mobility Shift Assay. *J. Biochem. Biophys. Methods* **2000**, *42* (1–2), 31–34.
- (11) Hudson, R. H. E.; Ghorbani-Choghamarani, A. Selective Fluorometric Detection of Guanosine-Containing Sequences by 6-Phenylpyrrolocytidine in DNA. *Synlett* **2007**, *2007* (06), 870–873.
- (12) Sugiyama, T.; Hasegawa, G.; Niikura, C.; Kuwata, K.; Imamura, Y.; Demizu, Y.; Kurihara, M.; Kittaka, A. PNA Monomers Fully Compatible with Standard Fmoc-Based Solid-Phase Synthesis of Pseudocomplementary PNA. *Bioorganic Med. Chem. Lett.* **2017**, *27* (15), 3337–3341.

Chapter 3

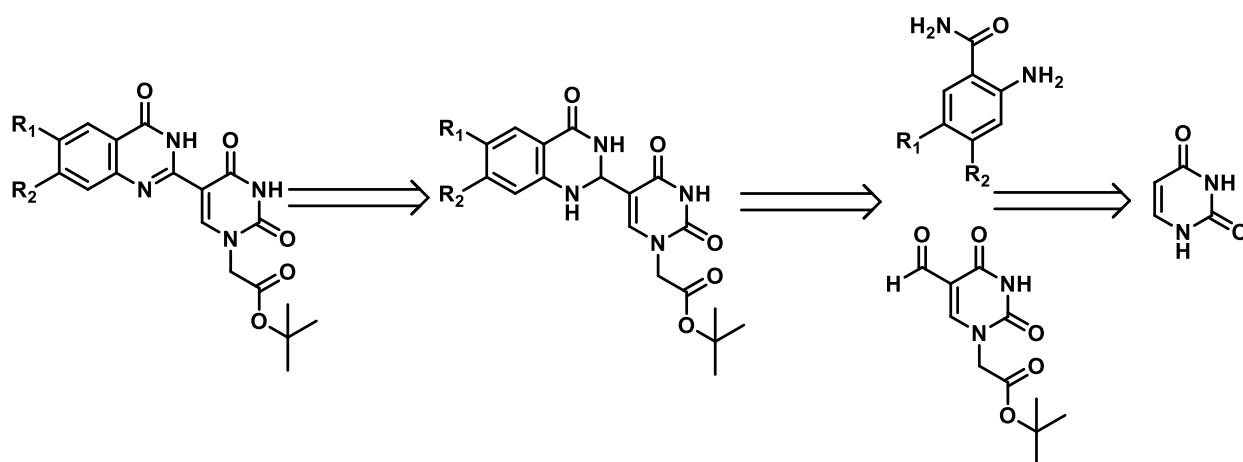
Modified fluorescent dihydroquinazolinone/ quinazolinone heterocyclic frameworks based on uracil scaffold

3.1 Introduction

Fluorescent nucleobase analogues are chemically modified nucleobases which are able to maintain their chemical and biological functional properties. This includes base stacking and base pairing. As a result of their usefulness, these molecules have become an incredibly important tool within chemistry and biology as they inform the molecular-level comprehension of nucleic acid structures as well as their locations and interactions.¹ In 1969, Stryer reported a class of emissive compounds including formycin and 2-aminopurine (2AP)². This study showed that fluorescent analogues can indeed facilitate studies of nucleic acids conformation and interactions. The study has led to further work and the creation of a variety of fluorescent nucleobases. As natural nucleobases are generally non-fluorescent, significant modifications to their structure is essential before they can be useful as an emissive tools. These types of chemical modifications can either be made with an eye to preserving Watson–Crick base-pairing ability (that is, retaining ‘canonical’ pairing), or more dramatic changes to the nucleobase architecture can be made, resulting in non-canonical designs.¹

The basic requirements that are imposed upon new the nucleobase fluorophore analogue synthesis includes the following: (a) to maintain the structural similarity to the canonical nucleobases; (b) to display emission at long wavelengths; (c) to retain sufficient emission quantum efficiency to be utilized in real time fluorescence-based assays; and, importantly, (d) to show the sensitivity to different environments that is manifested in markedly different photophysical parameters in different environment. Thus, fluorescent nucleobase analogues that respond to changes in their microenvironment are valuable for studying nucleic acid structure, dynamics, and recognition.¹ Here we describe the synthesis of a quinazolinone-based uracil scaffold (**Scheme**

3.1) as well as their basic photophysical characteristics. We demonstrate that the molecular rigidity plays a key role in the fluorescent property of quinazolinone-based uracil scaffold as a fluorescent PNA probe by generating higher quantum yields in lower temperatures or a more viscous solvent. Furthermore, we studied the effect of electron-donating and electron-withdrawing groups on the fluorescent response of the quinazolinone-based uracil scaffold compounds. An advantage of this molecular system is the ease of synthesis from readily available and inexpensive starting materials (**Scheme 3.1**).



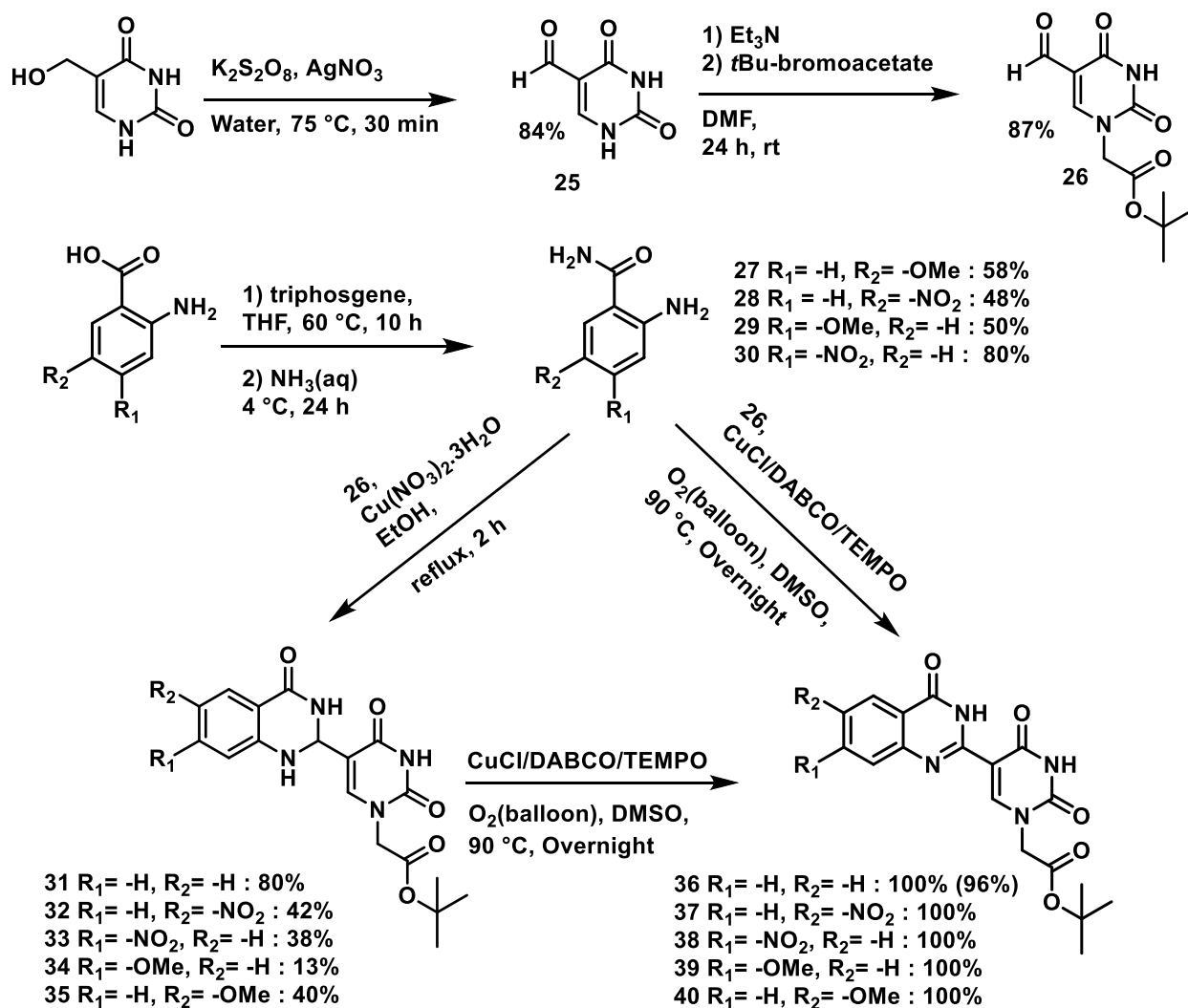
Scheme 3.1 Retro-synthesis of quinazolinone uracil-based scaffolds

3.2 Synthesis of quinazolinone-based uracil scaffold as a PNA monomer

The synthesis of the quinazolinone-based PNA monomer is illustrated in **Scheme 3.2** starting with the synthesis of 5-formyluracil (**25**) from 5-hydroxymethyl uracil according to the standard chemistry tested in Hudson's group. In the next step, 5-formyluracil (**25**) was condensed with ethyl bromoacetate in basic DMF to do the *N1* alkylation.

In order to test the effect of electron-withdrawing and electron-donating groups on the fluorescent properties of quinazolinone and dihydroquinazolinone compounds, methoxy and nitro 2-amino benzamide compounds were synthesized from 2-amino benzoic acid compounds by following the

reported patent⁴³. In order to increase the yield of these reactions, triphosgene was used (instead of phosgene) and isatoic anhydride intermediate compound collected at room temperature and then amination with liquid ammonia was done and reactions kept in lower temperatures. In the next step, 5-formyluracil was condensed with different 2-aminobenzamide compounds using copper (II) nitrate as a catalyst to give substituted dihydroquinazolinone compounds.



Scheme 3.2. Synthesis of modified quinazolinone based uracil scaffold tert-butyl- acetate

3.3 Approaches for the synthesis of quinazolinones

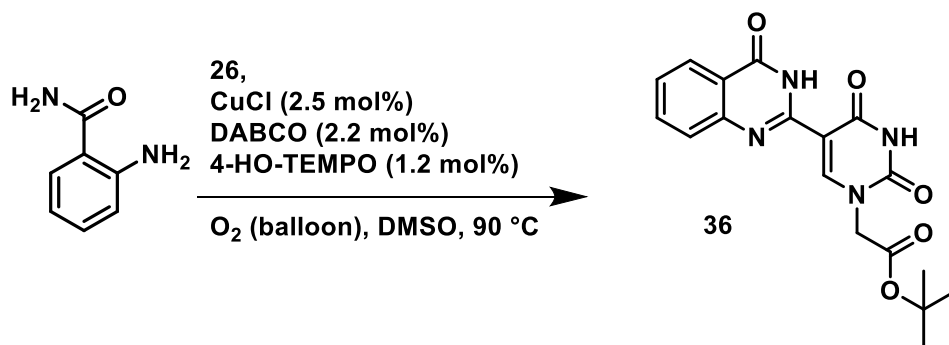
Substituted quinazolinones have been synthesized by a number of methods involving several substrates such as 2-aminobenzaldehyde and 2-aminobenzoketones or 2-amino-N arylbenzamidines or 2-halophenylmethanamines⁴⁴. The condensation of 2-aminobenzylamines with aldehydes using copper (II) nitrate in refluxed ethanol followed by subsequent oxidation with strong oxidants such as 2,3-dichloro-5,6-dicyano-1,4-benzoquinone (DDQ), MnO₂ and NaClO provides a conventional but simple method to synthesize quinazolinones⁴⁵. However, despite the synthetic usefulness of this approach, the reported oxidizing conditions suffer from the drawbacks that a stoichiometric amount of nonrenewable oxidant has to be used and the yields are not satisfactory. Therefore, more efficient and environmentally friendly catalytic systems are needed to render this method to be synthetically more attractive.

So, we tested different facile and efficient approach for the aerobic oxidative synthesis of substituted dihydroquinazolinones and by using a one-pot reaction of aldehydes with 2-aminobenzylamines and CuCl/DABCO/4-HO-TEMPO as the catalysts under mild conditions (**Scheme 3.3**). The copper/N-ligand/TEMPO catalytic system has been proven to be a powerful promoter for the aerobic oxidation of primary alcohols^{46,47}, but its applications in the oxidative dehydrogenation synthesis of nucleobase scaffold heterocycles of have not been reported yet. This work provides the first example toward this goal.

The study was initiated by conducting the reaction of anthranilamide (1 equiv) with N1-alkylated-5-formyluracil **26** (1 equiv). First, the two starting materials were allowed to condense in situ; then 4-HO-TEMPO **4** (0.2 equiv) was added as the catalyst and the reaction system was charged with an oxygen balloon. As expected, the target molecule **36** was obtained, but the yield was poor due to the oxidative decomposition of dihydroquinazolinone intermediate (**Table 3.1, entry 1**).

To improve the yield, copper salts were employed together with TEMPO to catalyze the reaction. The catalytic systems based on copper and TEMPO has proved to be very effective for the aerobic oxidation of alcohols⁴⁵. We hoped that these systems might work equally well to affect the dehydrogenation of dihydroquinazolinone compounds. To our delight, the reaction did improve

when CuCl was used, and the yield of **36** was raised up to 43% (**Table 2.1, entry 3**). The yield of the reaction was further improved by the addition of monodentate N-containing ligands such as Et₃N, DABCO (1,4-diazabicyclo[2.2.2]octane), and DMAP (*N,N*-dimethylpyridin-4-amine) (**Table 3.1., entries 4-8**)



Scheme 3.3. CuCl/DABCO/TEMPO-catalyzed one-pot aerobic oxidative synthesis of modified quinazolinones

entry	copper	ligand	TEMPO	solvent	yield (%)
1			4-HO	toluene	32
2	CuBr		4-HO	DMF	22
3	CuCl		4-HO	DMF	43
4	CuCl	Et ₃ N	4-HO	CH ₃ CN	62
5	CuCl	Et ₃ N	4-HO	CH ₃ CN	80
6	CuCl	DMAP	4-HO	DMSO	86
7	CuCl	DABCO	4-HO	DMSO	12 ^b
8	CuCl	DABCO	4-HO	DMSO	96

Table 3.1. Optimization on the Catalytic Aerobic Oxidative Synthesis of Quinazolinone^a

^aAnthranilamide (1 mmol) and alkylated formyluracil (1 mmol) were dissolved in solvent (8 mL) in a 25 mL flask, and the mixture was stirred at 80 °C until the condensation completed (about 2 h). Then copper

salts (0.025 mmol), DABCO (0.022 mmol), and TEMPO (0.012 mmol) were added to the reaction mixture and stirring was continued at 80 °C under oxygen until anthranilamide was consumed completely as monitored by TLC.

^bUnder nitrogen.

3.4 Photophysical properties

UV-Vis spectra and fluorescence studies of **31 to 40** have been investigated in order to calculate the molar absorbance coefficient (ϵ) and quantum yield (Φ) under different solvents (**Table 3.2**). The values indicate that generally, the quantum yield in ethanol is greater than the other solvents for dihydroquinazolinone compounds.

Compound #	$\Phi_{\text{(EtOH)}}$	$\Phi_{\text{(DMSO)}}$	$\Phi_{\text{(THF)}}$	$\lambda_{\text{max}} \text{ (nm)}$	$\epsilon \left(\frac{\text{L}}{\text{mol.cm}} \right)^{\text{c}}$
31	0.015	0.002	0.001	341	$\epsilon_{341} = 67970$
32^b	0.008	0.003	0.001	417	$\epsilon_{417} = 65500$
33^b	0.007	0.001	0.001	417	$\epsilon_{417} = 65430$
34	0.014	0.003	0.003	321	$\epsilon_{325} = 39220$
35	0.019	0.004	0.003	321	$\epsilon_{325} = 39120$

Table 3.2. Photophysical properties ^a of dihydroquinazolinone compounds 31-35

^a The quantum yields were determined using emission wavelengths range between 340 and 640 nm with an excitation wavelength of 325 nm.

^b Excitation wavelength at 310 nm.

^c Calculated based on absorption in DMSO.

Molecular structure plays a major role in determining fluorescence parameters of aromatic molecules. Nonplanar molecules usually have structureless absorption and fluorescence spectra while planar and rigid molecules of the high-symmetry group show absorption and fluorescence spectra with well-resolved vibrational bands⁴⁸. Prior to 1970, it was believed that the ability of some molecules to emit fluorescence radiation was totally attributable to molecular rigidity. Berlman⁴⁹, however, showed later that rigidity in the S_0 state was not as important a factor as rigidity in the first excited S_1 excited state, that is, in maintaining a planar or near planar configuration. Currently, there is no doubt that the planarity and rigidity of a molecule play important roles in determining the fluorescence parameters of a compound. Thus, the dehydrogenation of dihydroquinazolinone compounds **31-35** (**Scheme 3.1.**) was done to add a π bond and make the molecule more rigid around the linker bond on the 5-position of uracil. This will fix the uracil and quinazolinone moiety in the same plane (**Figure 3.1. a and b**) and eventually increase the fluorescence quantum yield. Also, it may be further rigidified by an intramolecular hydrogen bond between the oxygen in the carbonyl group at 4-position of uracil and amide in heterocycle ring. (**Figure 3.1**) Moreover, in order to show the effect of molecular rigidity on fluorescent properties, the quantum yield calculation was done in three different temperatures and glycerol as a more viscous solvent. (**Table 3.3.**).

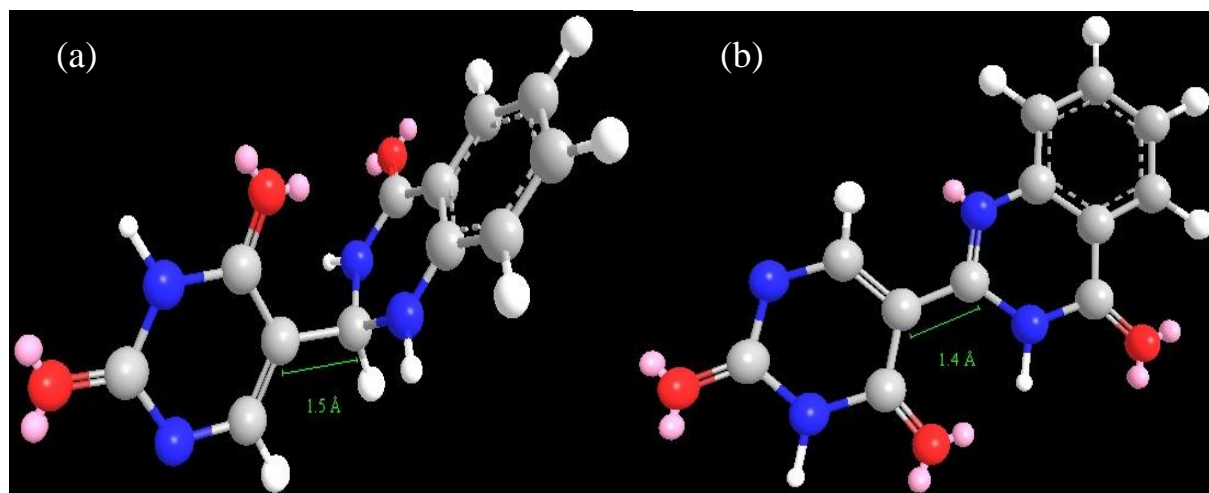
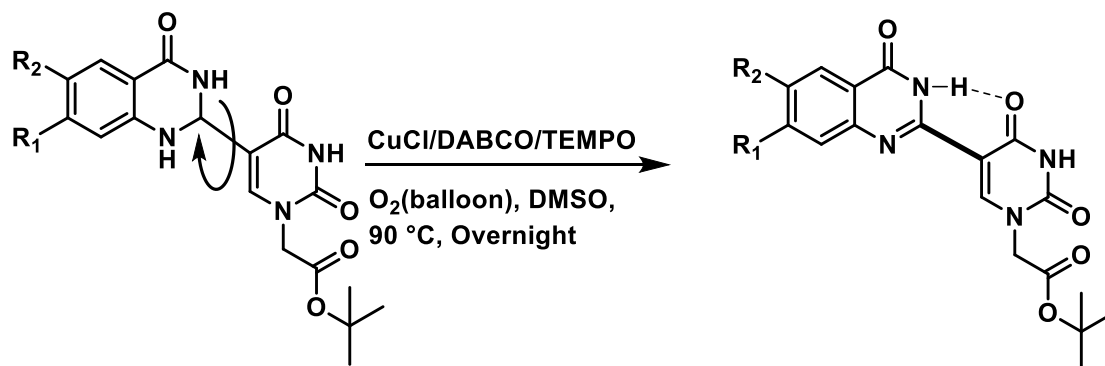


Figure 3.1. 3D Molecular structure at minimum energy state^a of modified dihydroquinazolinone (a) and quinazolinone (b) compounds.

^a Using energy minimization in MM2 calculation by Chem3D software.

Compound #	Φ (EtOH)	Φ (DMSO)	Φ (THF)	Φ (Glycerol)	λ_{\max} (nm)	ϵ ($\frac{L}{mol.cm}$) ^c	T (°C)
36	0.012	0.006	0.008	0.083	331	$\epsilon_{331} = 36391$	23
	0.006	0.002		0.031			60
	0.038						15
37^b		0.003	0.004	0.024	417	$\epsilon_{417} = 65499$	23
	NA [*]	0.001					60
							15
38^b		0.001	0.003	0.018	417	$\epsilon_{417} = 65532$	23
	NA [*]	<0.001					60
							15
39	0.023	0.009	0.016	0.076	340	$\epsilon_{340} = 39120$	23
	0.006	0.007		0.059			60
	0.041						15
40	0.035	0.011	0.019	0.106	340	$\epsilon_{340} = 39042$	23
	0.017	0.008		0.062			60
	0.076						15

Table 3.3. Photophysical properties a of quinazolinone compounds 36-40.

^{*} Compound was not soluble in ethanol

^a The quantum yields were determined using emission wavelengths range between 340 and 640 nm with an excitation wavelength of 330 nm.

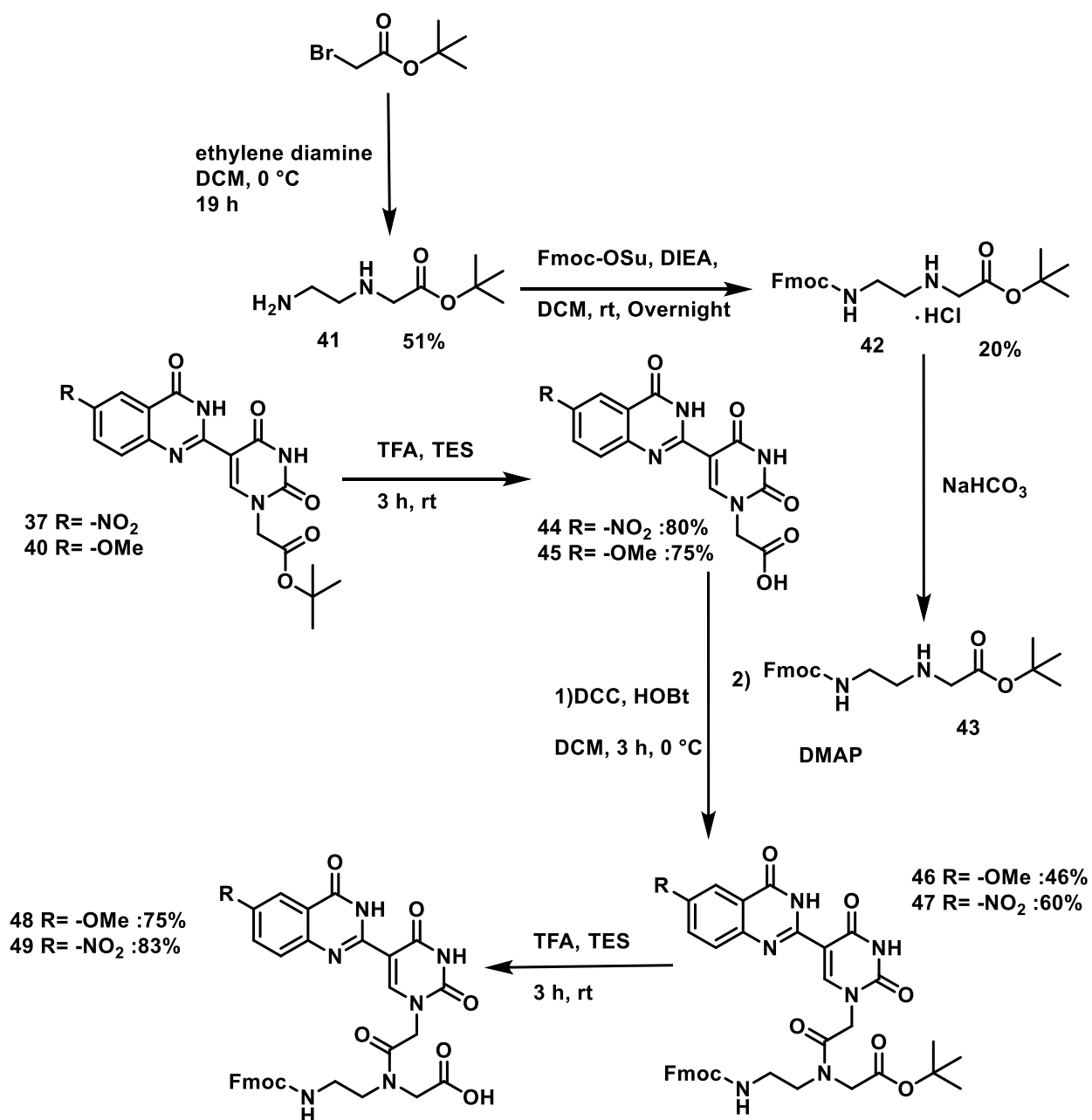
^b Excitation wavelength at 310 nm.

^c Calculated based on absorption in DMSO

Based on the values from (Table 3.3.) quinazolinone compounds (36-40) show greater quantum yields than dihydroquinazolinones 31-35, however, the solubility of these compounds is weaker and in some cases insoluble in organic solvents. Also, it shows that by using a more viscous

solvent (glycerol) or in lower temperature the quantum yield will be stronger by making the fluorescence molecule more rigid, which explains the aforementioned rotation around nucleobase linker (**Figure 3.1.**).

These quinazolinone based uracil scaffolds can bind to DNA and RNA through base pairs and making the DNA duplex more stable as a fluorescent molecule. In order to study the effect of electron-donating and electron-withdrawing groups on the fluorescent properties in oligomer level as well as stabilization effect upon hybridization to complementary DNA oligomers, compound **37** and **40** were chosen to make PNA monomers and oligomerization. (**Scheme 3.4**).



Scheme 3.4. Synthesis of quinazolinone based uracil scaffold PNA monomer

The tert-butyl-Fmoc-based aminoethylglycine backbone was synthesized as a hydrochloride salt in by using ethyl diamine followed by adding Fmoc-OSu and DIEA and stored in the freezer as a hydrochloride salt. The hydrochloride salt backbone was extracted in dichloromethane to yield **43** as a clear and colourless oil.

The tert-butyl alkylacetate of the quinazolinone based uracil scaffolds was hydrolyzed using trifluoroacetic acid, to obtain the carboxylic acid functional group for attachment to the aminoethylglycine backbone. The quinazolinone based nucleobase was then reacted with a solution of hydroxybenzotriazole (HOBt), dicyclohexylcarbodiimide (DCC) which act as the coupling agents, and 4-dimethylaminopyridine (DMAP) which acts as the base. The activated nucleobase is then reacted with the protected aminoethylglycine (**43**) backbone to form the PNA monomer. The tert-butyl ester protecting the C-terminus of the PNA monomer is then hydrolyzed using trifluoroacetic acid solution to form the C- terminus carboxylic acid.

After C-terminus ester hydrolysis, which gives desired PNA monomer, the oligomerization can be done. The monomers were characterized using ^1H NMR and ^{13}C NMR spectroscopy as well as high-resolution mass spectrometry (HRMS). ^1H NMR spectra show several rotamer structures (see supplemental data).

3.5 Conclusion

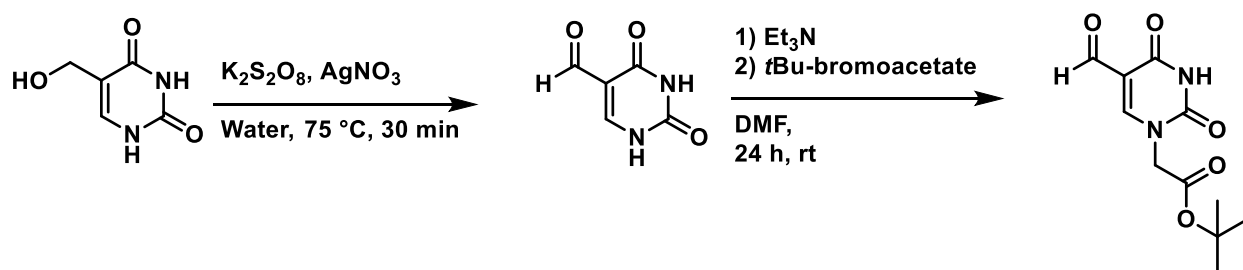
We synthesized PNA monomers carrying quinazolinone moiety and characterized them by their fluorescence quantum yield response in different solvents and three different temperatures which shows promising result that may be used as a reporter in PNA probes with expected stabilization of the formed duplex structure. It was found that emission of quinazolinone based uracil analogues is sensitive to the rigidity of the molecule which indicates that PNA probe containing quinazolinone moiety may be a good candidate for reporting binding events by showing “ON-OFF” fluorescence upon hybridization to complementary oligomers.

3.6 Future work

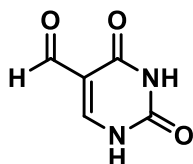
Incorporation of quinazolinone-based PNA monomer into PNA oligomer is underway. PNA sequences H-GTAGA**X**CACT-Lys-NH₂ (X= **48** or **49**) have been synthesized and their

thermal melting point and fluorescent response upon hybridization with complementary DNA sequences will be studied. The ability of these PNA oligomers to be used as a reporter probe will be evaluated.

3.6 Experimental Procedure

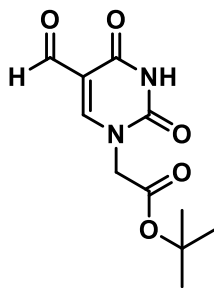


5-formyluracil (25)

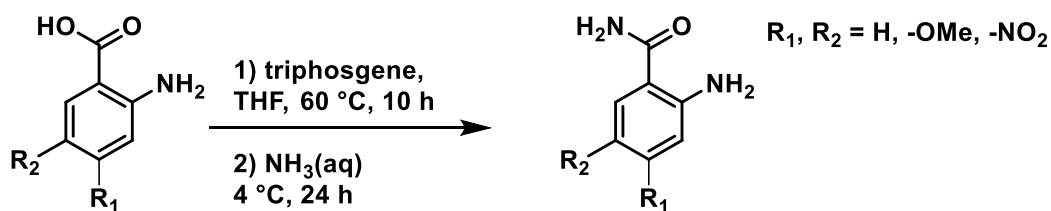


Hydroxymethyluracil (4.0 g, 28 mmol), was dissolved in 100 mL water by heating to $75\text{ }^\circ\text{C}$. Then the solution was cooled down to $40\text{ }^\circ\text{C}$. $\text{K}_2\text{S}_2\text{O}_8$ (13.6 g, 49.6 mmol) and AgNO_3 (0.14 g, 0.8 mmol) were added and the product began to slowly precipitate. The reaction was stirred for 15 min at $35\text{ }^\circ\text{C}$ and 10 min at room temperature. The suspension was then placed at $4\text{ }^\circ\text{C}$ for 1 h. the product was collected by filtration, washed with cold water and dried to yield **2** (3.2 g, 22.7 mmol, 84%) as a white solid. Spectra matched those reported by Integrated Spectral Database System of Organic Compounds with data that were obtained from the National Institute of Advanced Industrial Science and Technology (Japan). ^1H NMR (400 MHz, $\text{DMSO}-d_6$) δ 11.96 (s, 1H), 11.50 (s, 1H), 9.74 (s, 1H), 8.13 (s, 1H). $^{13}\text{C}\{^1\text{H}\}$ NMR (101 MHz, $\text{DMSO}-d_6$) δ 186.9, 162.9, 150.9, 149.7, 110.6.

***tert*-Butyl (uracil-5-formaldehyde-1-yl) acetate (26)**

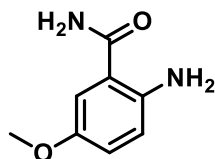


5-formyluracil (2.0 g, 14.28 mmol) was dissolved in 50 mL added to dry DMF and heated to 40 °C to dissolve and cooled down to room temperature. Et₃N (2 mL, 14.28 mmol) was added to the solution. *tert*-Butyl bromoacetate (2.11 mL, 14.28 mmol) was added drop wisely to the stirred mixture within 30 min and stirring was continued for 24 h under N₂ atmosphere. The solvent was removed in vacuo and the residue was extracted with ethyl acetate and water. The organic layer was washed with brine, dried by Na₂SO₄ and concentrated in vacuo to give 7 as a pure white solid product (3.16 g, 12.43 mmol, 87%). Spectroscopic analysis conformed to previous reports. ¹H NMR (400 MHz, DMSO-*d*₆) δ 11.92 (s, 1H), 9.79 (s, 1H), 8.51 (s, 1H), 4.56 (s, 2H), 4.02 (q, *J* = 7.1 Hz, 1H), 1.98 (s, 1H), 1.42 (s, 12H). ¹³C{¹H} NMR (101 MHz, DMSO-*d*₆) δ 186.8, 167.0, 164.1, 163.7, 162.7, 154.1, 152.4, 150.4, 110.7, 102.6, 82.8, 60.3, 50.5, 50.4, 28.0, 27.9, 14.5.



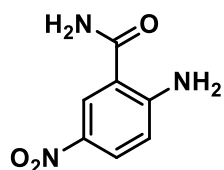
Synthesis of -nitro and -methoxy benzamide compounds

2-Amino-5-methoxybenzamide (27)



2-amino-5-methoxybenzoic acid (0.350 g, 2.5 mmol) dissolved in 4 mL THF, heated to 60 °C, triphosgene (0.25 g, 0.8 mmol) added and stirred for 10 h and checked by TLC. The solution cooled down to room temperature the isatoic anhydride intermediate filtered and collected. Cold 1N ammonia added to the collected intermediate and stirred for 24 h at 4 °C and checked by TLC. The crude solution was taken up in 10 ml EtOAc/Hexanes (1:1) mixture and the resulting precipitate filtered and washed with water and ether to give (0.240 g 1.4 mmol, 58%) of compound **2** as a brown solid. Spectra matched those reported by Integrated Spectral Database System of Organic Compounds with data that were obtained from the National Institute of Advanced Industrial Science and Technology (Japan). ¹H NMR (400 MHz, DMSO-*d*₆) δ 7.75 (s, 1H), 7.10 (d, *J* = 2.9 Hz, 1H), 7.08 (s, 1H), 6.84 (dd, *J* = 8.9, 2.9 Hz, 1H), 6.64 (d, *J* = 8.9 Hz, 1H), 6.12 (s, 2H), 3.68 (s, 3H). ¹³C{¹H} NMR (101 MHz, DMSO-*d*₆) δ 171.4, 149.6, 144.9, 120.3, 118.2, 114.4, 112.9, 56.0.

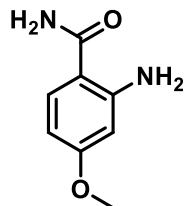
2-Amino-5-nitrobenzamide (28)



2-amino-5-nitrobenzoic acid (0.785 g, 4.5 mmol) dissolved in 10 mL THF, heated to 60 °C, triphosgene (0.45 g, 1.5 mmol) added and stirred for 10 h and checked by TLC. The solution cooled down to room temperature the isatoic anhydride intermediate filtered and collected. Cold 1N ammonia added to the collected intermediate and stirred for 24 h at 4 °C and checked by TLC. The turbid solution was filtered and washed with water and ether to give (0.430 g, 2.3 mmol, 48%) of compound **2** as a yellow solid. Spectra matched those reported by Integrated Spectral Database System of Organic Compounds with data that were obtained from the National Institute of Advanced Industrial Science and Technology (Japan). ¹H NMR (400 MHz, DMSO-*d*₆) δ 8.56 (d, *J* = 2.6 Hz, 1H), 8.21 (s, 1H), 8.02 (dd, *J* = 9.2, 2.6 Hz, 1H), 7.90 (s, 2H), 7.41 (s, 1H), 6.80 (d, *J*

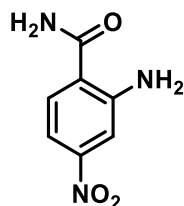
= 9.2 Hz, 1H). $^{13}\text{C}\{^1\text{H}\}$ NMR (101 MHz, DMSO- d_6) δ 170.1, 156.2, 135.2, 128.0, 126.9, 116.4, 112.5.

2-Amino-4-methoxybenzamide (29)



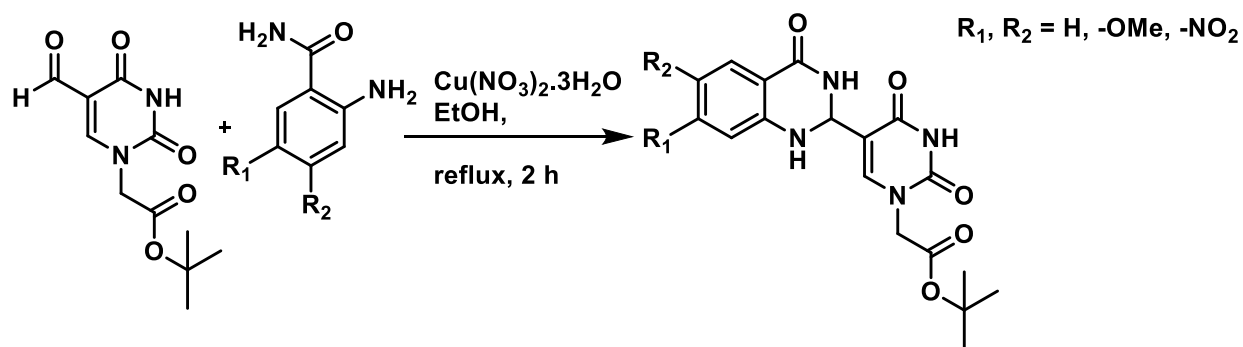
2-amino-4-methoxybenzoic acid (0.501 g, 3 mmol) dissolved in 6 mL THF, heated to 60 °C, triphosgene (0.3 g, 1 mmol) added and stirred for 10 h and checked by TLC. Cold 1N ammonia added to the collected intermediate and stirred for 24 h at 4 °C and checked by TLC. The turbid solution was filtered and washed with water and ether to give 0.250 g (1.5 mmol, 50%) of compound **2** as a white solid. Spectra matched those reported by Integrated Spectral Database System of Organic Compounds with data that were obtained from the National Institute of Advanced Industrial Science and Technology (Japan). ^1H NMR (400 MHz, DMSO- d_6) δ 7.49 (d, J = 8.8 Hz, 1H), 6.74 (s, 2H), 6.20 (d, J = 2.6 Hz, 1H), 6.07 (dd, J = 8.8, 2.6 Hz, 1H), 3.70 (s, 3H).

2-Amino-4-nitrobenzamide (30)

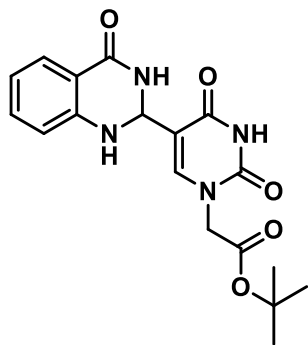


2-amino-4-nitrobenzoic acid (0.549 g, 3 mmol) dissolved in 6 mL THF, heated to 60 °C, triphosgene (0.3 g, 1 mmol) added and stirred for 5 h and checked by TLC. The solution cooled down to room temperature and THF removed under reduced pressure. The solution cooled down to room temperature the isatoic anhydride intermediate filtered and collected. Cold 1N ammonia added to the collected intermediate and stirred for 24 h at 4 °C and checked by TLC. The turbid solution was filtered and washed with water and ether to give (0.430 g 2.3 mmol, 80%) of

compound **2** as an orange solid. Spectra matched those reported by Integrated Spectral Database System of Organic Compounds with data that were obtained from the National Institute of Advanced Industrial Science and Technology (Japan). ^1H NMR (400 MHz, $\text{DMSO}-d_6$) δ 8.03 (s, 1H), 7.74 (d, $J = 8.6$ Hz, 1H), 7.57 (d, $J = 2.4$ Hz, 1H), 7.46 (s, 1H), 7.25 (dd, $J = 8.6, 2.4$ Hz, 1H), 7.02 (s, 2H).



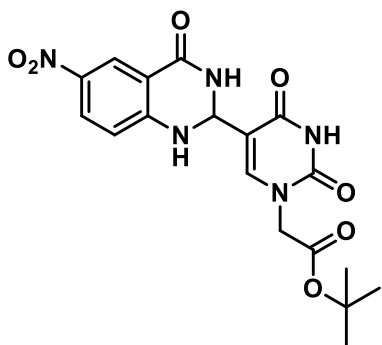
tert-butyl 2-(2,4-dioxo-5-(4-oxo-1,2,3,4-tetrahydroquinazolin-2-yl)-3,4-dihydropyrimidin-1(2H)-yl)acetate (31**)**



0.50 g (2 mmol) of **7** dissolved in 10 ml reflux ethanol, 36 mg (0.13 mmol) of $\text{Cu}(\text{NO}_3)_2 \cdot 3\text{H}_2\text{O}$ and 0.14 g (1 mmol) of 2-amino benzamide added to the solution and reaction mixture stirred for 2 h and checked by TLC, solution cooled down to room temperature and the resulting precipitate filtered and washed with EtOH and MeOH to give **8** (0.298 g, 0.8 mmol, 80%) as a white solid. ^1H NMR (400 MHz, $\text{DMSO}-d_6$) δ 11.62 (s, 1H), 7.95 (d, $J = 1.8$ Hz, 1H), 7.82 (s,

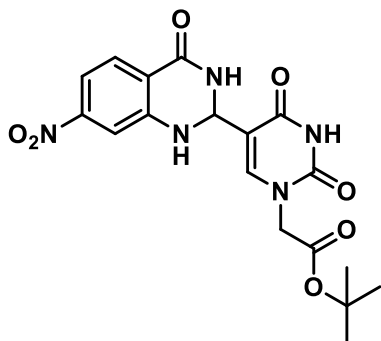
1H), 7.62 (dd, $J = 7.8, 1.6$ Hz, 1H), 7.25 (ddd, $J = 8.5, 7.2, 1.7$ Hz, 1H), 6.78 (d, $J = 8.1$ Hz, 1H), 6.75 – 6.66 (m, 2H), 5.68 (d, $J = 2.0$ Hz, 1H), 4.48 (s, 2H), 1.40 (s, 9H). $^{13}\text{C}\{^1\text{H}\}$ NMR (101 MHz, DMSO- d_6) δ 167.5, 163.9, 163.3, 150.9, 148.2, 144.5, 133.7, 127.9, 117.9, 115.3, 112.9, 82.2, 60.4, 50.1, 28.1. HRMS (ESI/Q-TOF) m/z : $[\text{M}]^+$ Calcd for $\text{C}_{18}\text{H}_{20}\text{N}_4\text{O}_5$ 372.1434; Found 372.1428.

tert-butyl 2-(5-(6-nitro-4-oxo-1,2,3,4-tetrahydroquinazolin-2-yl)-2,4-dioxo-3,4-dihydropyrimidin-1(2H)-yl) acetate (32)



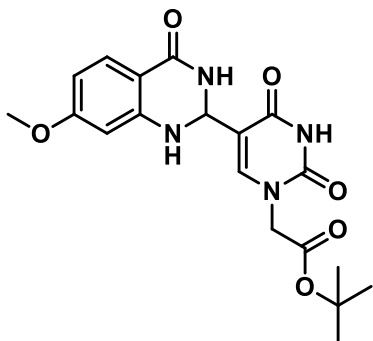
0.50 g (2 mmol) of **7** dissolved in 10 ml reflux ethanol, 36.2 mg (0.15 mmol) of $\text{Cu}(\text{NO}_3)_2 \cdot 3\text{H}_2\text{O}$ and 0.18 g (1 mmol) of 2-amino-5-nitrobenzamide added to the solution and reaction mixture stirred for 2 h and checked by TLC, solution cooled down to room temperature and the resulting precipitate filtered and washed with EtOH and MeOH to give **8** (176 mg, 0.42 mmol, 42%) as a yellow solid. ^1H NMR (400 MHz, DMSO- d_6) δ 11.67 (s, 1H), 8.41 (dd, $J = 8.3, 2.4$ Hz, 2H), 8.30 (s, 1H), 8.09 (dd, $J = 9.1, 2.8$ Hz, 1H), 7.81 (s, 1H), 6.84 (d, $J = 9.1$ Hz, 1H), 5.85 (t, $J = 2.1$ Hz, 1H), 4.47 (s, 2H), 1.39 (s, 9H). $^{13}\text{C}\{^1\text{H}\}$ NMR (101 MHz, DMSO- d_6) δ 167.7, 162.9, 161.6, 152.4, 150.9, 144.4, 137.5, 129.2, 124.5, 114.9, 113.0, 112.9, 82.3, 61.0, 49.9, 28.1. HRMS (ESI/Q-TOF) m/z : $[\text{M}]^+$ Calcd for $\text{C}_{18}\text{H}_{19}\text{N}_5\text{O}_7$ 417.1284; Found 417.1271.

tert-butyl 2-(5-(7-nitro-4-oxo-1,2,3,4-tetrahydroquinazolin-2-yl)-2,4-dioxo-3,4-dihydropyrimidin-1(2H)-yl) acetate (33)



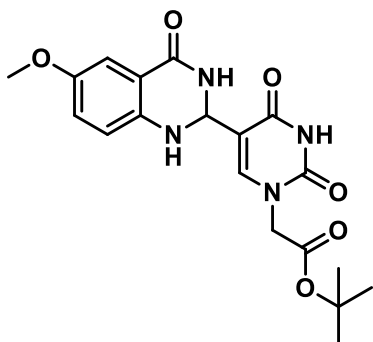
0.50 g (2 mmol) of **7** dissolved in 10 ml reflux ethanol, 36.2 mg (0.15 mmol) of $\text{Cu}(\text{NO}_3)_2 \cdot 3\text{H}_2\text{O}$ and 0.18 g (1 mmol) of 2-amino-5-nitrobenzamide added to the solution and reaction mixture stirred for 2 h and checked by TLC, solution cooled down to room temperature and the resulting precipitate filtered and washed with EtOH and MeOH to give **8** (160 mg, 0.38 mmol, 38%) as a yellow solid. ^1H NMR (600 MHz, $\text{DMSO}-d_6$) δ 11.62 (s, 1H), 8.34 (s, 1H), 7.79 (d, $J = 8.5$ Hz, 1H), 7.74 (s, 1H), 7.59 (d, $J = 2.3$ Hz, 1H), 7.43 – 7.37 (m, 2H), 5.73 (s, 1H), 4.43 (s, 2H), 1.34 (s, 9H). $^{13}\text{C}\{^1\text{H}\}$ NMR (101 MHz, $\text{DMSO}-d_6$) δ 166.5, 162.9, 161.6, 152.4, 150.9, 144.4, 137.5, 129.2, 124.5, 114.8, 113.0, 112.9, 82.3, 61.0, 49.9, 27.3. HRMS (ESI/Q-TOF) m/z : $[\text{M}]^+$ Calcd for $\text{C}_{18}\text{H}_{19}\text{N}_5\text{O}_7$ 417.1284; Found 417.1270

tert-butyl 2-(5-(7-methoxy-4-oxo-1,2,3,4-tetrahydroquinazolin-2-yl)-2,4-dioxo-3,4-dihydropyrimidin-1(2H)-yl) acetate (34)

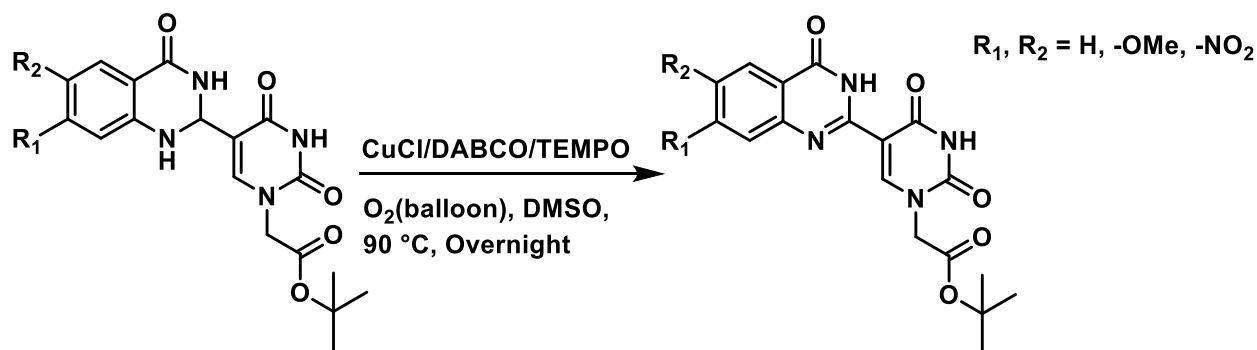


0.25 g (1 mmol) of **7** dissolved in 10 ml reflux ethanol, 18.1 mg (0.075 mmol) of Cu(NO₃)₂·3H₂O and 83 mg (0.5 mmol) of 2-amino-4-methoxybenzamide added to the solution and reaction mixture stirred for 10 h and checked by TLC, solution cooled down to room temperature and the resulting precipitate filtered and washed with EtOH and MeOH to give **8** (51 mg, 0.13 mmol, 13%) as a yellow solid. ¹H NMR (400 MHz, DMSO-*d*₆) δ 12.37 (s, 1H), 12.03 (s, 1H), 9.02 (s, 1H), 8.02 (d, *J* = 8.7 Hz, 1H), 7.12 – 7.01 (m, 2H), 4.70 (s, 2H), 3.89 (s, 3H), 1.45 (s, 9H). ¹³C{¹H} NMR (101 MHz, DMSO-*d*₆) δ 167.2, 164.6, 164.5, 160.1, 151.3, 150.7, 150.1, 149.6, 128.1, 116.1, 114.8, 108.2, 103.2, 82.7, 56.1, 50.7, 28.1. HRMS (ESI/Q-TOF) *m/z*: [M]⁺ Calcd for C₁₉H₂₂N₄O₆ 402.1539; Found 402.1536

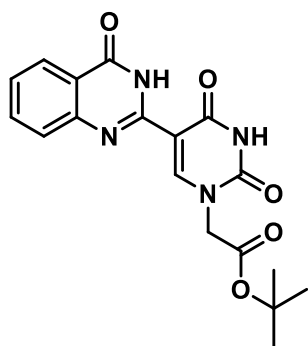
tert-butyl 2-(5-(6-methoxy-4-oxo-1,2,3,4-tetrahydroquinazolin-2-yl)-2,4-dioxo-3,4-dihydropyrimidin-1(2H)-yl) acetate (35)



0.25 g (1 mmol) of **7** dissolved in 10 ml reflux ethanol, 18.1 mg (0.075 mmol) of Cu(NO₃)₂·3H₂O and 83 mg (0.5 mmol) of 2-amino-5-methoxybenzamide added to the solution and reaction mixture stirred for 4 h and checked by TLC, solution cooled down to room temperature and the resulting precipitate filtered and washed with EtOH and MeOH to give **8** (155 mg, 0.40 mmol, 40%) as a yellow solid. ¹H NMR (400 MHz, DMSO-*d*₆) δ 11.61 (s, 1H), 8.00 (t, *J* = 1.8 Hz, 1H), 7.82 (s, 1H), 7.16 (d, *J* = 3.0 Hz, 1H), 6.93 (dd, *J* = 8.7, 3.0 Hz, 1H), 6.77 (d, *J* = 8.8 Hz, 1H), 6.38 (d, *J* = 1.7 Hz, 1H), 5.62 (t, *J* = 1.7 Hz, 1H), 4.48 (s, 2H), 3.69 (s, 3H), 1.40 (s, 9H). ¹³C{¹H} NMR (101 MHz, DMSO-*d*₆) δ 167.5, 163.9, 163.3, 152.2, 150.9, 144.5, 142.5, 121.8, 116.9, 116.0, 112.7, 110.4, 82.2, 60.6, 55.7, 50.0, 28.1. HRMS (ESI/Q-TOF) *m/z*: [M]⁺ Calcd for C₁₉H₂₂N₄O₆ 402.1539; Found 402.1537

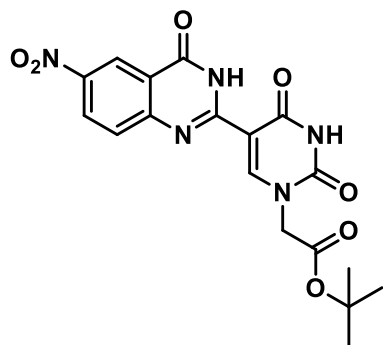


tert-butyl 2-(2,4-dioxo-5-(4-oxo-3,4-dihydroquinazolin-2-yl)-3,4-dihydropyrimidin-1(2H)-yl)acetate (36)



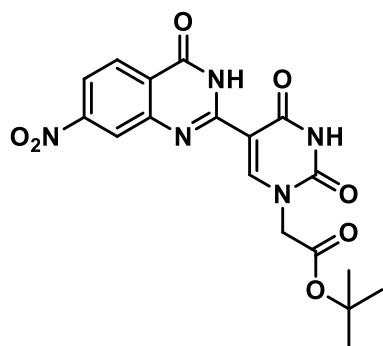
0.15 g, (0.4 mmol) were fully dissolved in 1 mL DMSO at 60 °C. To the same solution were added CuCl (1.2 mg, 0.01 mmol), 4-HO-TEMPO (1 mg, 0.005 mmol), and DABCO (1 mg, 0.009 mmol), and the mixture was stirred at 90 °C for several hours under O₂ atmosphere (balloon). After completion of the reaction (monitored by TLC), the reaction was cooled down to room temperature and the resulting precipitate was washed with water and ethanol to give the product **1b** (0.15, 0.4 mmol, 100%) as a white solid. ¹H NMR (400 MHz, DMSO-*d*₆) δ 12.46 (s, 1H), 9.27 (s, 1H), 8.38 (d, *J* = 7.9 Hz, 1H), 8.08 (t, *J* = 7.7 Hz, 1H), 7.90 (d, *J* = 8.2 Hz, 1H), 7.74 (t, *J* = 7.5 Hz, 1H), 4.96 (s, 2H), 1.71 (s, 9H). ¹³C{¹H} NMR (151 MHz, DMSO-*d*₆) δ 166.88, 164.31, 150.51, 150.00, 149.16, 134.86, 126.40, 126.29, 121.54, 110.00, 103.54, 82.83, 50.85, 40.88, 40.74, 40.60, 40.47, 40.33, 40.19, 40.05, 28.22. HRMS (ESI/Q-TOF) *m/z*: [M]⁺ Calcd for C₁₈H₁₈N₄O₅ 370.1277; Found 370.1279

tert-butyl 2-(5-(6-nitro-4-oxo-1,4-dihydroquinazolin-2-yl)-2,4-dioxo-3,4-dihydropyrimidin-1(2H)-yl) acetate (37)



To 6-nitro substituted dihydrobenzoquinazolinone compound (0.13 g, 0.31 mmol) added 1 mL DMSO and dissolved at 60 °C. To the same solution were added CuCl (2.9 mg, 0.02 mmol), 4-HO-TEMPO (2 mg, 0.012 mmol), and DABCO (2 mg, 0.022 mmol), and the mixture was stirred at 90 °C overnight under O₂ atmosphere (balloon). After completion of the reaction (monitored by TLC), the reaction was cooled down to room temperature and the resulting precipitate was washed with water and ethanol to give the product as a yellow solid (0.13 g, 0.31 mmol 100%). ¹H NMR (400 MHz, DMSO-*d*₆) δ 12.51 (s, 1H), 9.15 (s, 1H), 8.80 (d, *J* = 2.7 Hz, 1H), 8.55 (dd, *J* = 9.0, 2.8 Hz, 1H), 7.77 (d, *J* = 9.0 Hz, 1H), 4.74 (s, 2H), 1.46 (s, 9H). ¹³C{¹H} NMR (101 MHz, DMSO-*d*₆) δ 167.1, 159.9, 152.2, 144.6, 129.2, 128.7, 122.6, 121.2, 82.8, 50.9, 28.1. HRMS (ESI/Q-TOF) *m/z*: [M]⁺ Calcd for C₁₈H₁₇N₅O₇ 415.1128; Found 415.1130

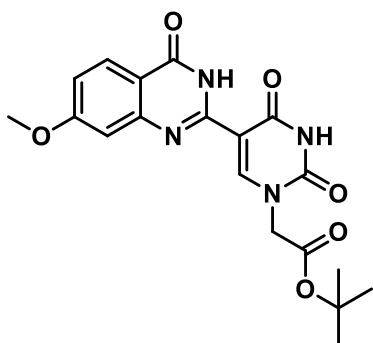
tert-butyl 2-(5-(7-nitro-4-oxo-1,4-dihydroquinazolin-2-yl)-2,4-dioxo-3,4-dihydropyrimidin-1(2H)-yl)acetate (38)



To 7-nitro substituted dihydrobenzoquinazolinone compound (0.12 g, 0.29 mmol) added 1 mL DMSO and dissolved at 60 °C. To the same solution were added CuCl (2.9 mg, 0.02 mmol), 4-HO-TEMPO (2 mg, 0.012 mmol), and DABCO (2 mg, 0.022 mmol), and the mixture was stirred

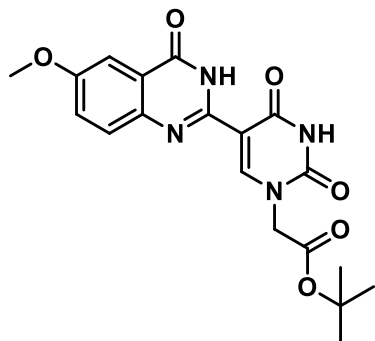
at 90 °C overnight under O₂ atmosphere (balloon). After completion of the reaction (monitored by TLC), the reaction was cooled down to room temperature and the resulting precipitate was washed with water and ethanol to give the product as a yellow solid. (0.12 g, 0.29 mmol, 100%). ¹H NMR (400 MHz, DMSO-*d*₆) δ 12.50 – 12.39 (m, 2H), 9.12 (s, 1H), 8.36 – 8.27 (m, 2H), 8.18 (dd, *J* = 8.7, 2.2 Hz, 1H), 4.72 (s, 2H), 1.46 (s, 9H). ¹³C{¹H} NMR (101 MHz, DMSO-*d*₆) δ 167.1, 159.7, 151.8, 151.6, 151.4, 150.0, 149.6, 128.8, 125.7, 121.9, 119.8, 102.7, 82.8, 50.9, 28.1. HRMS (ESI/Q-TOF) *m/z*: [M]⁺ Calcd for C₁₈H₁₇N₅O₇ 415.1128; Found 415.1133

tert-butyl 2-(5-(7-methoxy-4-oxo-1,4-dihydroquinazolin-2-yl)-2,4-dioxo-3,4-dihydropyrimidin-1(2H)-yl) acetate (39)

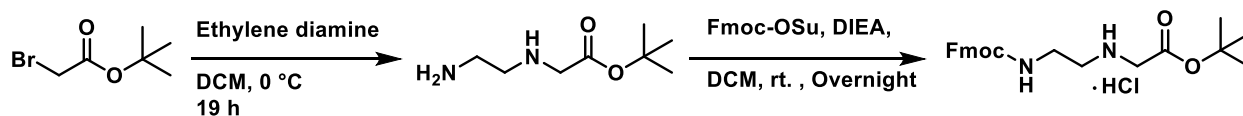


To 7-methoxy substituted dihydrobenzoquinazolinone compound (0.14 g, 0.35 mmol) added 1 mL DMSO and dissolved at 60 °C. To the same solution were added CuCl (2.9 mg, 0.02 mmol), 4-HO-TEMPO (2 mg, 0.012 mmol), and DABCO (2 mg, 0.022 mmol), and the mixture was stirred at 90 °C overnight under O₂ atmosphere (balloon). After completion of the reaction (monitored by TLC), the reaction was cooled down to room temperature and the resulting precipitate was washed with water and ethanol to give the product as a yellow solid. (0.14 g, 0.35 mmol, 100%). ¹H NMR (400 MHz, DMSO-*d*₆) δ 12.37 (s, 1H), 12.03 (s, 1H), 9.02 (s, 1H), 8.02 (d, *J* = 8.7 Hz, 1H), 7.12 – 7.01 (m, 2H), 4.70 (s, 2H), 3.89 (s, 3H), 1.45 (s, 9H). ¹³C {¹H} NMR (101 MHz, DMSO-*d*₆) δ 167.2, 164.7, 164.5, 160.1, 151.3, 150.7, 150.1, 149.7, 128.1, 116.1, 114.8, 108.2, 103.2, 82.7, 56.1, 50.7, 28.1. HRMS (ESI/Q-TOF) *m/z*: [M]⁺ Calcd for C₁₉H₂₀N₄O₆ 400.1383; Found 400.1379

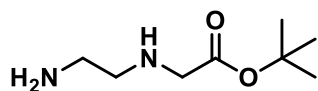
tert-butyl 2-(5-(6-methoxy-4-oxo-3,4-dihydroquinazolin-2-yl)-2,4-dioxo-3,4-dihydropyrimidin-1(2H)-yl)acetate (40)



To 6-methoxy substituted dihydrobenzoquinazolinone compound (0.14 g, 0.35 mmol) added 1 mL DMSO and dissolved at 60 °C. To the same solution were added CuCl (2.9 mg, 0.02 mmol), 4-HO-TEMPO (2 mg, 0.012 mmol), and DABCO (2 mg, 0.022 mmol), and the mixture was stirred at 90 °C overnight under O₂ atmosphere (balloon). After completion of the reaction (monitored by TLC), the reaction was cooled down to room temperature and the resulting precipitate was washed with water and ethanol to give the product as a yellow solid. (0.14 g, 0.35 mmol, 100%). ¹H NMR (400 MHz, DMSO-*d*₆) δ 12.37 (s, 1H), 12.03 (s, 1H), 9.02 (s, 1H), 8.02 (d, *J* = 8.7 Hz, 1H), 7.12 – 7.01 (m, 2H), 4.70 (s, 2H), 3.89 (s, 3H), 1.45 (s, 9H). ¹³C{¹H} NMR (101 MHz, DMSO-*d*₆) δ 167.2, 164.7, 164.5, 160.1, 151.3, 150.7, 150.1, 149.7, 128.1, 116.1, 114.8, 108.2, 103.2, 82.7, 56.1, 50.7, 28.1. HRMS (ESI/Q-TOF) *m/z*: [M]⁺ Calcd for C₁₉H₂₀N₄O₆ 400.1383; Found 400.1382



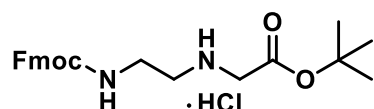
tert-butyl (2-aminoethyl)glycinate (41)



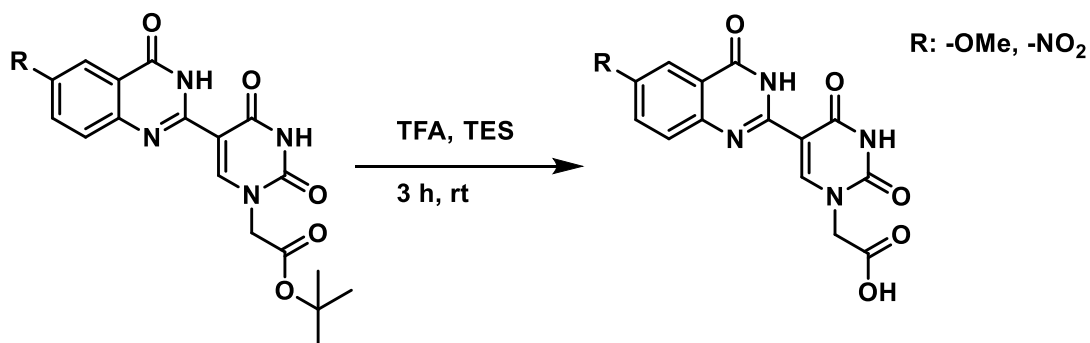
6.9 mL of *t*Bu-bromoacetate **1** mixed with 37.5 mL of Dichloromethane and added dropwise to the mixture of 25 mL ethylenediamine (dissolved in 175 mL Dichloromethane) on the ice bath. The reaction continued for 19 hours. Then extracted with water (90 mL ×2) and dichloromethane (60 mL ×3); dried with Sodium sulfate and concentrated in *vacuo* to give (15.8 g, 90 mmol, 51%)

of ester **2** as a colorless liquid. ^1H NMR (400 MHz, Chloroform-*d*) δ 3.22 (s, 2H), 2.74 – 2.66 (m, 2H), 2.64 – 2.52 (m, 2H), 1.39 (s, 9H).

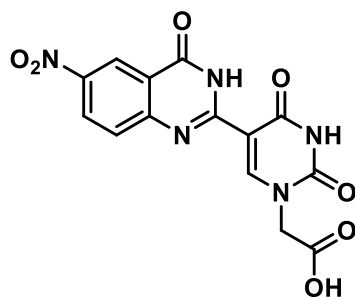
tert-butyl (2-((((9H-fluoren-9-yl)methoxy)carbonyl)amino)ethyl)glycinate (42**)**



15.0 g (88 mmol) of ester **2** and 15.2 mL diisopropylethylamine (90 mmol) were added and dissolved in 680 mL dichloromethane. 26.3 g (77mmol) of Fmoc-OSu **3** dissolved in 192 mL Dichloromethane and added drop wisely at room temperature for 70 min. The reaction mixture stirred overnight and washed with 1 M HCl (3×100 mL) and brine (100 mL). Organic layer dried with sodium sulfate and filtered. The solution was partially concentrated to 50 mL in *vacuo* and cooled in a deep freezer (-20 °C) overnight. The white precipitate was filtered the other day and washed with Dichloromethane and mother liquor returned to freezer to get more product **4** (8 g, 19 mmol, 20%) as a white precipitate. ^1H NMR (400 MHz, DMSO-*d*₆) δ 7.91 – 7.80 (m, 3H), 7.68 (dd, J = 16.3, 7.9 Hz, 2H), 7.46 – 7.23 (m, 5H), 4.36 – 4.27 (m, 2H), 4.22 (q, J = 7.3 Hz, 1H), 3.20 (s, 1H), 3.07 (q, J = 6.2 Hz, 2H), 2.58 (t, J = 6.4 Hz, 1H), 1.41 (s, 9H). $^{13}\text{C}\{^1\text{H}\}$ NMR (101 MHz, DMSO-*d*₆) δ 171.9, 156.7, 144.4, 141.2, 129.4, 128.0, 127.7, 127.5, 125.6, 121.8, 120.6, 120.5, 110.1, 80.5, 65.8, 51.3, 48.7, 47.2, 40.8, 28.2. This corresponded closely to the NMR spectra previously reported in the literature⁵⁰.

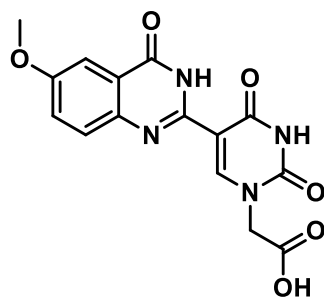


2-(5-(6-nitro-4-oxo-3,4-dihydroquinazolin-2-yl)-2,4-dioxo-3,4-dihydropyrimidin-1(2H)-yl)acetic acid(44)

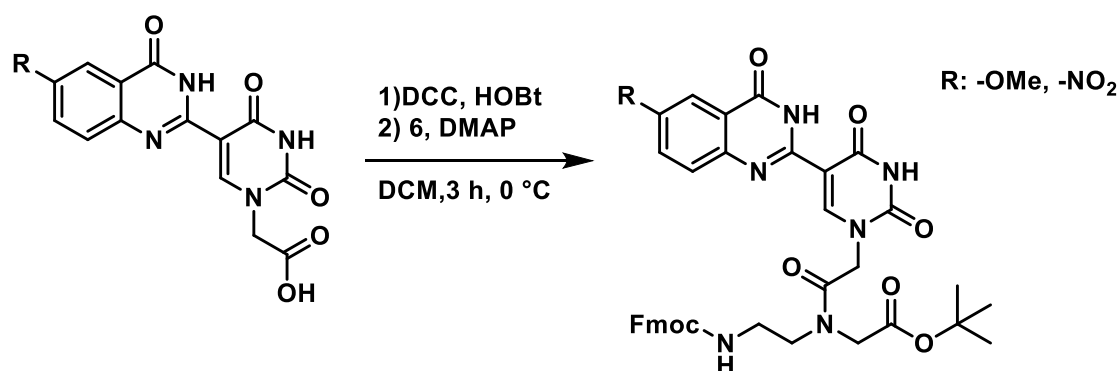


To (0.1 g, 0.24 mmol) of ester **8** added TFA (1 mL) and triethyl silane (3 drops). The reaction stirred for 2 hours at room temperature, then the excess of the acid was evaporated under a nitrogen stream and the product was washed by hexane and ethyl ether to give acid **9** as a yellow solid (70 mg, 0.19 mmol, 80%). ^1H NMR (400 MHz, DMSO- d_6) δ 13.39 (s, 1H), 12.49 (s, 1H), 9.16 (d, J = 1.4 Hz, 9H), 8.78 (q, J = 2.6 Hz, 9H), 8.54 (dq, J = 9.1, 2.6 Hz, 10H), 7.80 – 7.72 (m, 9H), 4.76 (s, 17H), 3.17 (s, 4H). ^{13}C { ^1H } NMR (101 MHz, DMSO- d_6) δ 169.4, 164.5, 160.0, 152.6, 152.3, 149.9, 144.5, 129.2, 128.7, 122.6, 121.2, 102.4, 56.5, 50.3, 19.0. HRMS (ESI/Q-TOF) m/z : $[\text{M}]^+$ Calcd for $\text{C}_{14}\text{H}_9\text{N}_5\text{O}_7$ 359.0502; Found 359.0509

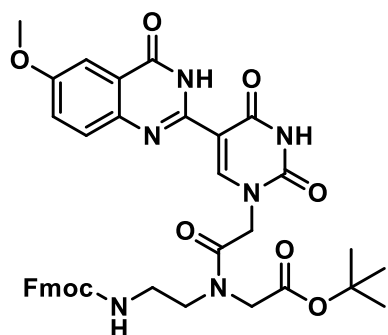
2-(5-(6-methoxy-4-oxo-3,4-dihydroquinazolin-2-yl)-2,4-dioxo-3,4-dihydropyrimidin-1(2H)-yl)acetic acid (45)



To (0.1 g, 0.25 mmol) of ester **8** added TFA (1 mL) and triethyl silane (3 drops). The reaction stirred for 2 hours at room temperature, then the excess of the acid was evaporated under a nitrogen stream and the product was washed by hexane and ethyl ether to give acid **9** as a light green solid (65 mg, 0.19 mmol, 75%). ^1H NMR (400 MHz, DMSO- d_6) δ 12.32 (s, 1H), 12.13 (s, 1H), 8.95 (s, 1H), 7.59 (d, J = 8.9 Hz, 1H), 7.51 (d, J = 3.0 Hz, 1H), 7.43 (dd, J = 8.9, 3.0 Hz, 1H), 4.72 (s, 2H), 3.88 (s, 3H). $^{13}\text{C}\{^1\text{H}\}$ NMR (101 MHz, DMSO- d_6) δ 169.6, 164.5, 160.4, 157.8, 150.2, 150.1, 146.9, 143.6, 128.9, 124.8, 122.1, 106.4, 103.5, 56.1, 50.0. HRMS (ESI/Q-TOF) m/z : $[\text{M}]^+$ Calcd for $\text{C}_{15}\text{H}_{12}\text{N}_4\text{O}_6$ 344.0757; Found 344.0759

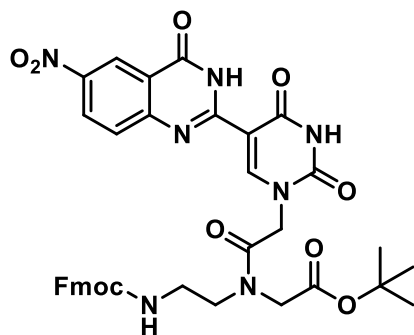


tert-butyl N-(2-((((9H-fluoren-9-yl)methoxy)carbonyl)amino)ethyl)-N-(2-(5-(6-methoxy-4-oxo-3,4-dihydroquinazolin-2-yl)-2,4-dioxo-3,4-dihydropyrimidin-1(2H)-yl)acetyl)glycinate (46**)**



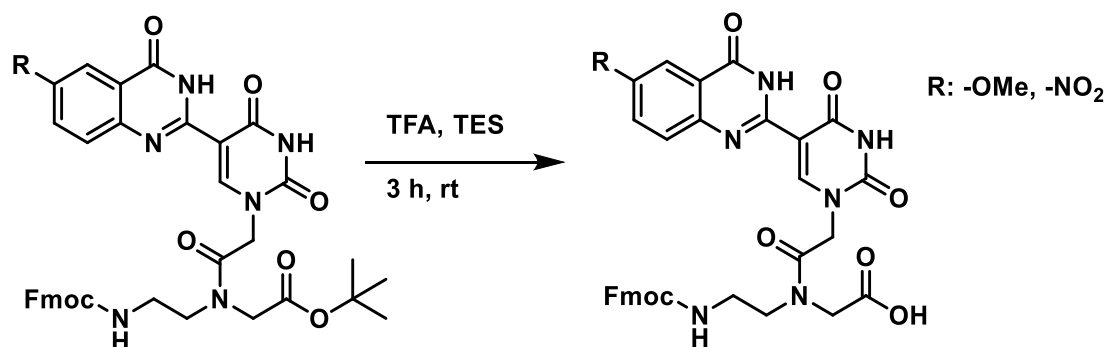
0.1 g (0.29 mmol) of **6** dissolved in 2 mL DMF at 0 °C HOBt (26 mg, 0.20 mmol) and DCC (70 mg, 0.34 mmol) added and stirred until precipitate formed. **6** (free base) (70 mg, 0.15 mmol) added and DMAP (1.8 mg, 0.015 mmol) added and reaction continued for 3 hours and checked by TLC. The mixture diluted with saturated aqueous NaHCO₃ and extracted with DCM and washed with brine and concentrated in *vacuo* and purified by column chromatography (1:1 to 4:1 ethyl acetate : hexanes) to yield as a white solid. (77 mg, 0.1 mmol, 66%). ¹H NMR (400 MHz, DMF-*d*₇) δ 8.31 (dd, *J* = 7.7, 3.6 Hz, 3H), 8.07 (dd, *J* = 10.0, 7.5 Hz, 3H), 7.84 (dd, *J* = 8.6, 6.2 Hz, 3H), 7.79 – 7.71 (m, 3H), 4.83 – 4.59 (m, 4H), 4.43 (d, *J* = 4.0 Hz, 2H), 4.01 (d, *J* = 2.4 Hz, 1H), 3.75 (s, 3H), 3.36 – 3.26 (m, 3H), 2.76 (q, *J* = 7.3 Hz, 1H), 1.84 (s, 9H). ¹³C{¹H} NMR (101 MHz, DMF-*d*₇) δ 169.99, 153.96, 144.68, 141.65, 129.81, 128.57, 128.17, 128.01, 128.00, 125.97, 122.27, 121.03, 110.63, 81.40, 68.20, 67.64, 67.23, 55.58, 55.30, 52.05, 48.40, 47.59. HRMS (ESI/Q-TOF) *m/z*: [M+Na]⁺ Calcd for C₃₈H₃₈N₆O₉Na 745.2598; Found 745.2590.

tert-butyl N-(2-((((9H-fluoren-9-yl)methoxy)carbonyl)amino)ethyl)-N-(2-(5-(6-nitro-4-oxo-3,4-dihydroquinazolin-2-yl)-2,4-dioxo-3,4-dihydropyrimidin-1(2H)-yl)acetyl)glycinate (47**)**

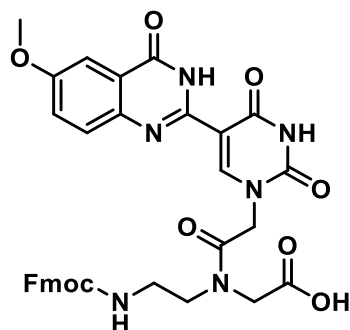


0.1 g (0.24 mmol) of **6** dissolved in 2 mL DMF at 0 °C HOBt (23 mg, 0.19 mmol) and DCC (70 mg, 0.34 mmol) added and stirred until precipitate formed. **6** (free base) (70 mg, 0.15 mmol) added and DMAP (1.8 mg, 0.015 mmol) added and reaction continued for 3 hours and checked by TLC. The mixture diluted with saturated aqueous NaHCO₃ and extracted with DCM and washed with brine and concentrated in *vacuo* and purified by column chromatography (1:1 to 4:1 ethyl acetate : hexanes) to yield as a yellow solid. (66 mg, 0.09 mmol, 60%). ¹H NMR (400 MHz, DMSO-*d*₆) δ 8.85 – 8.70 (m, 1H), 7.91 – 7.82 (m, 3H), 7.69 (dd, *J* = 10.0, 7.0 Hz, 2H), 7.47 – 7.18 (m, 5H),

4.01 (ddd, $J = 15.7, 14.1, 5.9$ Hz, 1H), 3.19 (d, $J = 3.2$ Hz, 4H), 2.90 (s, 1H), 2.75 – 2.56 (m, 7H), 1.42 (s, 9H). $^{13}\text{C}\{^1\text{H}\}$ NMR (101 MHz, Chloroform- d) δ 171.9, 146.0, 141.0, 128.7, 127.4, 127.2, 127.1, 126.9, 126.9, 125.2, 124.7, 121.0, 119.9, 119.8, 119.7, 107.7, 81.3, 57.3, 53.0, 51.4, 48.8, 47.9, 44.7, 33.9, 31.2, 28.1. HRMS (ESI/Q-TOF) m/z : $[\text{M}+\text{Na}]^+$ Calcd for $\text{C}_{37}\text{H}_{35}\text{N}_7\text{O}_{10}\text{Na}$ 760.2343; Found 760.2350.



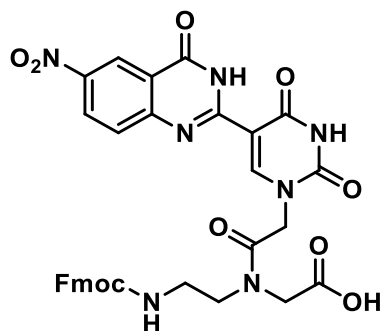
N-(2-((((9H-fluoren-9-yl)methoxy)carbonyl)amino)ethyl)-N-(2-(5-(6-methoxy-4-oxo-3,4-dihydroquinazolin-2-yl)-2,4-dioxo-3,4-dihydropyrimidin-1(2H)-yl)acetyl)glycine (48)



To (66 mg, 0.09 mmol) of ester **8** added TFA (1 mL) and triethyl silane (3 drops). The reaction stirred for 2 hours at room temperature, then the excess of the acid was evaporated under a nitrogen stream and the product was washed by hexane and ethyl ether to give acid **9** as a white solid (47 mg, 0.07 mmol, 75%). ^1H NMR (400 MHz, DMSO- d_6) δ 12.30 (s, 3H), 8.78 (s, 2H), 8.72 (s, 1H),

7.86 (dd, $J = 7.5, 5.1$ Hz, 6H), 7.68 (t, $J = 6.8$ Hz, 6H), 7.49 (ddd, $J = 8.4, 5.2, 1.6$ Hz, 8H), 7.38 (dt, $J = 7.9, 2.1$ Hz, 6H), 7.35 – 7.29 (m, 6H), 5.57 (s, 1H), 5.03 (s, 3H), 4.84 (s, 2H), 4.36 (d, $J = 6.9$ Hz, 4H), 4.29 (d, $J = 7.0$ Hz, 2H), 4.25 (t, $J = 3.4$ Hz, 4H), 4.02 (s, 3H), 3.88 (s, 3H), 1.27 – 1.03 (m, 9H). $^{13}\text{C}\{^1\text{H}\}$ NMR (101 MHz, DMSO) δ 172.8, 170.8, 167.2, 164.6, 160.6, 157.7, 156.8, 156.6, 150.4, 150.1, 144.3, 141.2, 141.1, 134.3, 128.1, 128.0, 127.8, 127.5, 125.6, 125.6, 120.6, 106.4, 103.1, 56.1, 49.4, 47.9, 47.2, 40.6, 40.4, 40.2, 39.9, 39.78, 39.6, 39.4, 36.7, 33.8, 25.8, 24.9. HRMS (ESI/Q-TOF) m/z : $[\text{M}+\text{Na}]^+$ Calcd for $\text{C}_{34}\text{H}_{36}\text{N}_6\text{O}_9\text{Na}$ 695.2441; Found 695.2458.

N-(2-((((9H-fluoren-9-yl)methoxy)carbonyl)amino)ethyl)-N-(2-(5-(6-nitro-4-oxo-3,4-dihydroquinazolin-2-yl)-2,4-dioxo-3,4-dihydropyrimidin-1(2H)-yl)acetyl)glycine (49)



To (58 mg, 0.07 mmol) of ester **8** added TFA (1 mL) and triethyl silane (3 drops). The reaction stirred for 2 hours at room temperature, then the excess of the acid was evaporated under a nitrogen stream and the product was washed by hexane and ethyl ether to give acid **9** as a light yellow solid (47 mg, 0.05 mmol, 83%). ^1H NMR (400 MHz, $\text{DMSO}-d_6$) δ 12.57 (s, 1H), 9.05 (d, $J = 3.4$ Hz, 2H), 8.81 (s, 3H), 8.55 (d, $J = 8.9$ Hz, 4H), 8.49 (s, 2H), 7.91 (d, $J = 7.2$ Hz, 3H), 7.86 (t, $J = 9.8$ Hz, 5H), 7.76 (dd, $J = 14.8, 8.1$ Hz, 6H), 7.69 (s, 3H), 7.46 – 7.29 (m, 11H), 5.07 (s, 2H), 4.87 (s, 2H), 4.68 (s, 3H), 4.13 (s, 2H), 4.03 (s, 2H), 3.56 (s, 4H), 3.28 (s, 8H), 2.92 (d, $J = 21.0$ Hz, 11H). $^{13}\text{C}\{^1\text{H}\}$ NMR (101 MHz, $\text{DMSO}-d_6$) δ 171.7, 169.7, 167.1, 163.5, 160.6, 157.8, 156.8, 156.6, 150.4, 150.1, 144.3, 141.2, 141.1, 134.3, 128.1, 128.0, 127.8, 127.5, 125.6, 125.6, 120.5, 106.4, 103.1, 49.4, 47.9, 47.2, 40.6, 40.4, 40.2, 39.9, 39.8, 39.6, 39.4, 36.7, 33.8, 25.8, 24.9. HRMS (ESI/Q-TOF) m/z : $[\text{M}+\text{Na}]^+$ Calcd for $\text{C}_{33}\text{H}_{27}\text{N}_7\text{O}_{10}\text{Na}$ 704.1717; Found 704.1739.

Quantum Yield determination

Fluorescence quantum yields (Φ_F) of the quinazolinone based monomer was determined using a Photon Technologies International Quanta Master 7/2005 spectrophotometer by the relative method⁵¹ using 9-10 diphenylanthracene (Φ_F in EtOH = 0.95)⁵² and tryptophan (Φ_F in water, pH 7.2 = 0.14)⁵³ as the reference standard in room temperature (**Table S2**). The quantum yields were determined using the integrated fluorescence intensity and an average of five emission scans for each compound and as a triplicate for each calculation. The quantum yield of the unknown $\Phi_{(x)}$ can be calculated by the following equation:

$$\Phi_s = \left(\frac{I_s}{I_{ref}} \right) \cdot \left(\frac{Abs_{ref}}{Abs_s} \right) \cdot \left(\frac{\eta^2_s}{\eta^2_{ref}} \right) \cdot \Phi_{ref}$$

Where $\Phi_{(ref)}$ is the quantum yield of the standard, **Abs** is the absorbance at the excitation wavelength, **I** is the integrated area in the emission curve, the subscripts **s** and **ref** refer to unknown and standard respectively and η is the refractive index of the solvent. By measuring a series of diluted solutions with various absorbance readings the following equation may be used:

$$\Phi_s = \left(\frac{Grad_s}{Grad_{ref}} \right) \cdot \left(\frac{\eta^2_s}{\eta^2_{ref}} \right) \cdot \Phi_{ref}$$

Where Grad is the gradient from the plot of the integrated area in the emission curve versus absorbance at the excitation wavelength.

References

- (1) Wilhelmsson, M. & Tor, Y. Fluorescent Analogues of Biomolecular Building Blocks: Design and Applications (*John Wiley & Sons*, **2016**).
- (2) Ward, D. C., Reich, E. & Stryer, L. Fluorescence studies of nucleotides and polynucleotides. I. Formycin, 2-aminopurine riboside, 2,6-diaminopurine riboside, and their derivatives. *J. Biol. Chem.* **1969**, 244, 1228–1237.
- (3) WO. Patent 2018/121400 AI, PCT/CN2017/117710
- (4) Portela-cubillo, F.; Scott, S.; Walton, J. C. 2- (Aminoaryl) Alkanone O -Phenyl Oximes : Versatile Reagents for Syntheses of Quinazolines. *Chem. Commun.*, **2008**, 2935-2937.
- (5) Sha, Q.; Arman, H.; Doyle, M. P. Three-Component Cascade Reactions with 2,3-Diketoesters: A Novel Metal-Free Synthesis of 5-Vinyl-Pyrrole and 4-Hydroxy-Indole Derivatives. *Org. Lett.* **2015**, 17 (15), 3876–3879.
- (6) Han, B.; Yang, X.-L.; Wang, C.; Bai, Y.-W.; Pan, T.-C.; Chen, X.; Yu, W. CuCl/DABCO/4-HO-TEMPO-Catalyzed Aerobic Oxidative Synthesis of 2-Substituted Quinazolines and 4H-3,1-Benzoxazines. *J. Org. Chem.* **2012**, 77 (2), 1136–1142.
- (7) Mase, N.; Mizumori, T.; Tatemoto, Y. ChemComm Aerobic Copper / TEMPO-Catalyzed Oxidation of Primary Alcohols to Aldehydes Using a Microbubble Strategy to Increase Gas Concentration in Liquid Phase Reactions. *Chem. Commun.*, **2011**, 47, 2086-2088.
- (8) Ijgorodov, N. I.; Downey, W. S. The Influence of Planarity and Rigidity on the Absorption and Fluorescence Parameters and Intersystem Crossing Rate Constant in Aromatic Molecules. *J. Phys. Chem.* **1994**, 98 (22), 5639–5643.
- (9) Berlman, I. B. Empirical Correlation between Nuclear Conformation and Certain Fluorescence and Absorption Characteristics of Aromatic Compounds. *J. Phys. Chem.* **1970**, 74 (16), 3085–3093.
- (10) Thomson, S. A.; Josey, J. A.; Cadilla, R.; Gaul, M. D.; Hassman, C. F.; Luzzio, M. J.; Pipe, A. J.; Reed, K. L.; Ricca, D. J.; Wiethe, R. W.; et al. *Tetrahedron*, **2002**, 51 (22), 1–16.
- (11) Dawseon, W. R.; Windsor, M. W. Fluorescence Yield of Aromatic Compounds. *J. Phys. Chem.*, **1968**, 72, 3251-3260. 4
- (12) Hamal, S.; Hrayama, F. Actinometría Determination of Absolute Fluorescence Quantum Yields. *J. Phys. Chem.*, **1983**, 277 (9), 83–89.
- (13) Kirby, E. P.; Steiner, R. F.; Kirby, E. P.; Steiner, R. F. The Influence of Solvent and Temperature upon the Fluorescence of Indole Derivatives1 H. *J. Phys. Chem.*, **1970**, 74 (28), 4480–4490.

Chapter 4

Conclusion and Outlook

PART 1:

The synthesis of a Fmoc protected thiouracil PNA monomers has been completed after the investigation of different highly acid-labile protecting groups for 2-thione group. This study has shown that the 4-methoxybenzyl protecting group that has been used for Boc-based oligomerization of pcPNA synthesis containing thiouracil residues is also suitable for Fmoc-based oligomerization. Moreover, the 2-methoxybenzyl protecting group was surprisingly robust and the origin of the resistance to acidolysis for the 2-methoxy group appears to be intramolecular stabilization of the protonated species; this extra stability cannot be expected without this particular structural feature. Also, considering the deprotection condition in Boc-based solid-phase peptide synthesis as the thiouracil protection most likely does not persist for Boc-based oligomer synthesis we hypothesized that having the acid-labile sulfur protection is not necessary during the oligomerization. Thus, the oligomerization of a 10-mer PNA sequence was completed with minimum evidence of an increase in truncation products and comparable purity to the previously synthesized PNA sequences using 2-thiouracil protected monomers. Thus, it was found that the protecting group is only necessary during the preparing thiouracil PNA monomer and it can be cleaved prior to the oligomerization. The Fmoc/Boc protected PNA monomer has also been synthesized for 2,6-diaminopurine and used in the synthesis of pseudo-complementary PNA sequences in order to destabilize the PNA-PNA duplex more.

In order to study the DNA strand invasion we developed a new technique which uses the fluorescent analysis. The study of DNA strand invasion using fluorescent techniques, the analyses of the results from melting curves demonstrate that the replacement of a C base with PhpC resulted in an increase in melting temperature. Secondly, as expected, a general increase in melting temperature was observed between DNA-PNA hetero-duplexes. Even though the PNA sequences were two base pairs shorter than their DNA partner, the decrease in repulsion due to the neutrality

of the PNA backbone resulted in increased T_m values. Finally, it appears that with regards to DNA-PNA bonding, 5T in PNA has a slightly stronger bonding interaction with DNA than does a 5U base. This was consistent across all cases when bonding to either the target DNA or target DNA (PhpC). Interestingly, when bonding to complementary PNA this phenomenon is reversed. This phenomenon requires further investigation but likely is a result of the different conformation of PNA-DNA versus PNA-PNA duplexes. The 5U and D monomer incorporation into a PNA shows that and its melting temperature against PNA and DNA shows that the synthesis of PNA sequences containing more pseudo-complementary bases can destabilize the PNA-PNA duplex while the DNA-PNA duplex is more stable. Fluorescence measurements were highly successful and were supportive of the original hypothesis. The target DNA (PhpC) baseline was initially compared to the target DNA (PhpC) paired to cDNA. The change between the “ON” and “OFF” states respectively was clearly evident as an overall change in fluorescence was approximately two-fold. Also, as expected, the fluorescence of the DNA-PNA hybrids in the “ON” state was intermediate between the free target DNA (PhpC) strand and its “OFF” partner. These results are encouraging because it is evident that a simple change in a binding partner can be used to induce a measurable change in fluorescence corresponding to its identity.

PART 2:

Synthesis of PNA monomer carrying functionalized quinazolinone moiety and study of the effect of electron-withdrawing and electron-donating groups has been done. The characterization by fluorescence quantum yield response in different solvents and three different temperatures shows a promising result. Based on the fluorescence studies, methoxy group as an electron-donating group on the 6-position has the highest fluorescence quantum yield. Quinazolinone-based uracil scaffolds show greater fluorescence quantum yields than dihydroquinazolinone compounds. Moreover, the observed emission spectra in lower temperature or glycerol as a more viscous solvent, show higher fluorescence quantum yields. It can be explained by the molecular 3D structure and rigidity as well as the hydrogen bonding between O4 in uracil ring with amide in the

heterocycle ring. So, these uracil analogues can be used as a reporter in PNA probes with expected stabilization of the formed duplex structure.

These results indicate that the PNA probe containing quinazolinone moiety may be a good candidate for reporting binding events by showing “ON-OFF” target effects upon hybridization to complementary nucleobases. In order to study these fluorescence uracil analogues in oligomer level, the incorporation of quinazolinone-based PNA monomer into PNA oligomer was done. Two different PNAs have been synthesized and their thermal melting point and fluorescent response upon hybridization with complementary DNA sequences will be studied as the future work. This PNA oligomer may be used as a reporter probe. Based on the fluorescence quantum yield of quinazolinone-based uracil compounds in different solvents and temperatures, the quinazolinone containing PNA probe may be used to monitor the state of hybridization by stabilizing the duplex structure and fluorescence response (single-stranded or duplex structure).

Supplemental Information

SUPPLEMENTAL INFORMATION.....	S1
General synthetic procedures	S2
Acidolysis studies and half-life calculations.....	S2
Time course studies on the acidolysis of thioesters	S4
Figure S2. ¹ H NMR spectra of ethyl 2-(2-(2-methoxybenzyl)thio)uracil-1-yl)acetate (14a) acidolysis in a solution of 2% TFA and 1% triethylsilane in CDCl ₃ . Benzylic methylene (*), <i>NI</i> - methylene (x).	S5
Figure S3. First order reaction curves for a) ethyl 2-(2-(<i>S</i> -(4 methoxybenzyl)thiouracil-1-yl)acetate, 12a, 17), and b) ethyl 2-(2-(<i>S</i> -(2 methyl-4-methoxybenzyl)thiouracil-1-yl)acetate, 9 treated with 2% TFA, 1% TES in CDCl ₃	S6
Oligomer synthesis.....	S7
RP-HPLC conditions and chromatograms.....	S7
Table S1. Observed high-resolution mass of synthesized PNA oligomers.....	S20
Table S2. Calculated quantum yield values for reference standards in different solvents and temperatures	S20
Figure S4. Emission at 446 nm of single stranded Target DNA (PhpC) upon excitation from 300 nm to 440 nm.	S21
UV-vis absorbance and Beer-Lambert Plots.....	S22
Emission scan spectra	S28
NMR Spectra	S30-105

General synthetic procedures

All chemicals were obtained from commercial sources and were of ACS reagent grade or higher and were used without further purification. Anhydrous and HPLC-grade solvents for PNA synthesis and chromatography were purchased from Caledon Laboratories. All other solvents were dried by passing through activated alumina columns. In all cases, sodium sulfate was used as the drying agent and solvent was removed by reduced pressure with Buchi Rotavapor. Thin-layer chromatography was performed on Silicycle Silica Gel TLC F-254 plates. Unless otherwise specified the R_f values are reported in the solvent system the reaction was monitored in. Flash chromatography was performed with Silicycle SiliaFlash® F60 230-400 mesh silica. All chemical shifts are reported in parts per million (δ), from tetramethylsilane (0 ppm), and are referenced to the residual proton in the respective solvent: CDCl_3 (7.26 ppm), $\text{DMSO}-d_6$ (2.49 ppm), $\text{methanol}-d_6$ (3.31 ppm) for ^1H NMR and CDCl_3 (77.0 ppm) and $\text{DMSO}-d_6$ (39.5 ppm) and $\text{methanol}-d_6$ (49.0 ppm) for ^{13}C NMR. Multiplicities are described as s (singlet), d (doublet), t (triplet), q (quartet), m (multiplet) and br s (broad singlet). Coupling constants (J) are reported in Hertz (Hz). Spectra were obtained on Bruker-400 and INOVA-400 and INOVA-600 instruments. The ^1H NMR and ^{13}C NMR for PNA monomers performed in CDCl_3 show the presence of rotamers. High-resolution mass spectra (HRMS) were obtained using electrospray ionization (ESI).

Acidolysis studies and half-life calculations

The change in the benzylic integration over time was plotted to fit a first-order reaction curve with the natural logarithm of the benzylic proton integration against the reaction time (**Figure S1**). A first-order reaction is dependent on the concentration of a single reactant (**Eq. 1**), thus the rate equation is expressed as:

$$\text{rate} = -\frac{d[A]}{dt} = k[A]$$

The integration of the first-order rate equation (**Eq. 2**) yields a linear equation (**Eq. 3**) with respect to the natural logarithm of the concentration of the reactant. By considering when the reaction

concentration has diminished by one-half (**Eq. 4**), an expression for the half-life of reaction emerges, (**Eq. 5**)

$$\int_{[A]_o}^{[A]} \frac{d[A]}{[A]} = \int_{t_o}^t -k dt \quad (2)$$

$$\ln[A] - \ln[A]_o = -kt \quad (3)$$

$$\frac{1}{2} = e^{-kt_{\frac{1}{2}}} \quad (4)$$

$$t_{\frac{1}{2}} = -\frac{\ln 2}{k} \quad (5)$$

Using the rate constant determined from **Figure S1**, the half-life of the acidolysis was estimated.

Time course studies on the acidolysis of thioesters

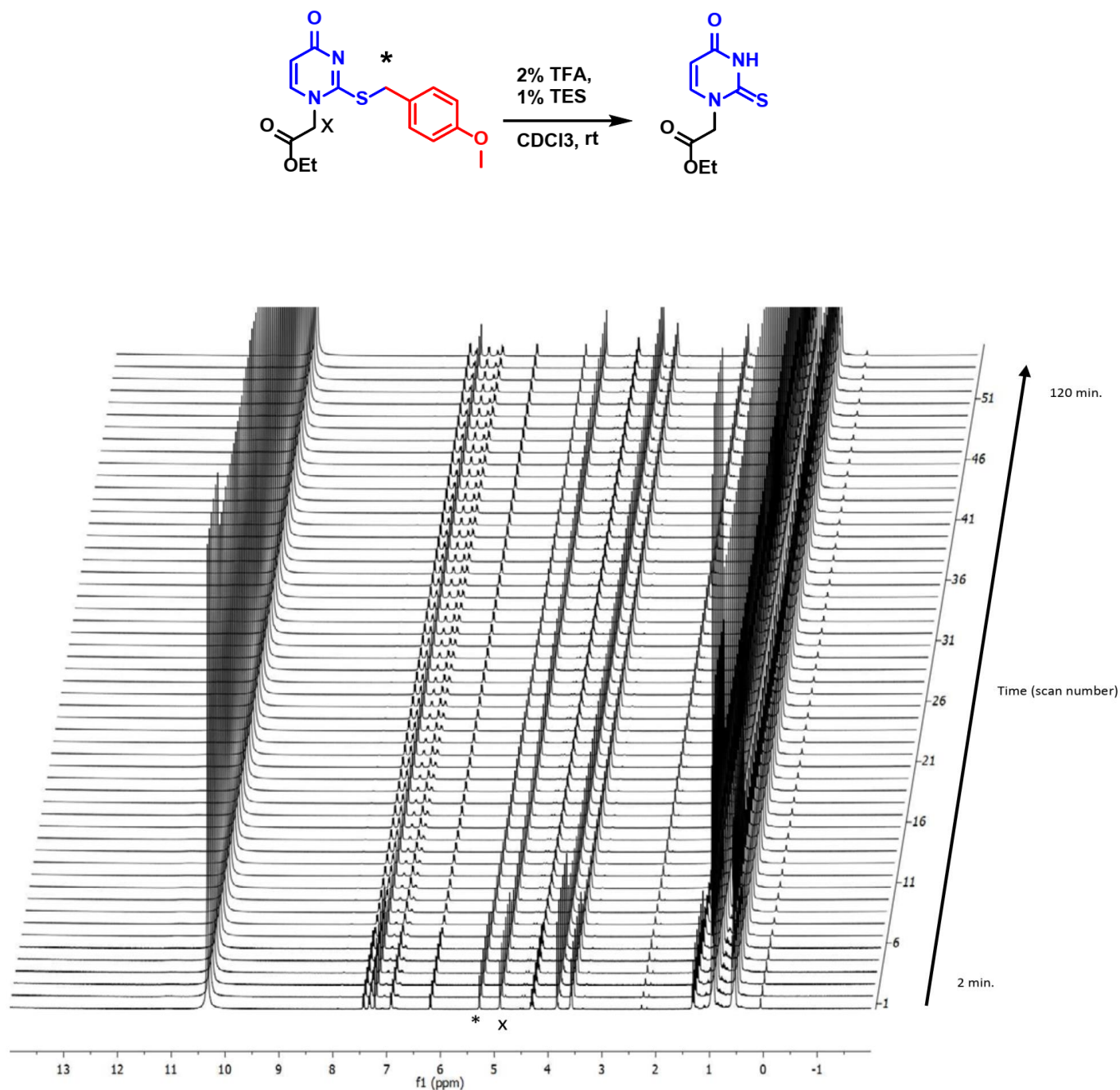


Figure S1. ¹H NMR spectra of ethyl 2-(2-((4-methoxybenzyl)thio)uracil-1-yl)acetate (12a) acidolysis in a solution of 2% TFA and 1% triethylsilane in CDCl₃. Benzylic methylene (*), N1-methylene (x).

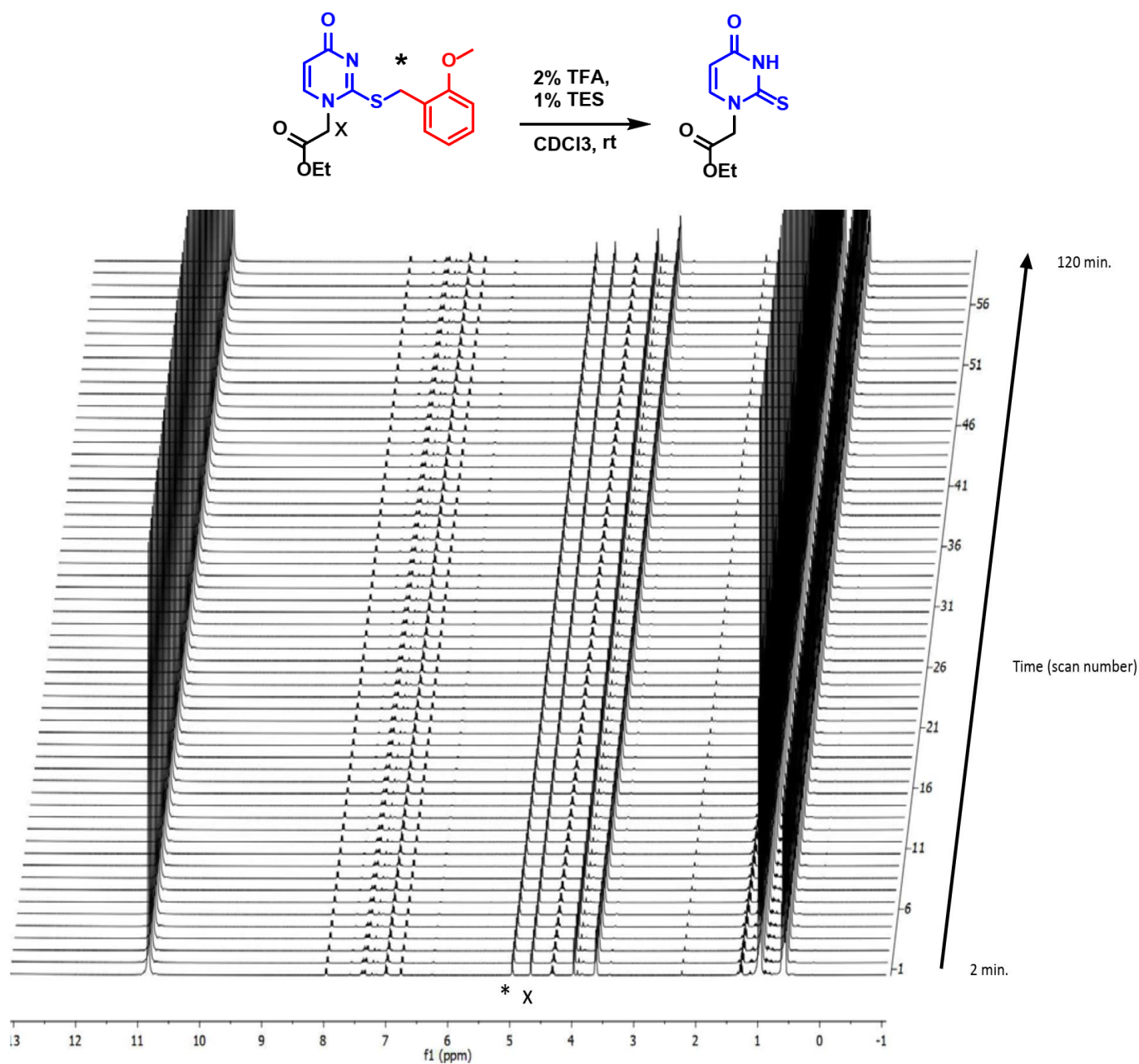


Figure S2. ¹H NMR spectra of ethyl 2-(2-(2-methoxybenzyl)thio)uracil-1-yl)acetate (14a) acidolysis in a solution of 2% TFA and 1% triethylsilane in CDCl₃. Benzylic methylene (*), N1-methylene (x).

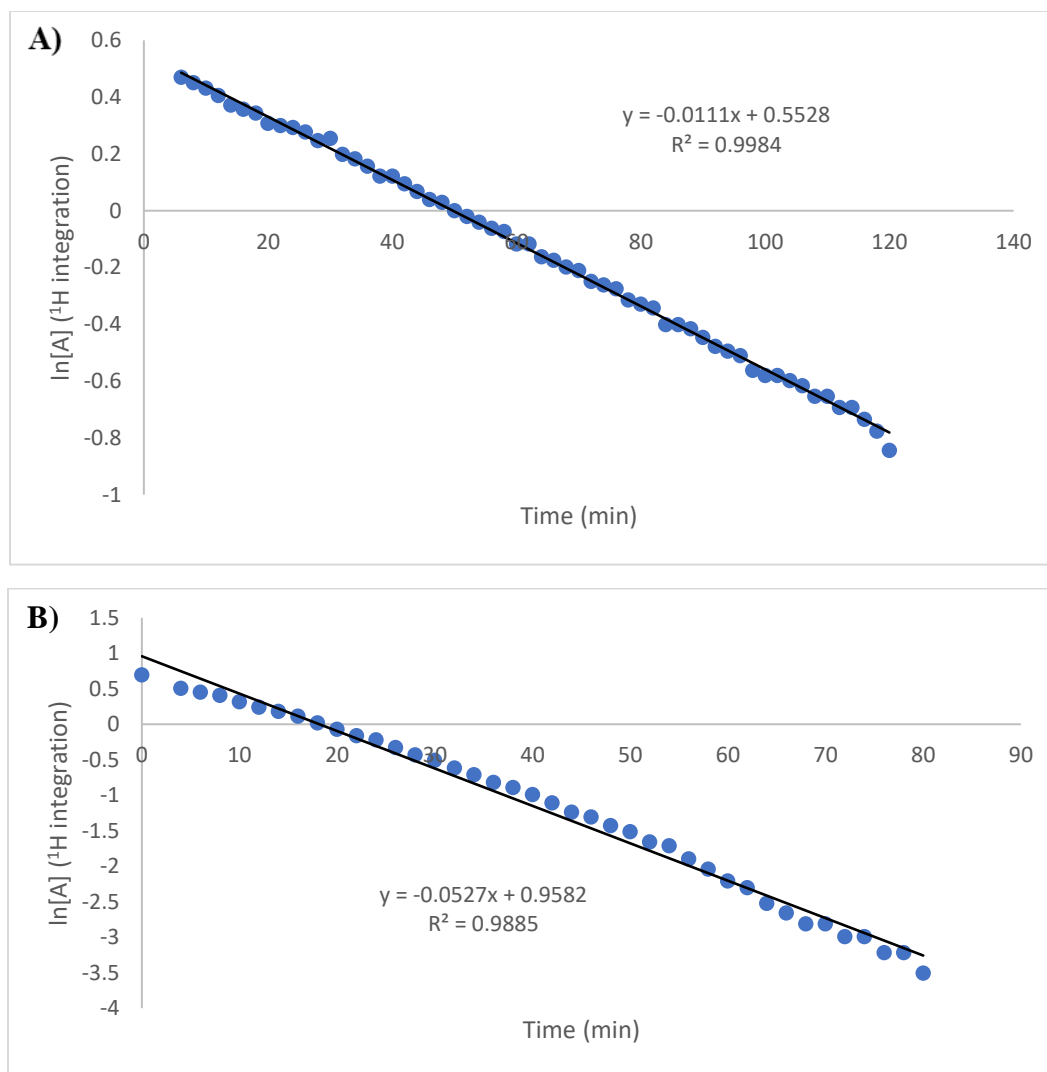


Figure S3. First order reaction curves for a) ethyl 2-(2-(S-(4 methoxybenzyl)thiouracil-1-yl)acetate, 12a, 17), and b) ethyl 2-(2-S-(2 methyl-4-methoxybenzyl)thiouracil-1-yl)acetate, 9 treated with 2% TFA, 1% TES in CDCl_3 .

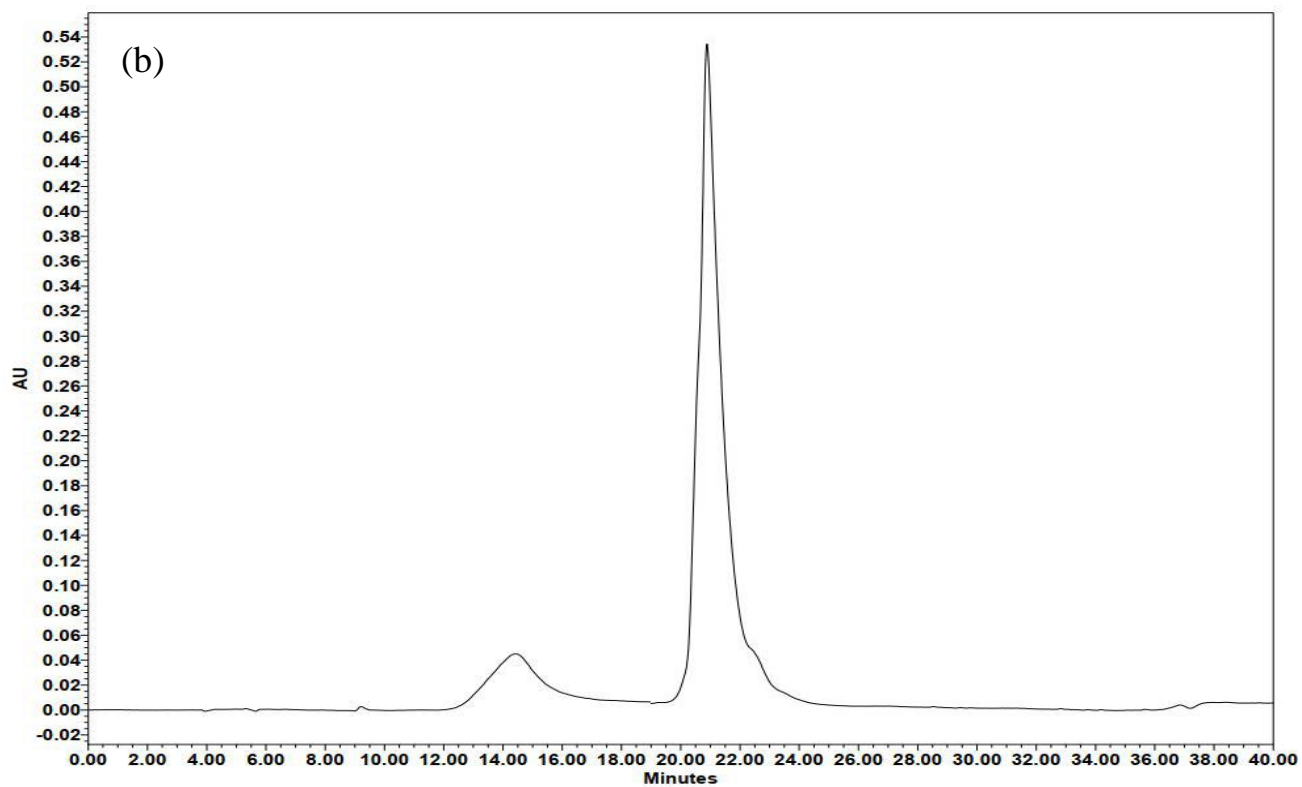
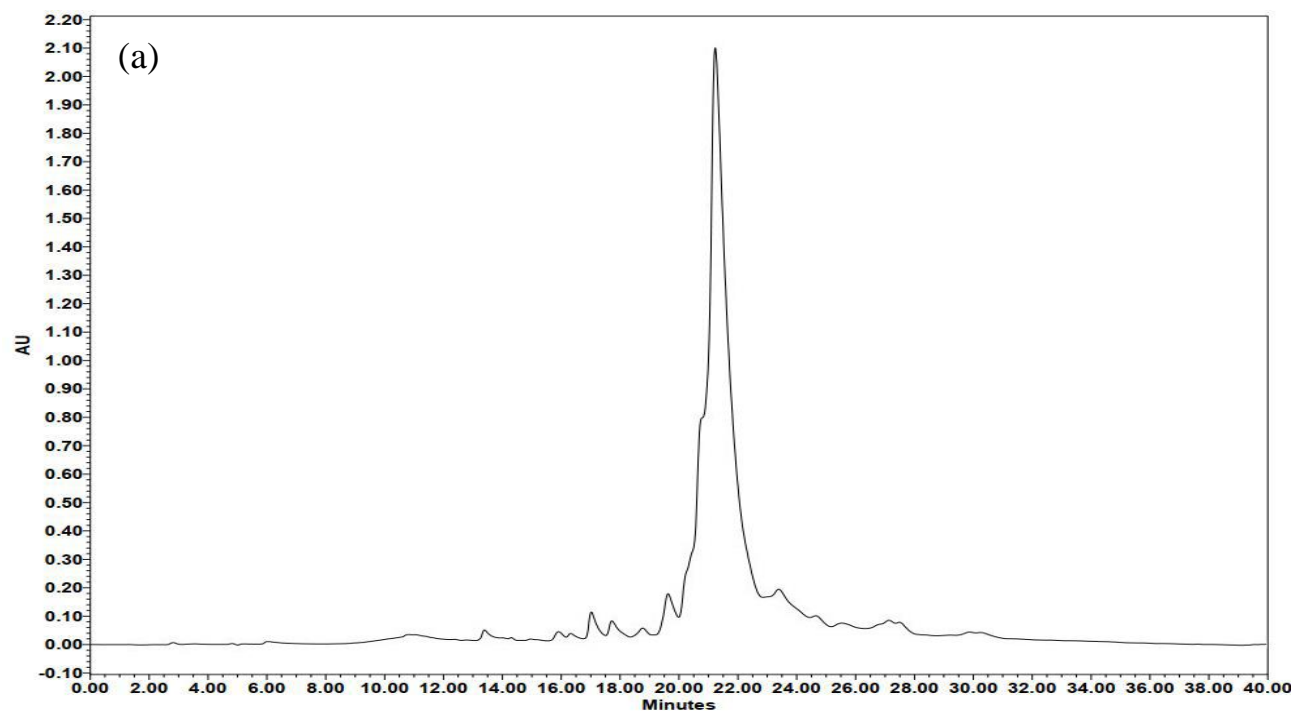
Oligomer synthesis

PNA oligomers were synthesized using the ABI 433A peptide synthesizer manufactured by Perkin Elmer Applied Biosystems. Oligomerization was carried out using newly synthesized ³U monomer, commercially available PNA monomers: Fmoc-A(Bhoc)-AEG-OH, Fmoc-G(Bhoc)-AEG-OH, and Fmoc-C(Bhoc)-AEG-OH, Fmoc-T(Bhoc)-AEG-OH (purchased from PolyOrg, Inc.), and N α -Fmoc-N ϵ -Boc-L-lysine (purchased from Chem-Impex Int'l Inc.), using standard Fmoc-based solid-phase synthesis protocol. Fmoc-RAM-PS was used as a solid support resin preloaded with lysine at 0.057 mmol/g. The synthesis was carried out on a 5.0 μ mol scale. Monomers were prepared with 25 μ mol dissolved in 110 μ L. Solutions of 0.4 M diisopropylethylamine in *N*-methyl-2-pyrrolidone (NMP) and 0.19 M HBTU in NMP were prepared for monomer coupling. Fmoc deprotection was performed using a solution of 20% 4-methylpiperidine in dimethylformamide. Unreacted terminal amino groups were capped with acetic anhydride, using a solution of 1:25:25 acetic anhydride: pyridine: NMP. Following automated synthesis, the resin was treated with a solution of 95 % trifluoroacetic acid and 5% triethylsilane to cleave the oligomer from the resin and remove the protecting group from the nucleobases (Bhoc) and amino group (Boc). The solvent was then evaporated under a nitrogen stream, the resulting residue was washed twice with cold ether, dissolved in a solution of 0.05% trifluoroacetic acid in water then purified by reverse-phase HPLC. Reverse-phase HPLC was performed on an Agilent Microsorb-MV 100-5 C18 250 \times 4.6 mm column heated to 50 °C. The purified PNA oligomer was eluted using a gradient (water/0.1 % trifluoroacetic acid to acetonitrile/0.1 % trifluoroacetic acid).

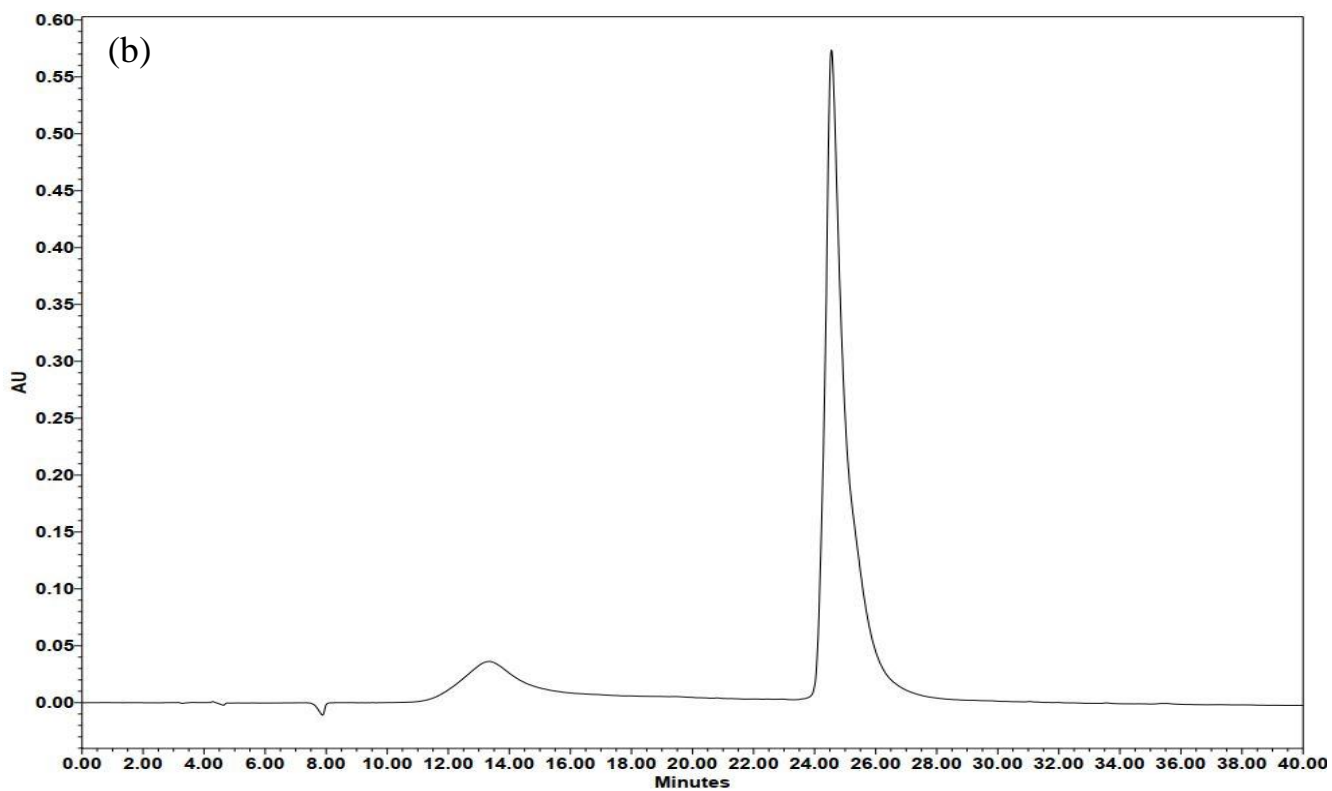
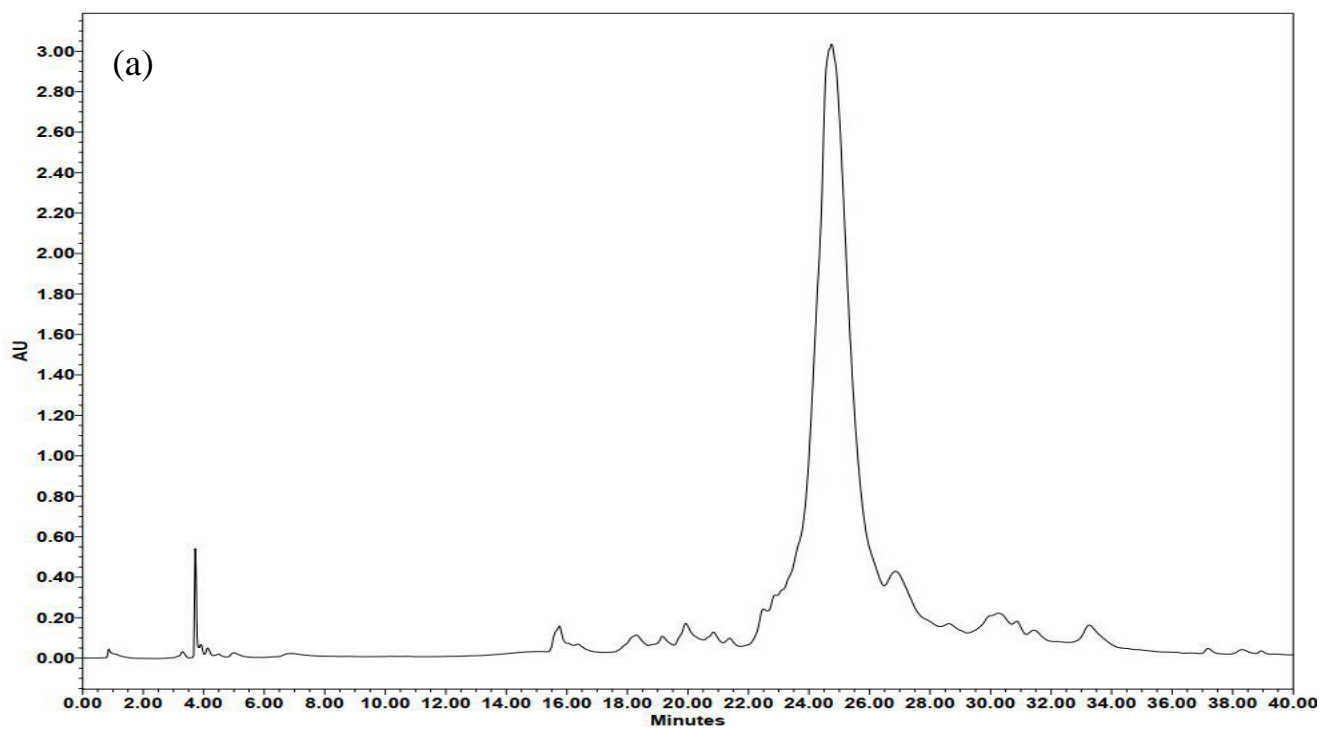
RP-HPLC conditions and chromatograms

For PNA oligomers: 0-50% B in 50 min and 50-100% B in 10 min (Mobile phase A: H₂O containing 0.1% TFA. Mobile phase B: acetonitrile containing 0.1% TFA) (unless otherwise stated). For DNA oligomers: 0-20% A in 20 min and 20-100% A in 10 min (Mobile phase A: Acetonitrile. Mobile phase B: 0.1 M TEAA buffer). The flow rate was 1 mL/min.

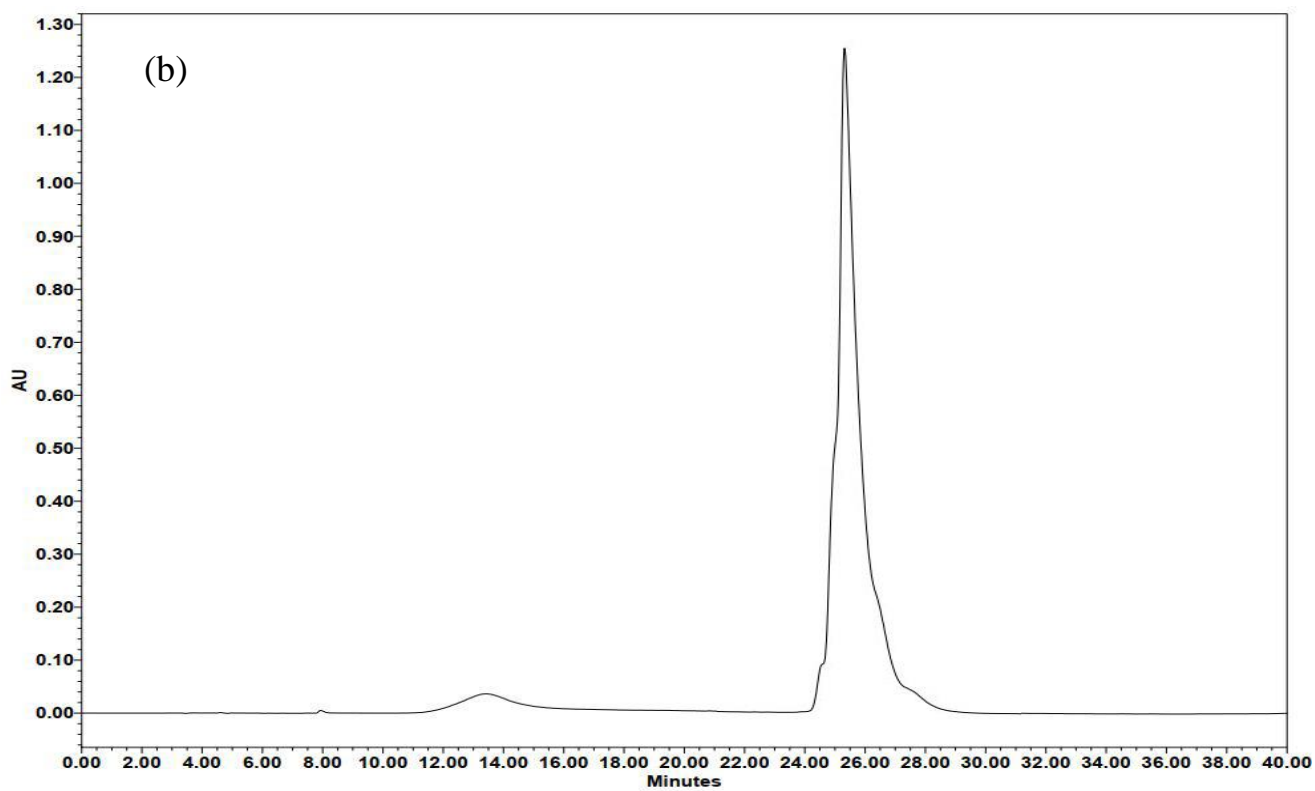
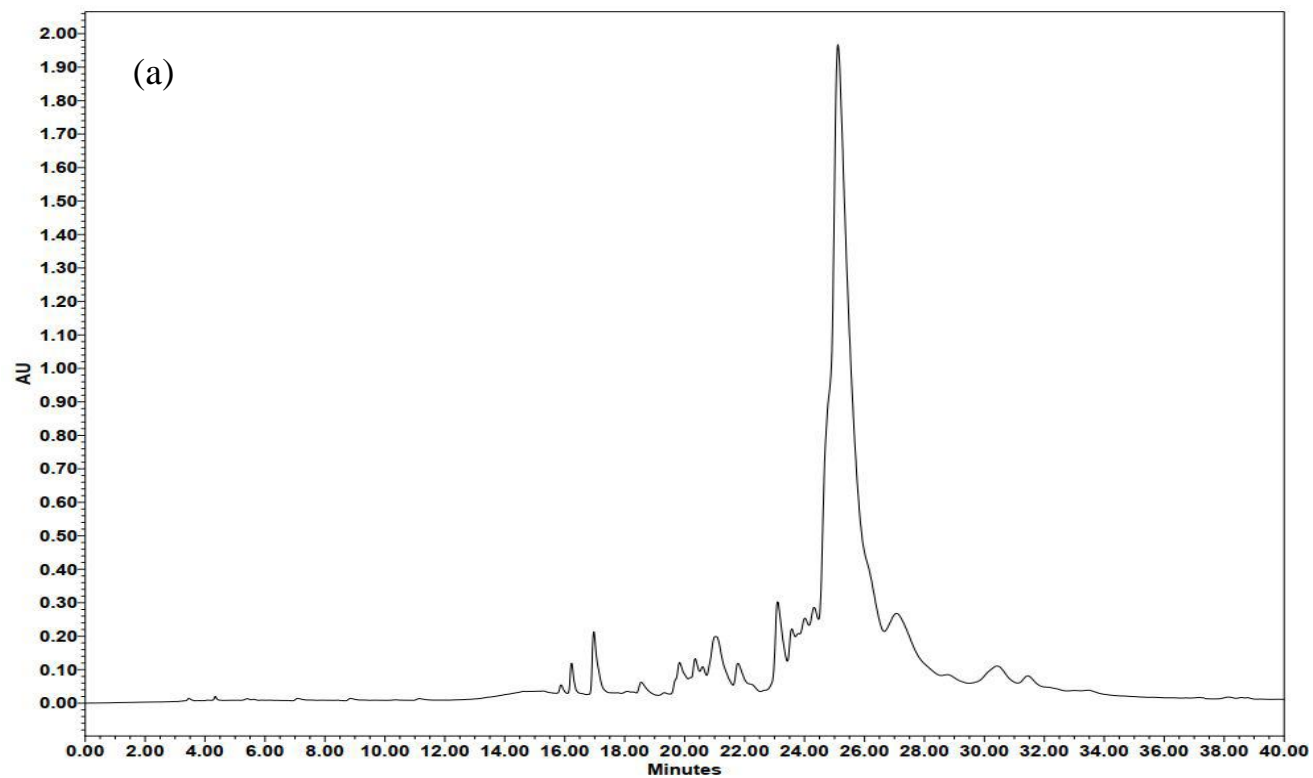
RP-HPLC chromatograms of the crude (a) and pure (b) PNA oligomer **H-Lys-AGTGATCTAC-Lys-NH₂**



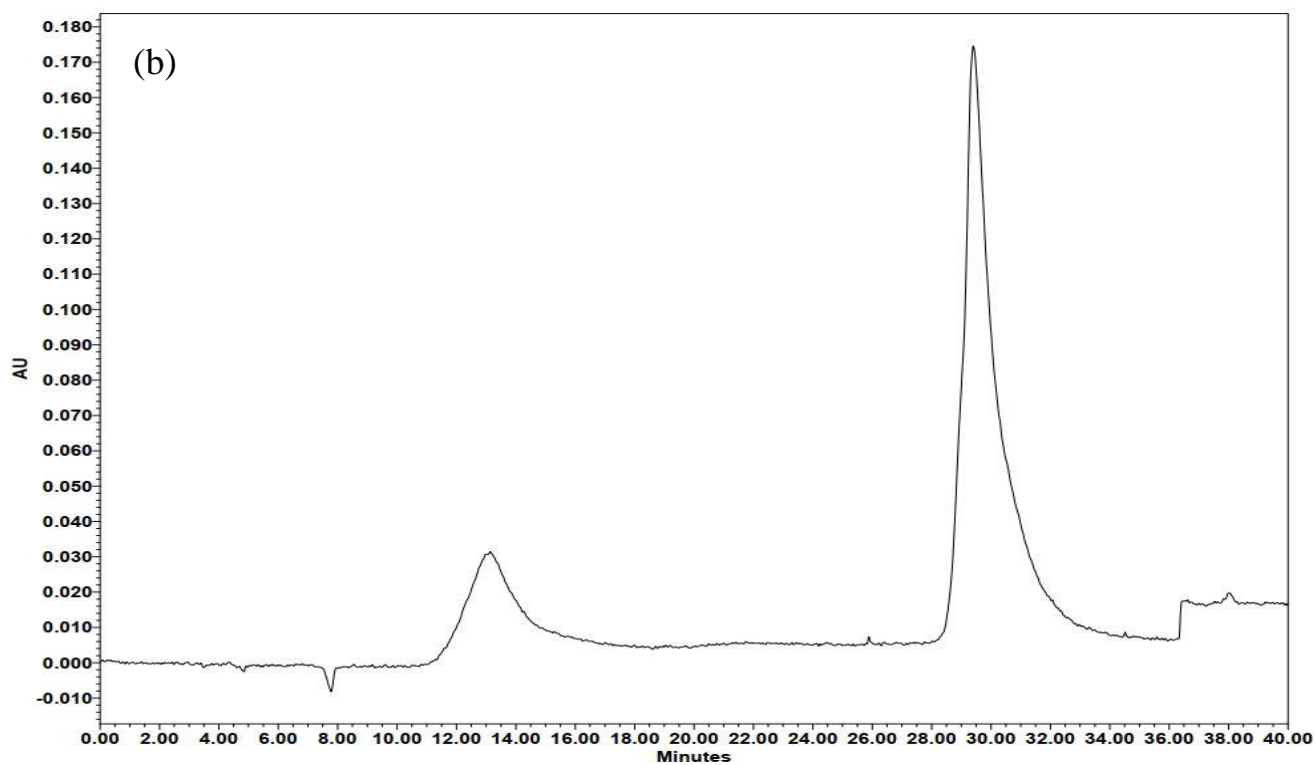
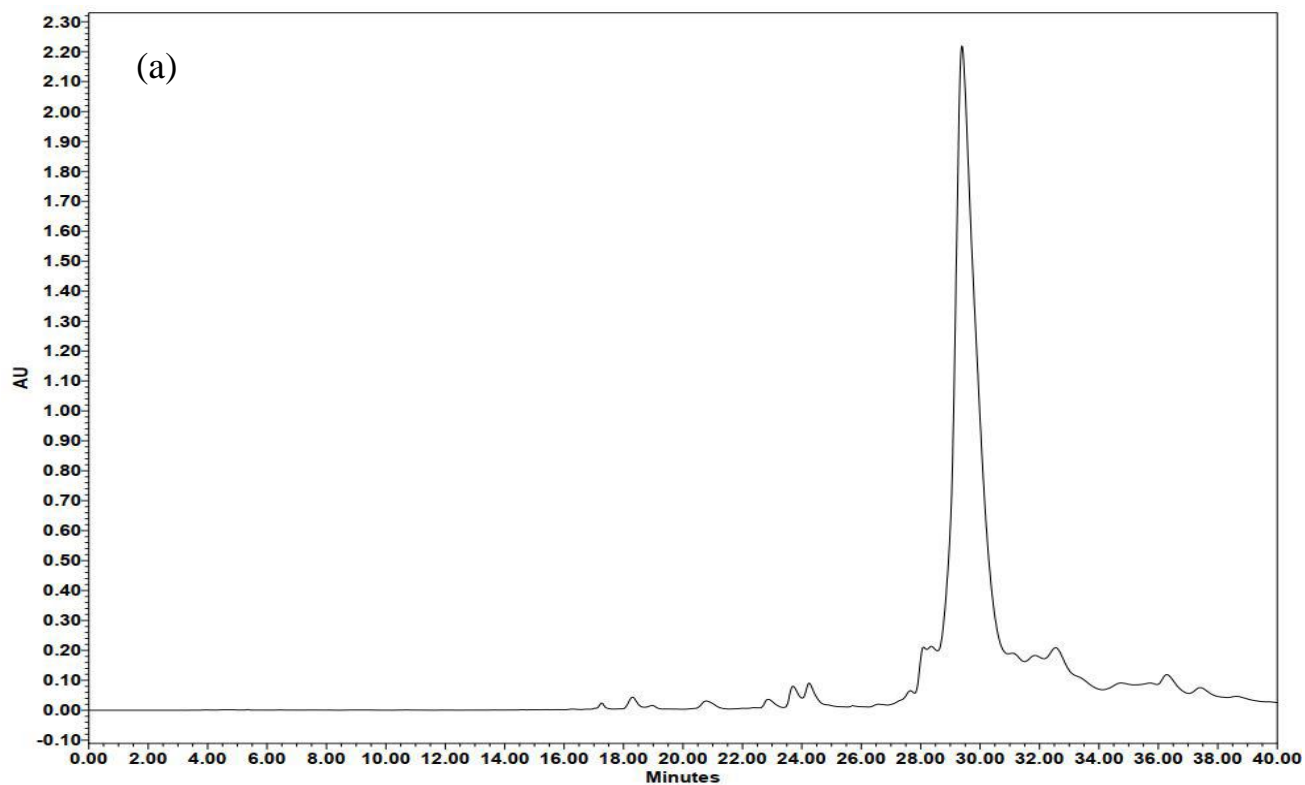
RP-HPLC chromatograms of the crude (a) and pure (b) PNA oligomer **H-Lys-G^sUAGA^sUCAC^sU-Lys-NH₂** (no PG for thiouracil)



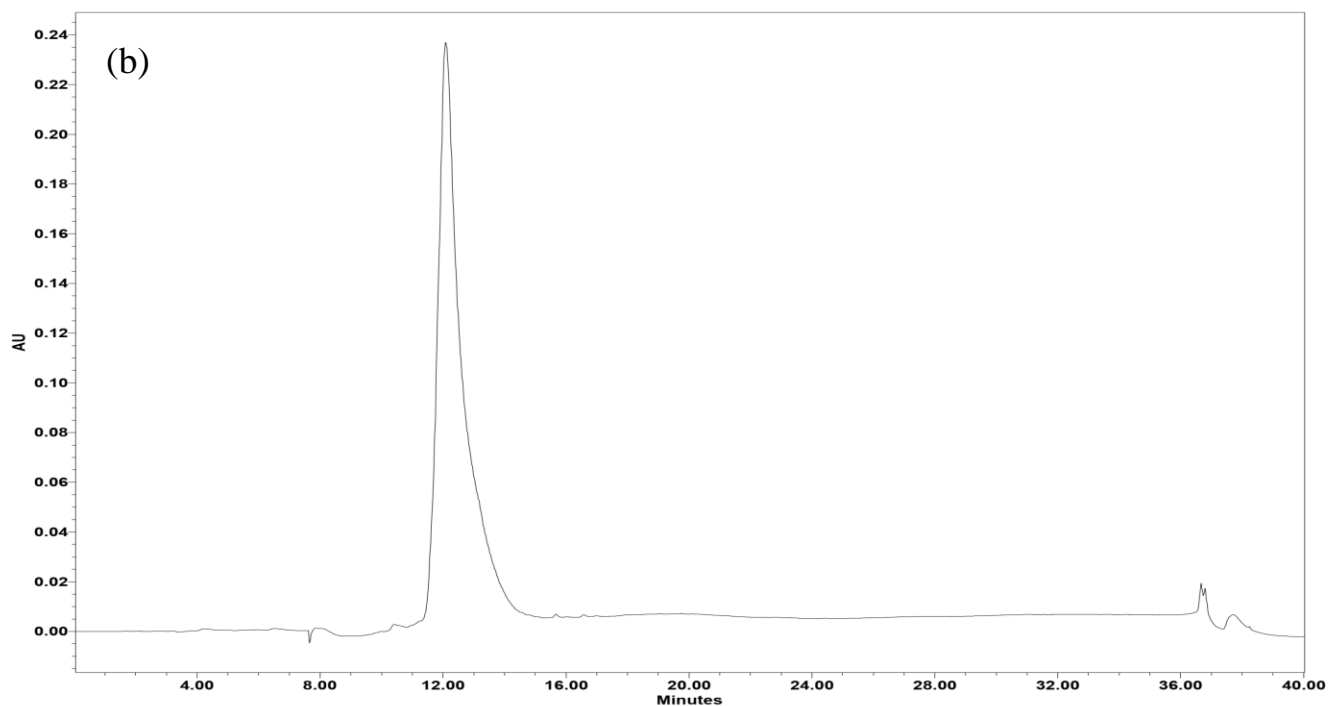
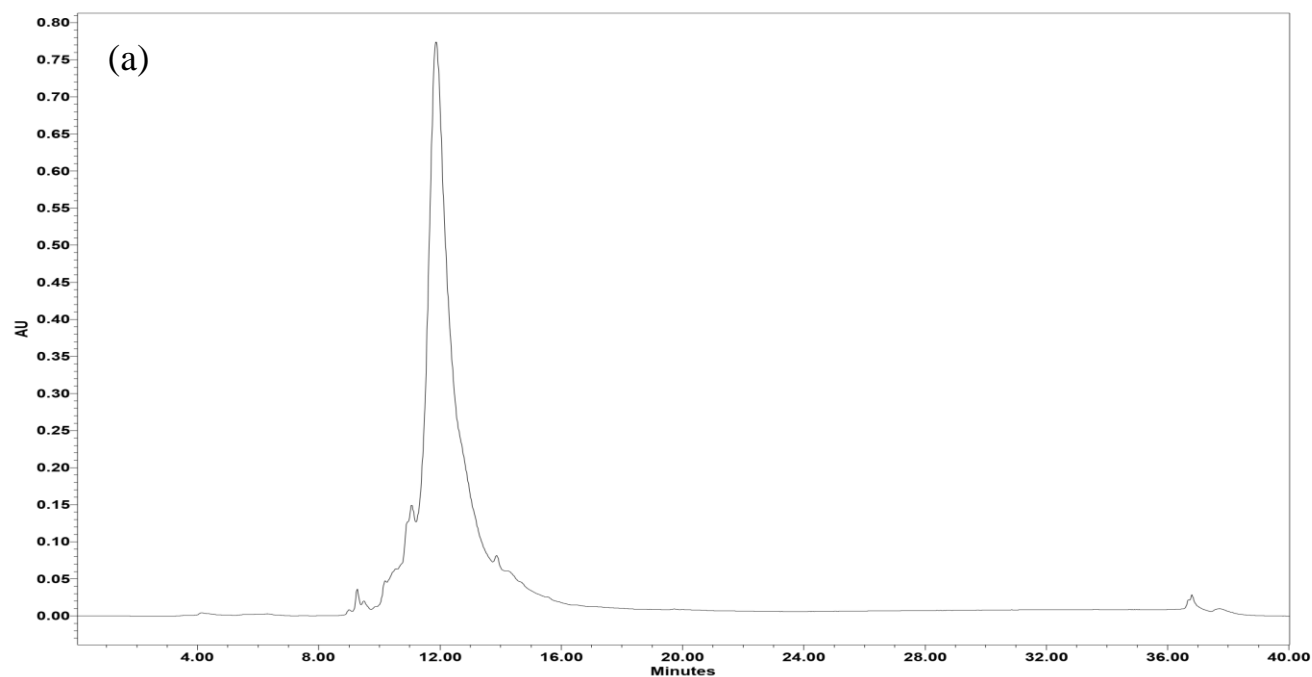
RP-HPLC chromatograms of the crude (a) and pure (b) PNA oligomer **H-Lys-G^sUAGA^sUCAC^sU-Lys-NH₂**



RP-HPLC chromatograms of the crude (a) and pure (b) PNA oligomer **H-Lys-G^sTAGA^sTCAC^sT-Lys-NH₂**

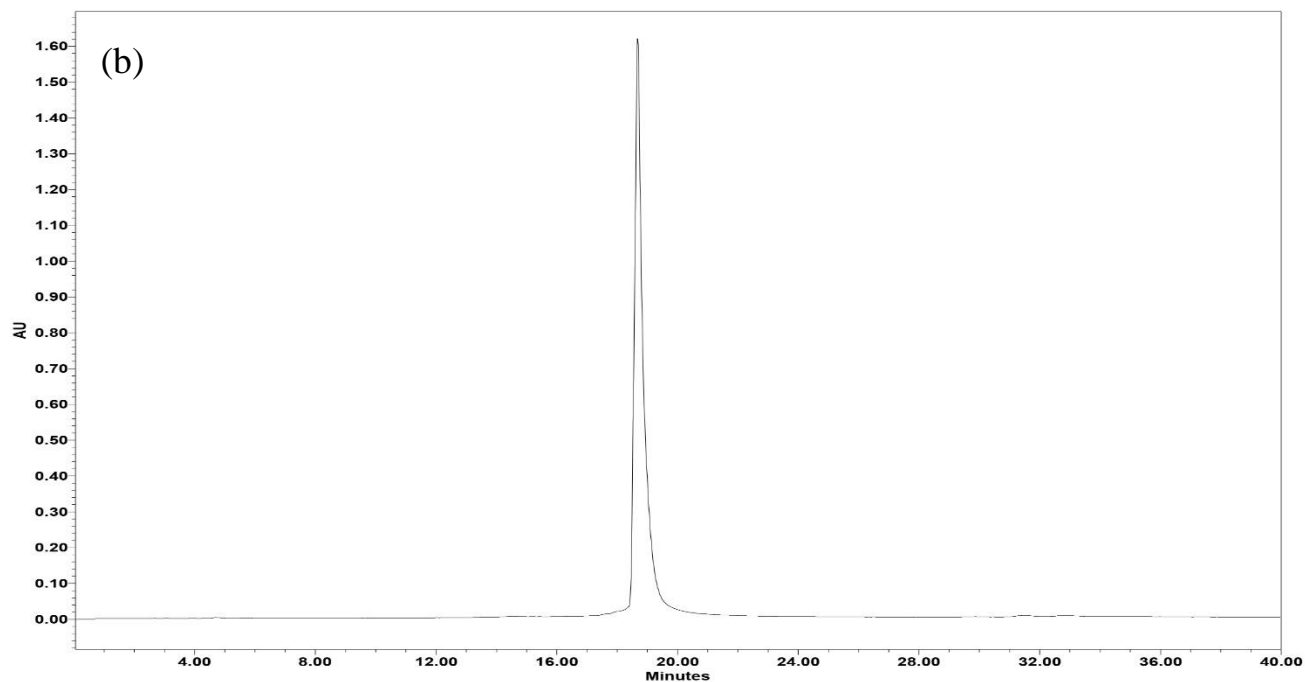
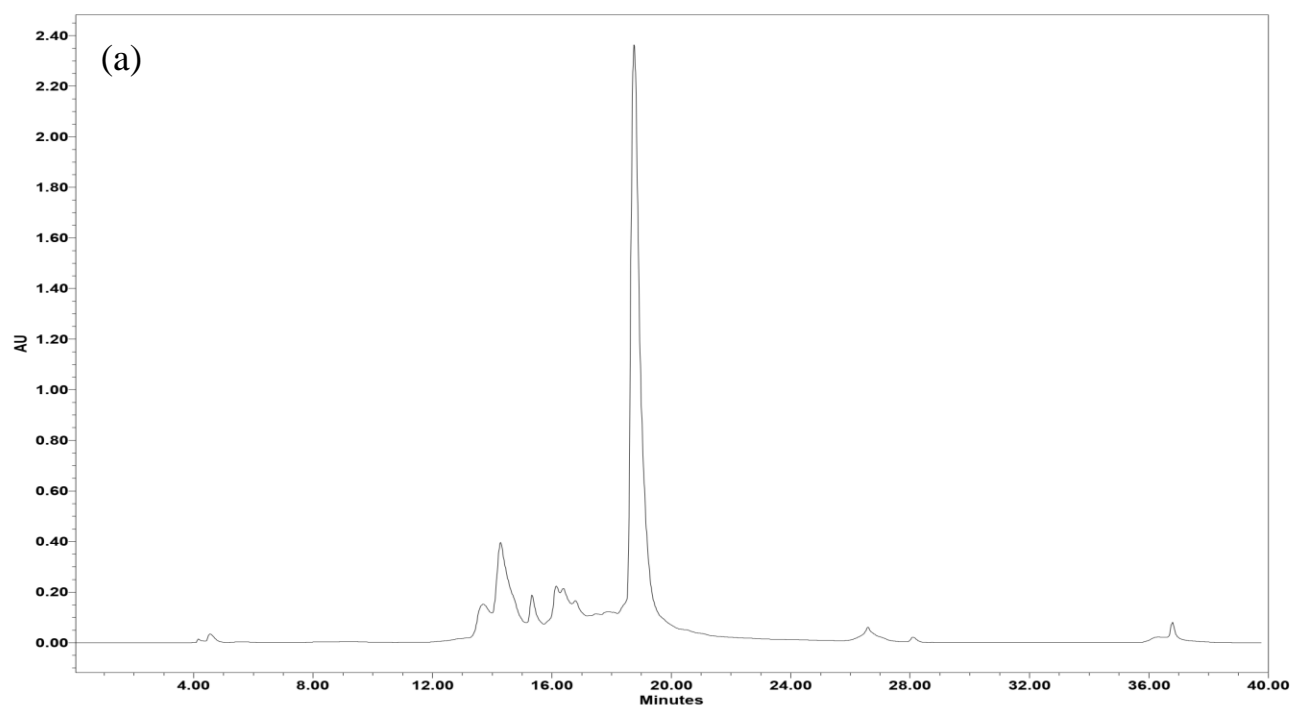


RP-HPLC chromatograms of the crude (a) and pure (b) PNA oligomer **H-Lys-AG^sUGA^sUC^sUAC-Lys-NH₂** *



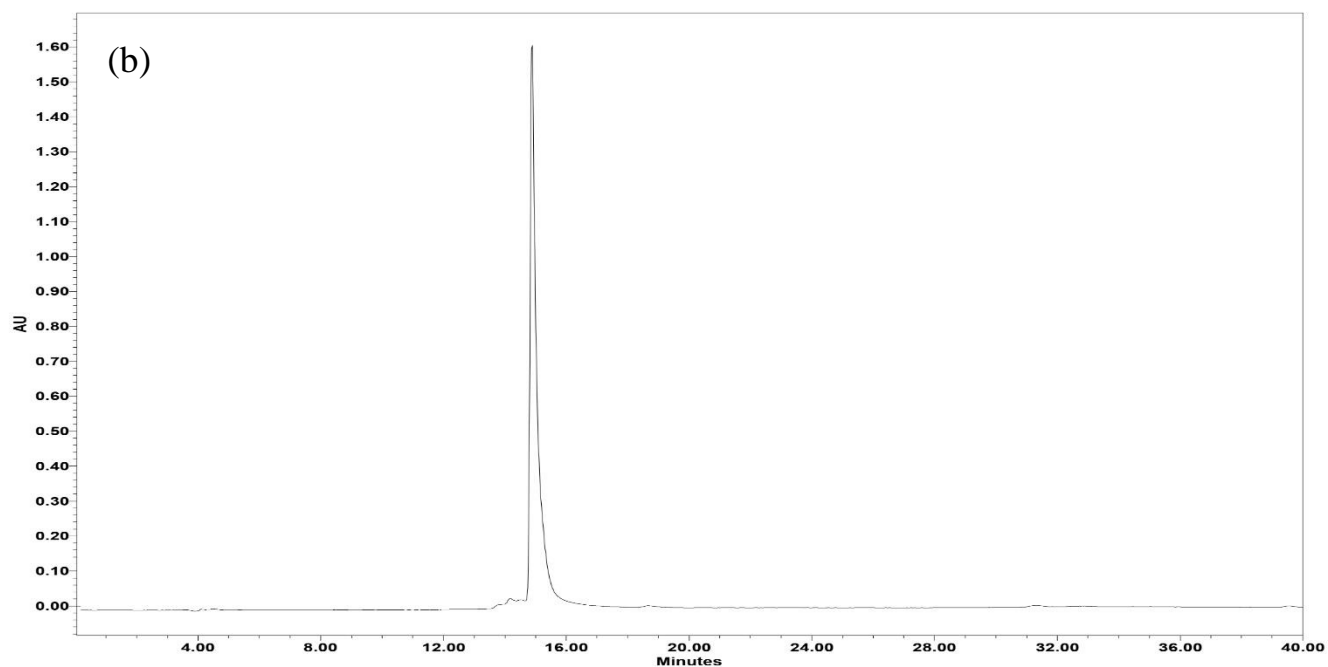
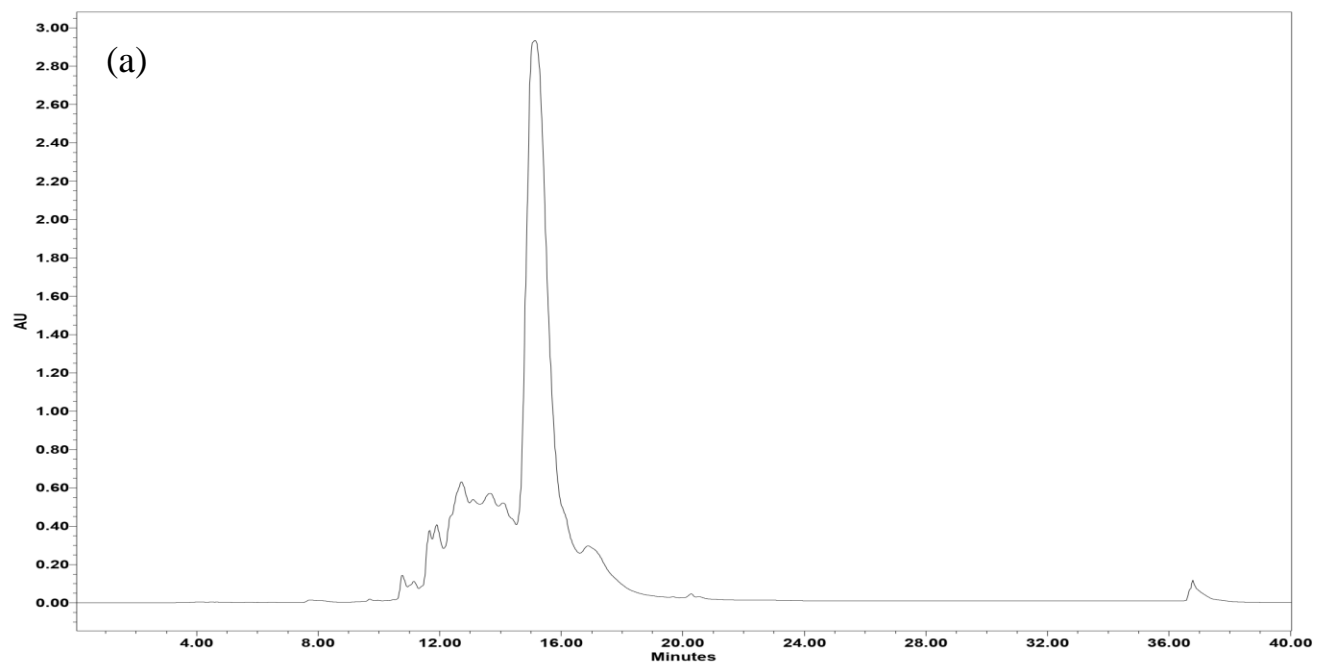
*0-50% B in 50 min and 50-100% B in 10 min (Mobile phase A: H₂O containing 0.1% TFA.
Mobile phase B: acetonitrile containing 0.1% TFA)

RP-HPLC chromatograms of the crude (a) and pure (b) PNA oligomer **H-Lys-DG^sUGD^sUC^sUDC-Lys-NH₂^{*}**



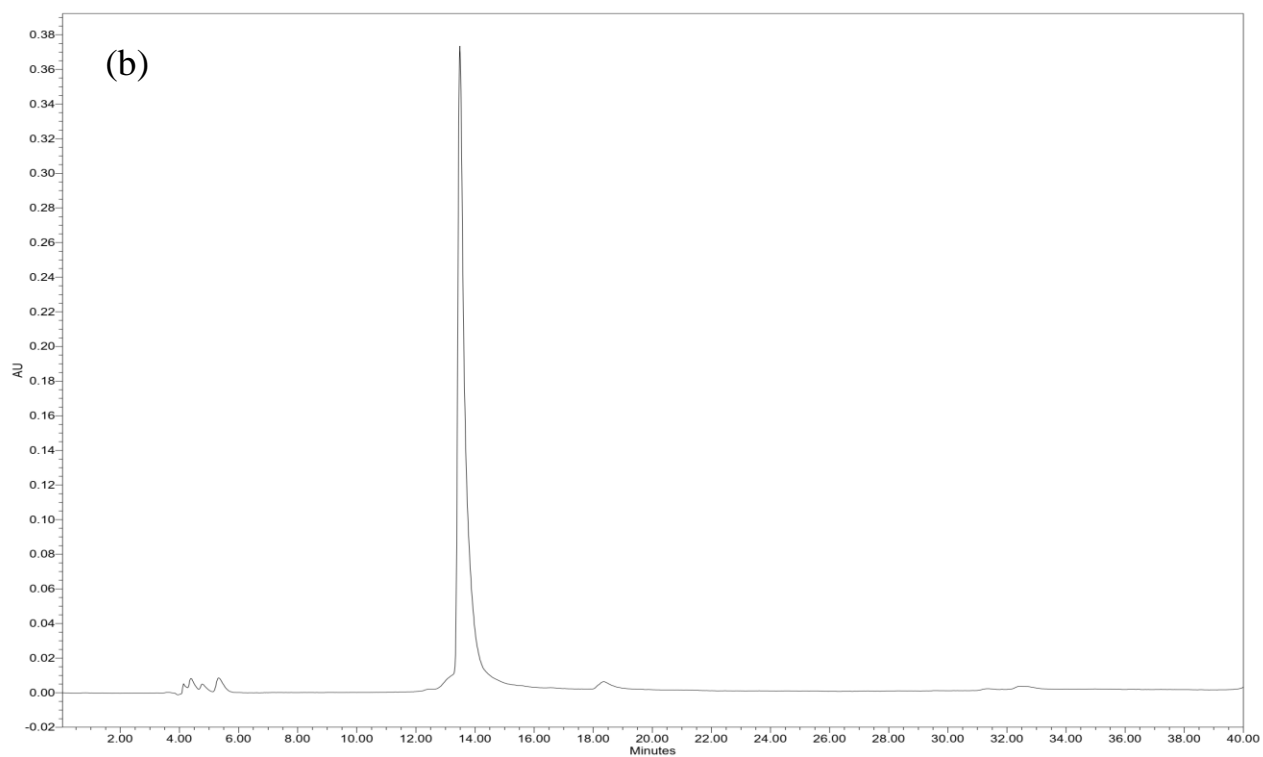
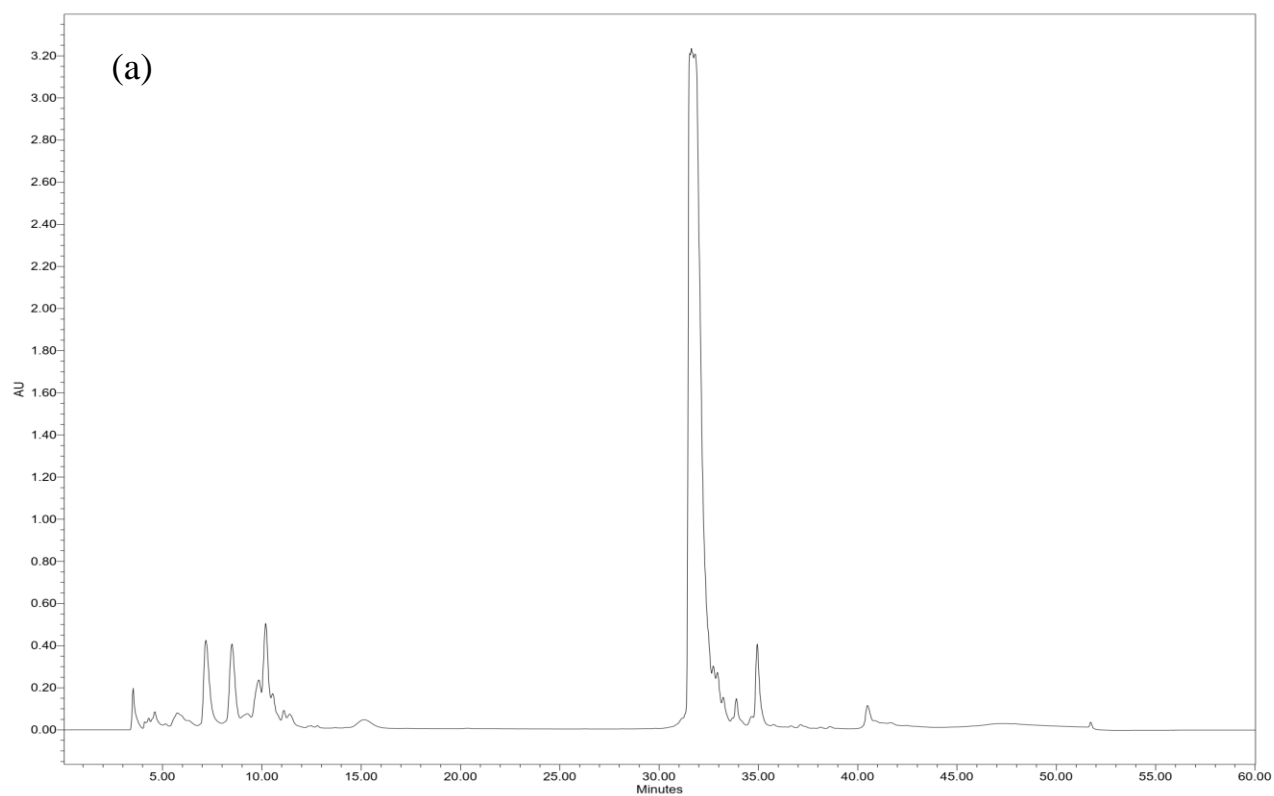
*0-50% B in 50 min and 50-100% B in 10 min (Mobile phase A: H₂O containing 0.1% TFA.
Mobile phase B: acetonitrile containing 0.1% TFA)

RP-HPLC chromatograms of the crude (a) and pure (b) PNA oligomer **H-Lys-G^sUDGD^sUCDCT-Lys-NH₂^{*}**

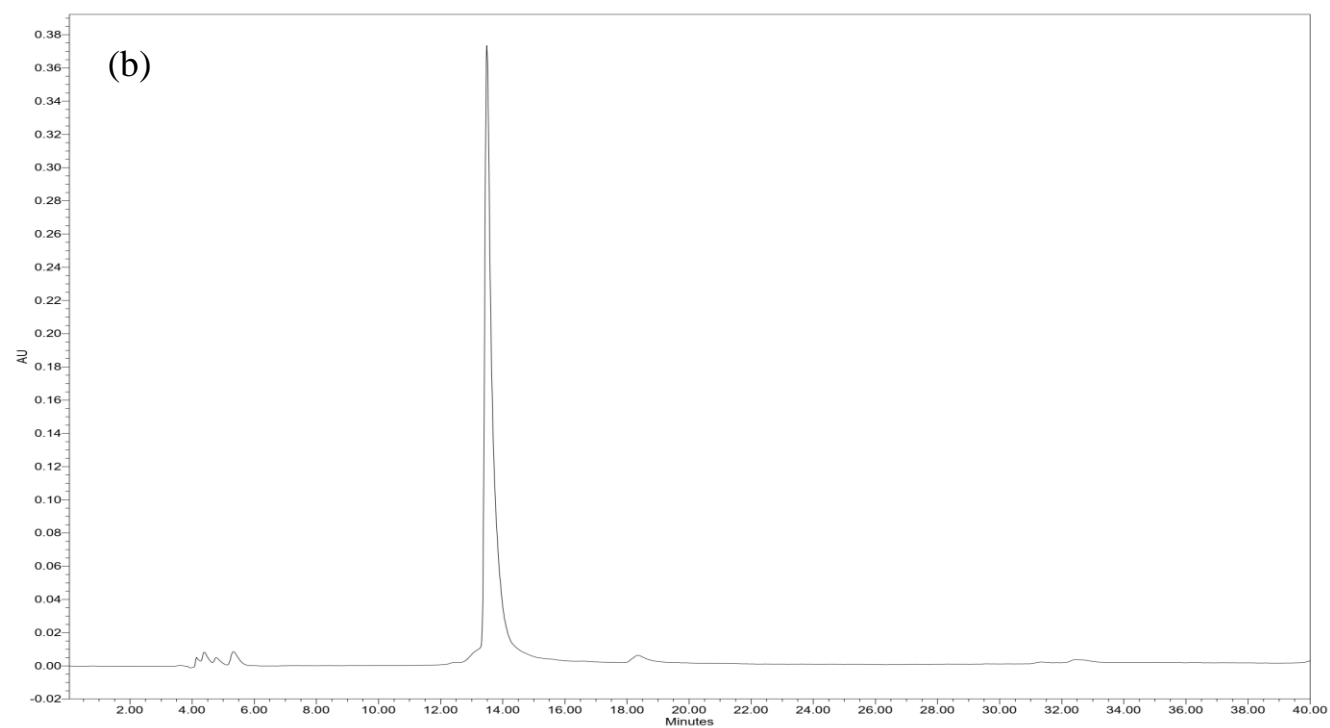
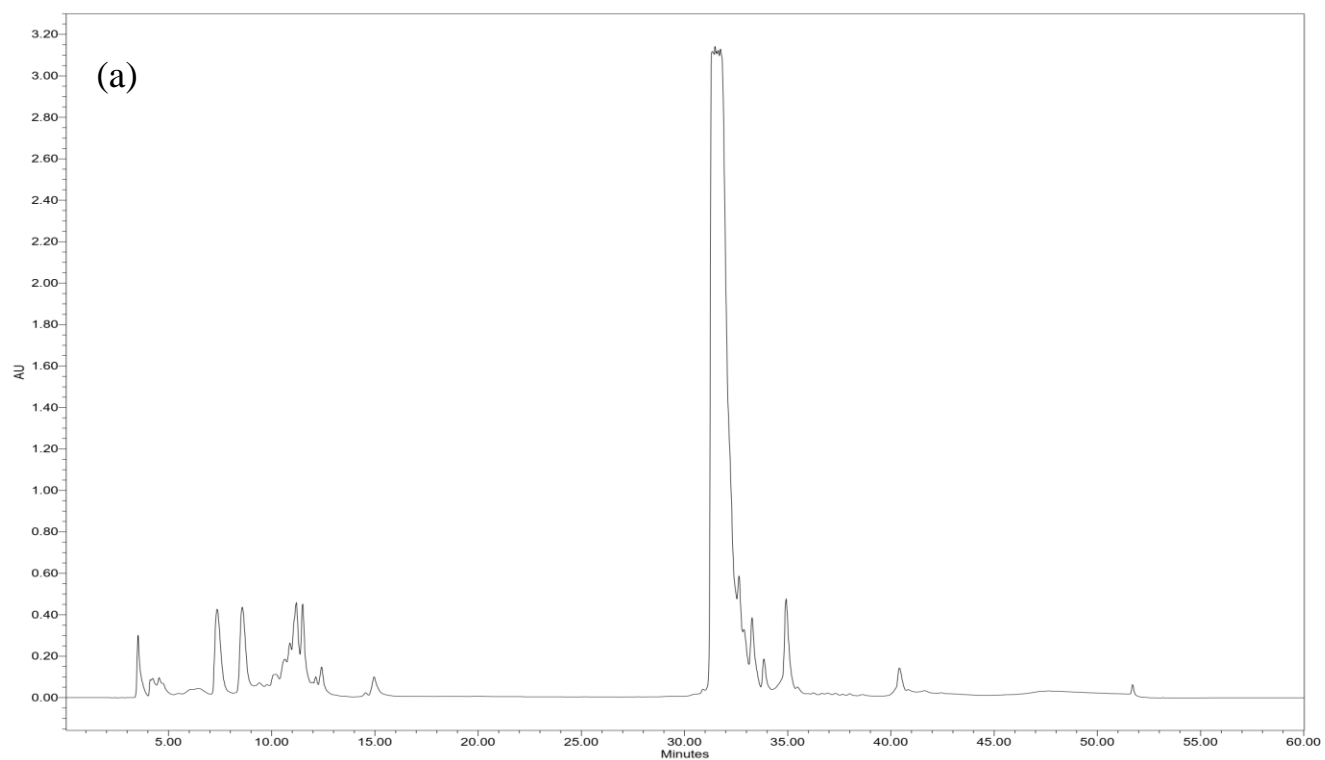


*0-50% B in 50 min and 50-100% B in 10 min (Mobile phase A: H₂O containing 0.1% TFA.
Mobile phase B: acetonitrile containing 0.1% TFA)

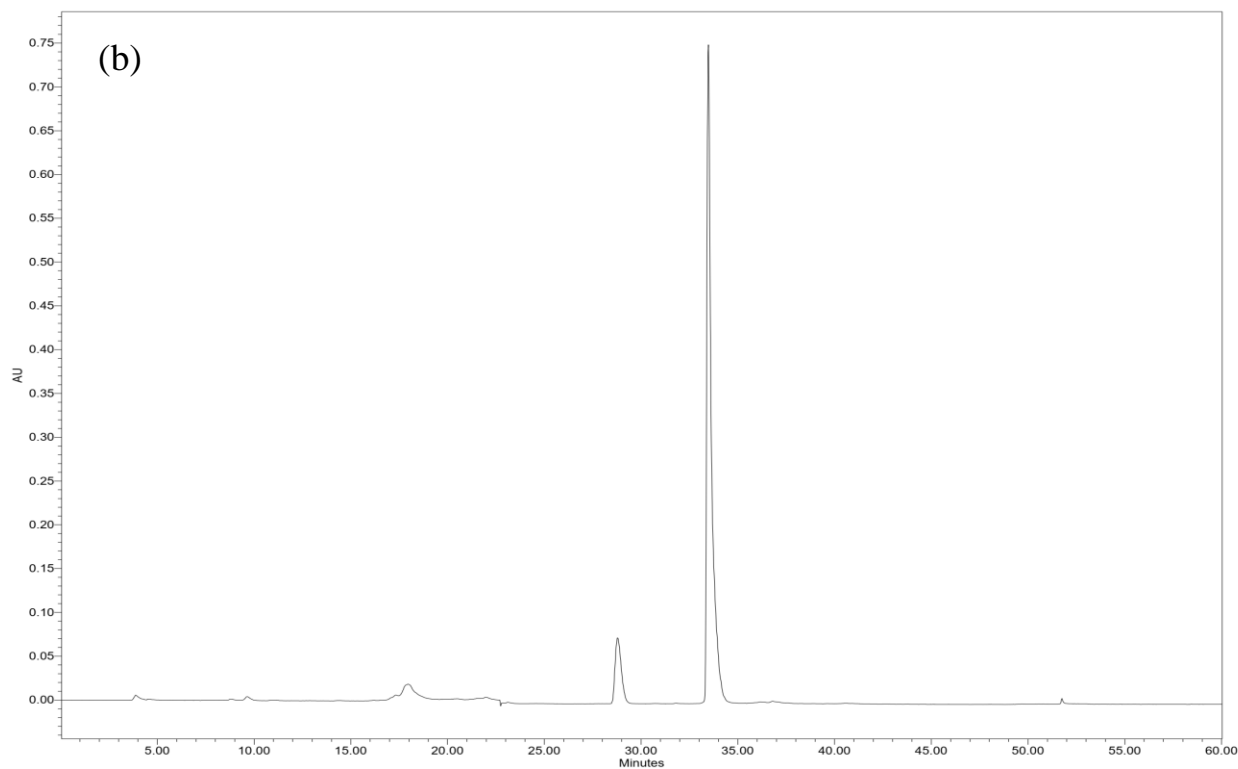
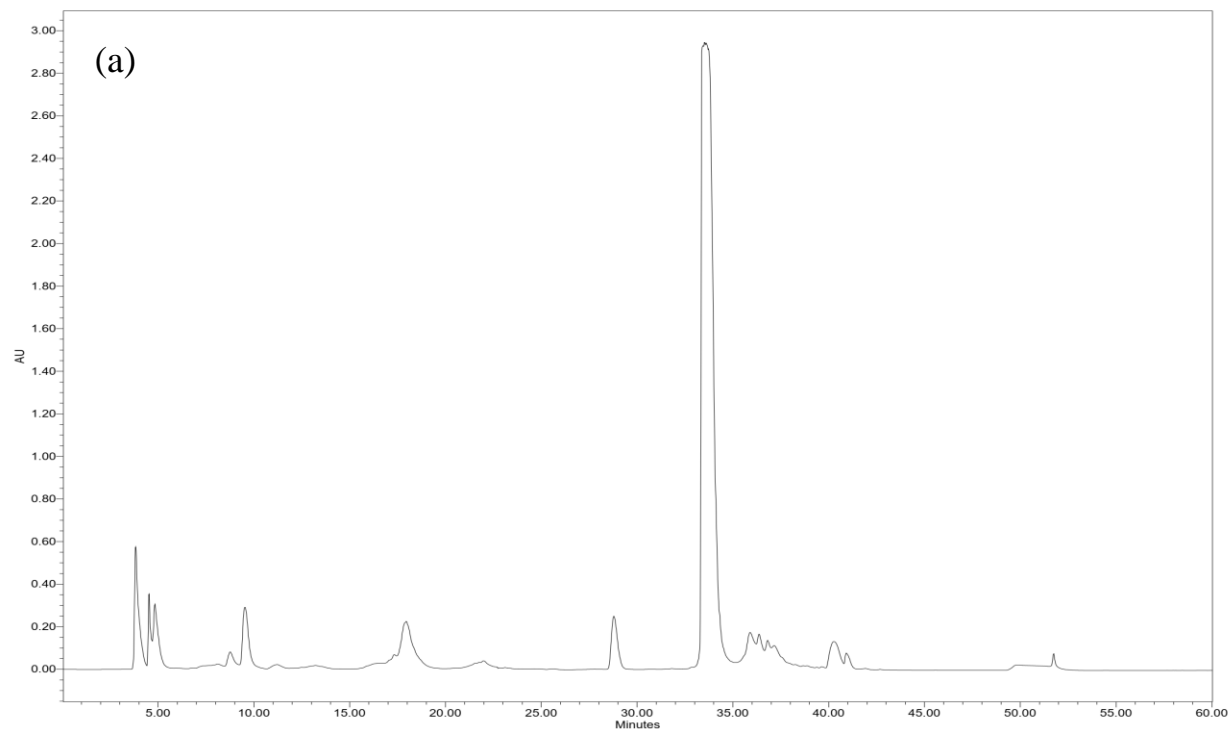
RP-HPLC chromatograms of the (a) crude (DMT-on) and (b) pure (DMT-off) PNA oligomer **5'**
AGTGATCTACCT 3'

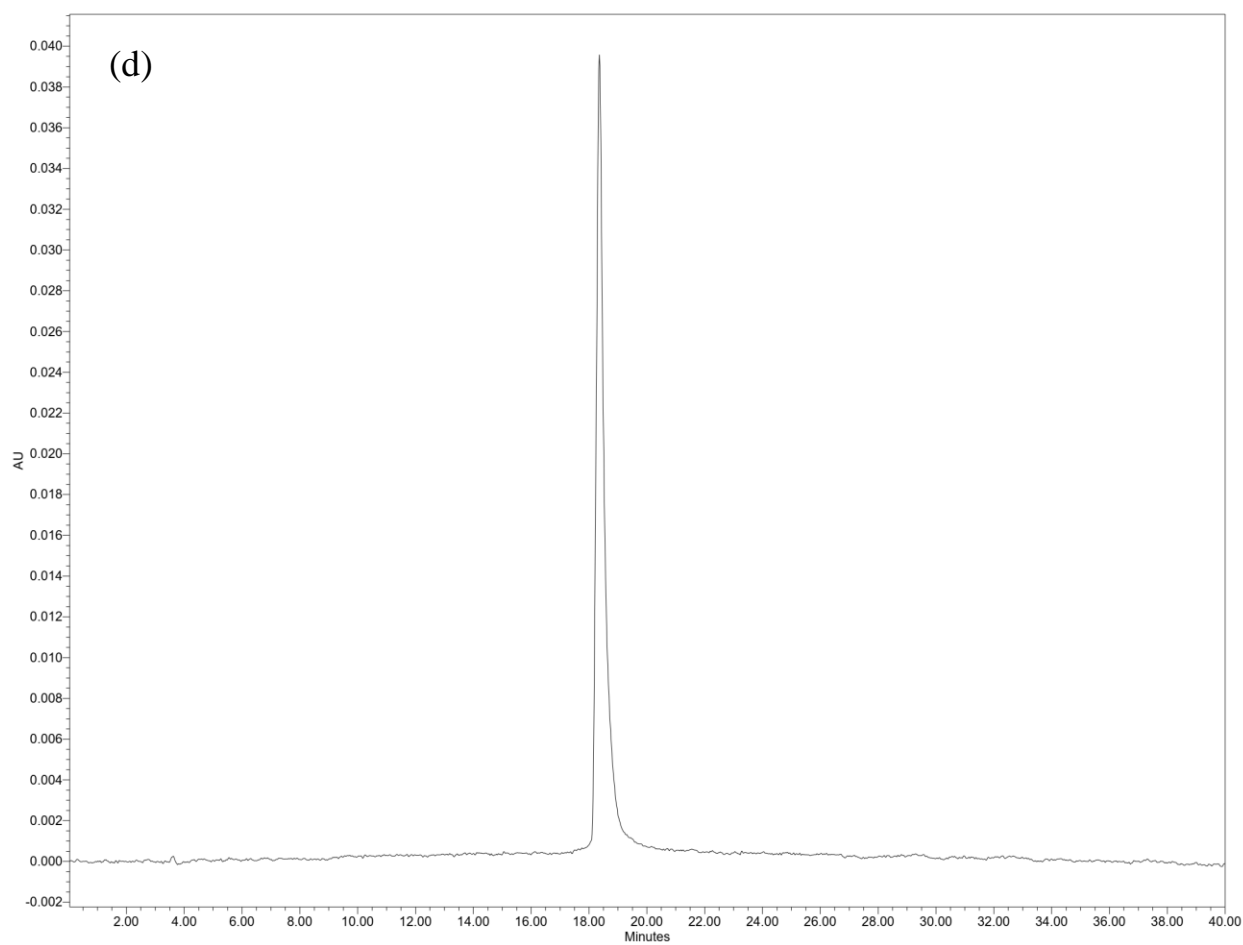
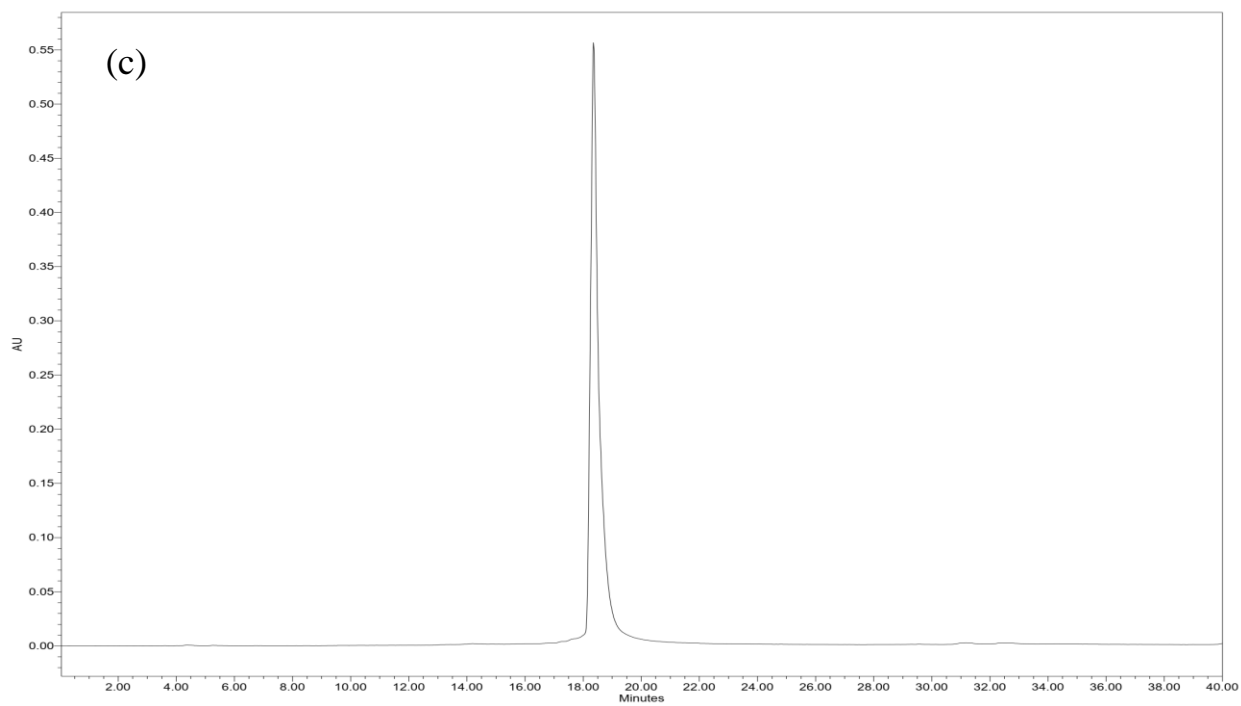


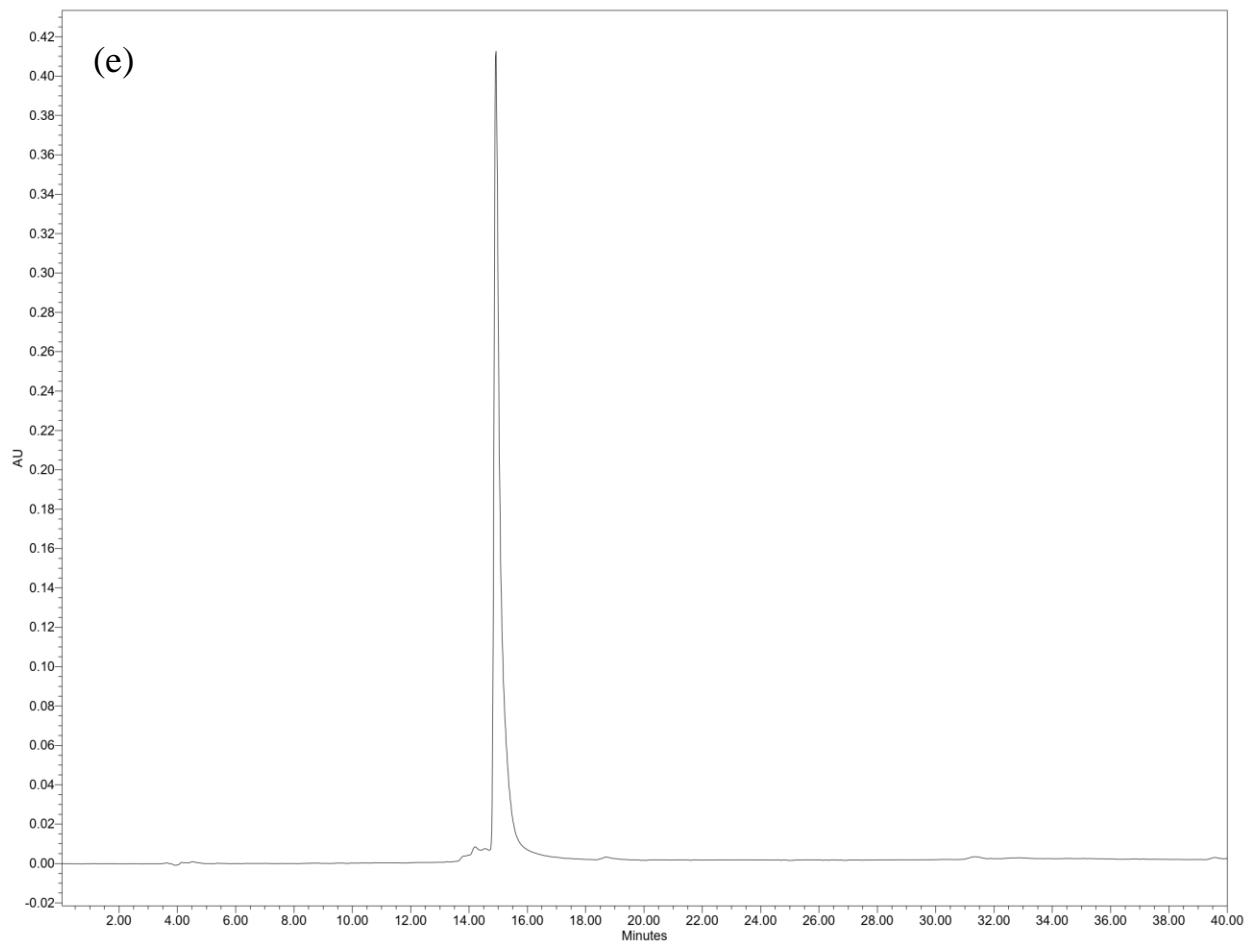
RP-HPLC chromatograms of the (a) crude (DMT-on) and (b) pure (DMT-off) PNA oligomer **5'**
AGGTAGATCACT 3' were used.



RP-HPLC chromatograms of the (a) crude (DMT-on) at 260 nm and (b) crude (DMT-on) at 360 nm (c) pure (DMT-on) at 260 nm (d) pure (DMT-on) at 360 nm (e) pure (DMT-off) at 260 nm
PNA oligomer 5' AGTGATCTAC(PhpC)T 3'







Sequence ^a (N → C)	Molecular formula	Calculated [M+Na] ⁺	Observed [M+Na] ⁺
H-Lys-AGTGTCTAC-Lys-NH ₂	C ₁₂₀ H ₁₅₉ N ₆₁ O ₃₃ Na	3005.2536	3005.2929
H-Lys-GTAGATCACT-Lys-NH ₂	C ₁₂₀ H ₁₅₉ N ₆₁ O ₃₃ Na	3005.2536	3005.2551
H-Lys-G ^S UAGA ^S UCAC ^S U-Lys-NH ₂	C ₁₁₇ H ₁₅₃ N ₆₁ O ₃₀ S ₃ Na	3011.1382	3011.2430
H-Lys-G ^S UAGA ^S UCAC ^S U-Lys-NH ₂ ^c	C ₁₁₇ H ₁₅₃ N ₆₁ O ₃₀ S ₃ Na	3011.1382	3011.2624
H-Lys-G ^S TAGA ^S TCAC ^S T-Lys-NH ₂	C ₁₂₀ H ₁₅₉ N ₆₁ O ₃₀ S ₃ Na ₂	1538.0874 ^b	1538.0963 ^b
H-Lys-AG ^S UGA ^S UC ^S UAC-Lys-NH ₂	C ₁₁₇ H ₁₅₃ N ₆₁ O ₃₀ S ₃ Na	3011.1382	3011.1431
H-Lys-DG ^S UGD ^S UC ^S UDC-Lys-NH ₂	C ₁₁₇ H ₁₅₆ N ₆₄ O ₃₀ S ₃ Na ₂	1539.5803 ^b	1539.6721 ^b
H-Lys-G ^S UDGD ^S UCDCT-Lys-NH ₂	C ₁₁₈ H ₁₅₈ N ₆₄ O ₃₁ S ₂ Na ₂	1538.5996 ^b	1538.7134 ^b

^a PNA sequences possess a free N-terminal amino group and C-terminal amide

^b Oligomer calculated and observed as the dicationic [M+2Na]²⁺

^c PNA sequences didn't have thiouracil protection during oligomerization

Table S1. Observed high-resolution mass of synthesized PNA oligomers

Reference Fluorophore	Φ (EtOH)	Φ (DMSO)	Φ (THF)	Φ (Glycerol)	Φ (water, pH 7.2)	T (°C)
9,10-diphenylanthracene	0.95 ^a	0.27	0.42	0.89		23
	0.79	0.24		0.81		60
	0.95					15
		0.27	0.35	0.31	0.14 ^a	23
		0.28				60
Tryptophan						15

^a Values extracted from literature.^{52,53}

Table S2. Calculated quantum yield values for reference standards in different solvents and temperatures

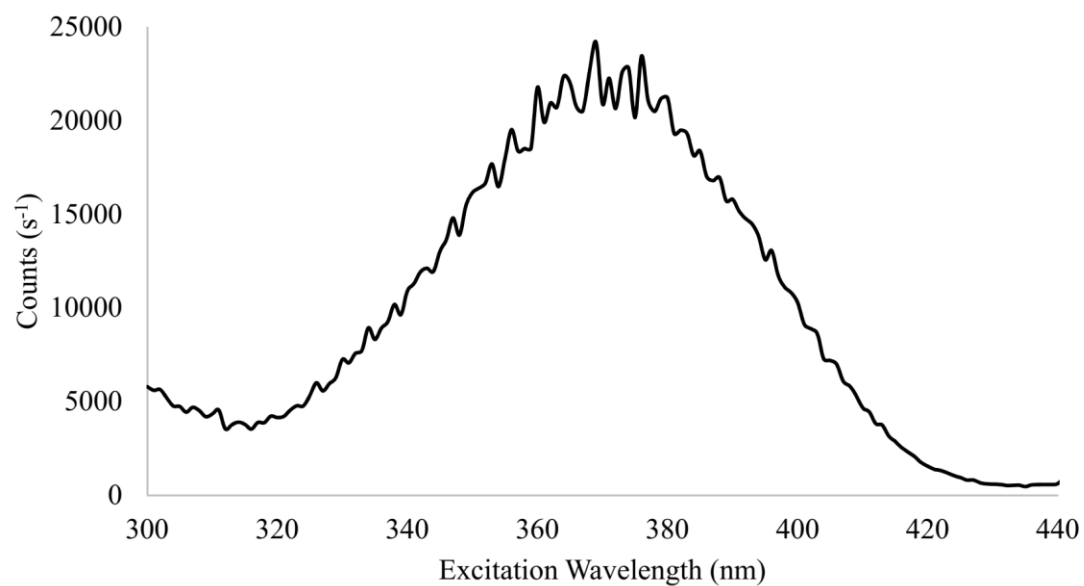
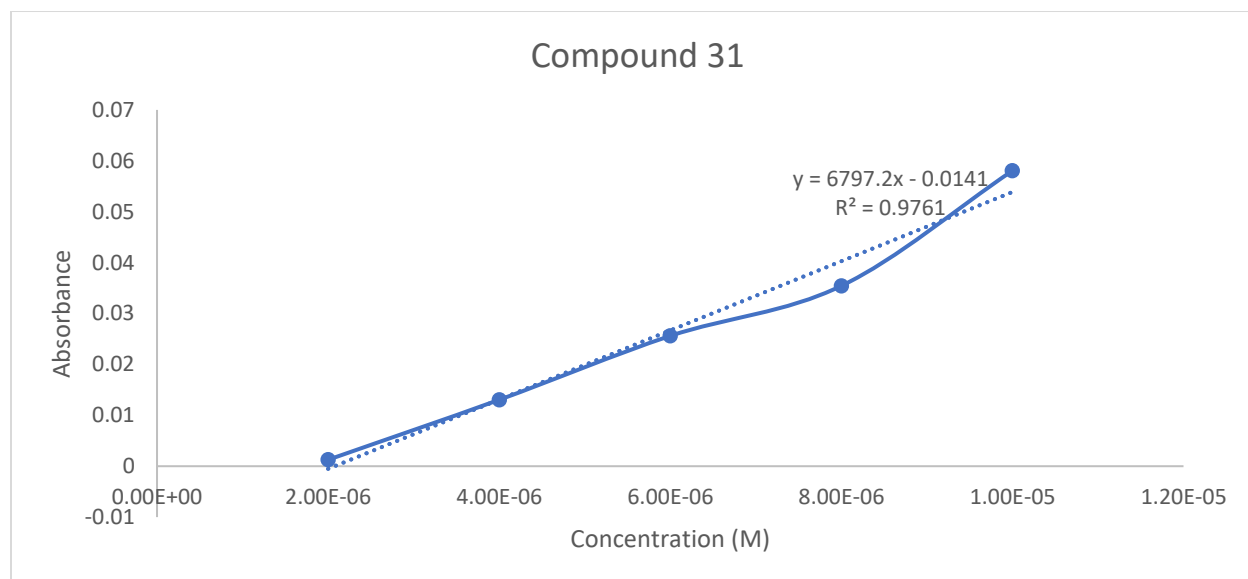
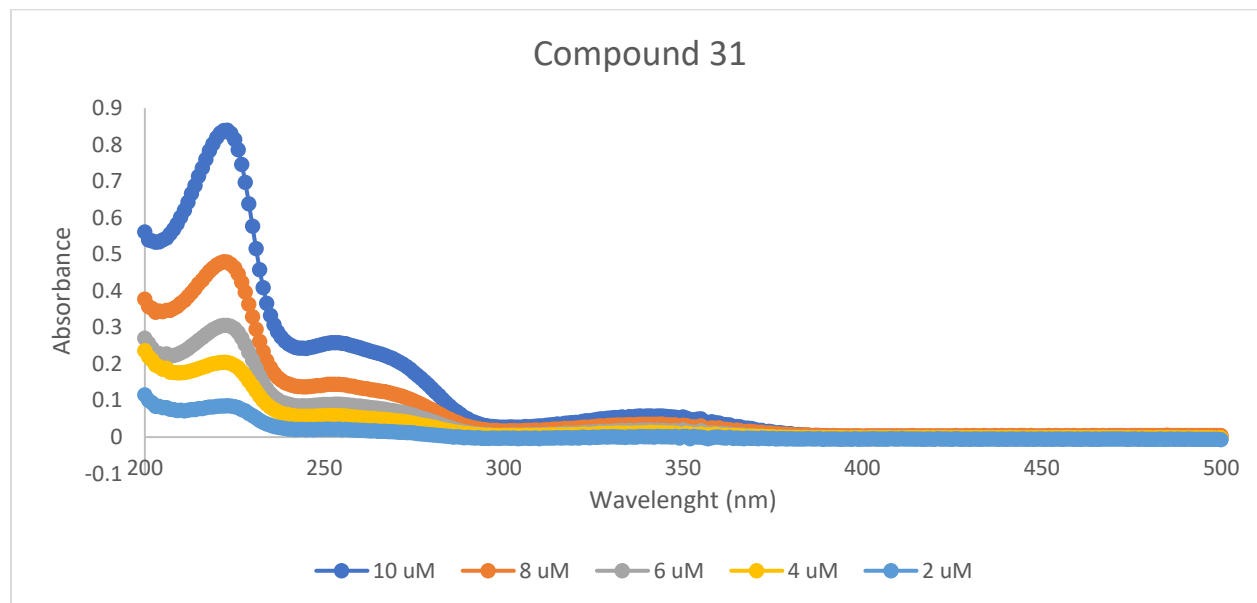
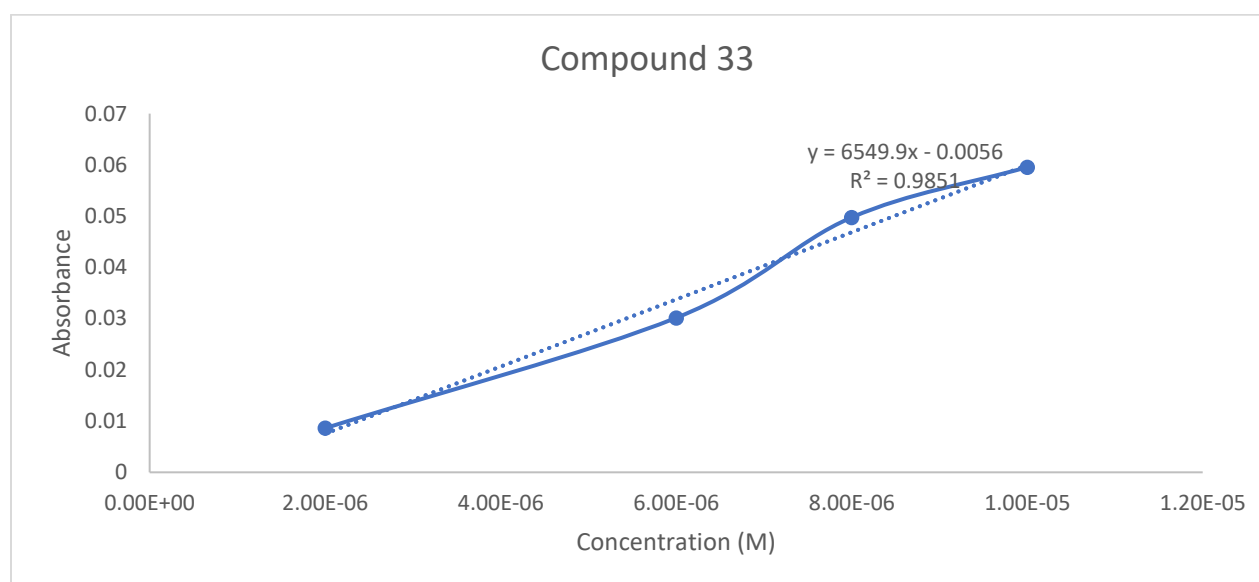
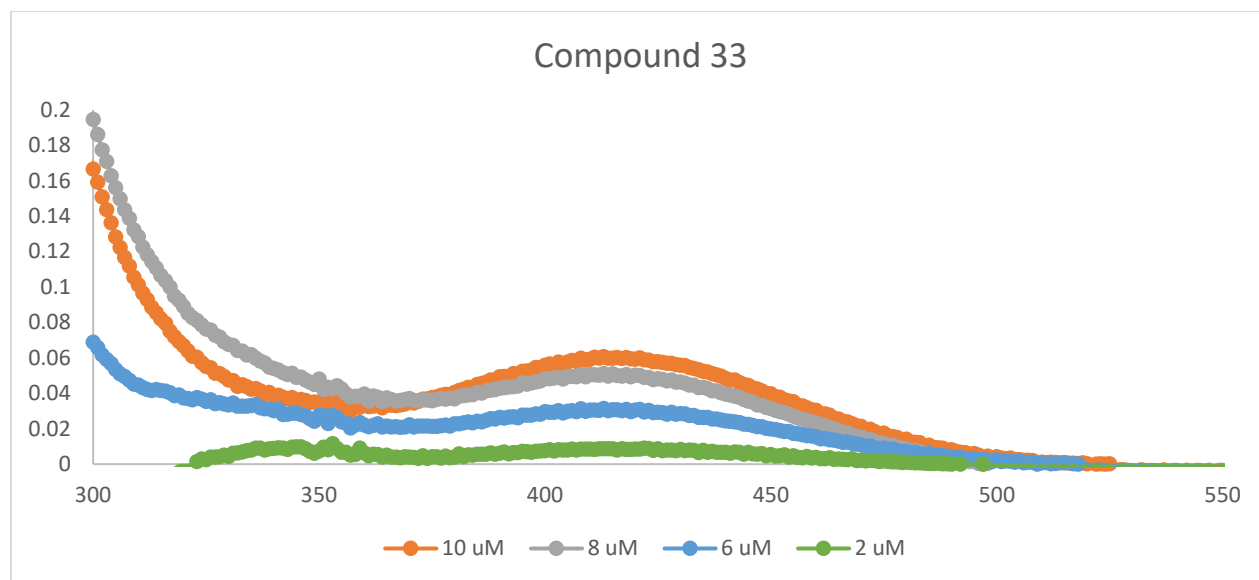
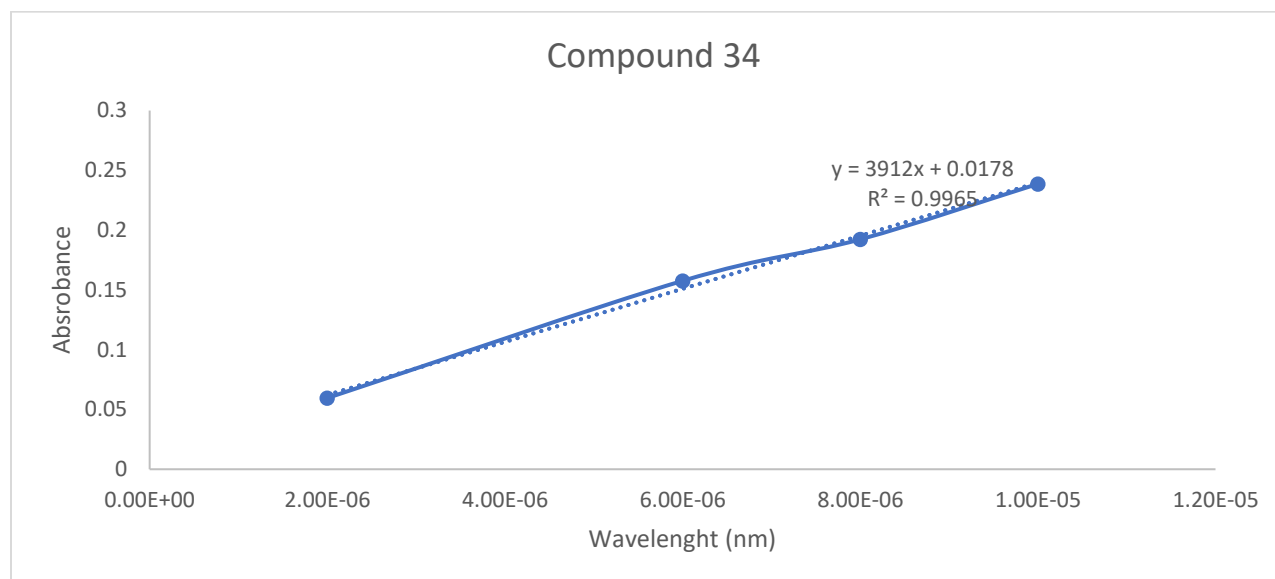
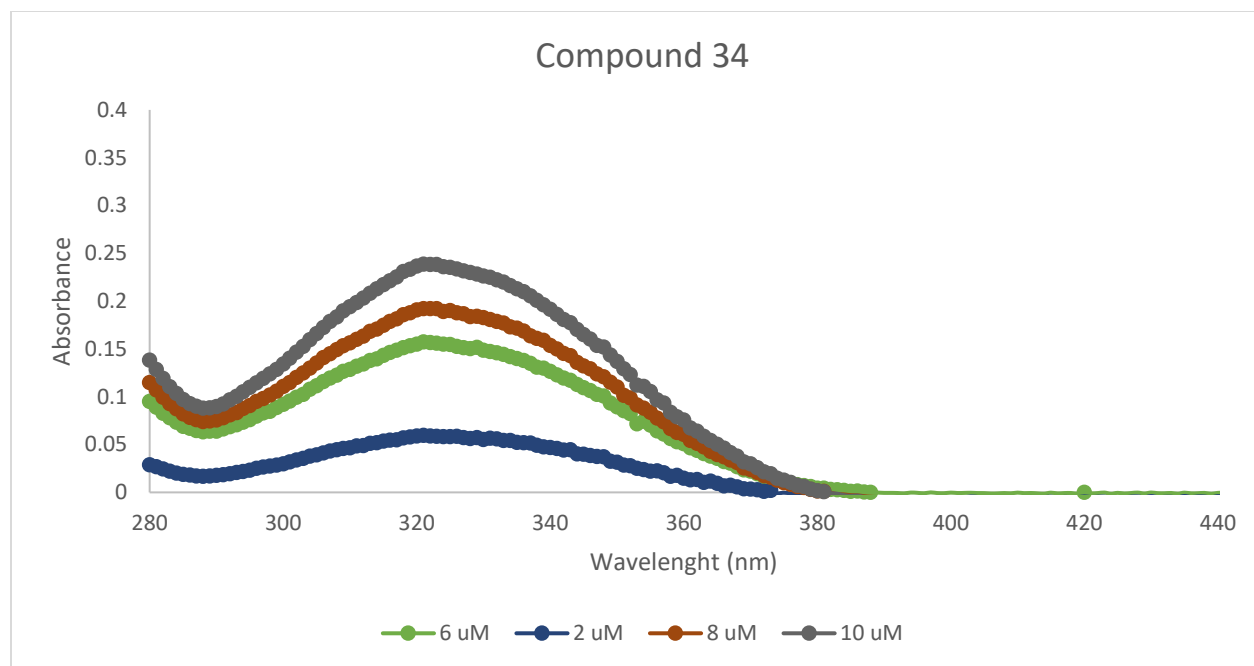


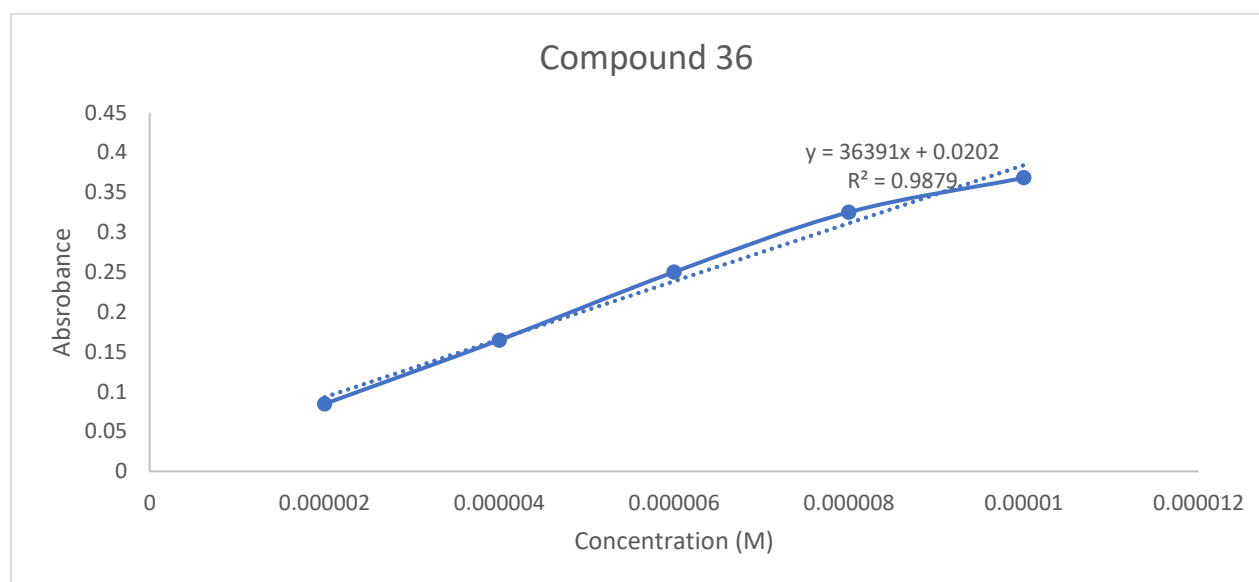
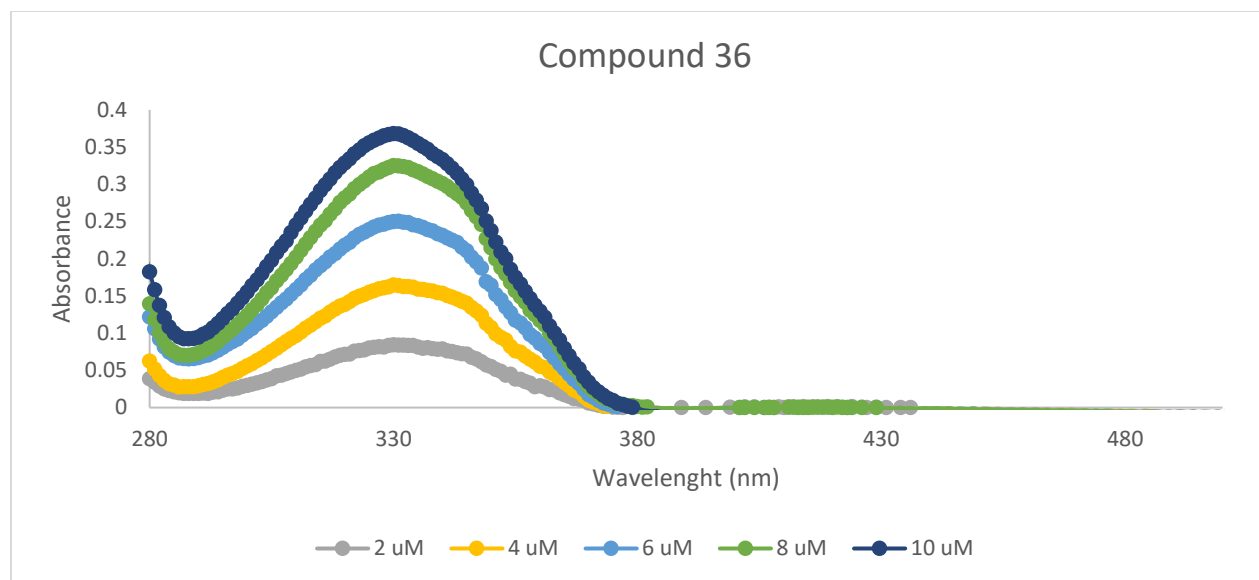
Figure S4. Emission at 446 nm of single-stranded Target DNA (PhpC) upon excitation from 300 nm to 440 nm.

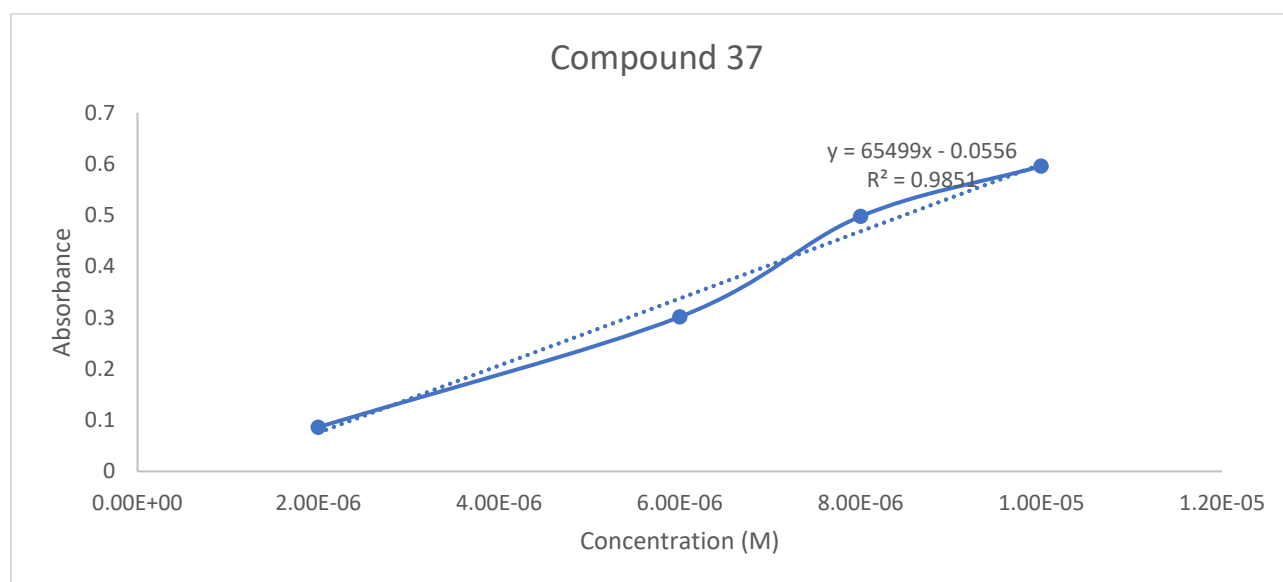
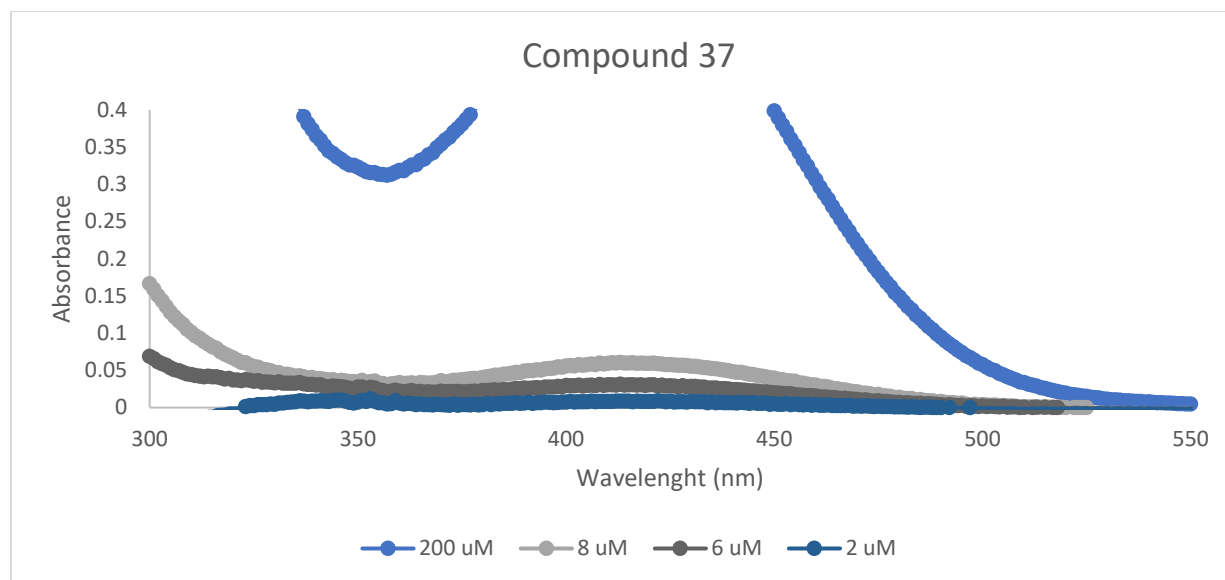
UV-vis absorbance and Beer-Lambert Plots

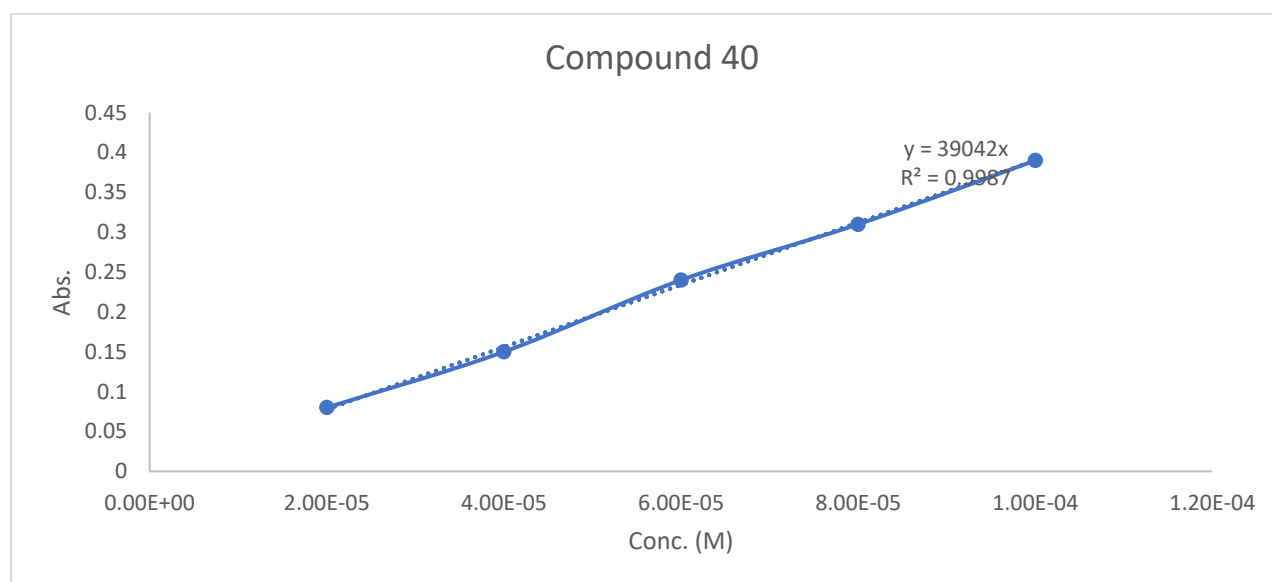
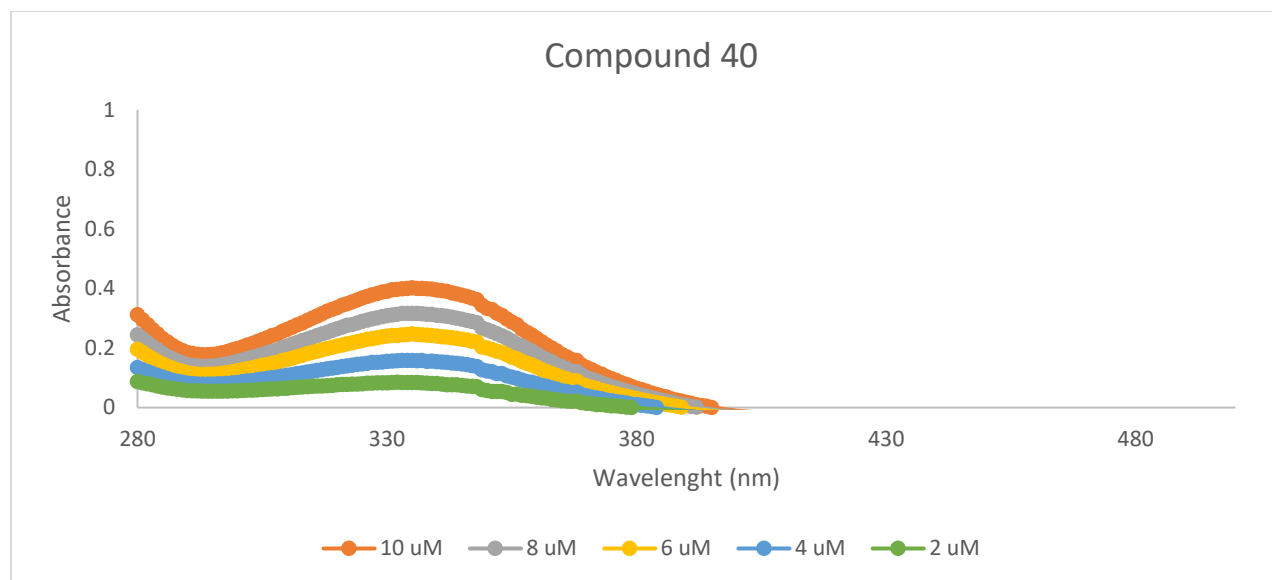




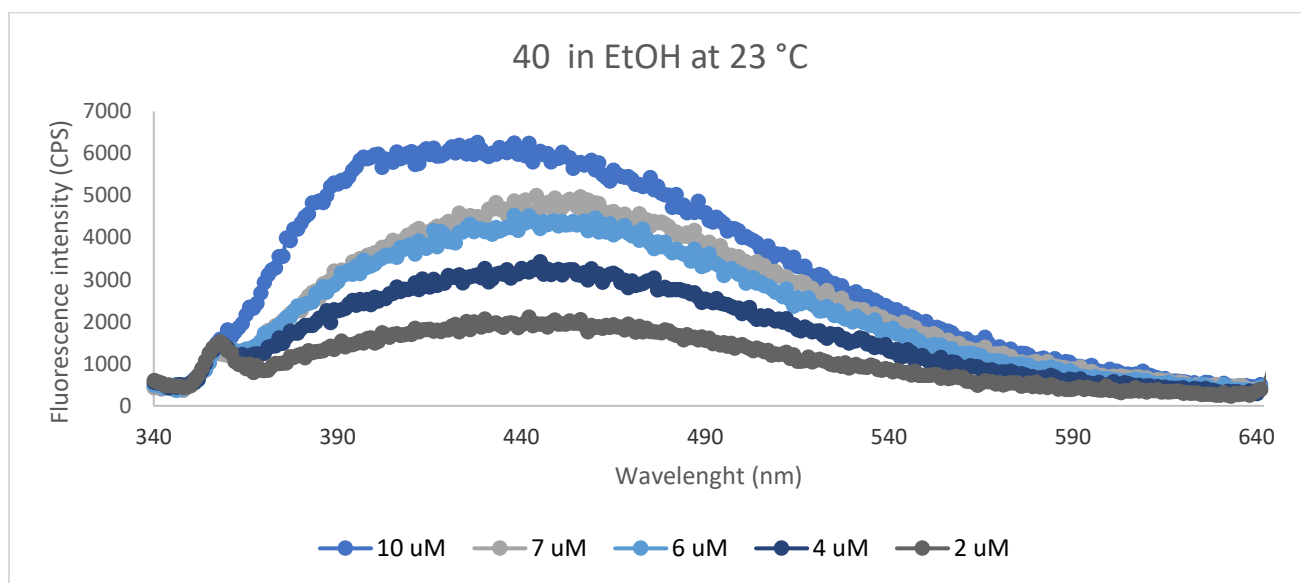
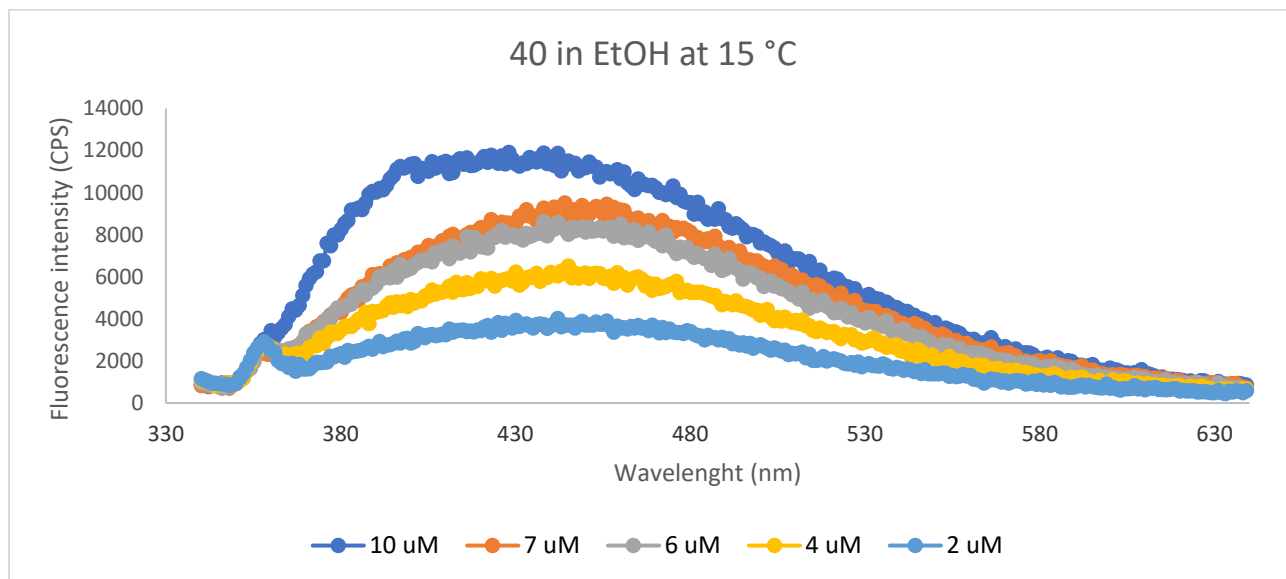


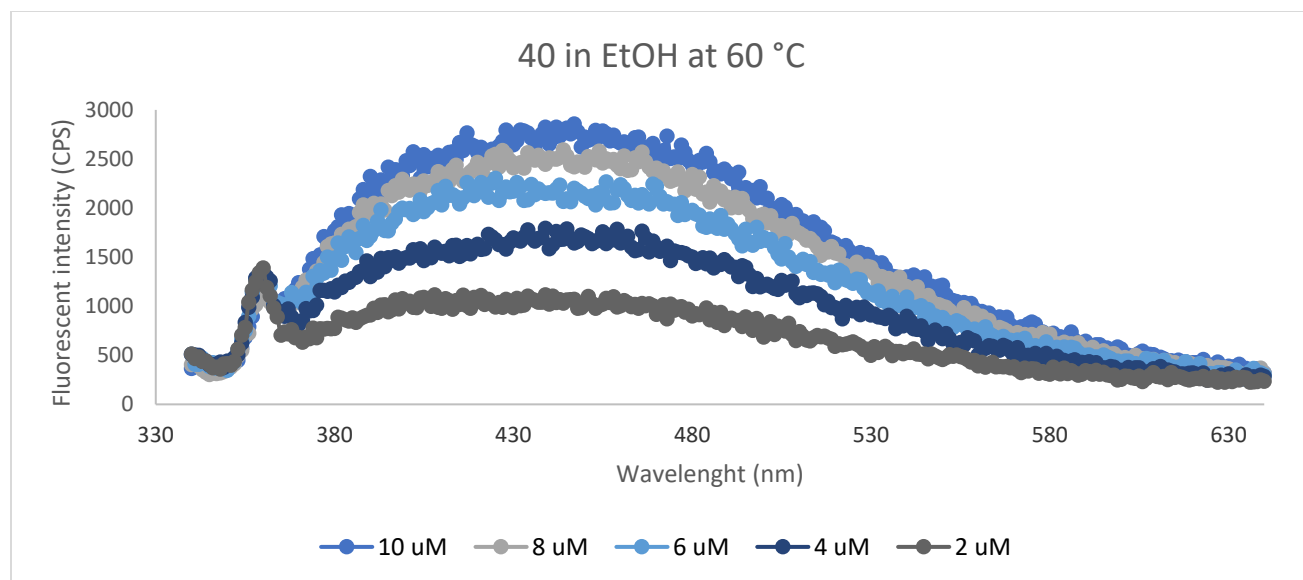






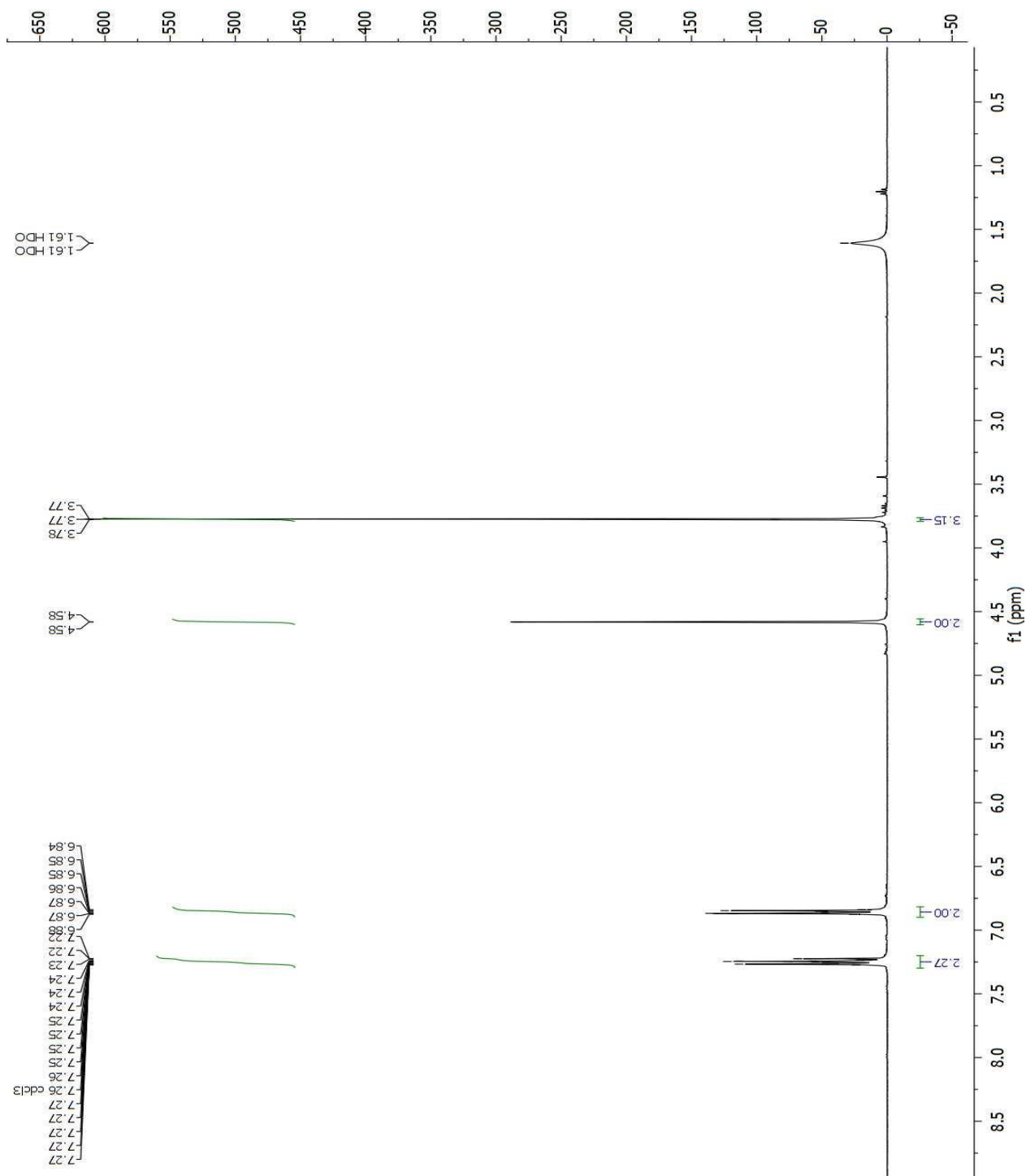
Emission spectra for compound **40** in different solvents and temperatures



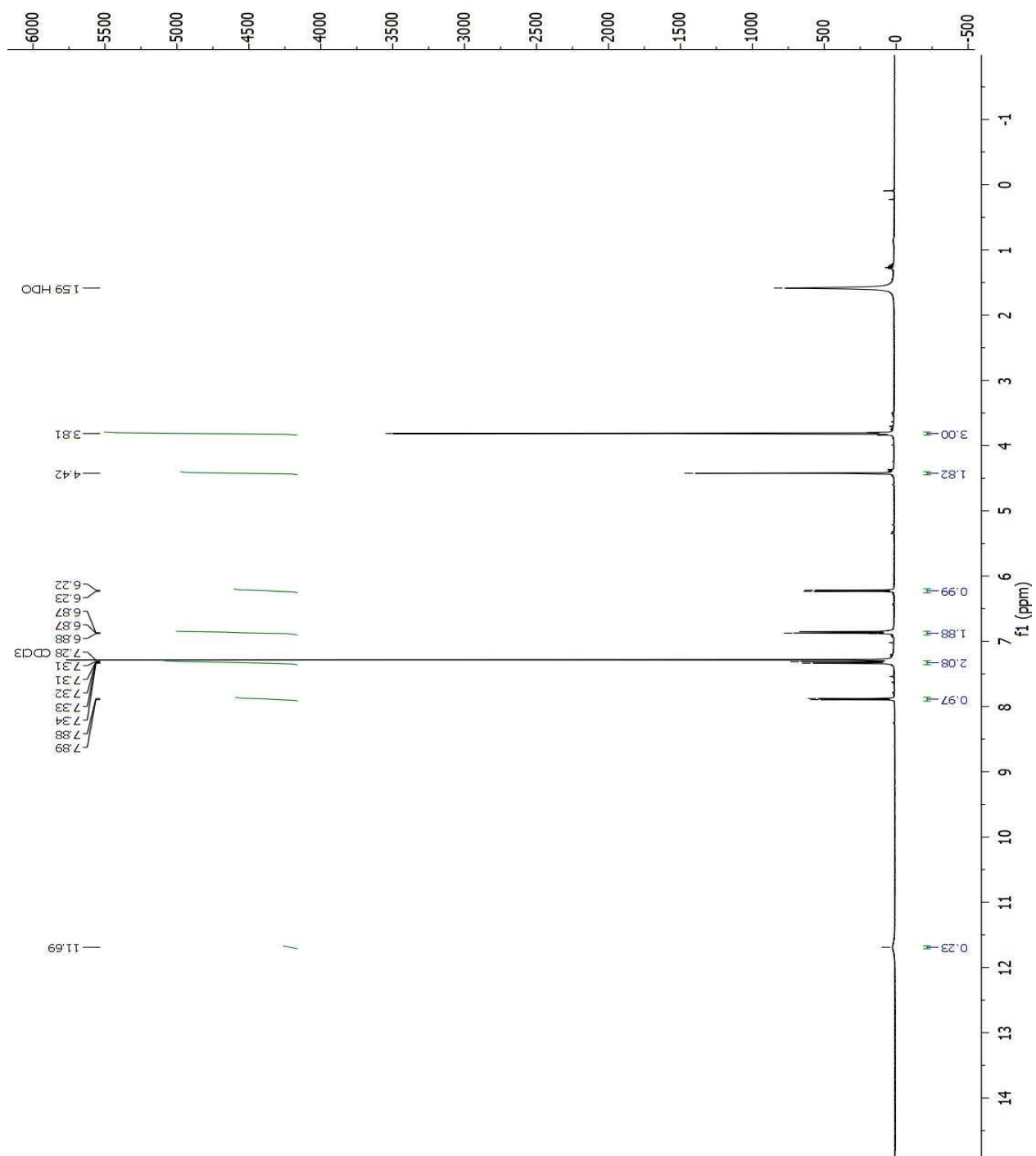


NMR Spectra

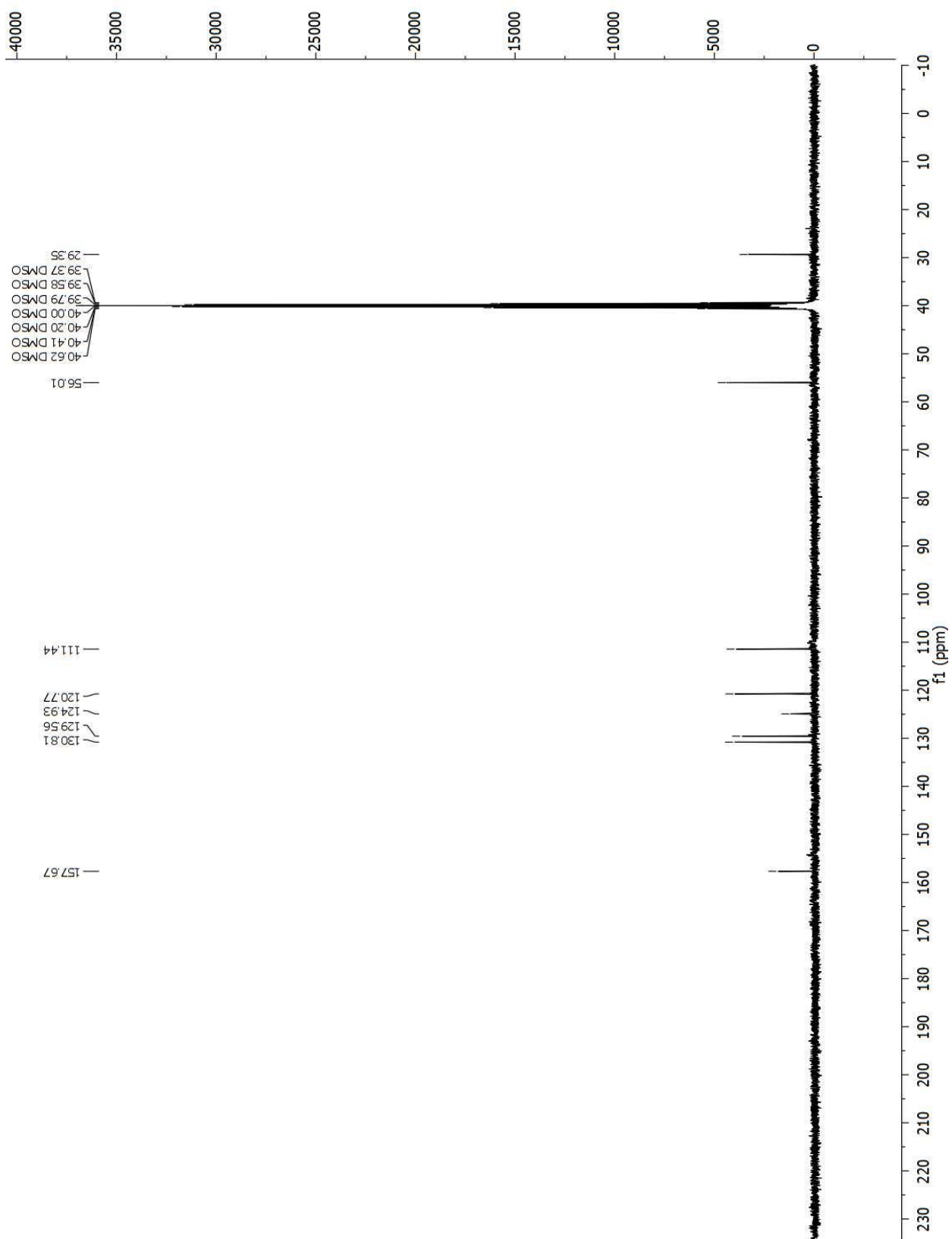
^1H NMR spectrum of 4-methoxybenzyl alcohol (2)



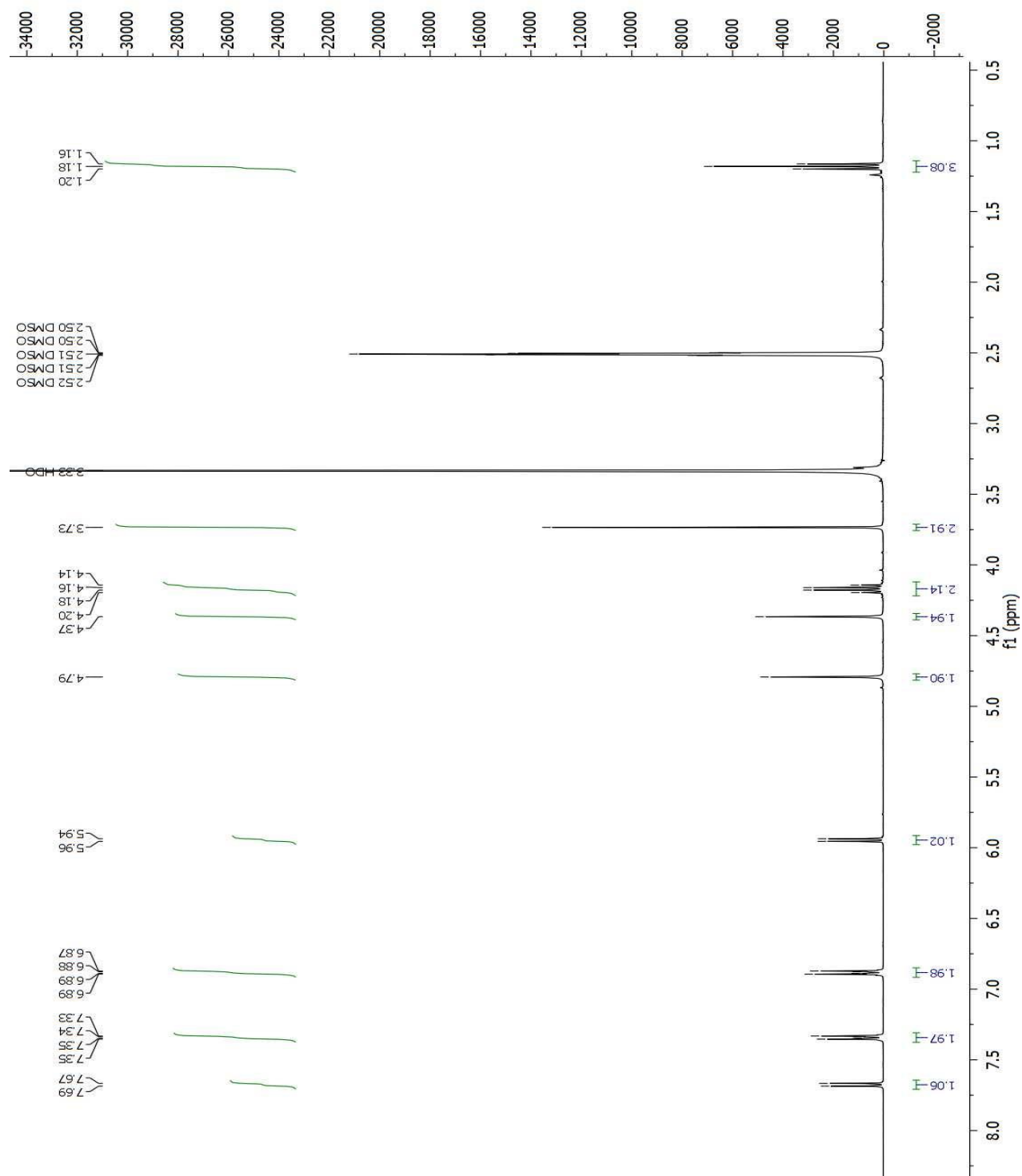
¹H NMR spectrum of 2-((4-methoxybenzyl)thio)pyrimidin-4(1H)-one (5)



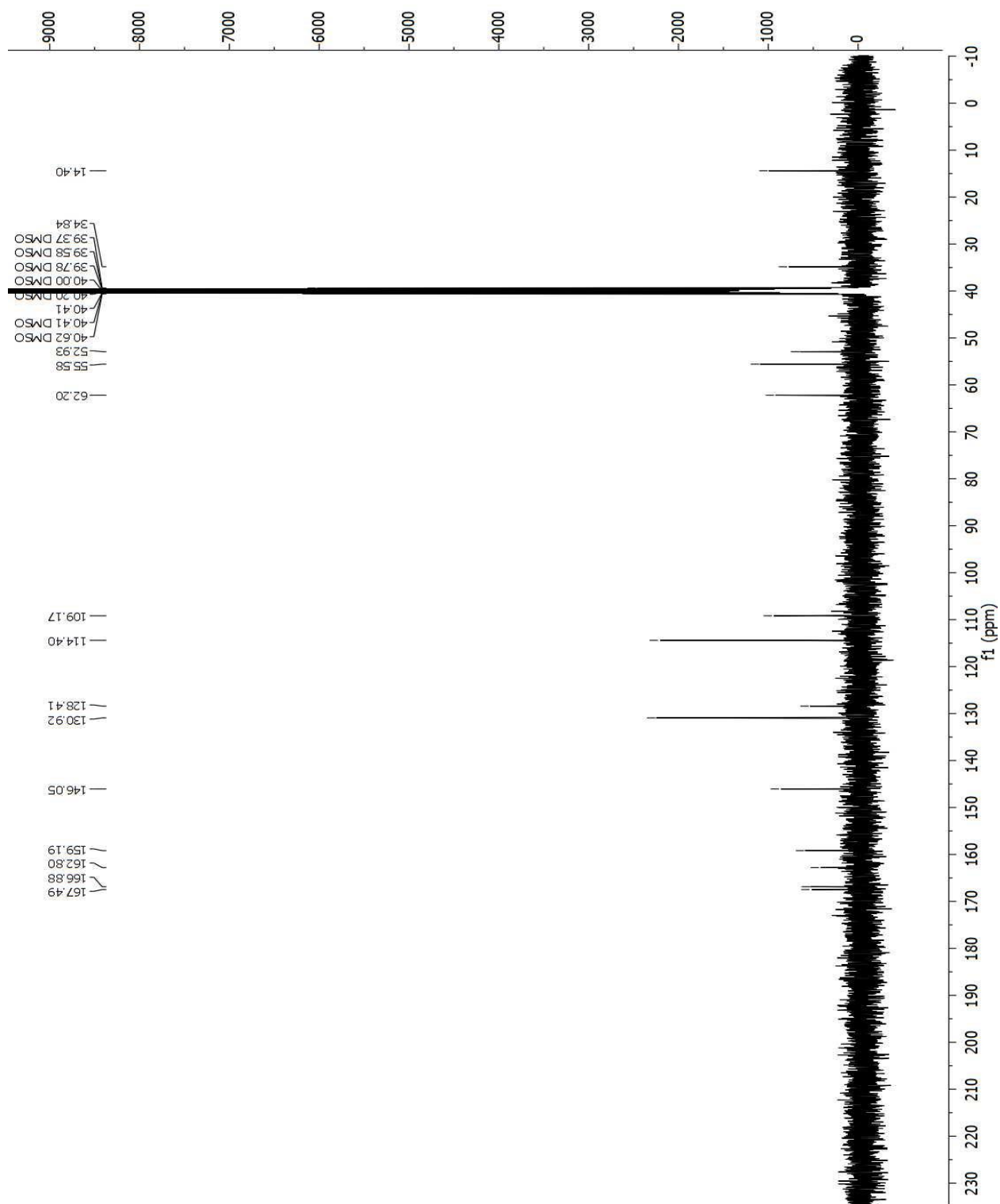
¹³C NMR spectrum of 2-((4-methoxybenzyl)thio)pyrimidin-4(1H)-one (5)



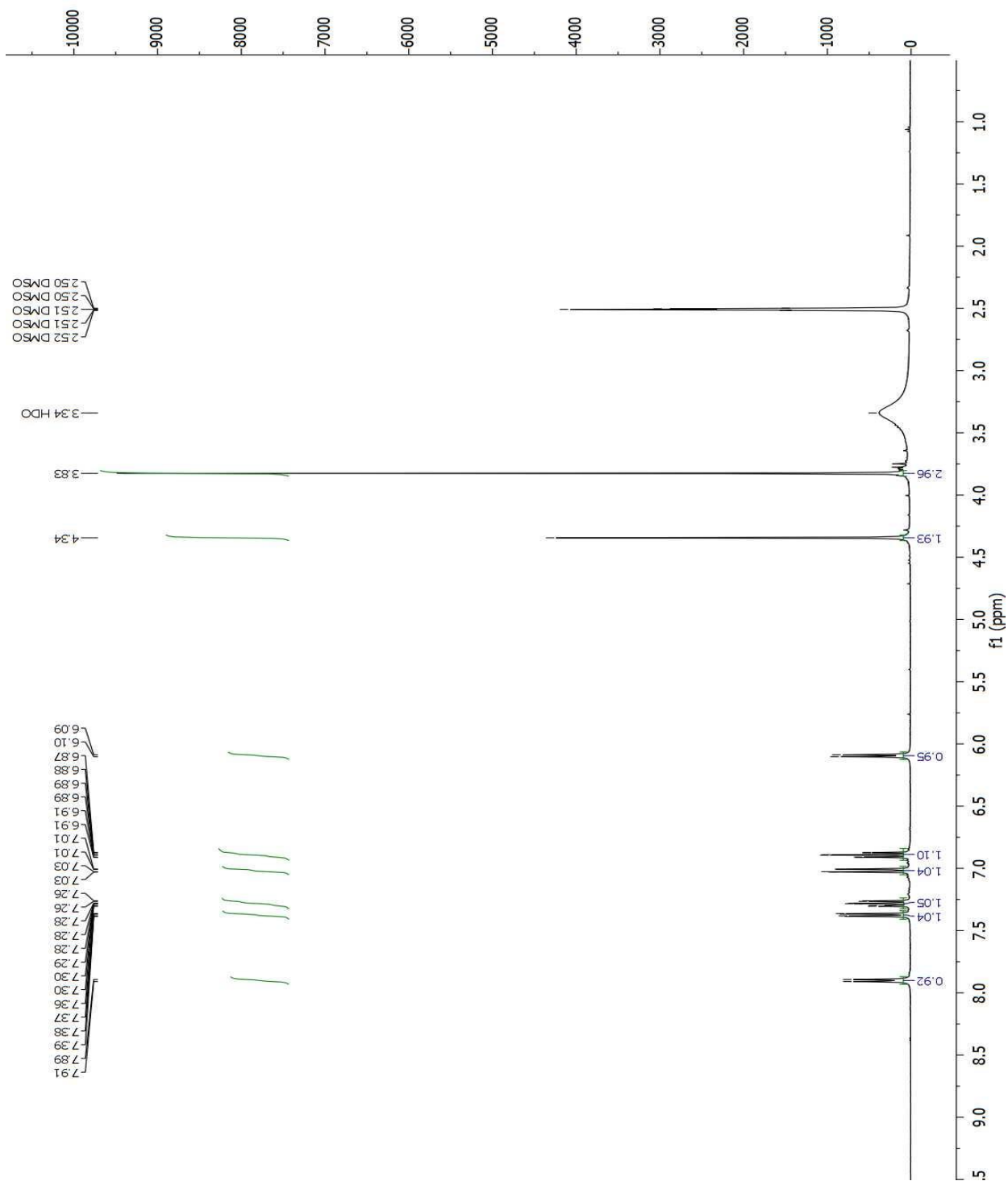
¹H NMR spectrum of *N*-1-(Ethoxycarbomethyl)-*S*-(4-methoxybenzyl)-2-thiouracil (6a)



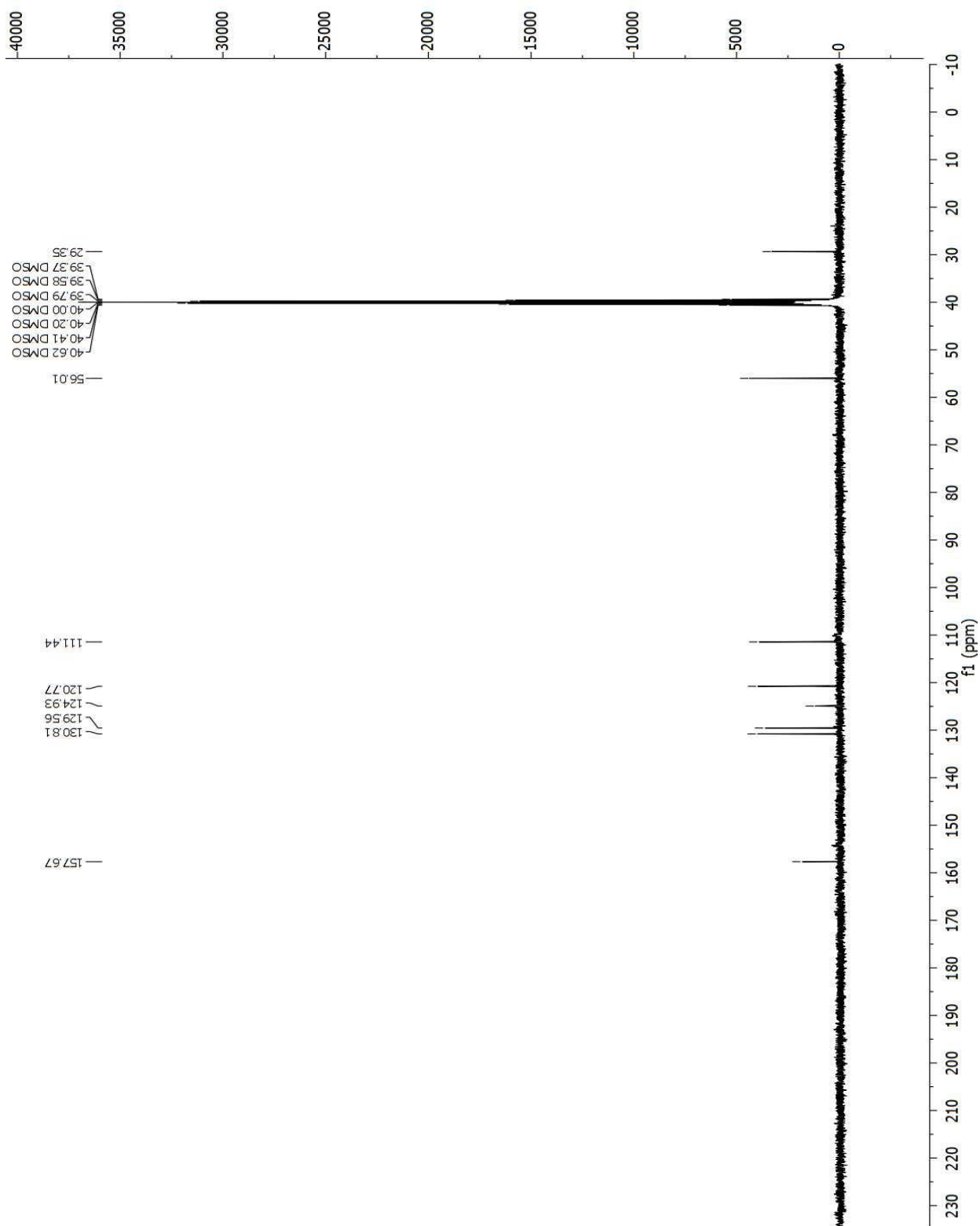
¹³C NMR spectrum of *N*-1-(Ethyloxycarbomethyl)-*S*-(4-methoxybenzyl)-2-thiouracil (6a)



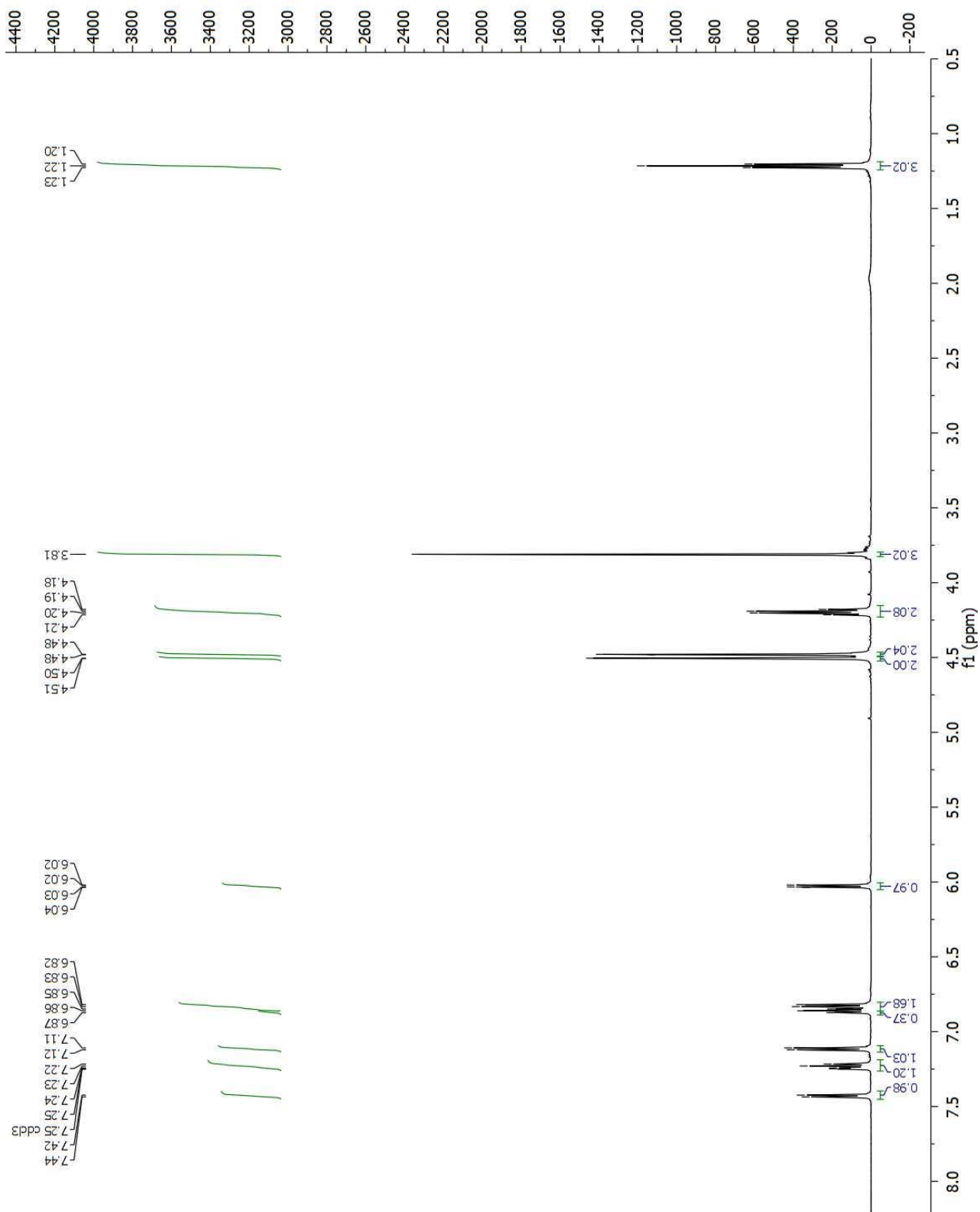
¹H NMR spectrum of 2-(2-methoxybenzyl) thiouracil (10)



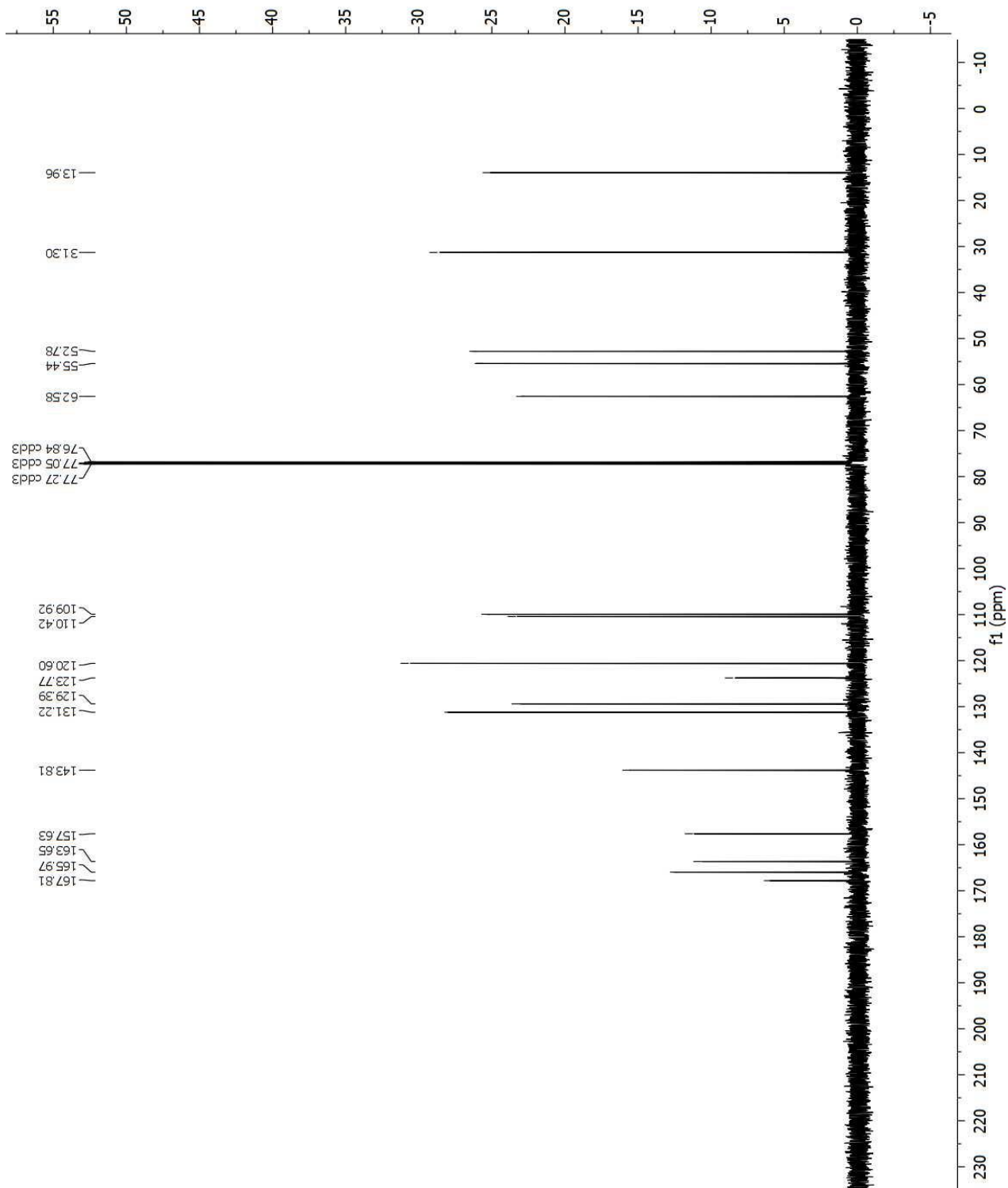
^{13}C NMR spectrum of 2-(2-methoxybenzyl) thiouracil (10)



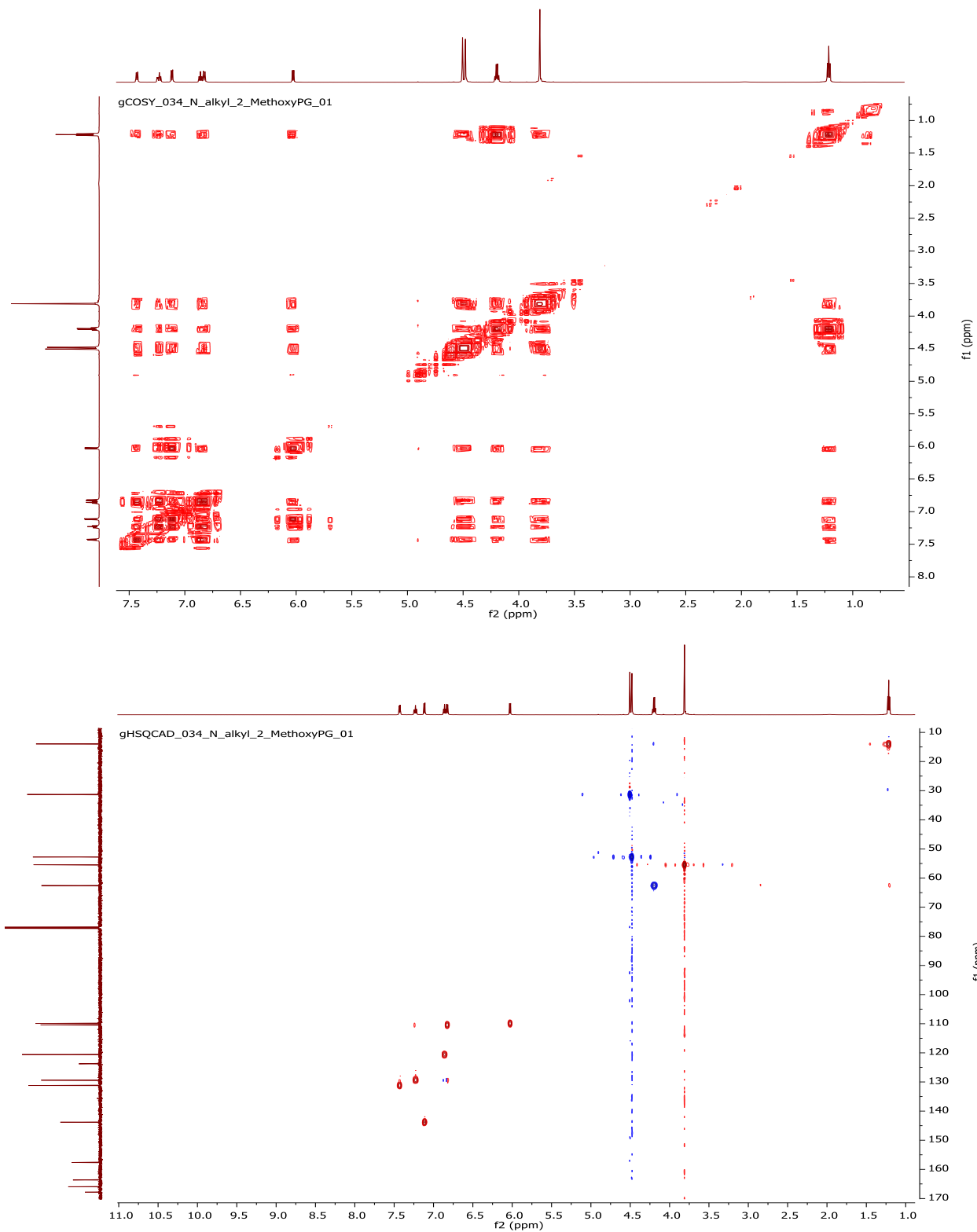
¹H NMR spectrum of *N*-1-(Ethyloxycarbomethyl)-*S*-(2-methoxybenzyl)-2-thiouracil (11a)



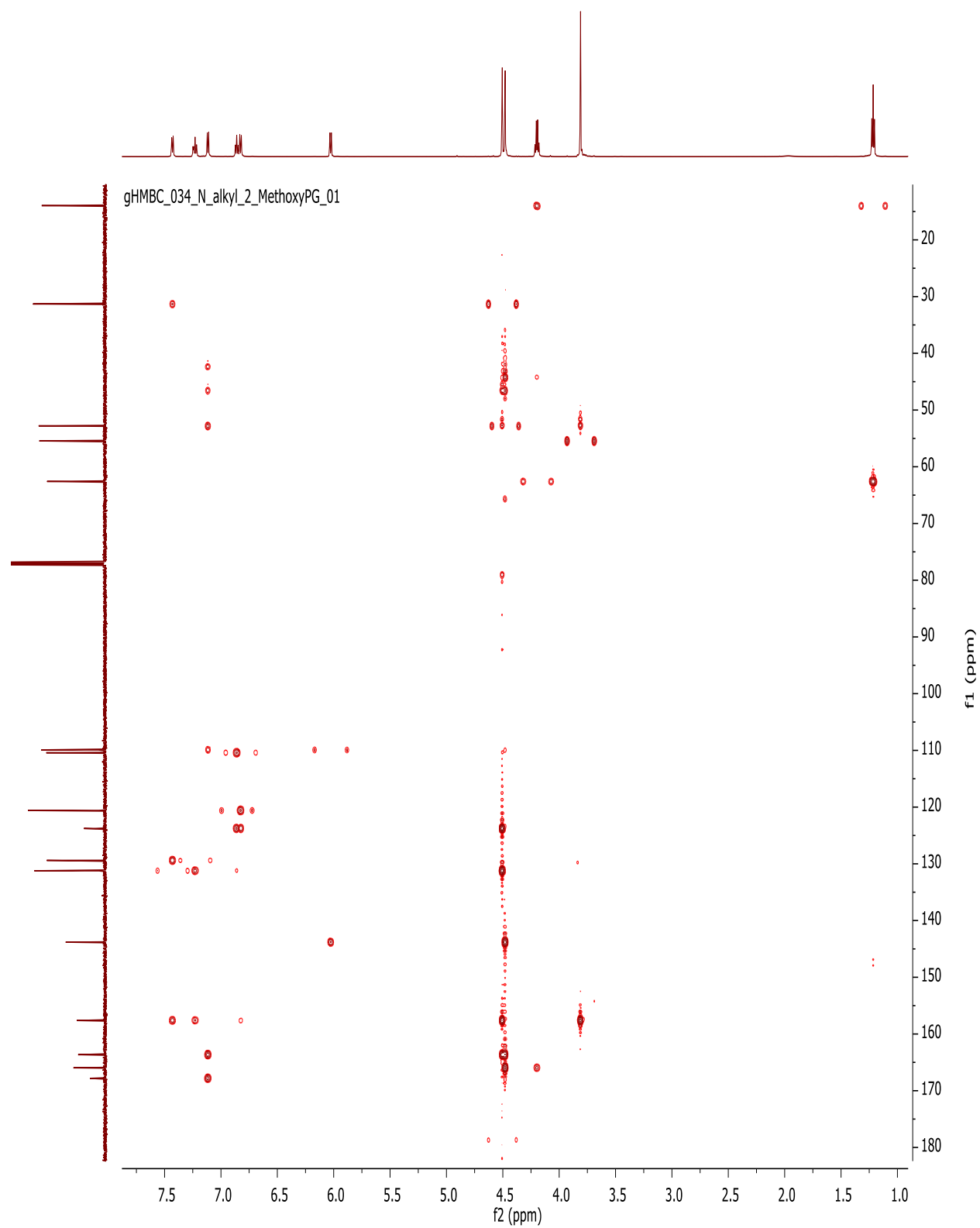
¹³C NMR spectrum of *N*-1-(Ethyloxycarbomethyl)-*S*-(2-methoxybenzyl)-2-thiouracil (11a)



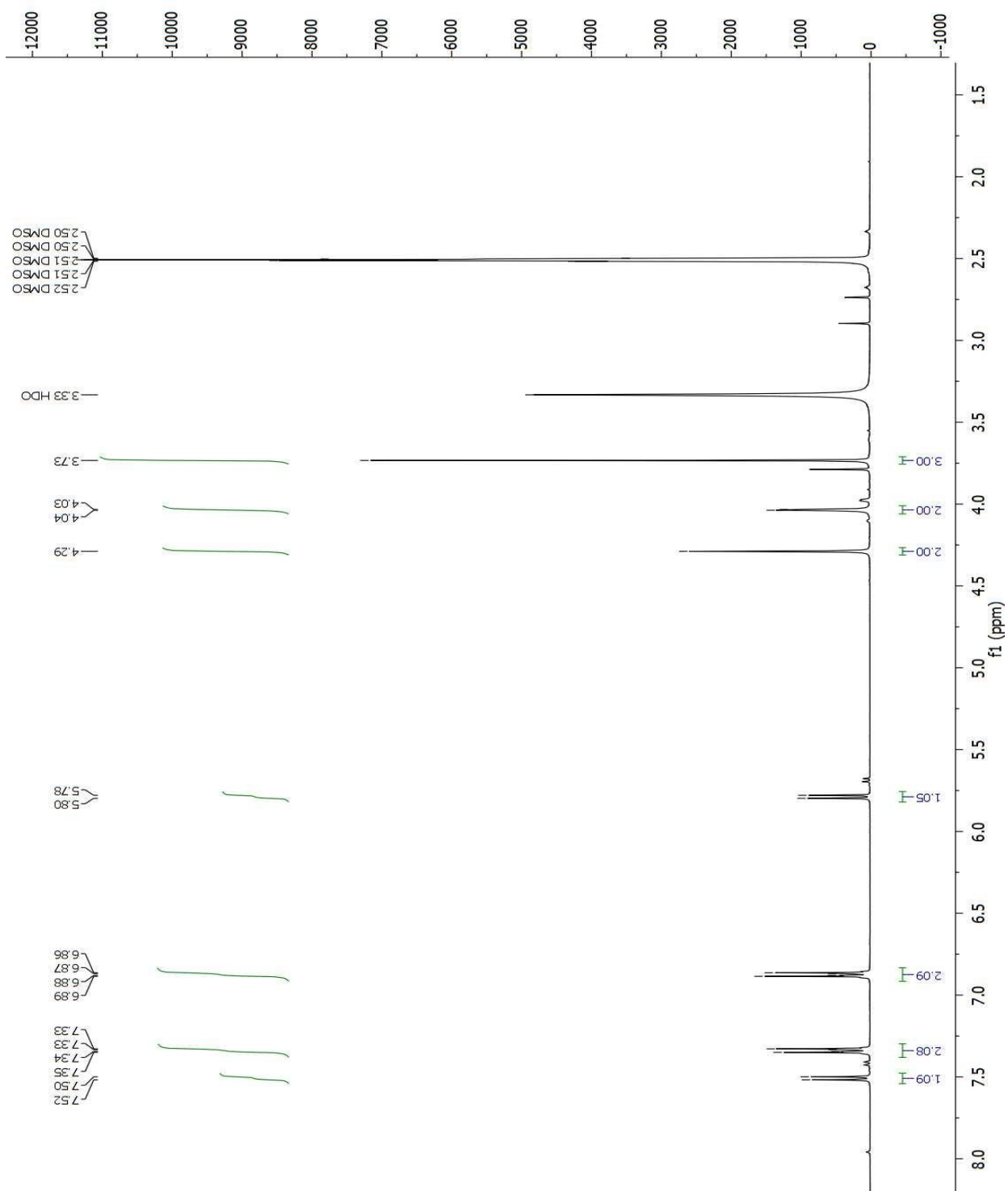
COSY and HSQC spectrum of *N*-1-(Ethoxycarboxymethyl)-*S*-(2-methoxybenzyl)-2-thiouracil (*11a*)



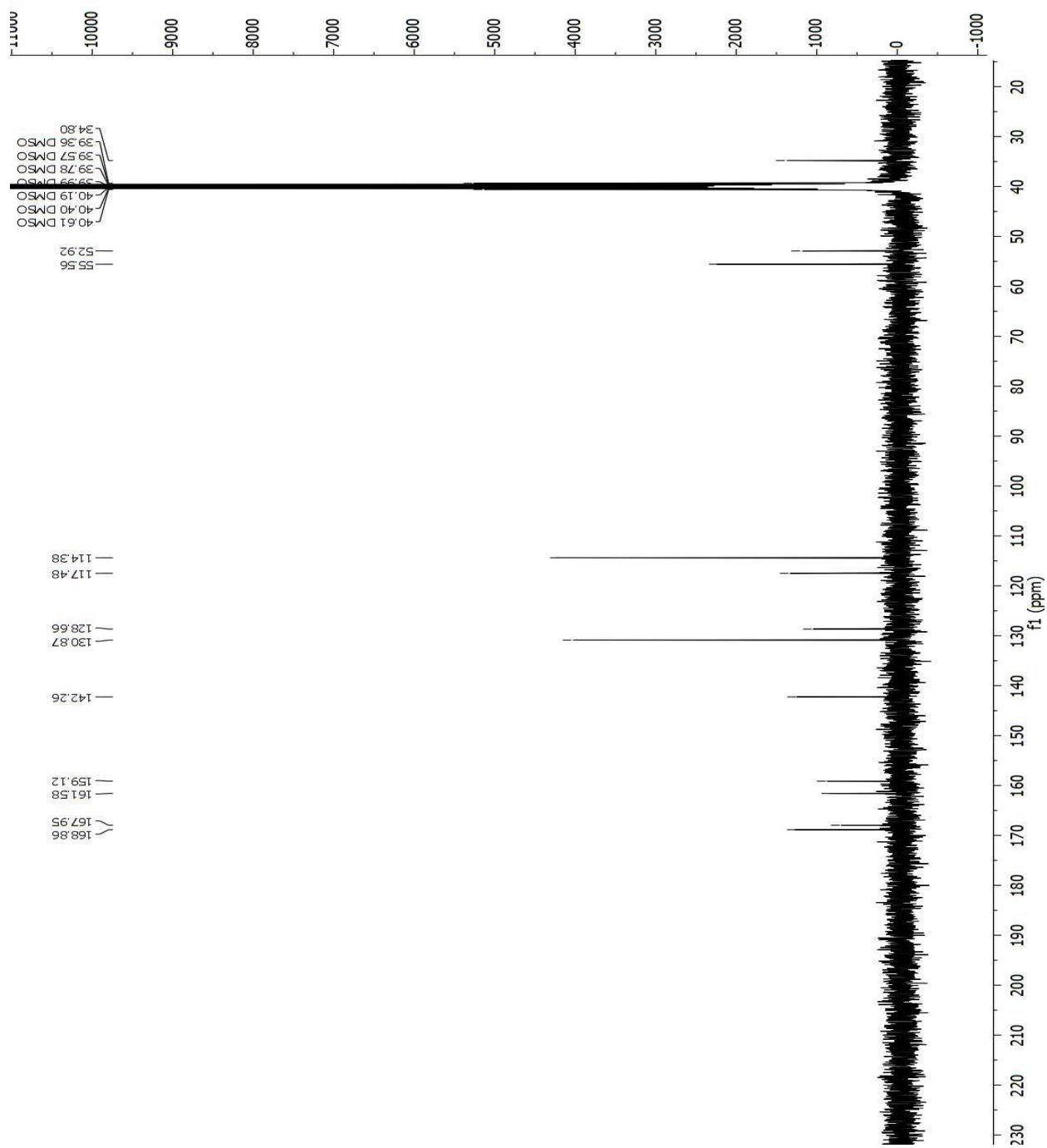
HMBC spectrum of *N*-1-(Ethyloxycarbomethyl)-*S*-(2-methoxybenzyl)-2-thiouracil (*11a*)



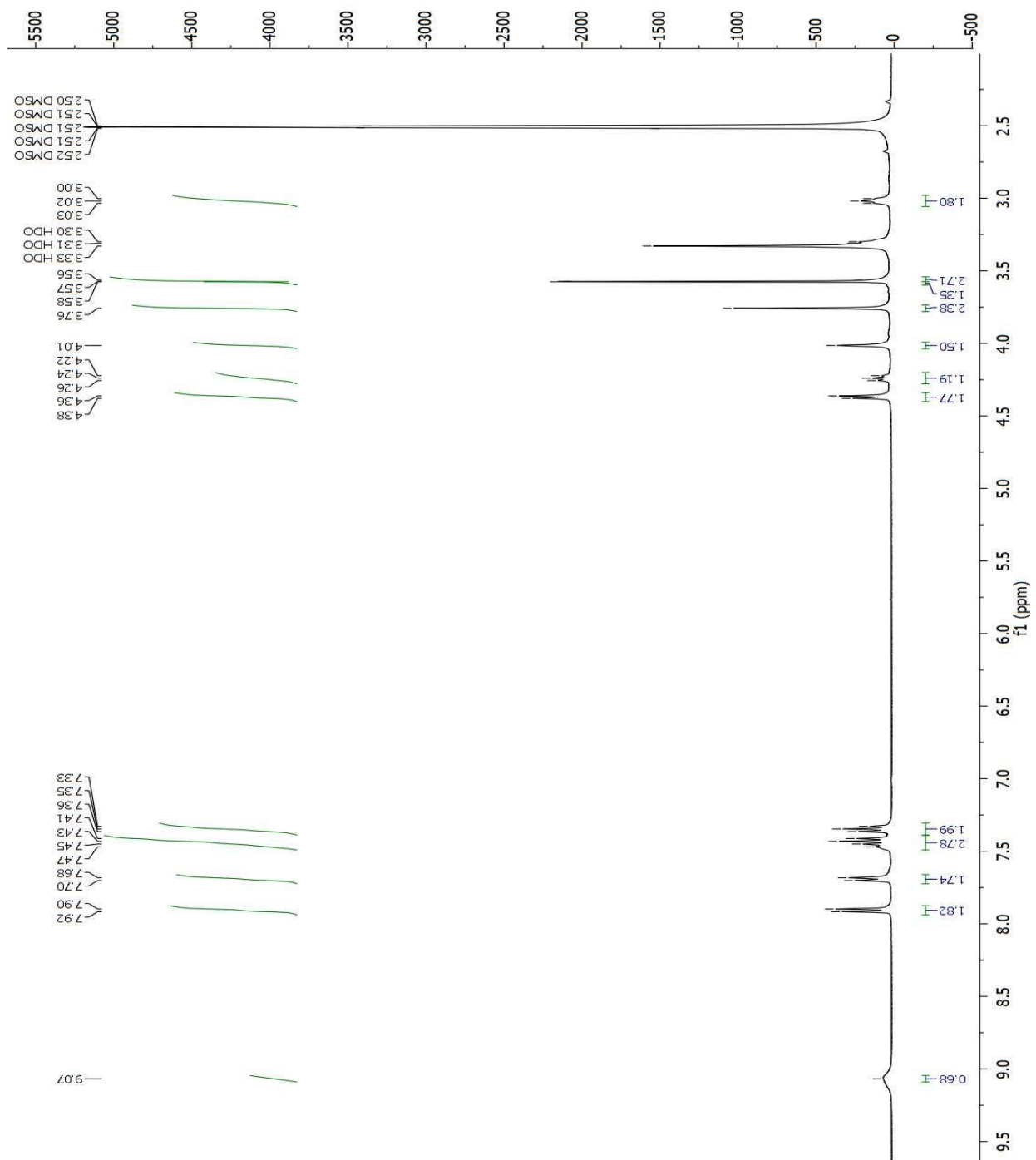
¹H NMR spectrum of 2-(2-((4-methoxybenzyl)thio)-4-oxopyrimidin-1(4H)-yl)acetic acid (12)



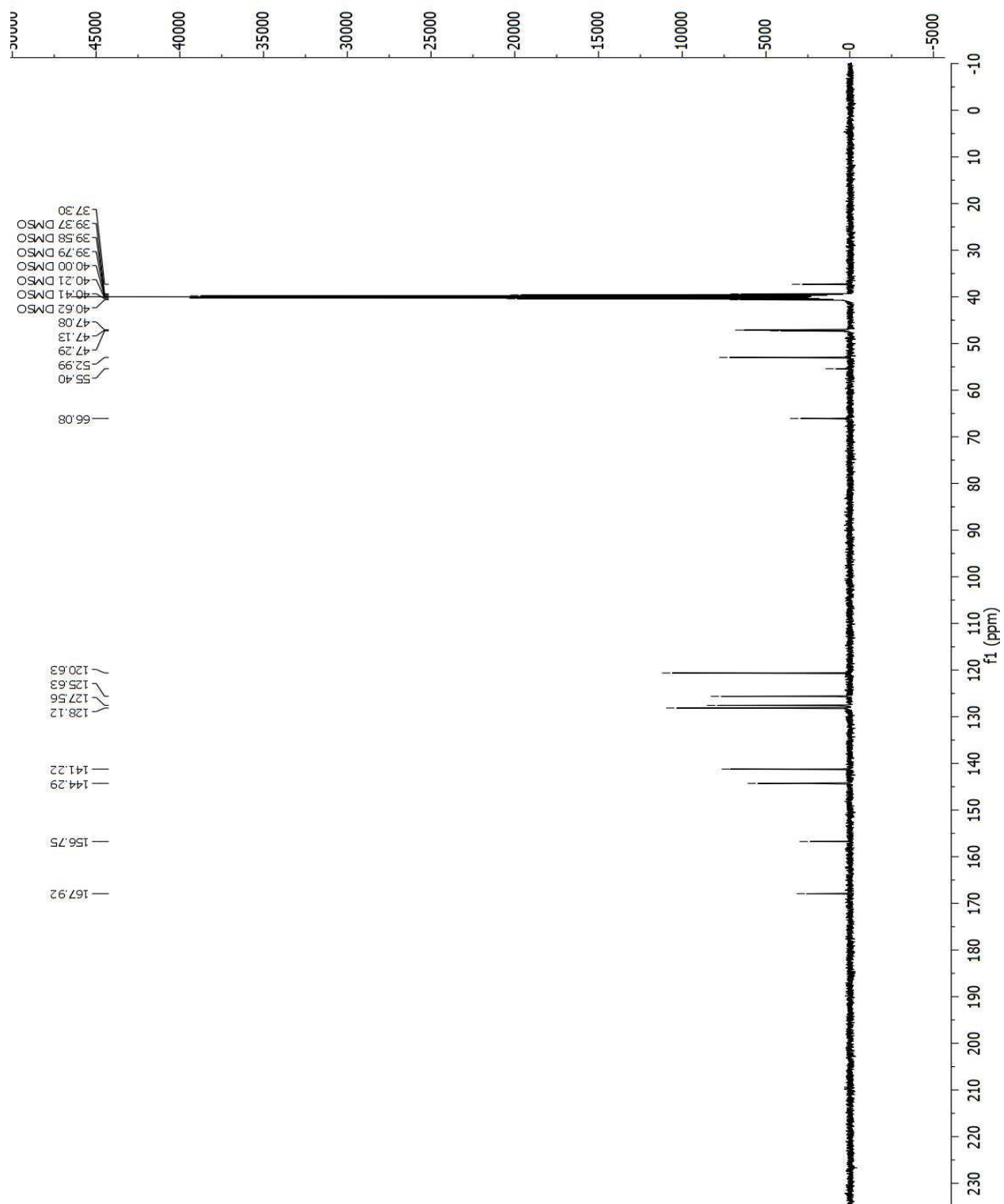
¹³C NMR spectrum of 2-(2-((4-methoxybenzyl)thio)-4-oxopyrimidin-1(4H)-yl)acetic acid (12)



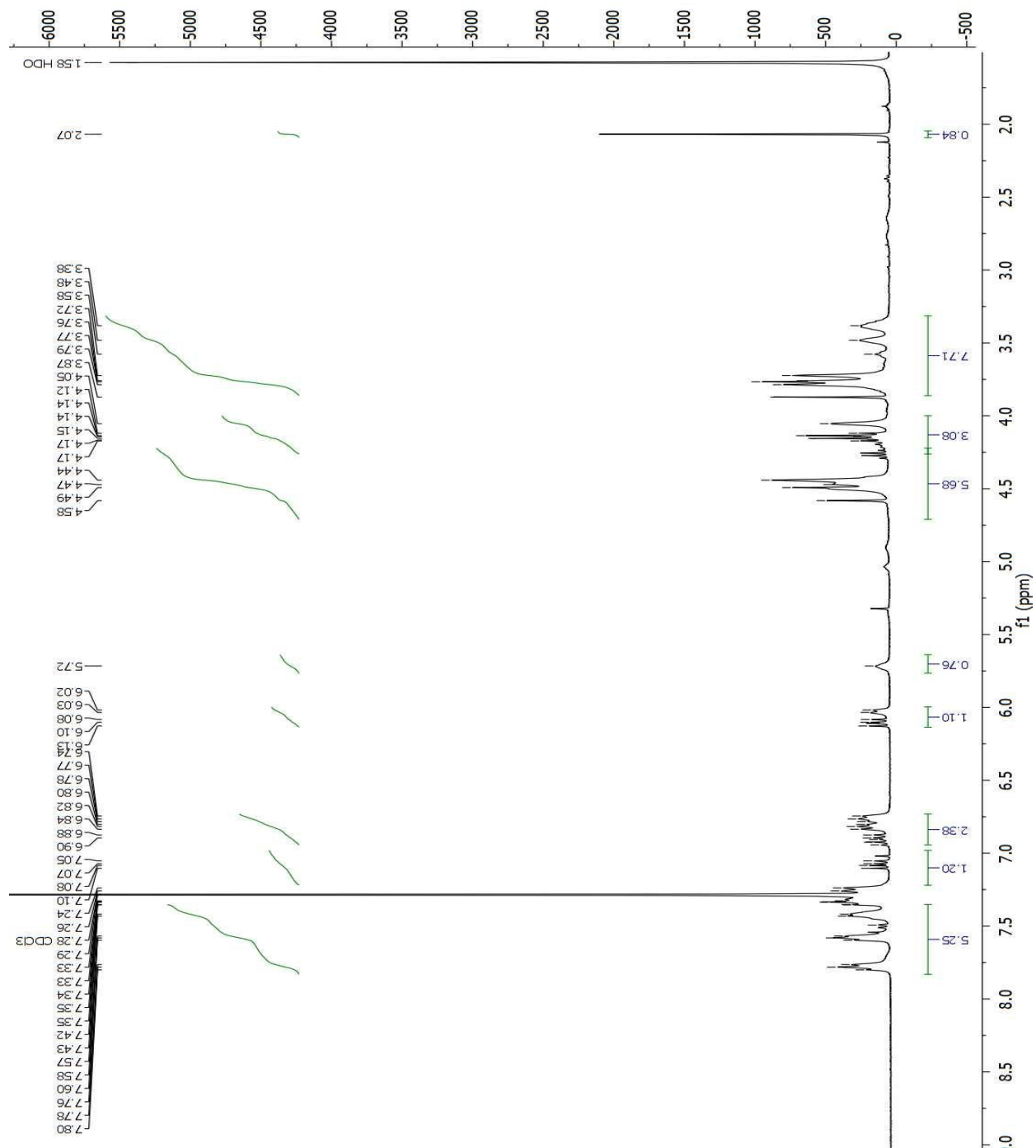
¹H NMR spectrum of methyl (2-((((9H-fluoren-9-yl)methoxy)carbonyl)amino)ethyl)glycinate (14)



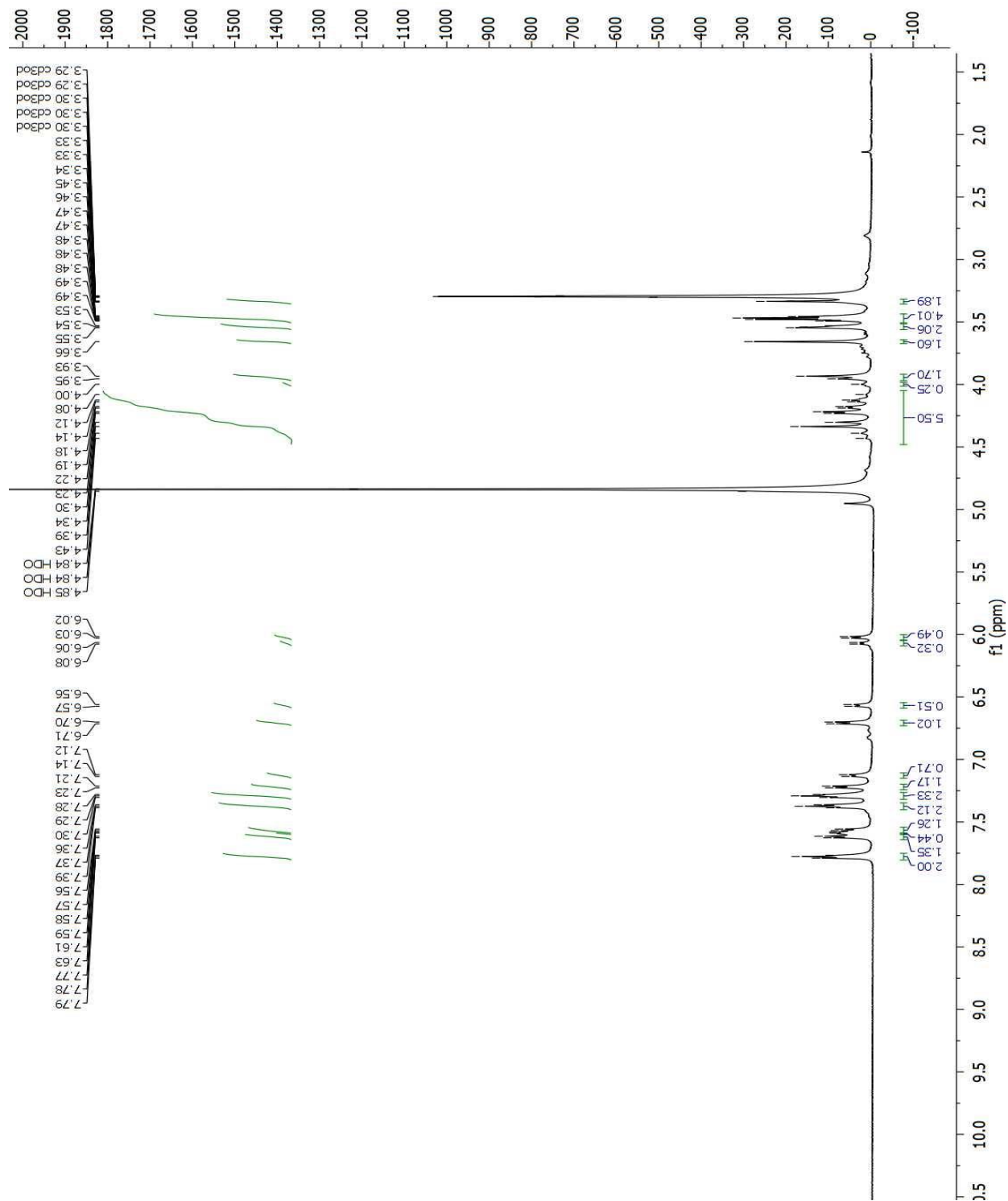
¹³C NMR spectrum of methyl (2-((((9H-fluoren-9-yl)methoxy)carbonyl)amino)ethyl)glycinate (14)



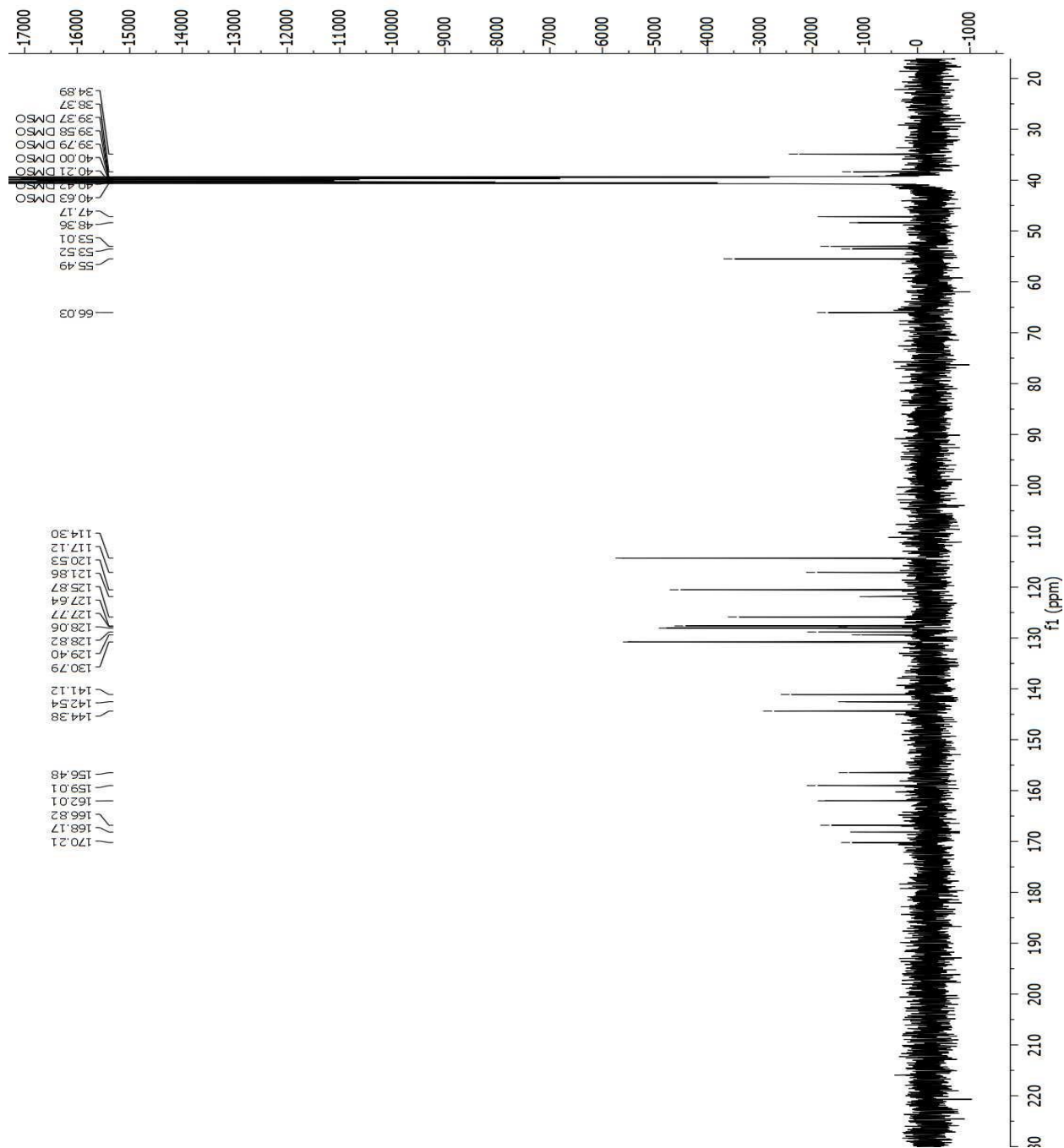
¹H NMR spectrum of methyl N-(2-((((9H-fluoren-9-yl)methoxy)carbonyl)amino)ethyl)-N-(2-(2-((4-methoxybenzyl)thio)-4-oxopyrimidin-1(4H)-yl)acetyl)glycinate (15)



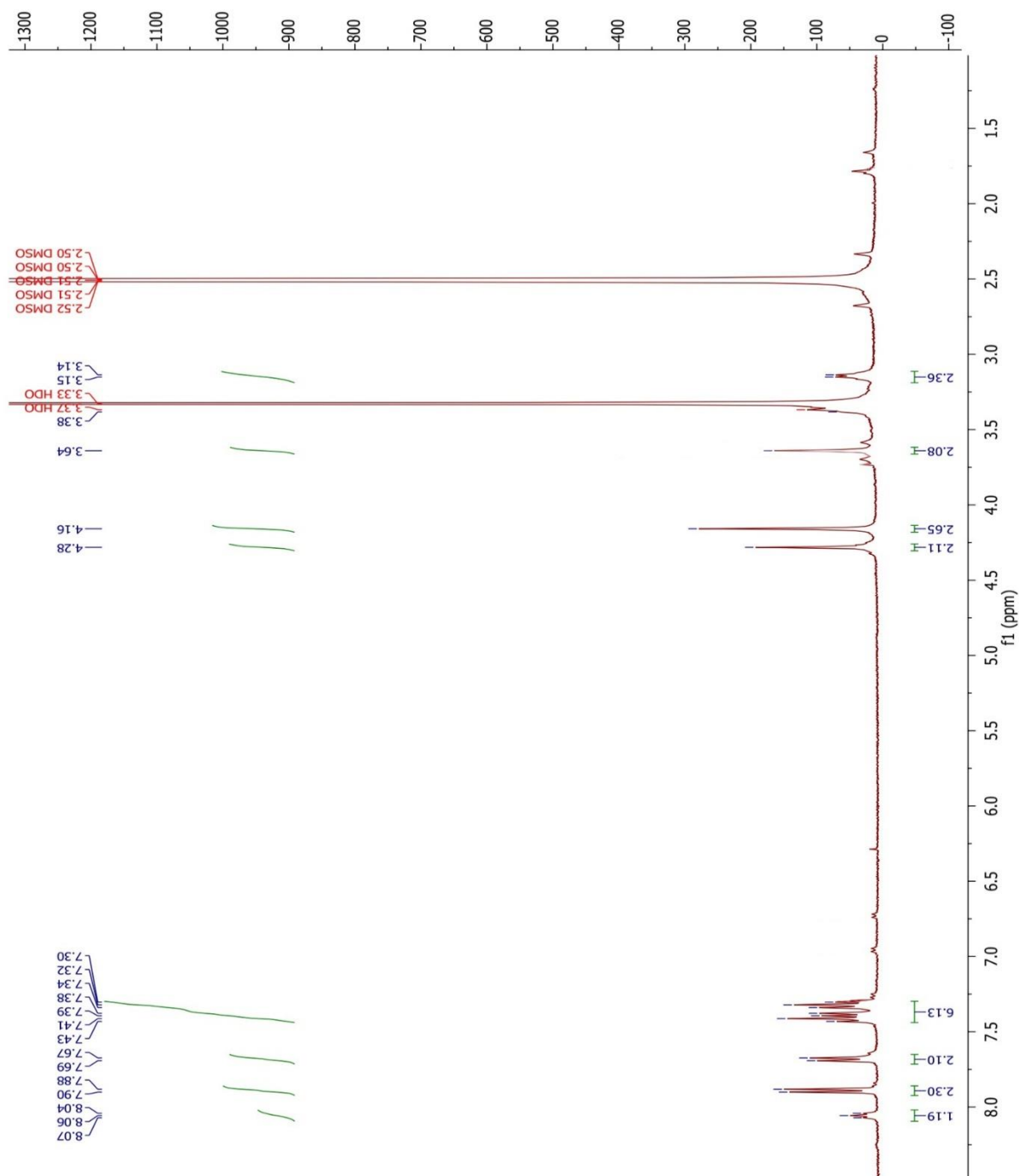
^1H NMR spectrum of N-(2-((((9H-fluoren-9-yl)methoxy)carbonyl)amino)ethyl)-N-(2-(2-((4-methoxybenzyl)thio)-4-oxopyrimidin-1(4H)-yl)acetyl)glycine (16)



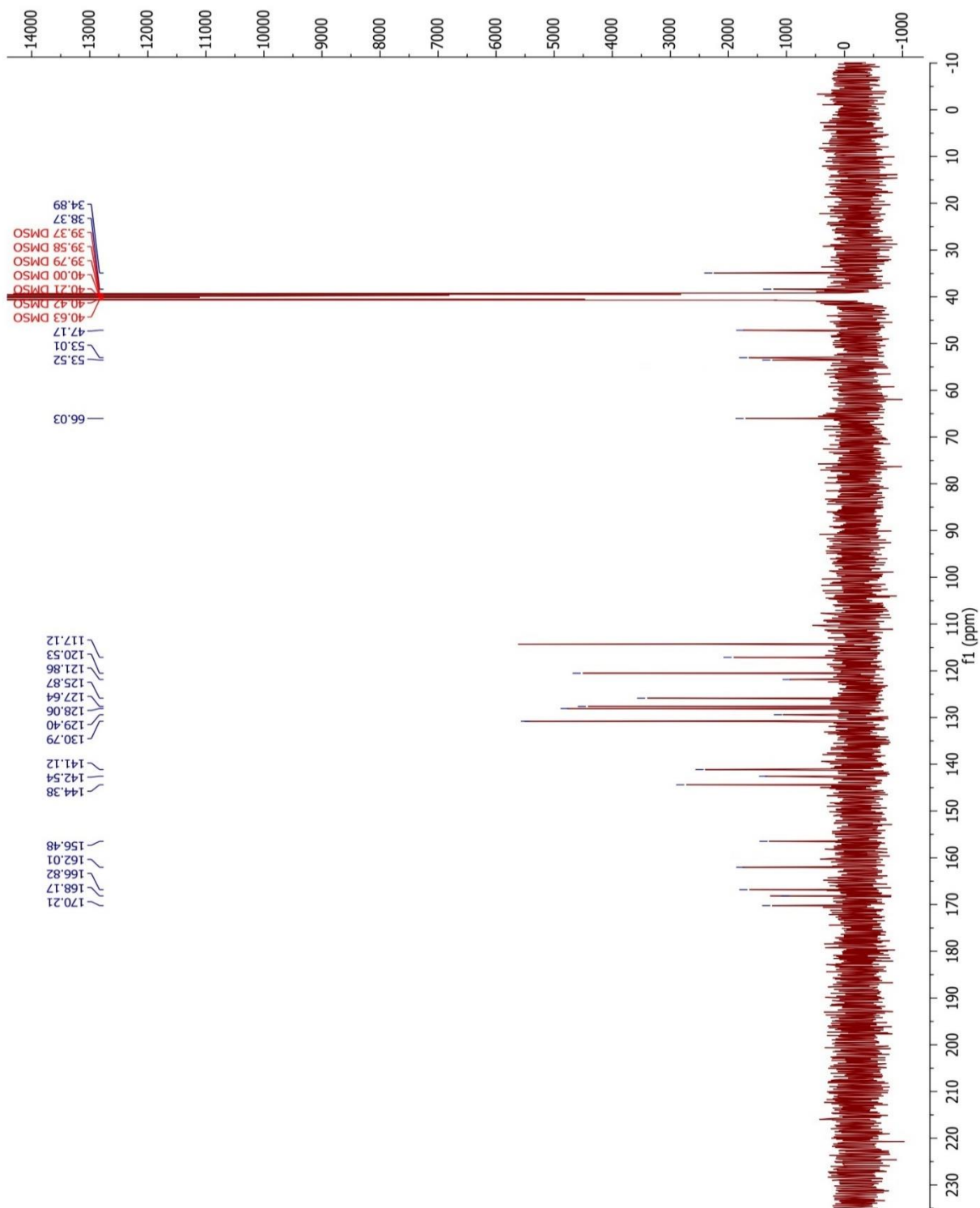
^{13}C NMR spectrum of N-(2-((((9H-fluoren-9-yl)methoxy)carbonyl)amino)ethyl)-N-(2-(2-((4-methoxybenzyl)thio)-4-oxopyrimidin-1(4H)-yl)acetyl)glycine (16)



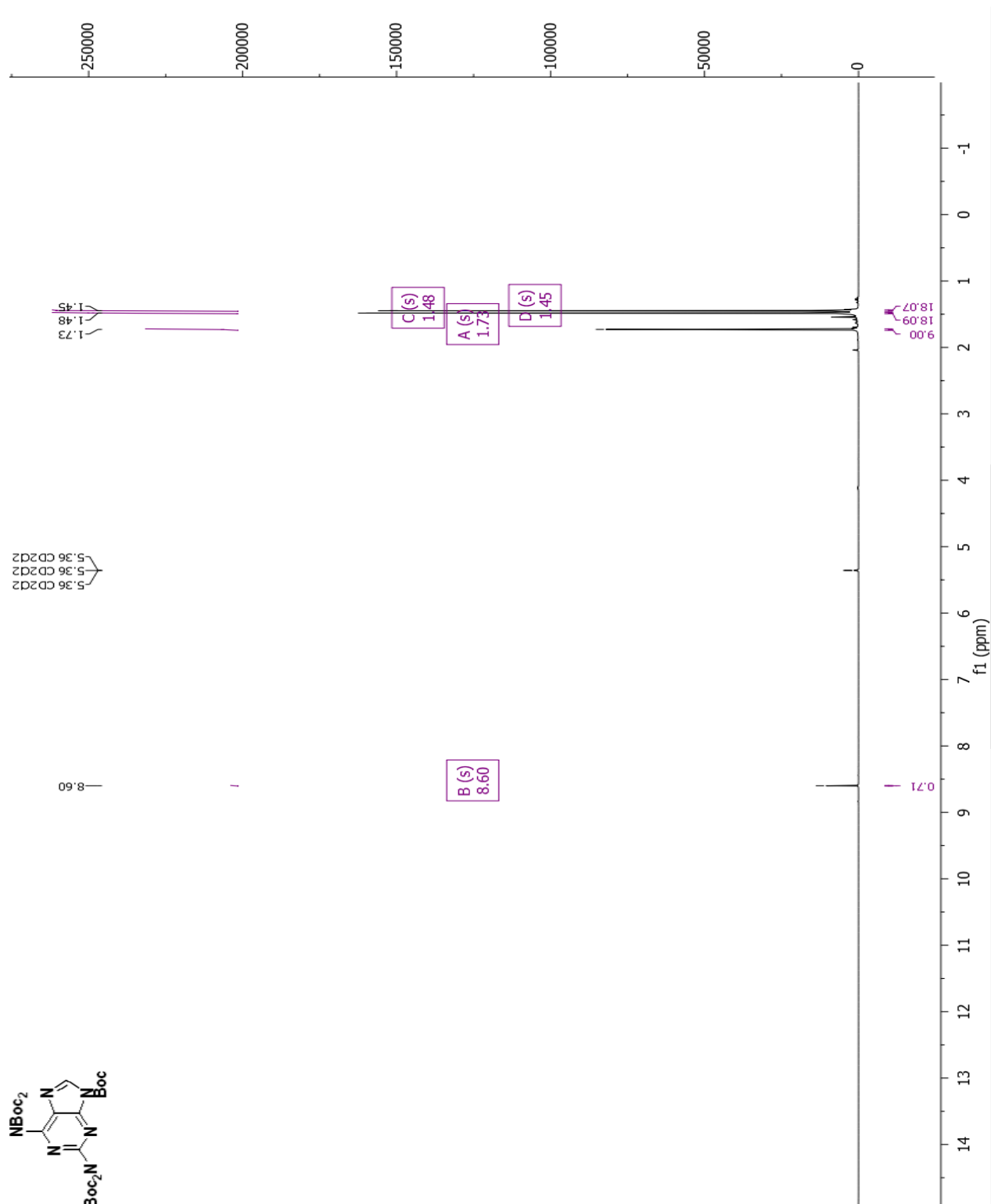
^1H NMR spectrum of N-(2-((((9H-fluoren-9-yl)methoxy)carbonyl)amino)ethyl)-N-(2-(4-oxo-2-thioxo-3,4-dihydropyrimidin-1(2H)-yl)acetyl)glycine (17)



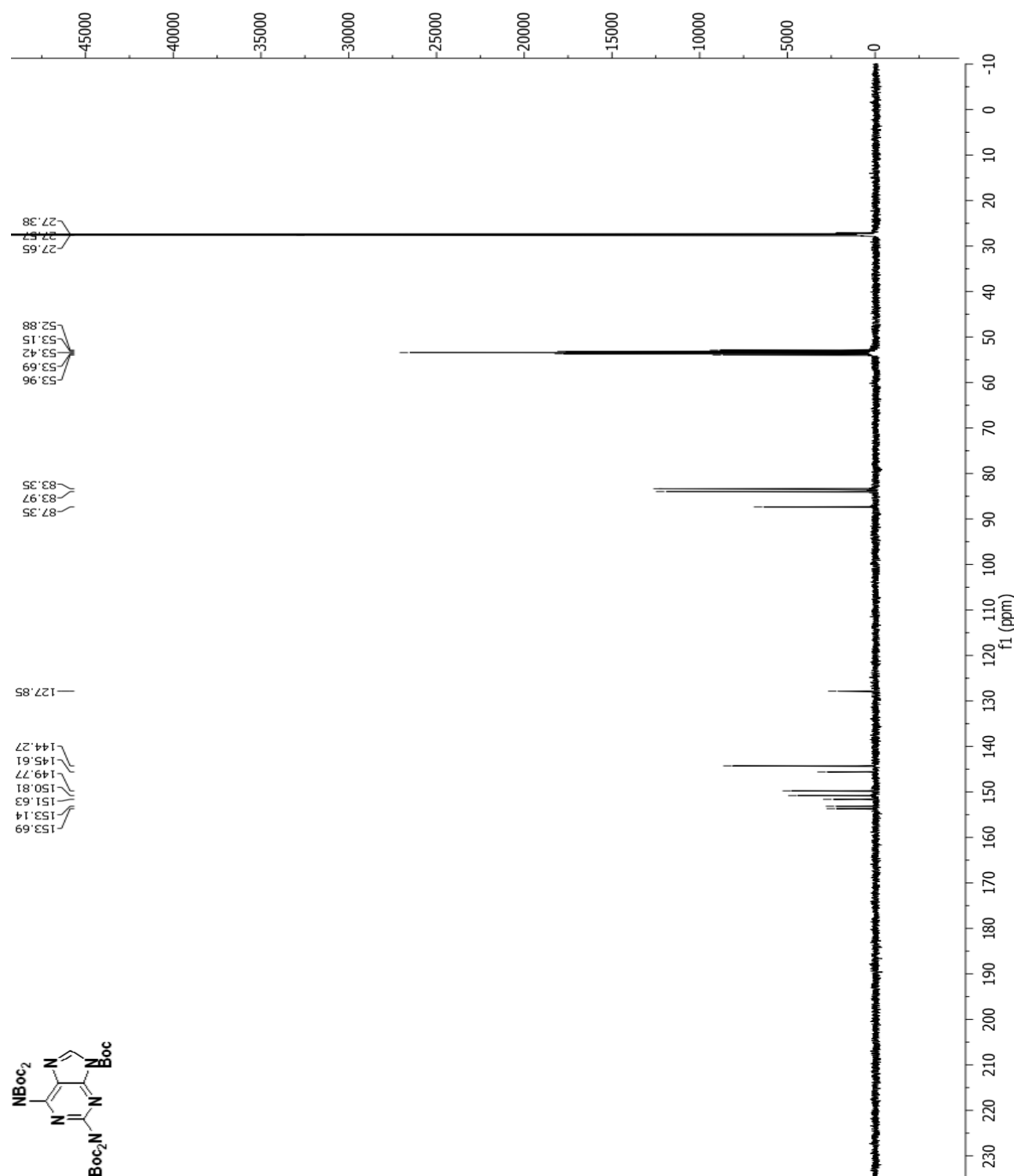
^{13}C NMR spectrum of N-(2-(((9H-fluoren-9-yl)methoxy)carbonyl)amino)ethyl)-N-(2-(4-oxo-2-thioxo-3,4-dihydropyrimidin-1(2H)-yl)acetyl)glycine (17)



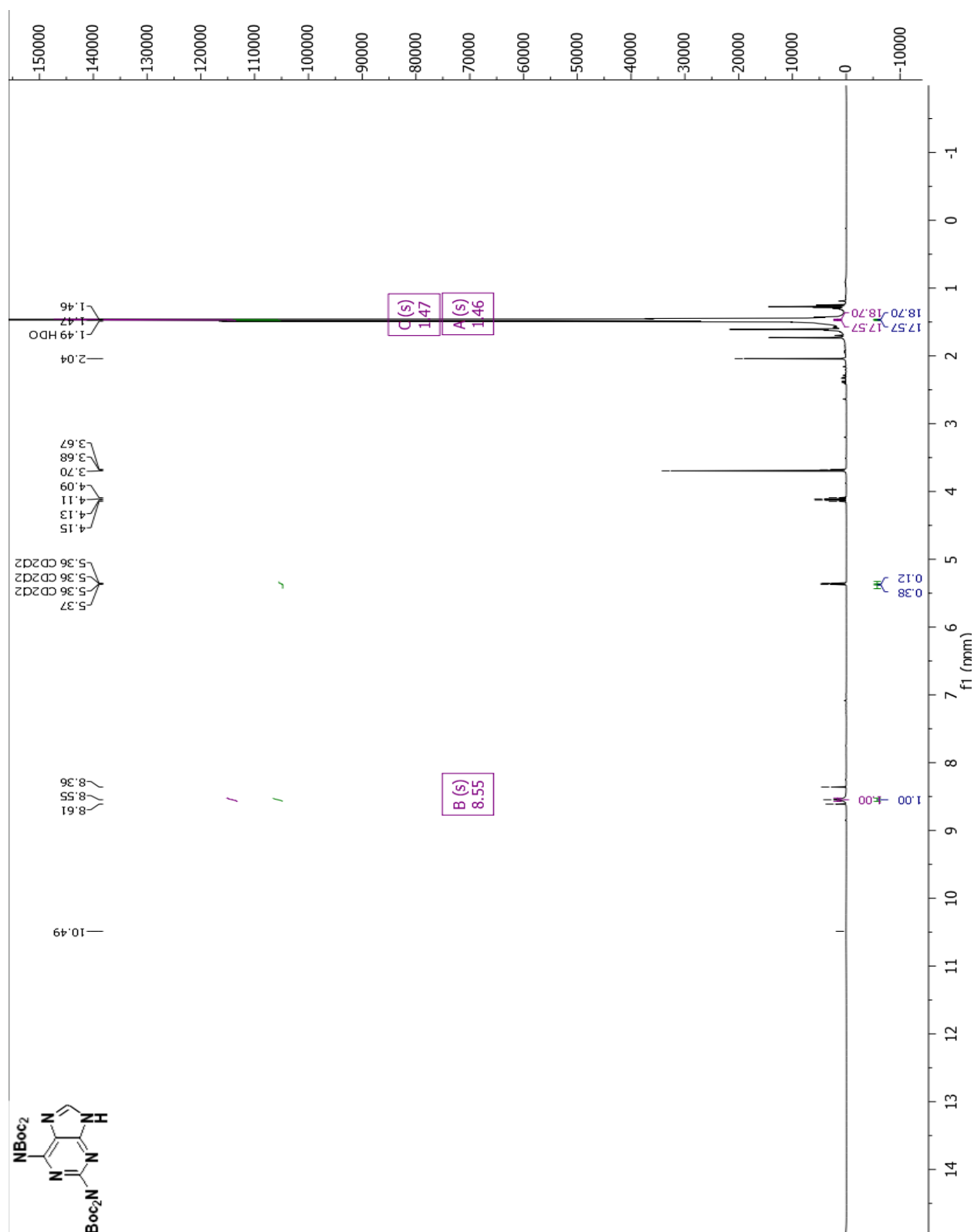
¹H NMR spectrum of tert-butyl 2,6-bis(bis(tert-butoxycarbonyl)amino)-9H-purine-9-carboxylate (19)



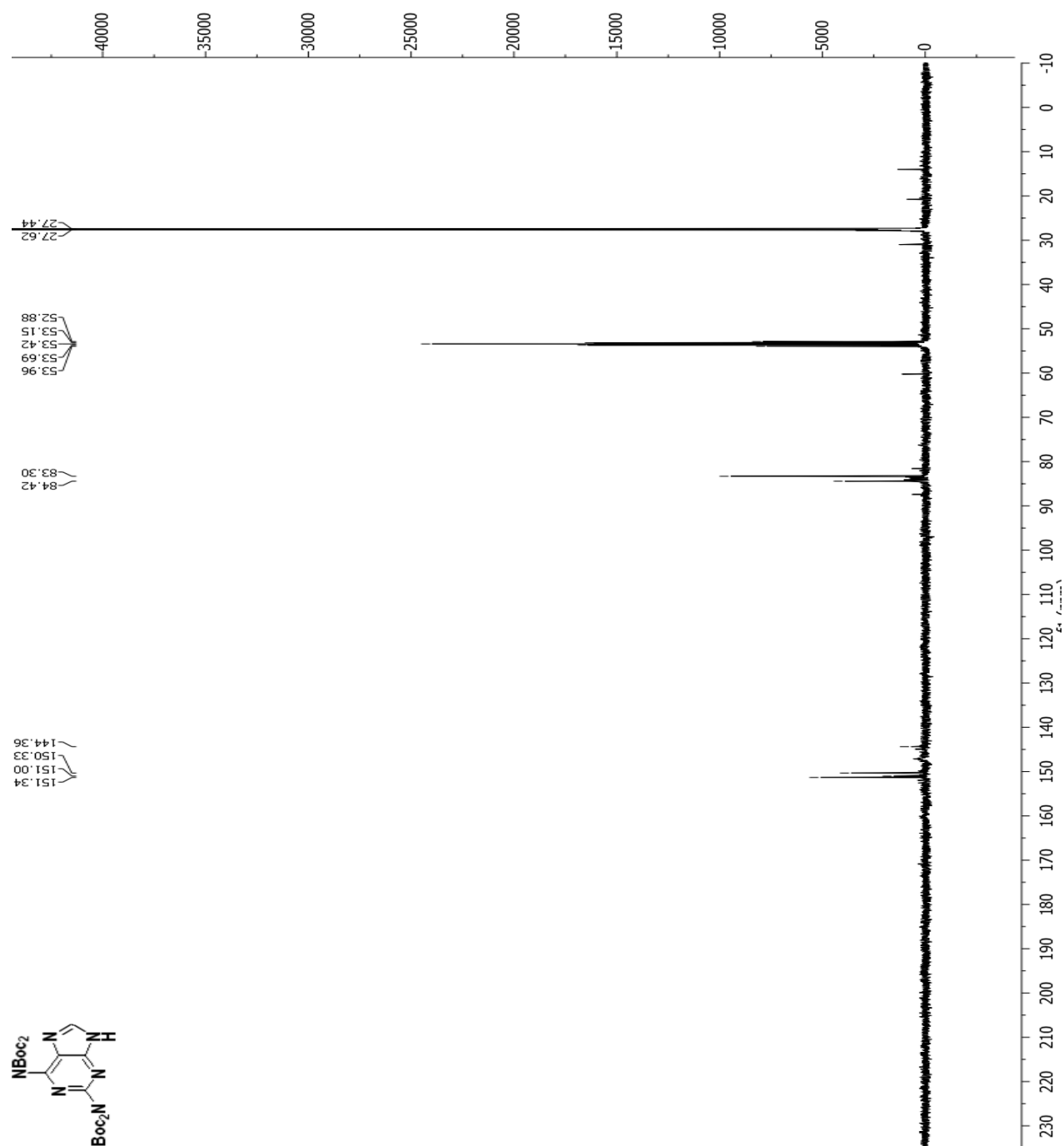
^{13}C NMR spectrum of tert-butyl 2,6-bis(bis(tert-butoxycarbonyl)amino)-9H-purine-9-carboxylate (19)



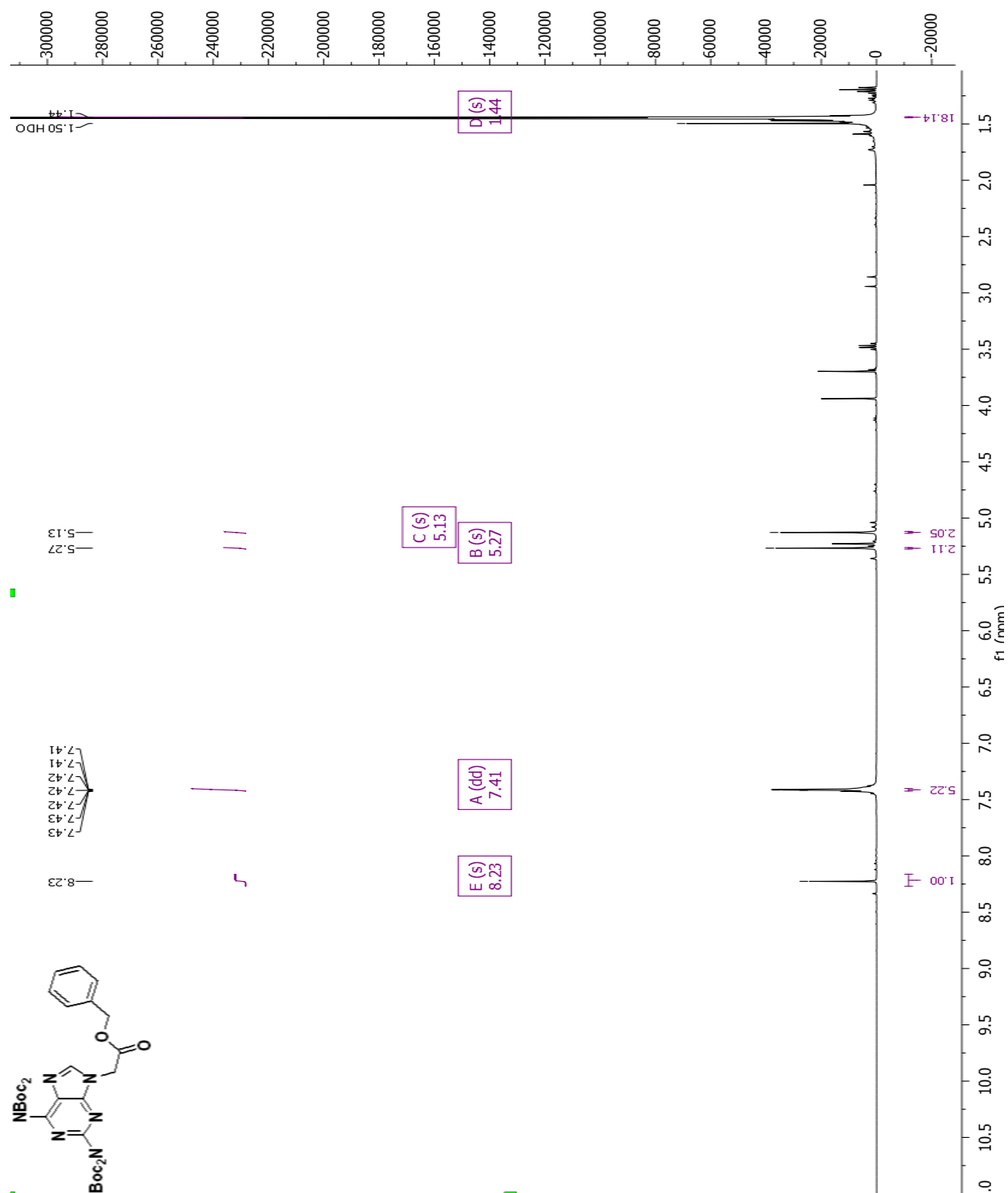
¹H NMR spectrum of di-tert-butyl (9H-purine-2,6-diyl)bis((tert-butoxycarbonyl)carbamate) (20)



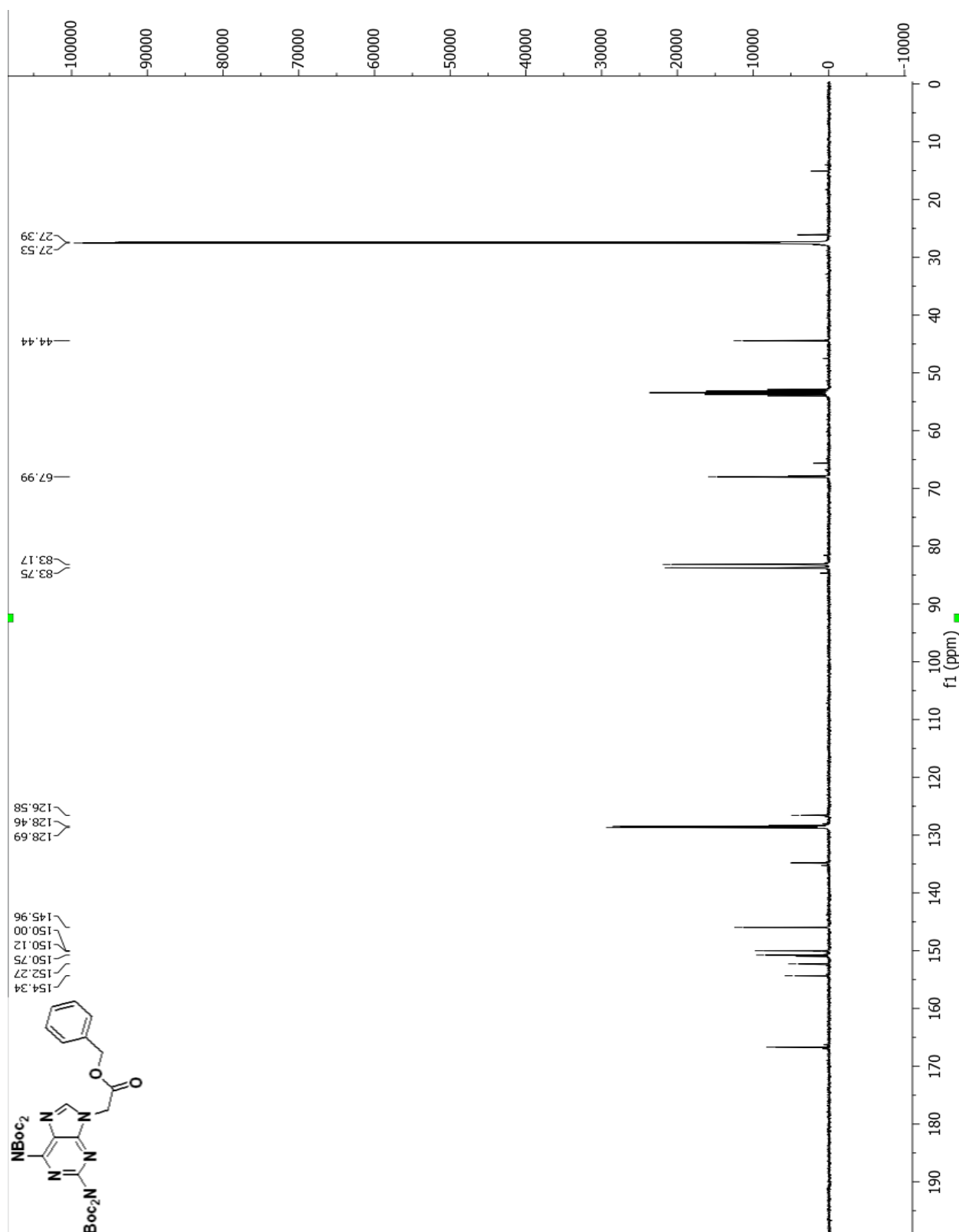
^{13}C NMR spectrum of di-tert-butyl (9H-purine-2,6-diyl)bis((tert-butoxycarbonyl)carbamate) (20)



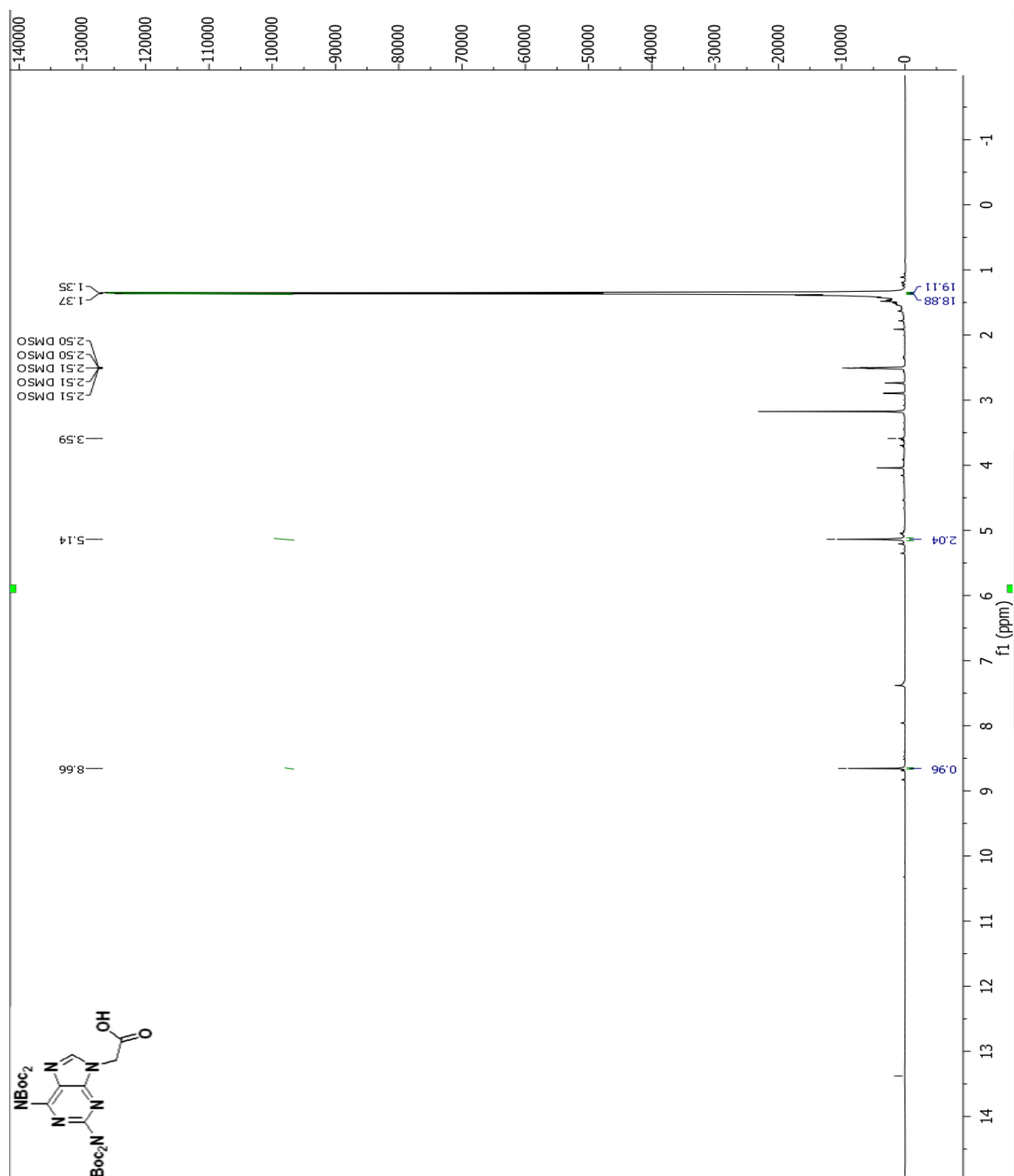
¹H NMR spectrum of benzyl 2-(2,6-bis(bis(tert-butoxycarbonyl)amino)-9H-purin-9-yl)acetate (21)



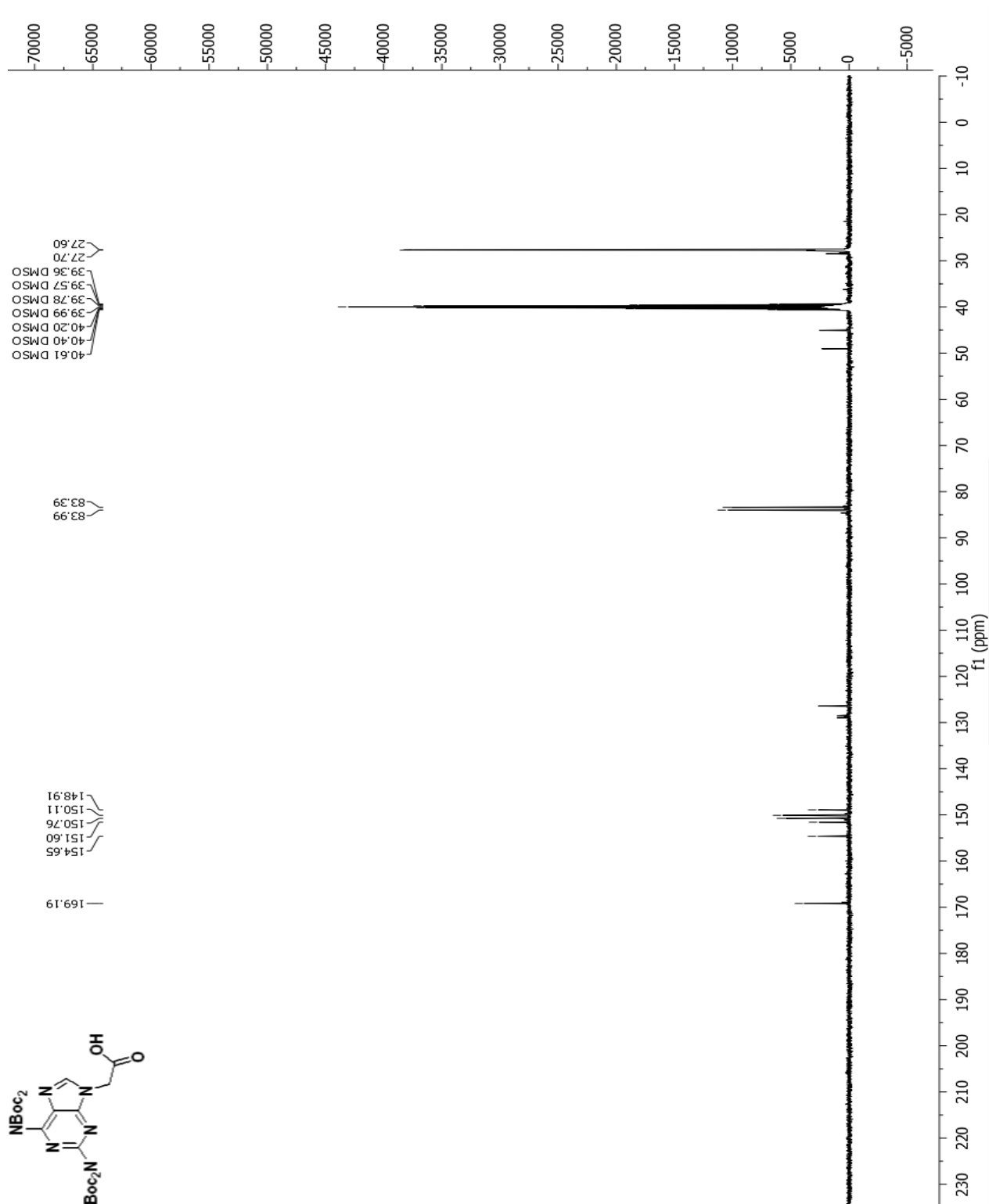
^{13}C NMR spectrum of benzyl 2-(2,6-bis(bis(tert-butoxycarbonyl)amino)-9H-purin-9-yl)acetate (21)



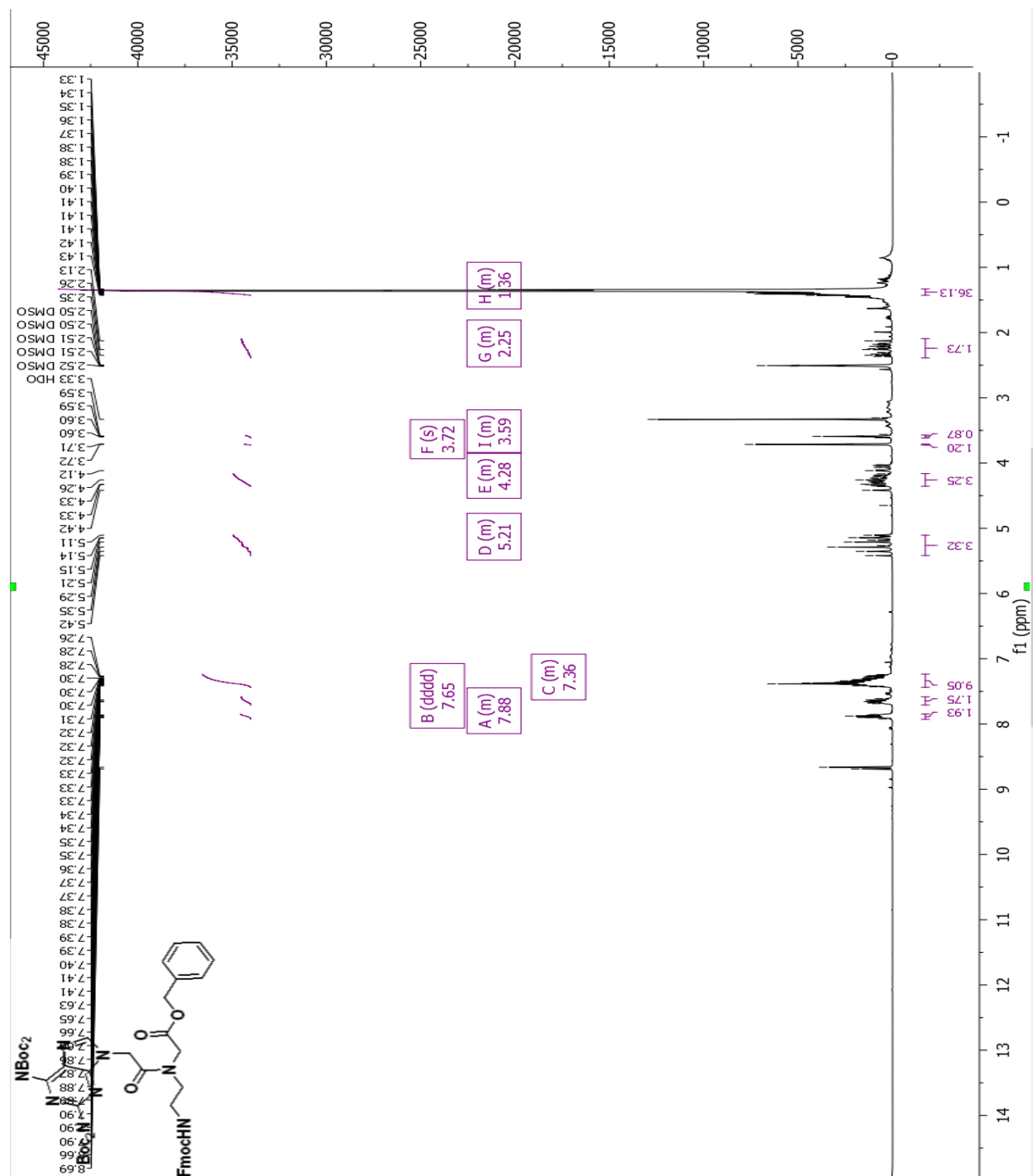
^1H NMR spectrum of 2-(2,6-bis(bis(tert-butoxycarbonyl)amino)-9H-purin-9-yl)acetic acid (22)



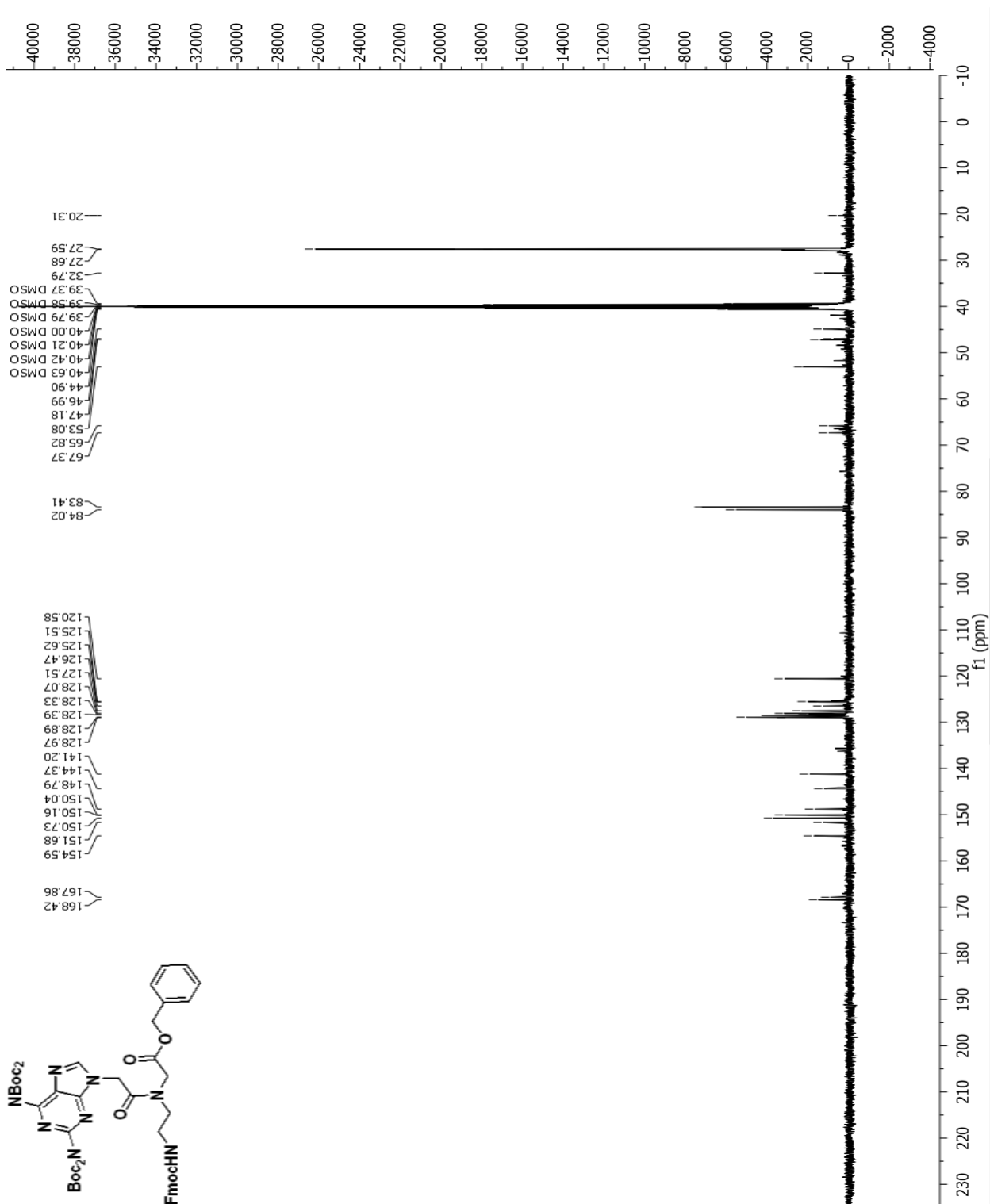
^{13}C NMR spectrum of 2-(2,6-bis(bis(tert-butoxycarbonyl)amino)-9H-purin-9-yl)acetic acid (22)

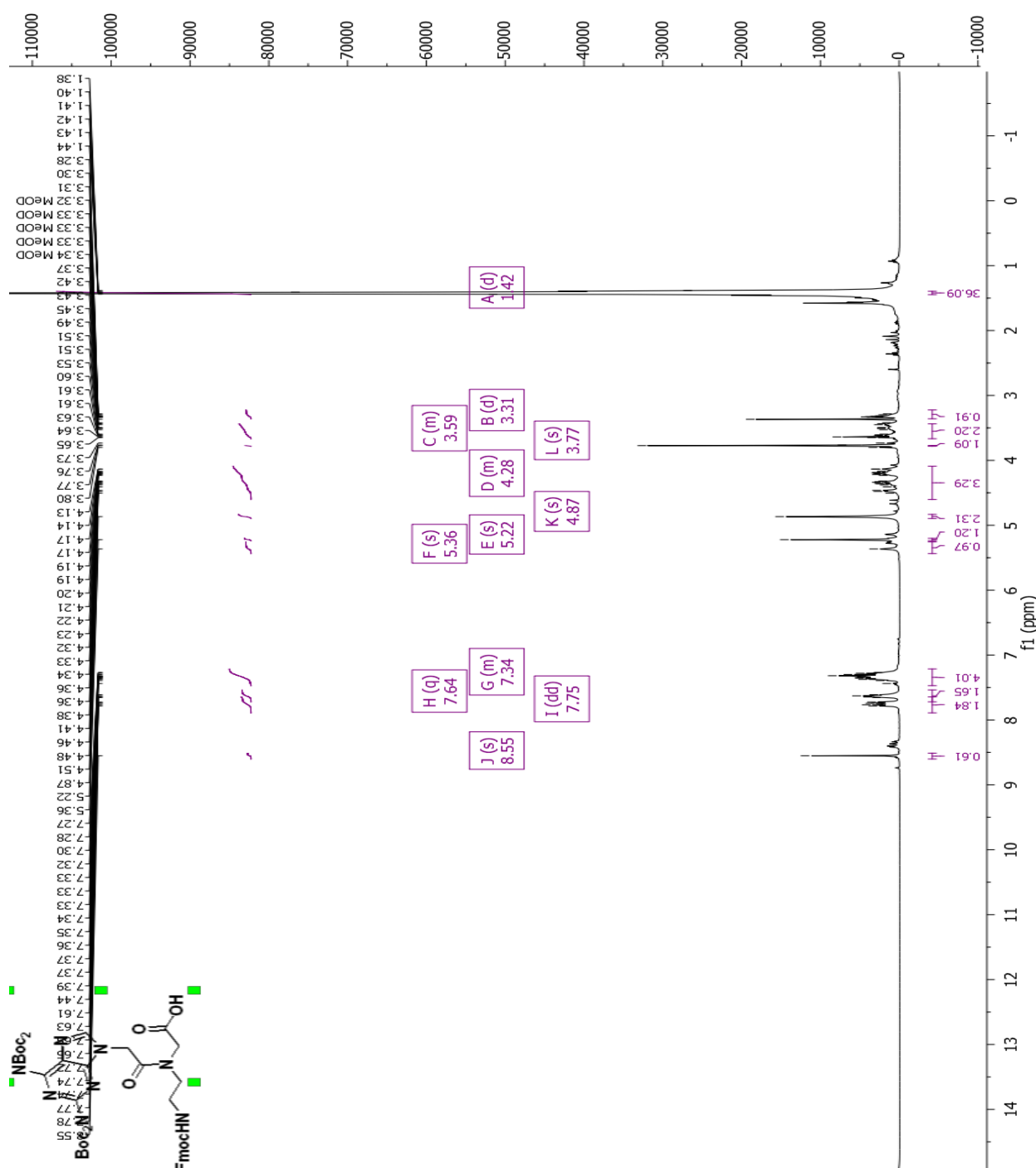


¹H NMR spectrum of benzyl N-(2-((((9H-fluoren-9-yl)methoxy)carbonyl)amino)ethyl)-N-(2-(2,6-bis(bis(tert-butoxycarbonyl)amino)-9H-purin-9-yl)acetyl)glycinate(23)

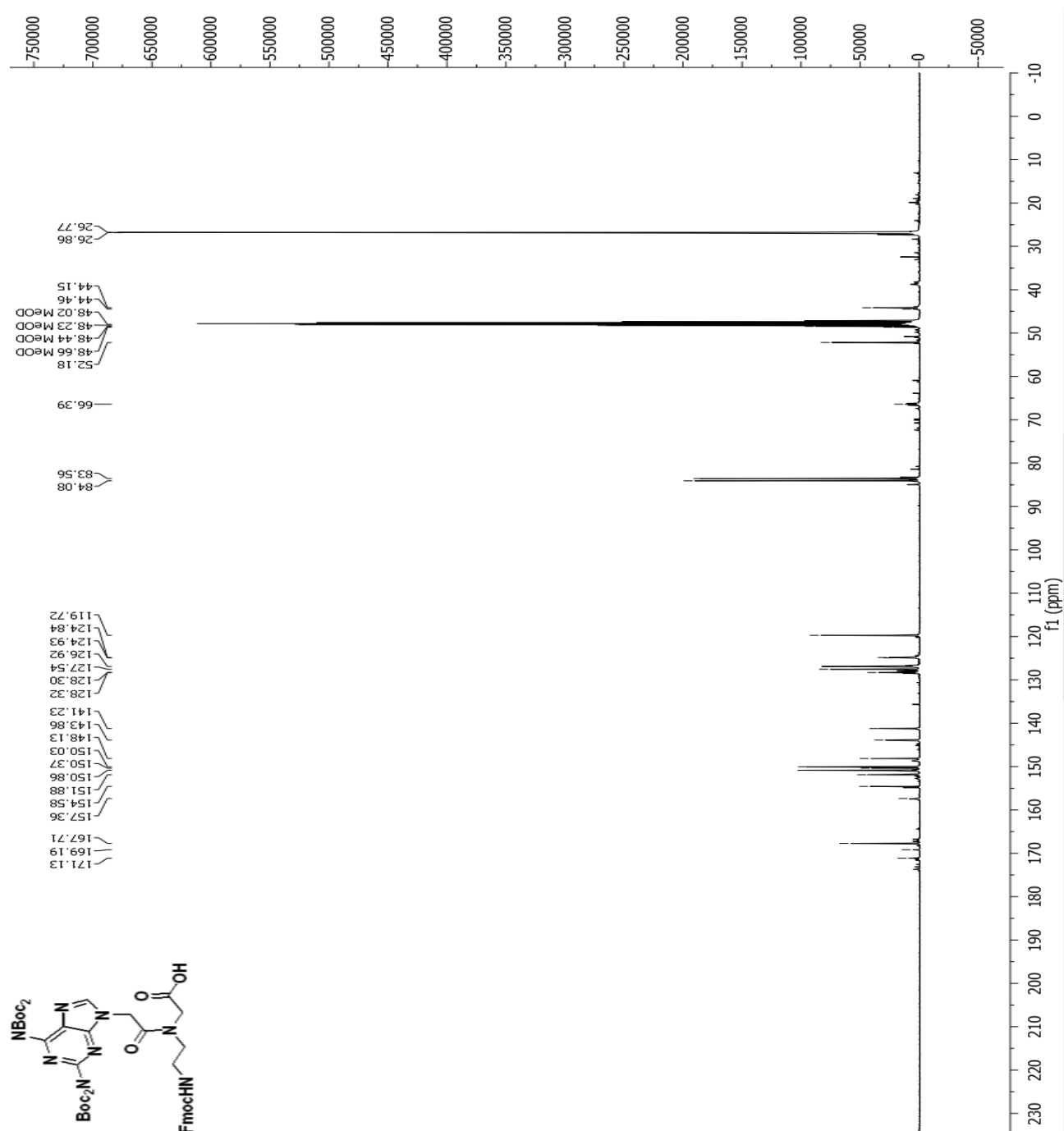


^{13}C NMR spectrum of benzyl N-(2-(((9H-fluoren-9-yl)methoxy)carbonyl)amino)ethyl)-N-(2-(2,6-bis(bis(tert-butoxycarbonyl)amino)-9H-purin-9-yl)acetyl)glycinate(23)

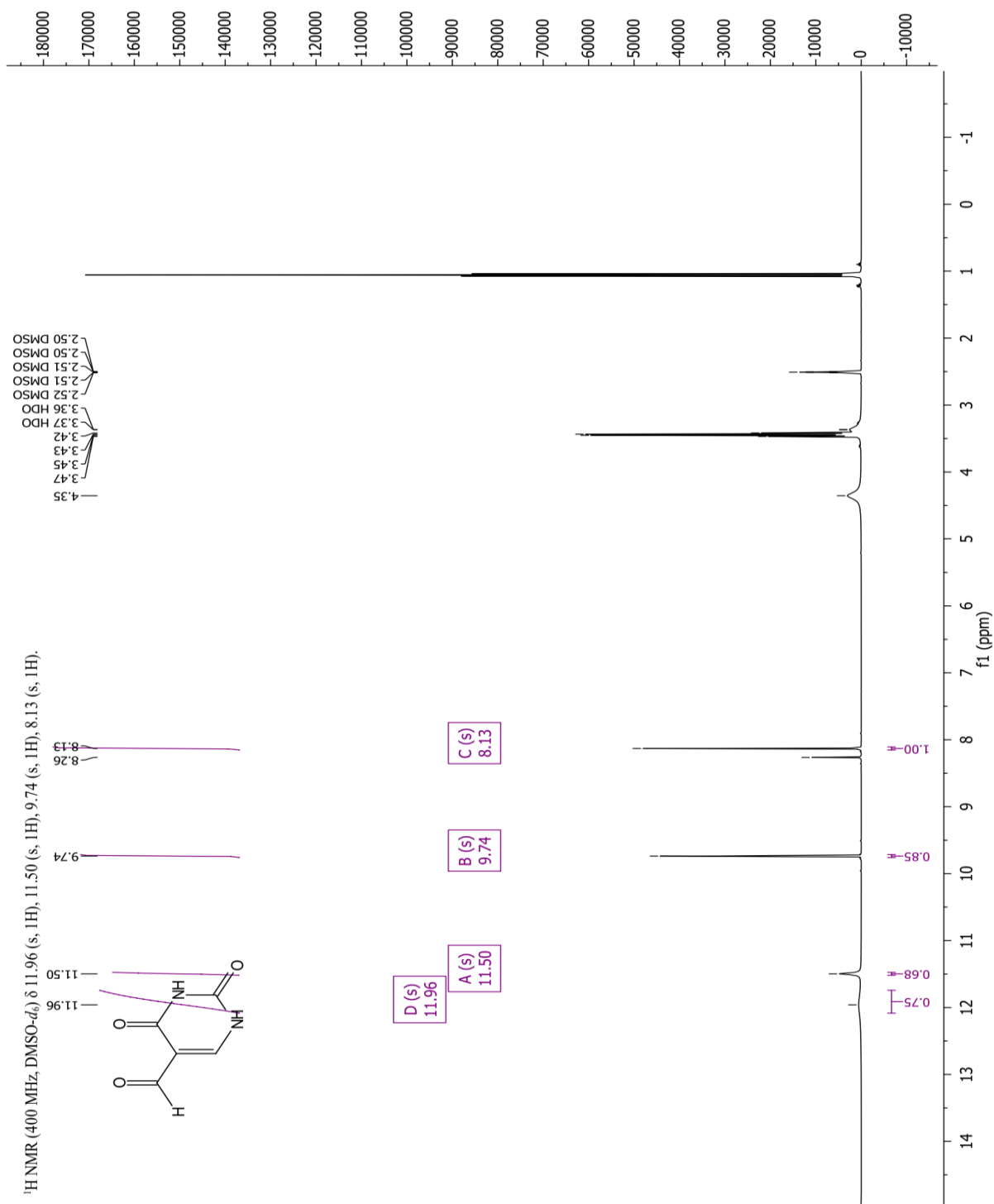




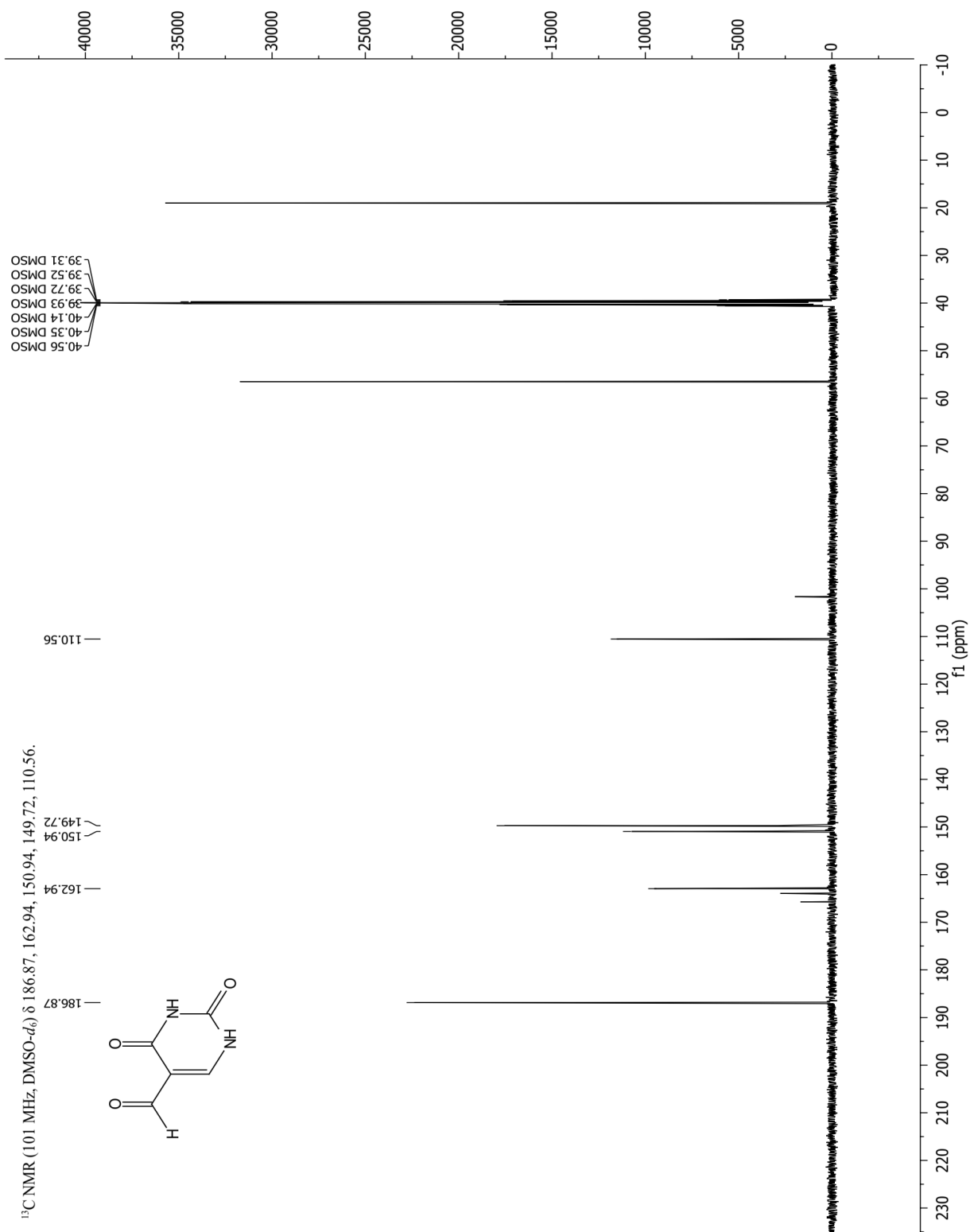
^{13}C NMR spectrum of N-(2-((((9H-fluoren-9-yl)methoxy)carbonyl)amino)ethyl)-N-(2-(2,6-bis(bis(tert-butoxycarbonyl)amino)-9H-purin-9-yl)acetyl)glycine (24)



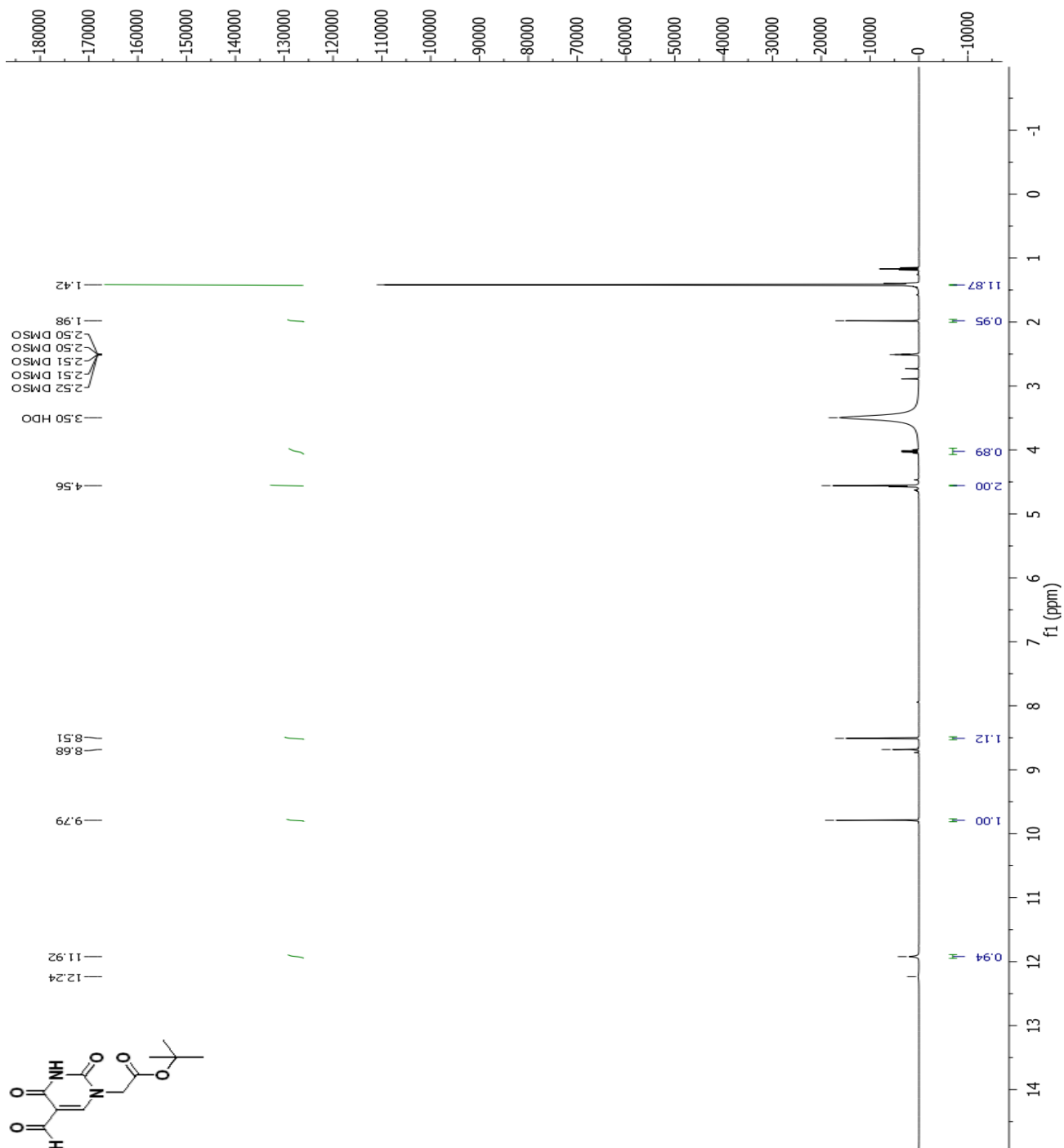
¹H NMR spectrum of 5-Formyluracil (25)



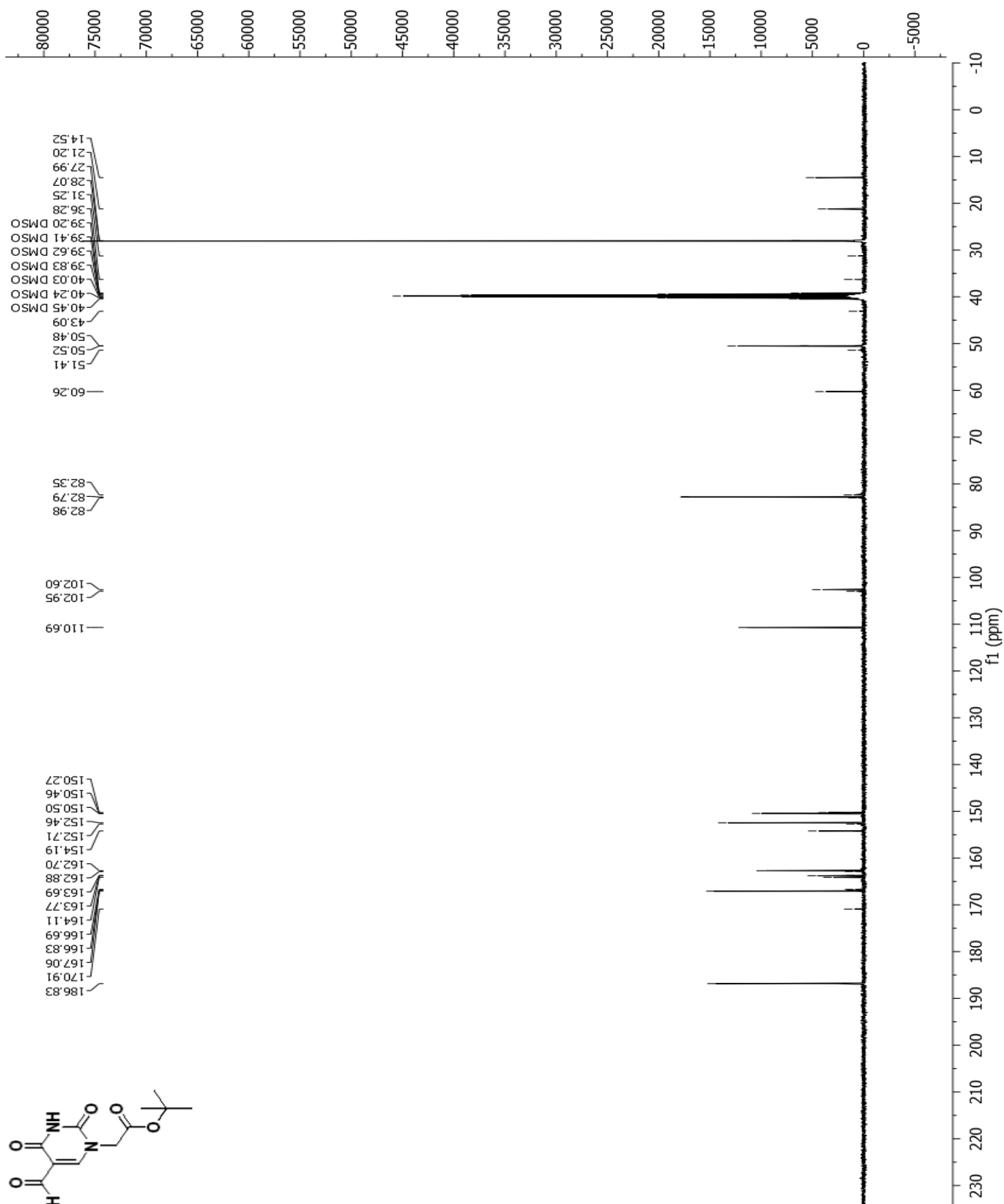
¹³C NMR spectrum of 5-Formyluracil (25)



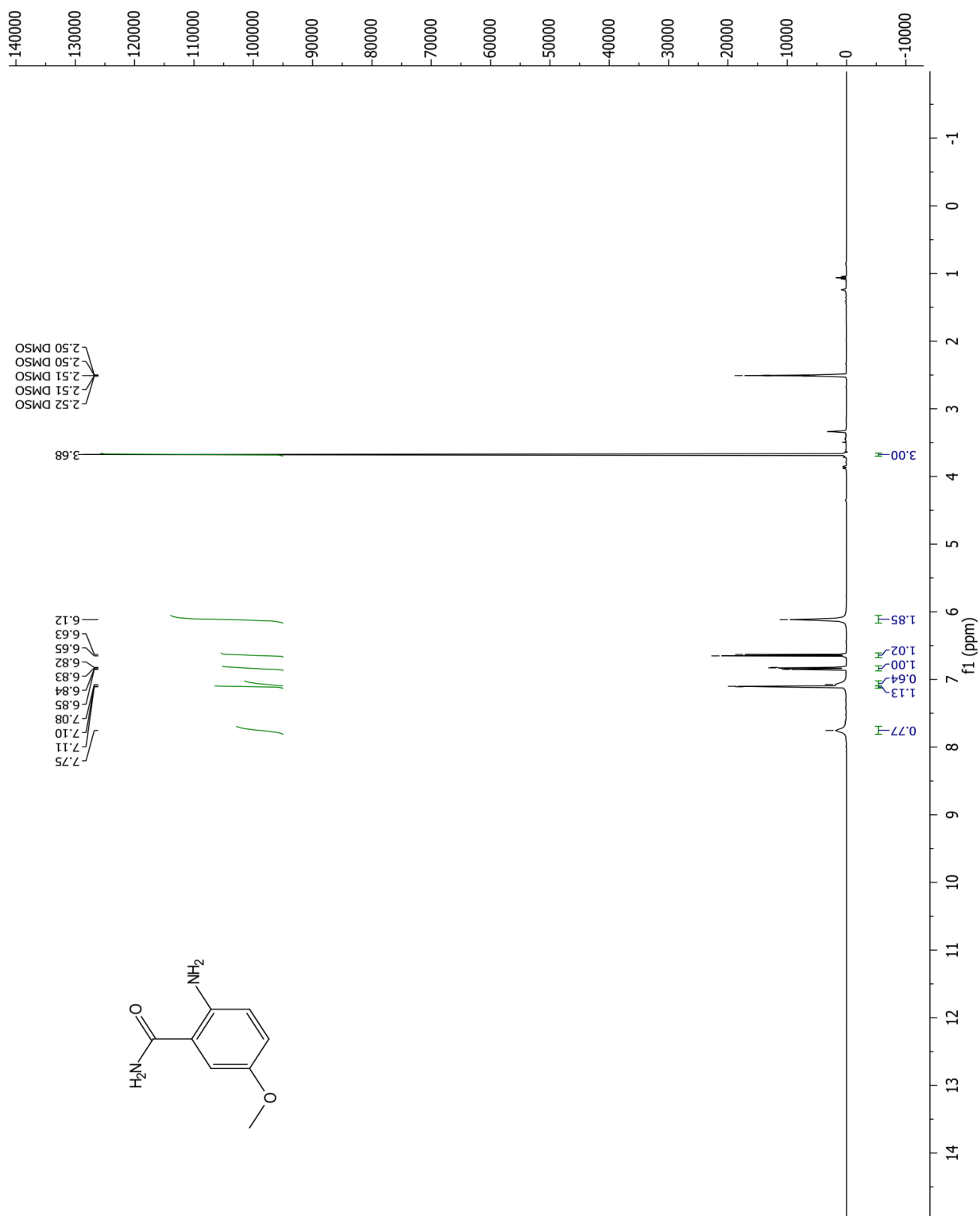
¹H NMR spectrum of *tert*-Butyl (uracil-5-formaldehyde-1-yl) acetate (26)



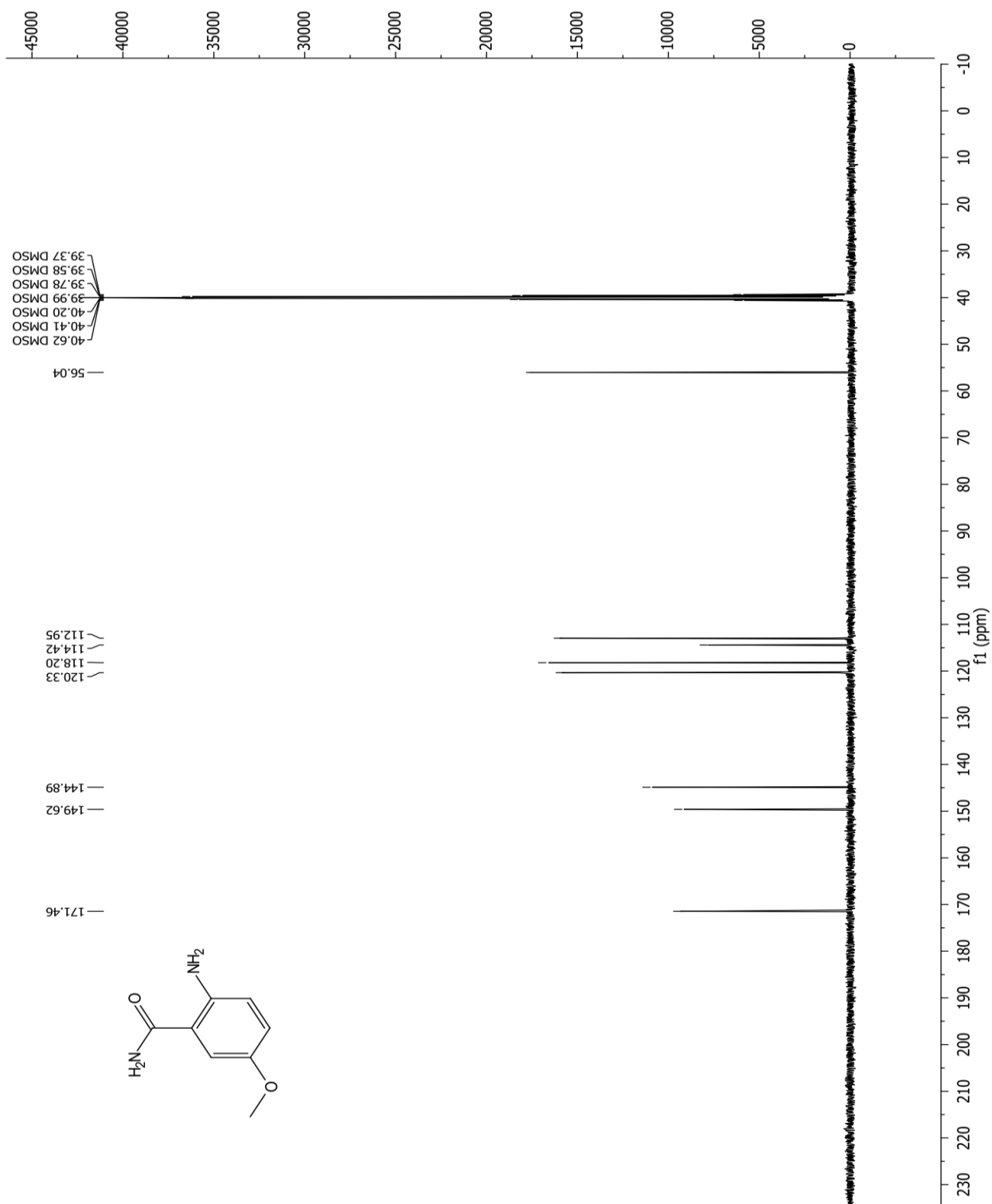
^{13}C NMR spectrum of *tert*-Butyl (uracil-5-formaldehyde-1-yl) acetate (26)



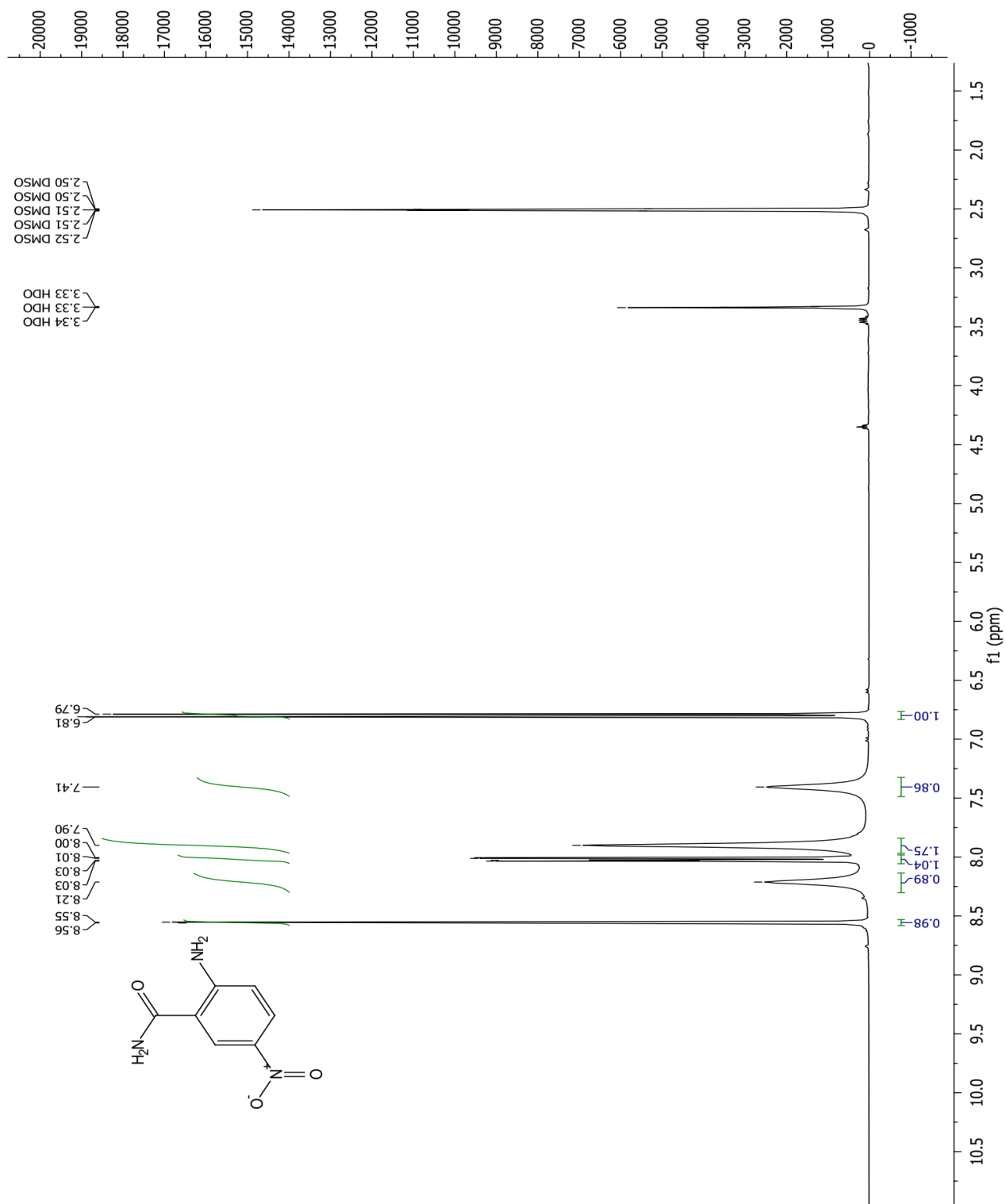
¹H NMR spectrum of 2-Amino-5-methoxybenzamide (27)



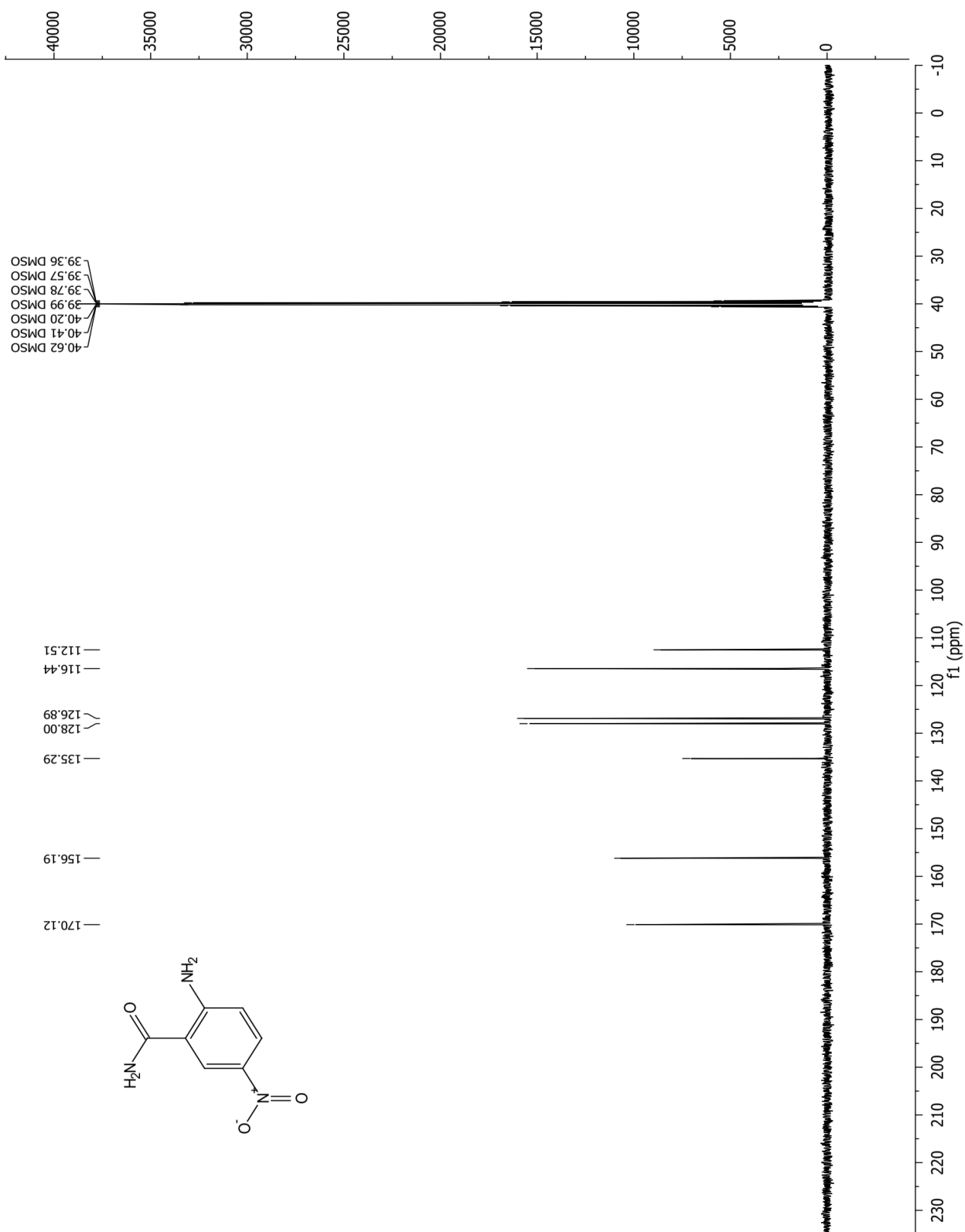
¹³C NMR spectrum of 2-Amino-5-methoxybenzamide (27)



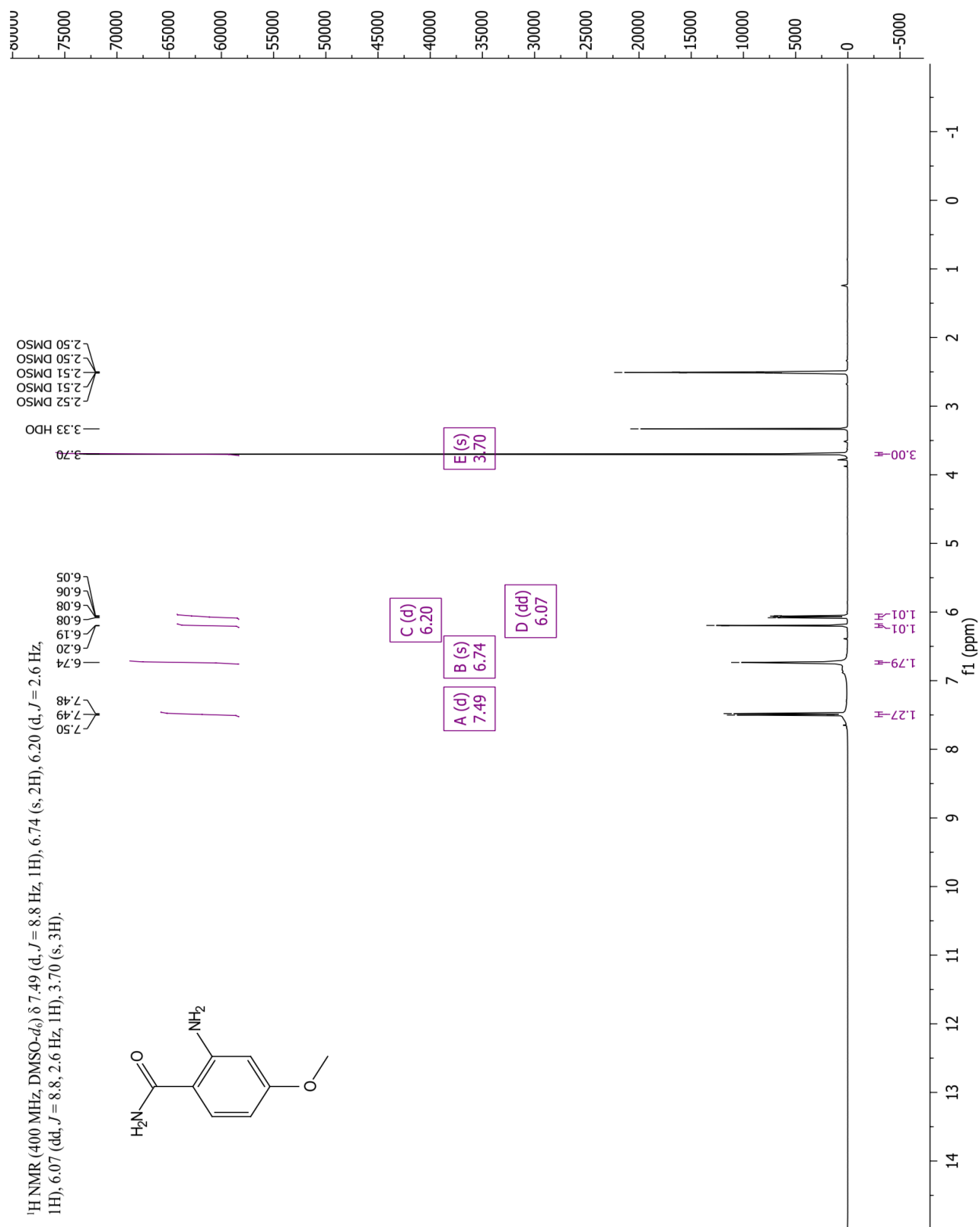
¹H NMR spectrum of 2-Amino-5-nitrobenzamide (28)



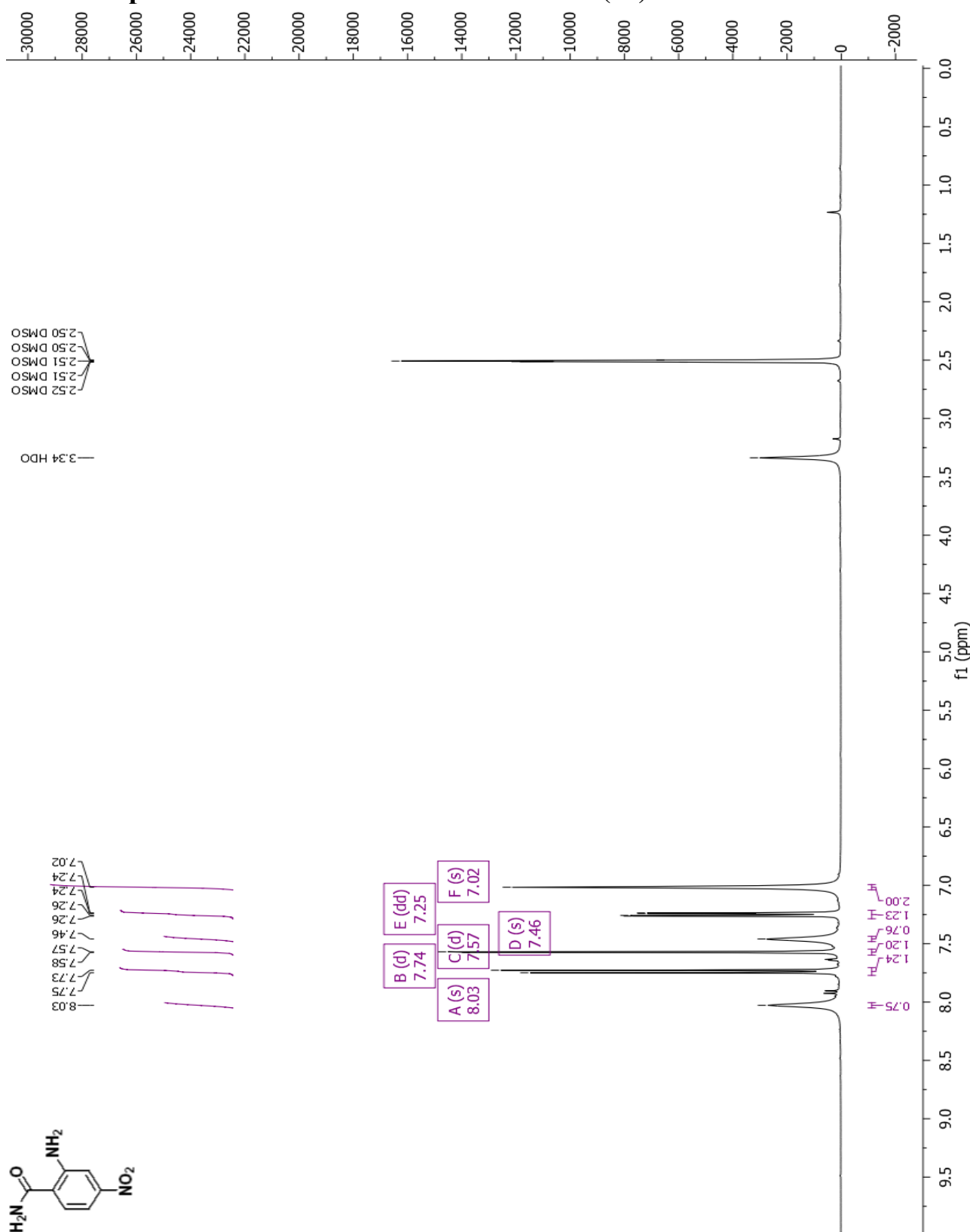
¹³C NMR spectrum of 2-Amino-5-nitrobenzamide (28)



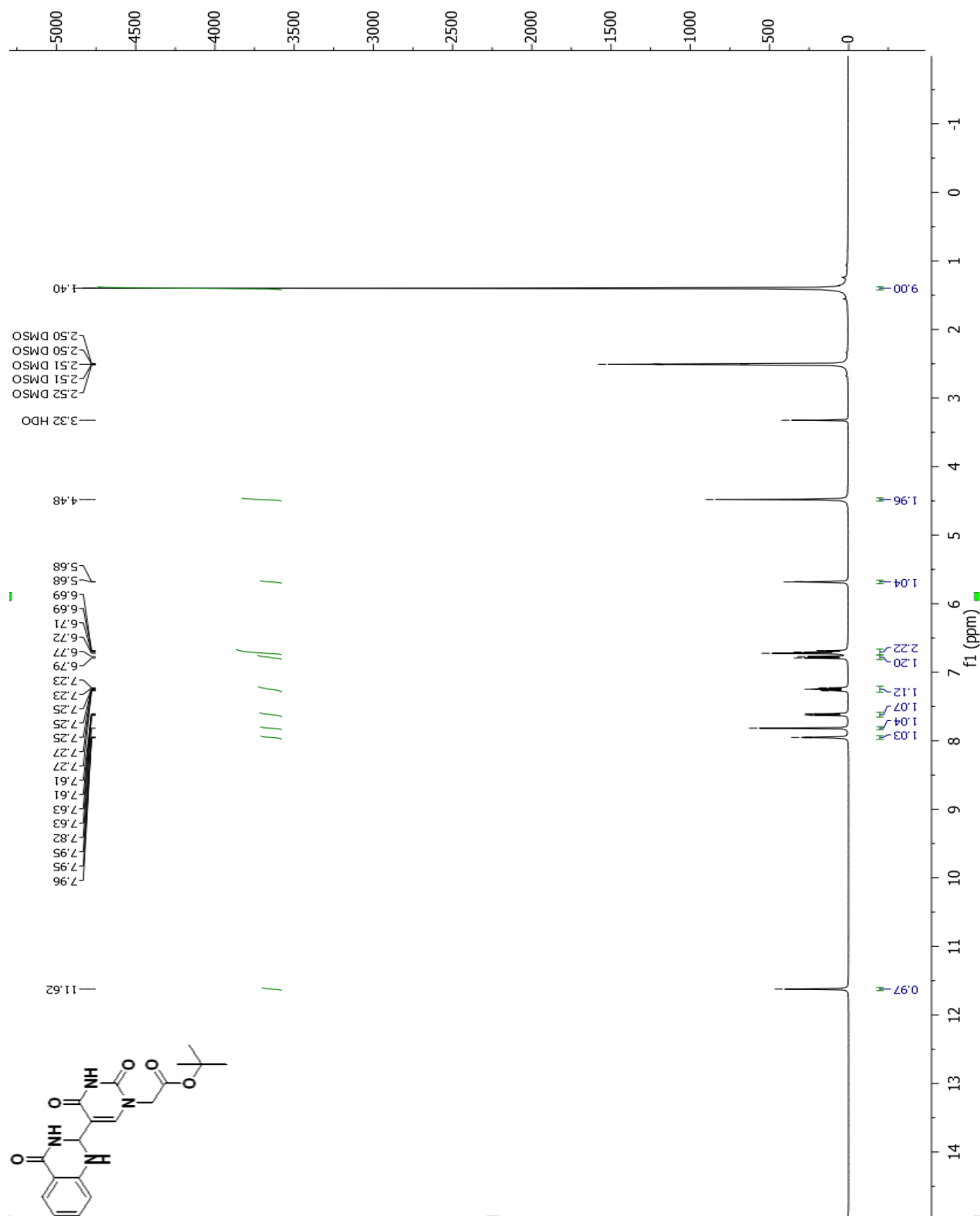
¹H NMR spectrum of 2-Amino-4-methoxybenzamide (29)



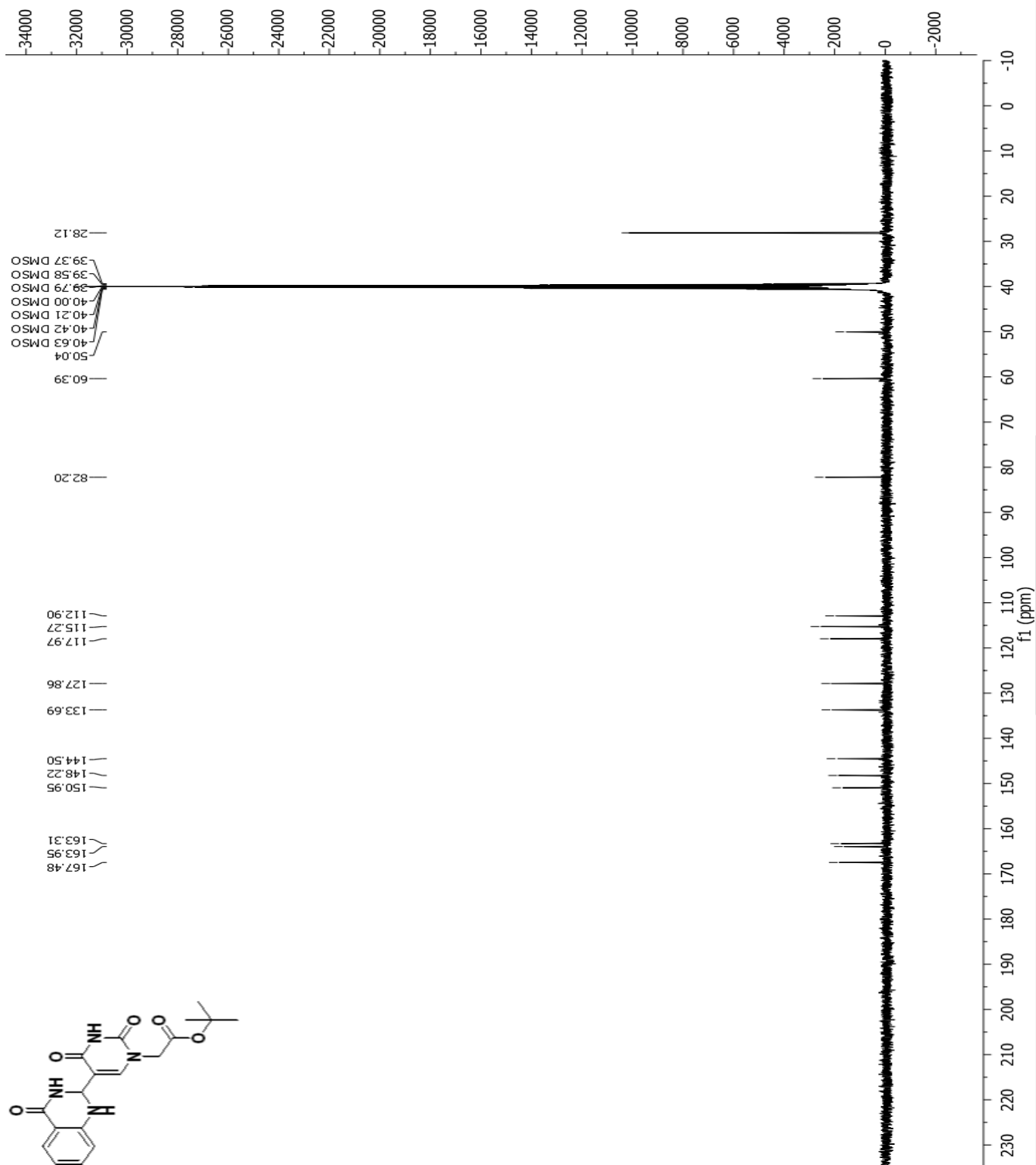
¹H NMR spectrum of 2-Amino-4-nitrobenzamide (30)



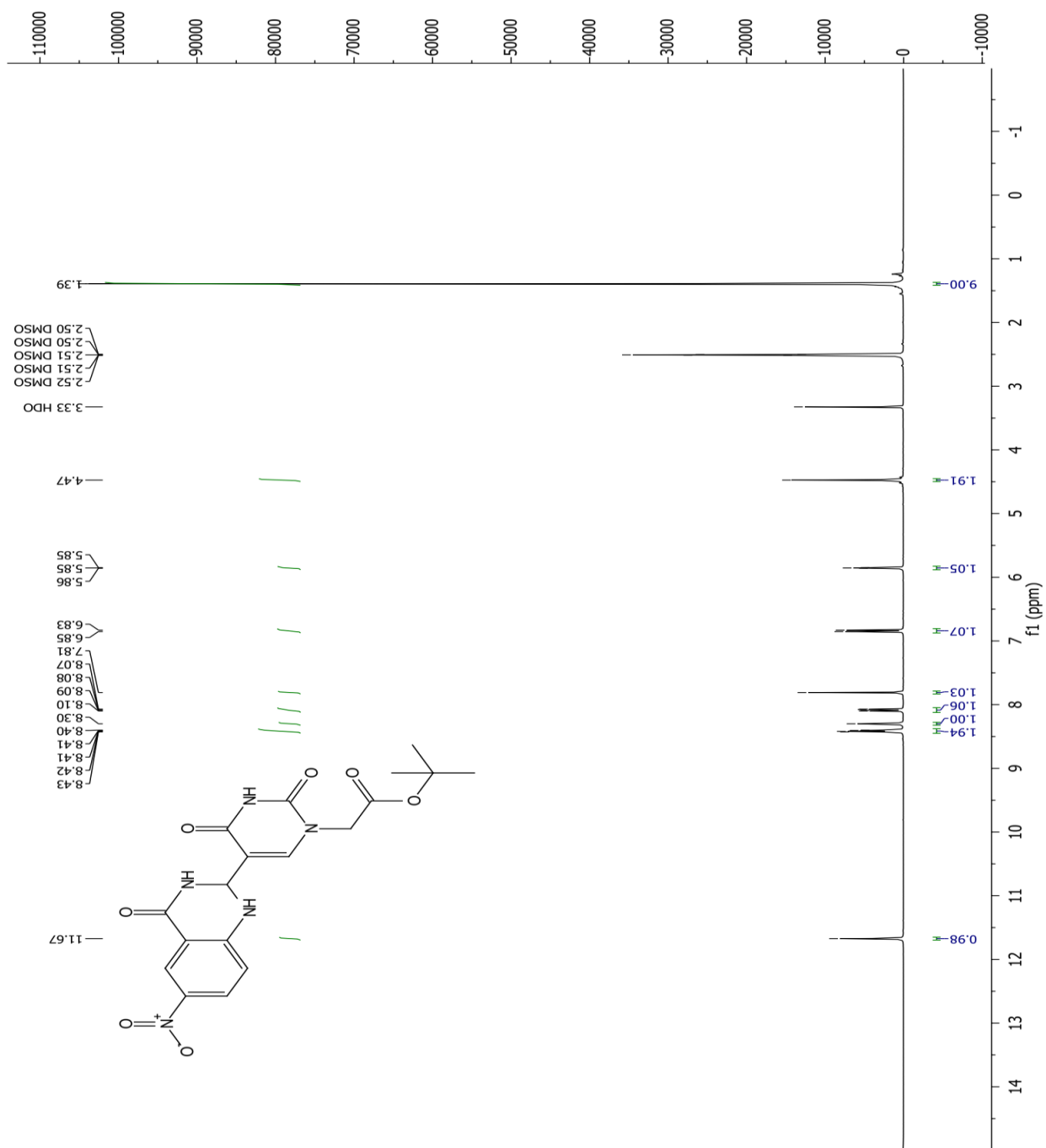
¹H NMR spectrum of tert-butyl 2-(2,4-dioxo-5-(4-oxo-1,2,3,4-tetrahydroquinazolin-2-yl)-3,4-dihydropyrimidin-1(2H)-yl)acetate (31)



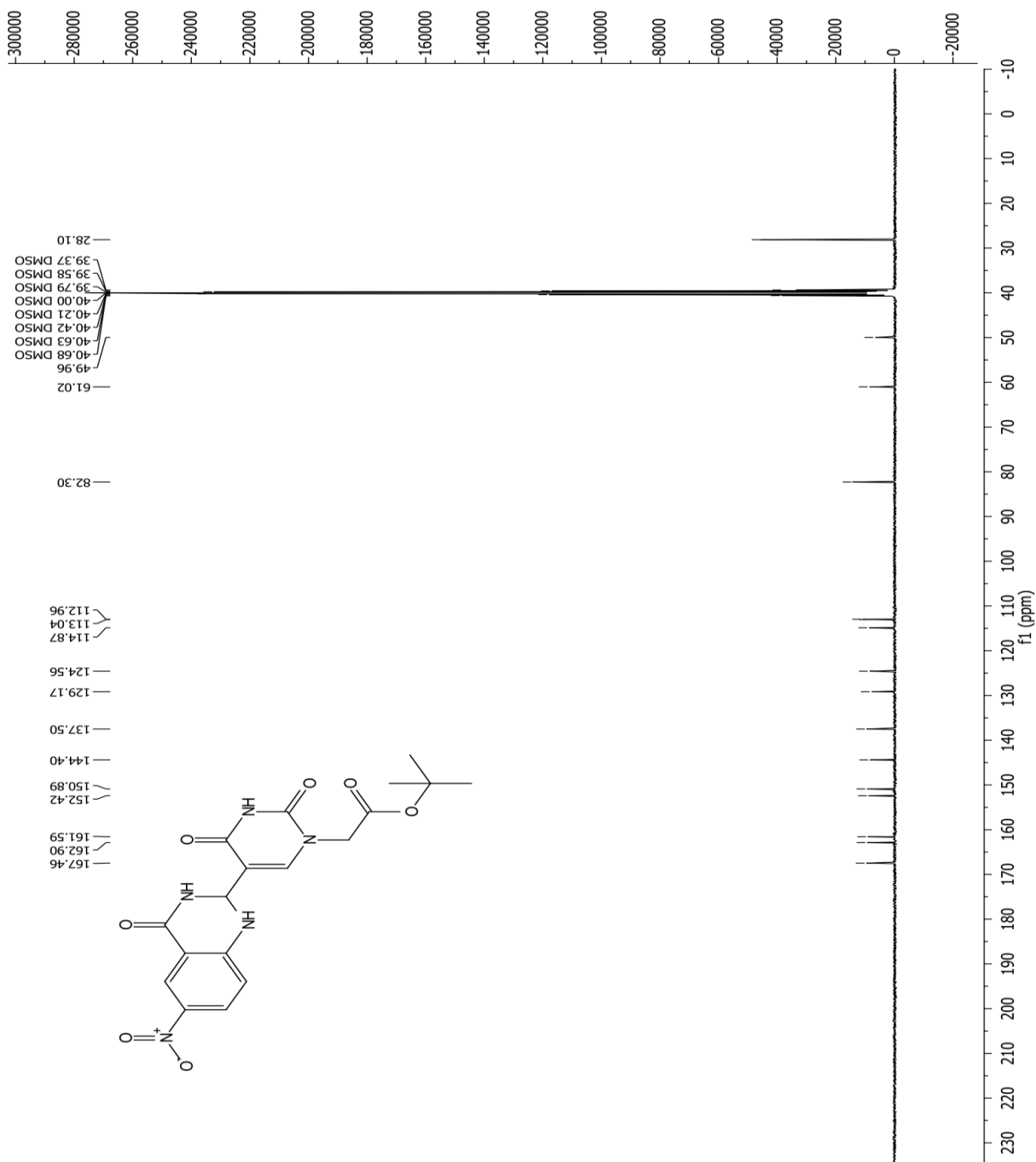
^{13}C NMR spectrum of tert-butyl 2-(2,4-dioxo-5-(4-oxo-1,2,3,4-tetrahydroquinazolin-2-yl)-3,4-dihydropyrimidin-1(2H)-yl)acetate (31)



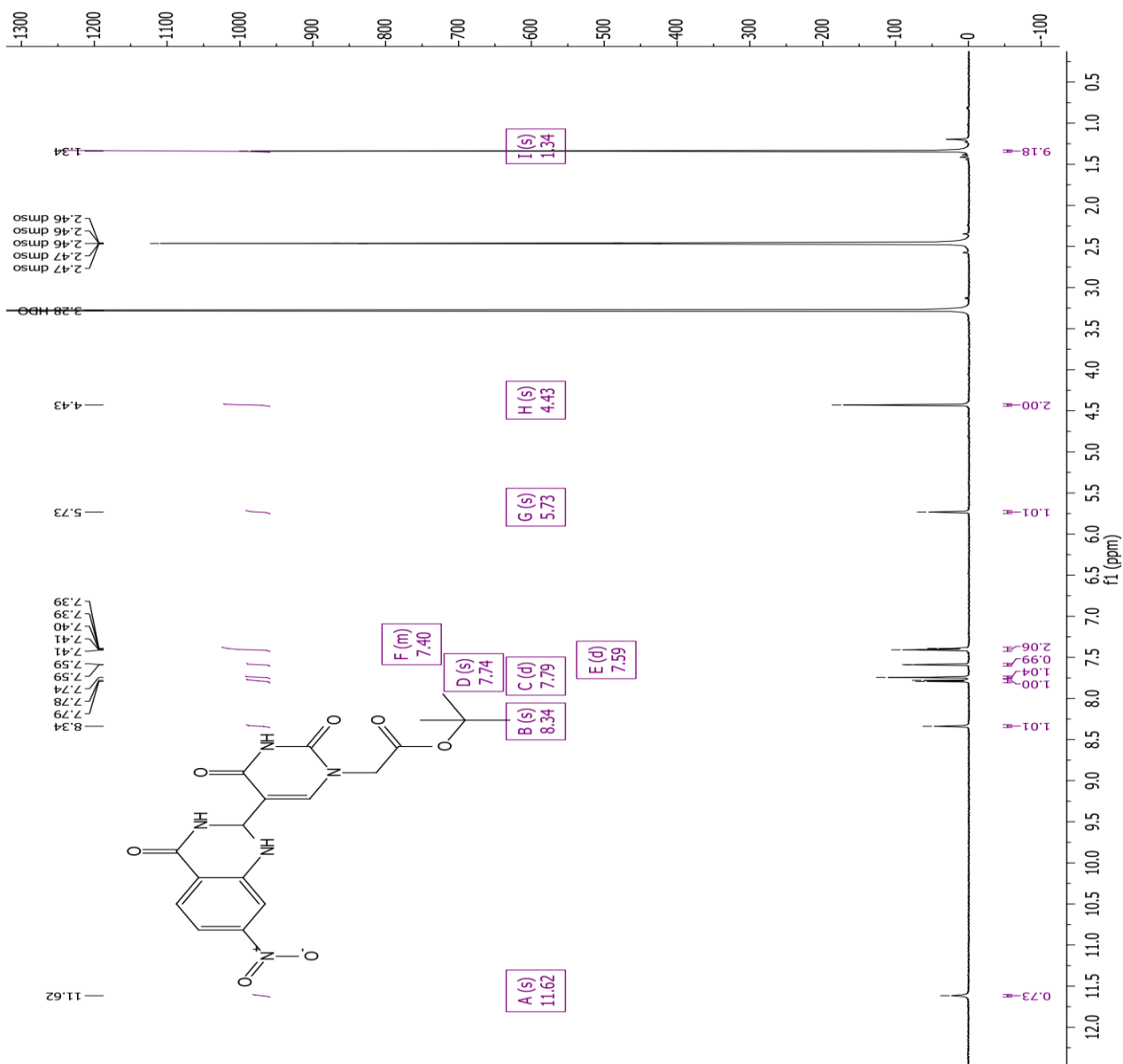
¹H NMR spectrum of tert-butyl 2-(5-(6-nitro-4-oxo-1,2,3,4-tetrahydroquinazolin-2-yl)-2,4-dioxo-3,4-dihydropyrimidin-1(2H)-yl) acetate (32)



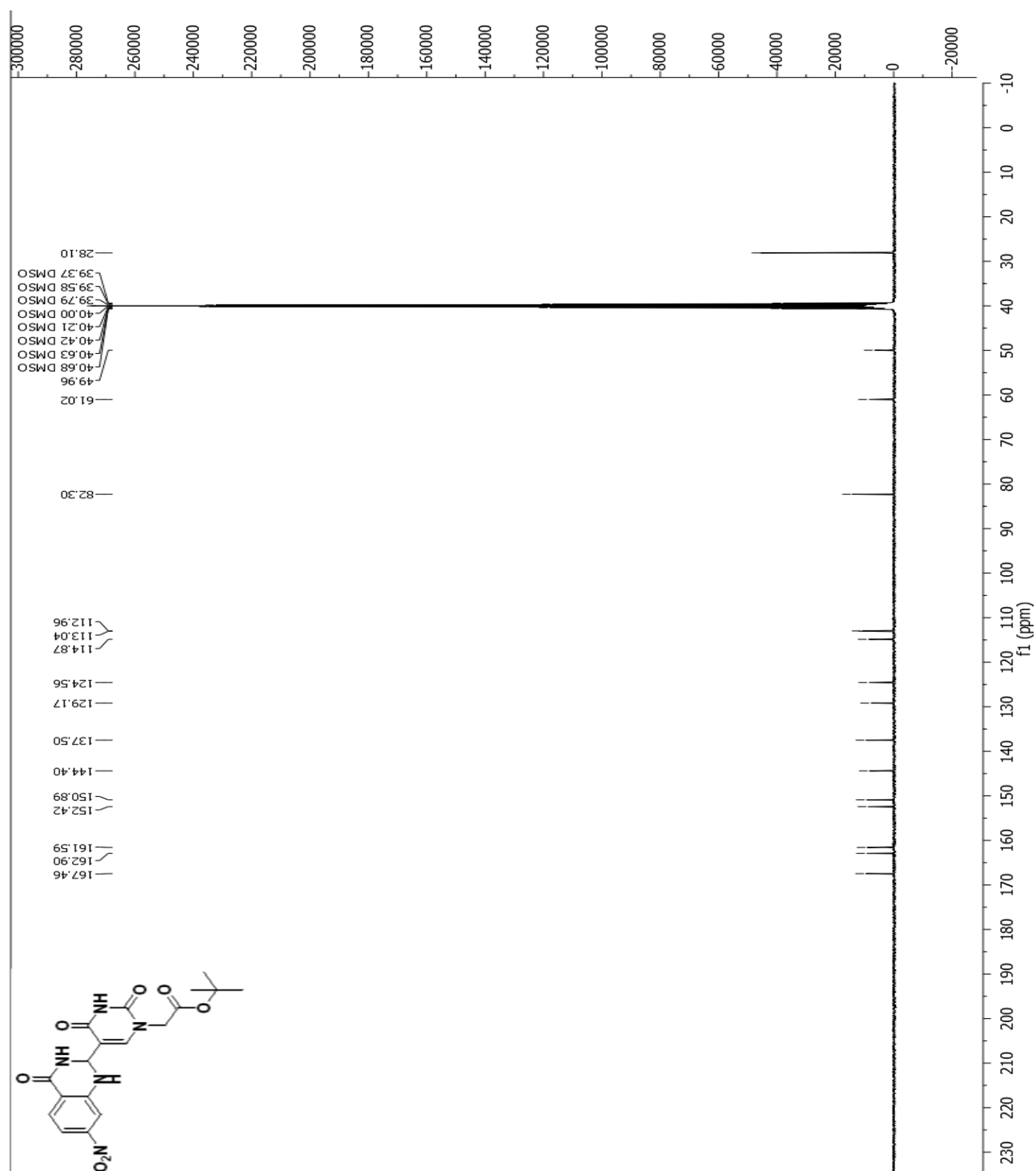
^{13}C NMR spectrum of tert-butyl 2-(5-(6-nitro-4-oxo-1,2,3,4-tetrahydroquinazolin-2-yl)-2,4-dioxo-3,4-dihydropyrimidin-1(2H)-yl) acetate (32)



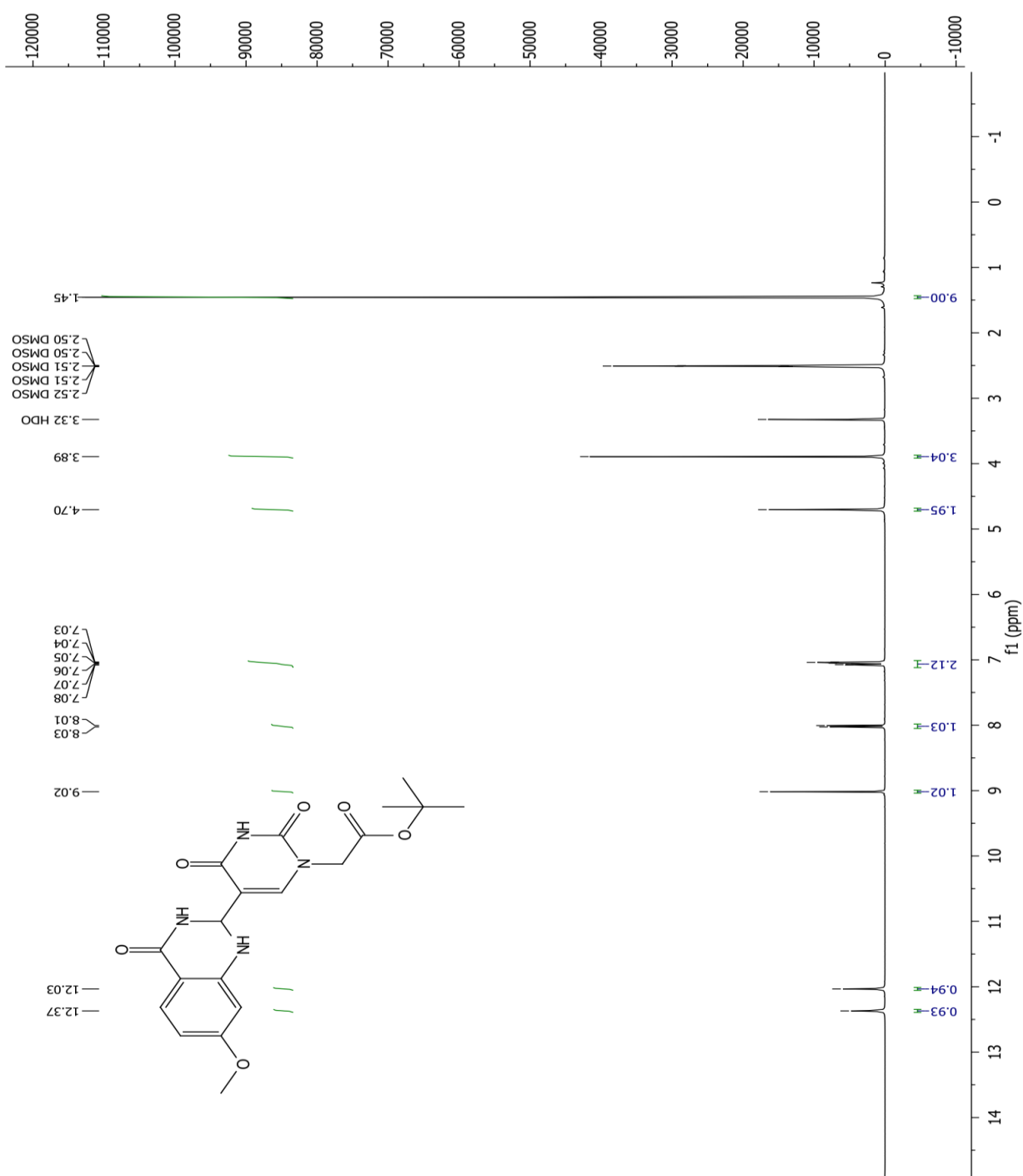
¹H NMR spectrum of tert-butyl 2-(5-(7-nitro-4-oxo-1,2,3,4-tetrahydroquinazolin-2-yl)-2,4-dioxo-3,4-dihydropyrimidin-1(2H)-yl) acetate (33)



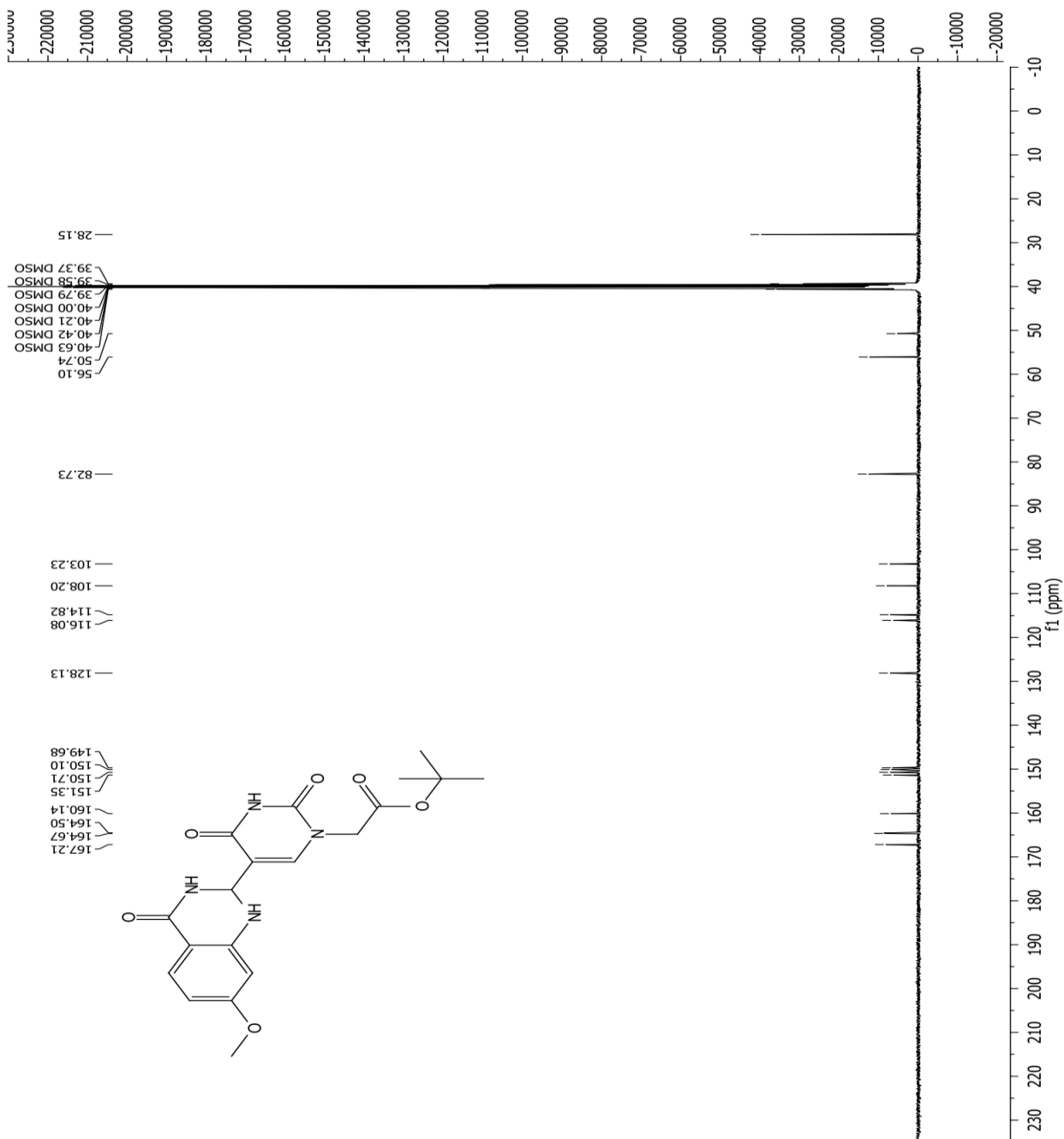
^{13}C NMR spectrum of tert-butyl 2-(5-(7-nitro-4-oxo-1,2,3,4-tetrahydroquinazolin-2-yl)-2,4-dioxo-3,4-dihydropyrimidin-1(2H)-yl) acetate (33)



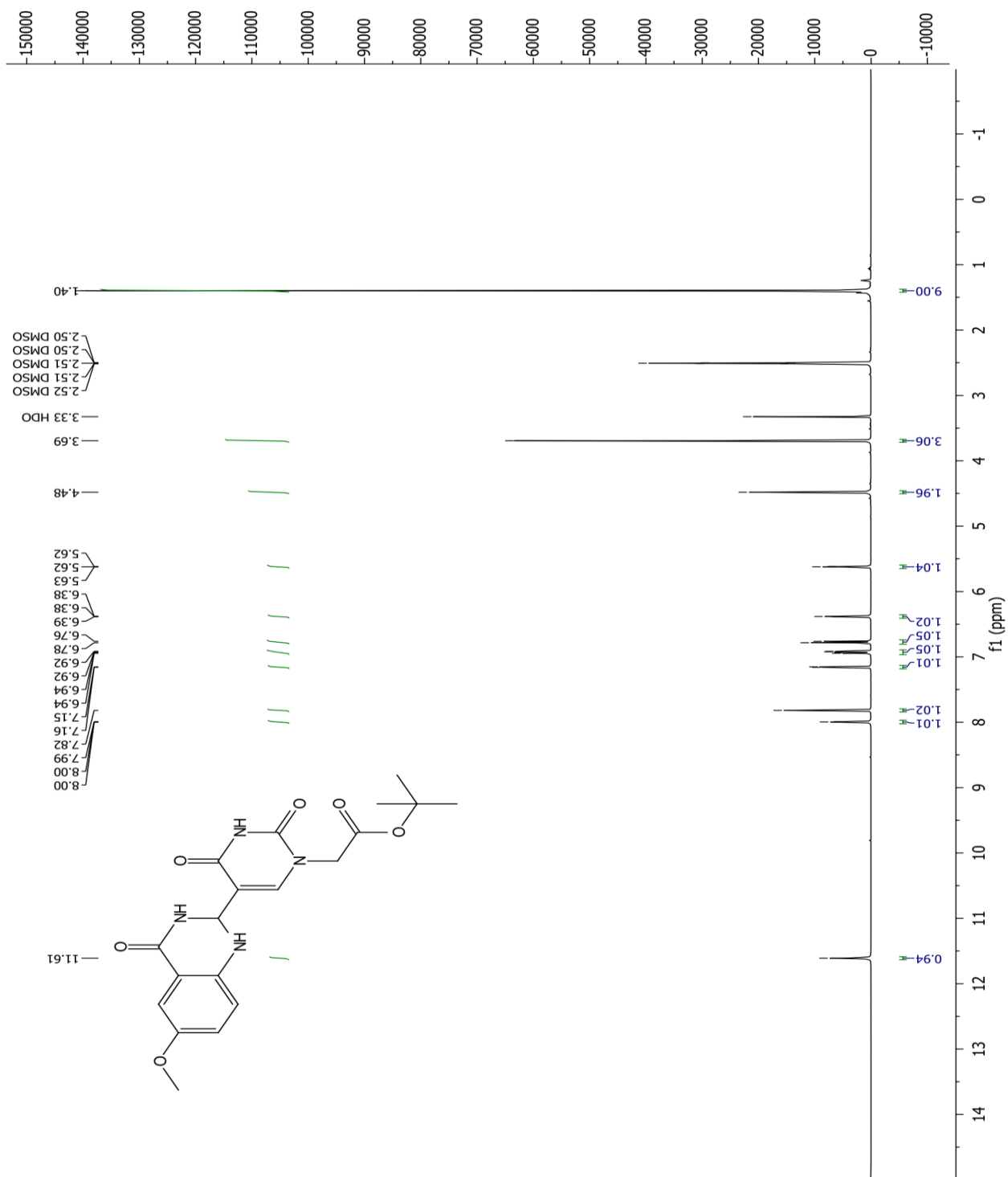
¹H NMR spectrum of tert-butyl 2-(5-(7-methoxy-4-oxo-1,2,3,4-tetrahydroquinazolin-2-yl)-2,4-dioxo-3,4-dihydropyrimidin-1(2H)-yl) acetate (34)



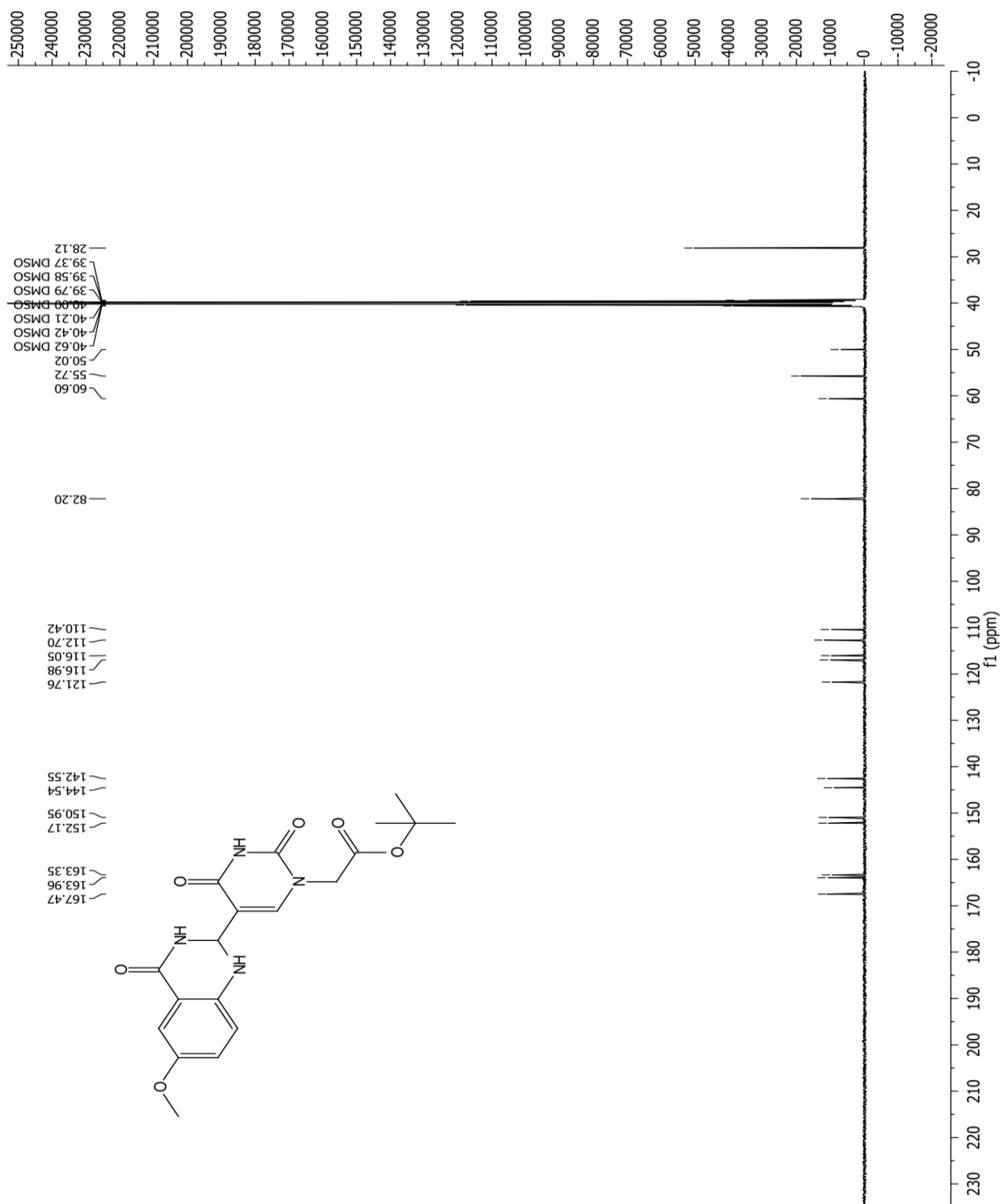
¹³C NMR spectrum of tert-butyl 2-(5-(7-methoxy-4-oxo-1,2,3,4-tetrahydroquinazolin-2-yl)-2,4-dioxo-3,4-dihydropyrimidin-1(2H)-yl) acetate (34)



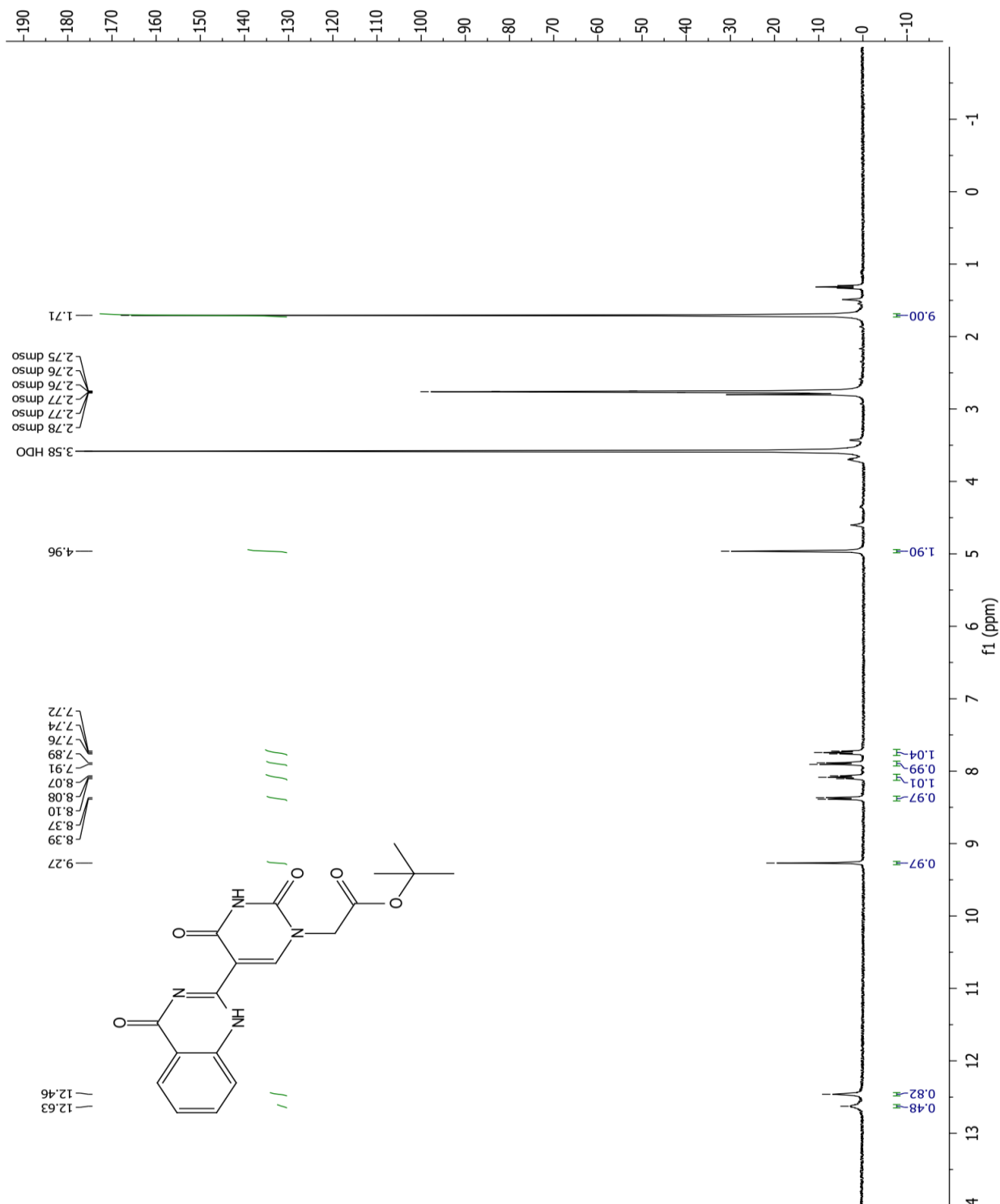
¹H NMR spectrum of tert-butyl 2-(5-(6-methoxy-4-oxo-1,2,3,4-tetrahydroquinazolin-2-yl)-2,4-dioxo-3,4-dihydropyrimidin-1(2H)-yl) acetate (35)



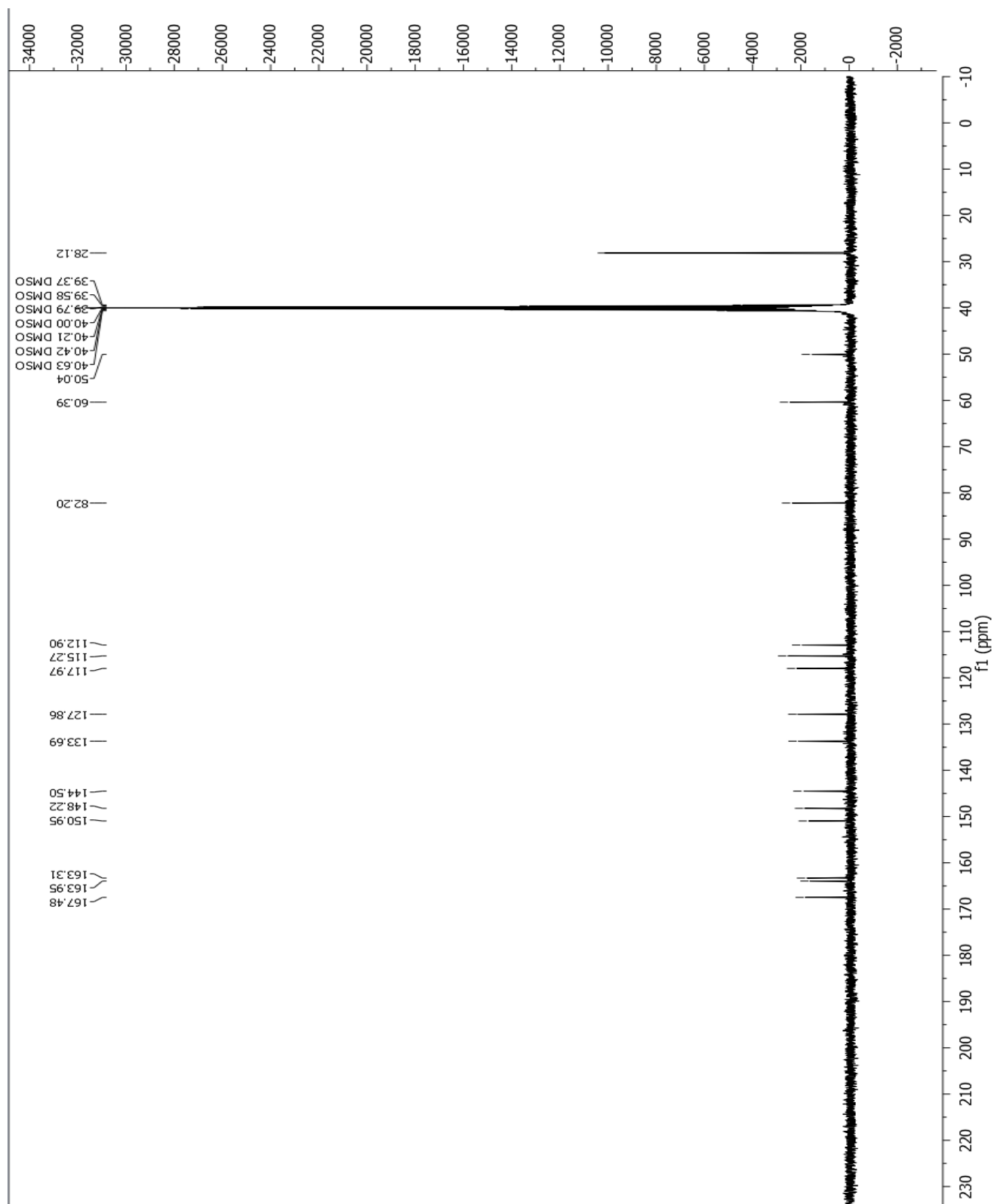
¹³C NMR spectrum of tert-butyl 2-(5-(6-methoxy-4-oxo-1,2,3,4-tetrahydroquinazolin-2-yl)-2,4-dioxo-3,4-dihydropyrimidin-1(2H)-yl) acetate (35)



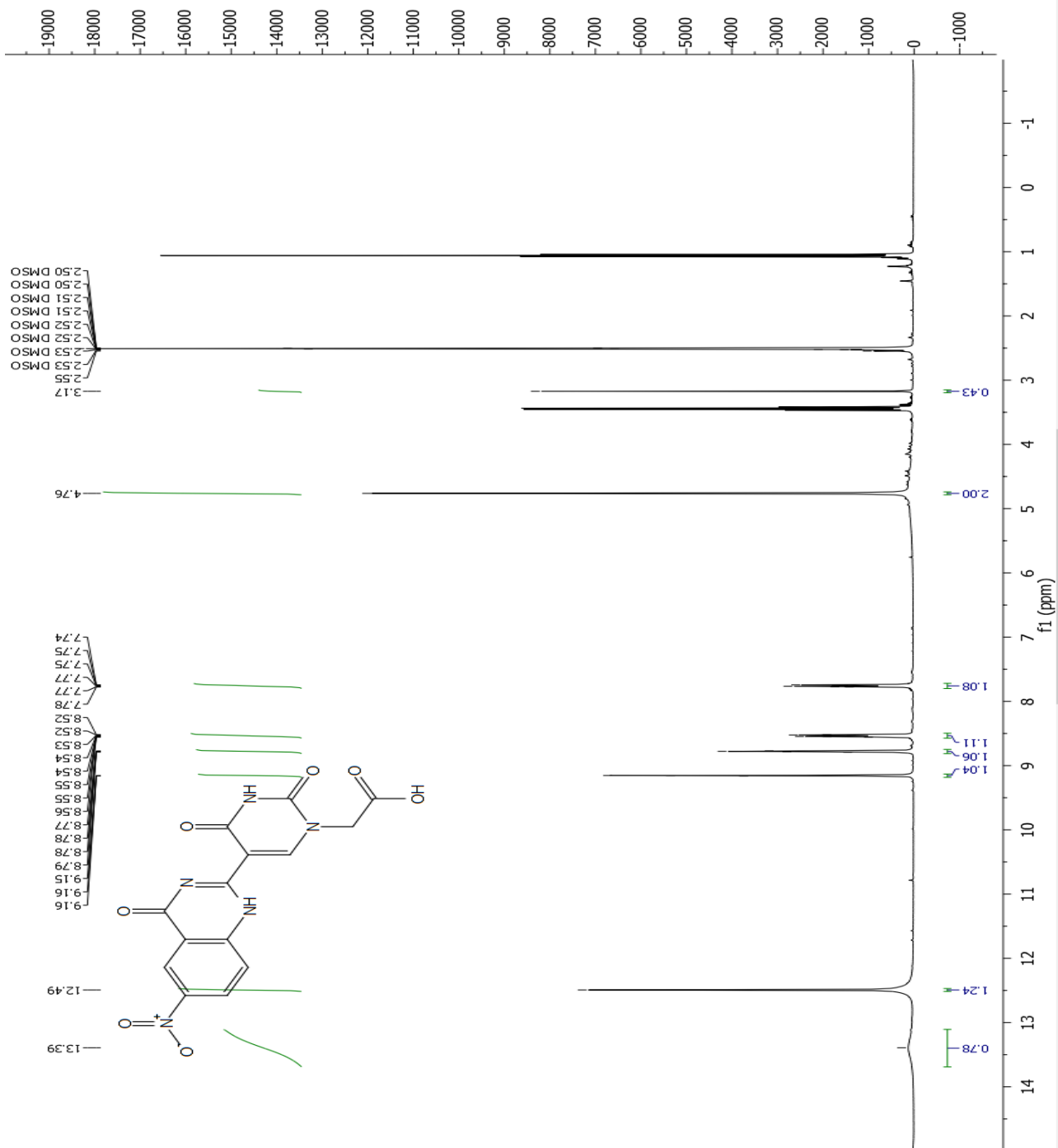
^1H NMR spectrum of tert-butyl 2-(2,4-dioxo-5-(4-oxo-3,4-dihydroquinazolin-2-yl)-3,4-dihydropyrimidin-1(2H)-yl)acetate (36)



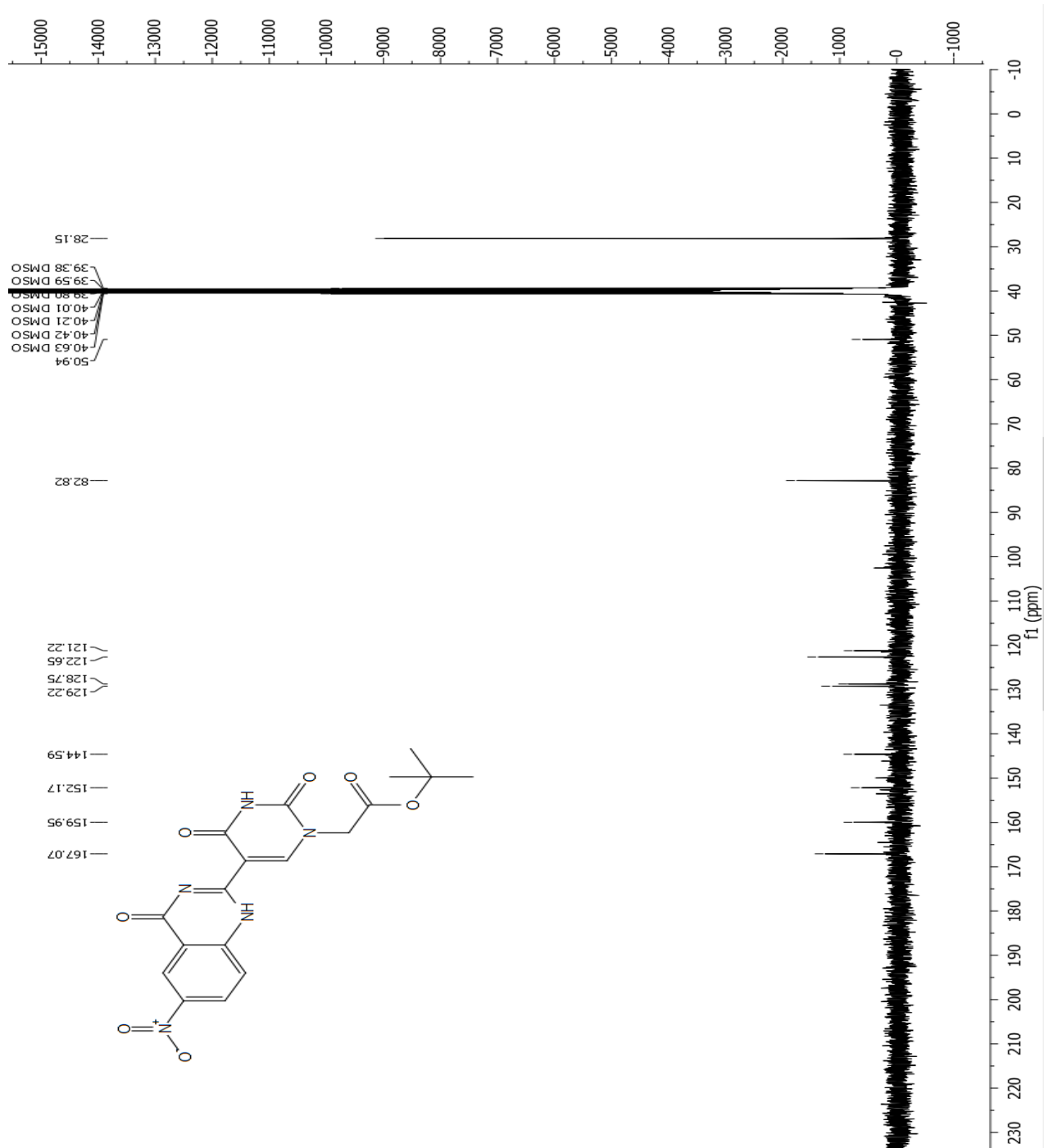
^{13}C NMR spectrum of tert-butyl 2-(2,4-dioxo-5-(4-oxo-3,4-dihydroquinazolin-2-yl)-3,4-dihydropyrimidin-1(2H)-yl)acetate (36)



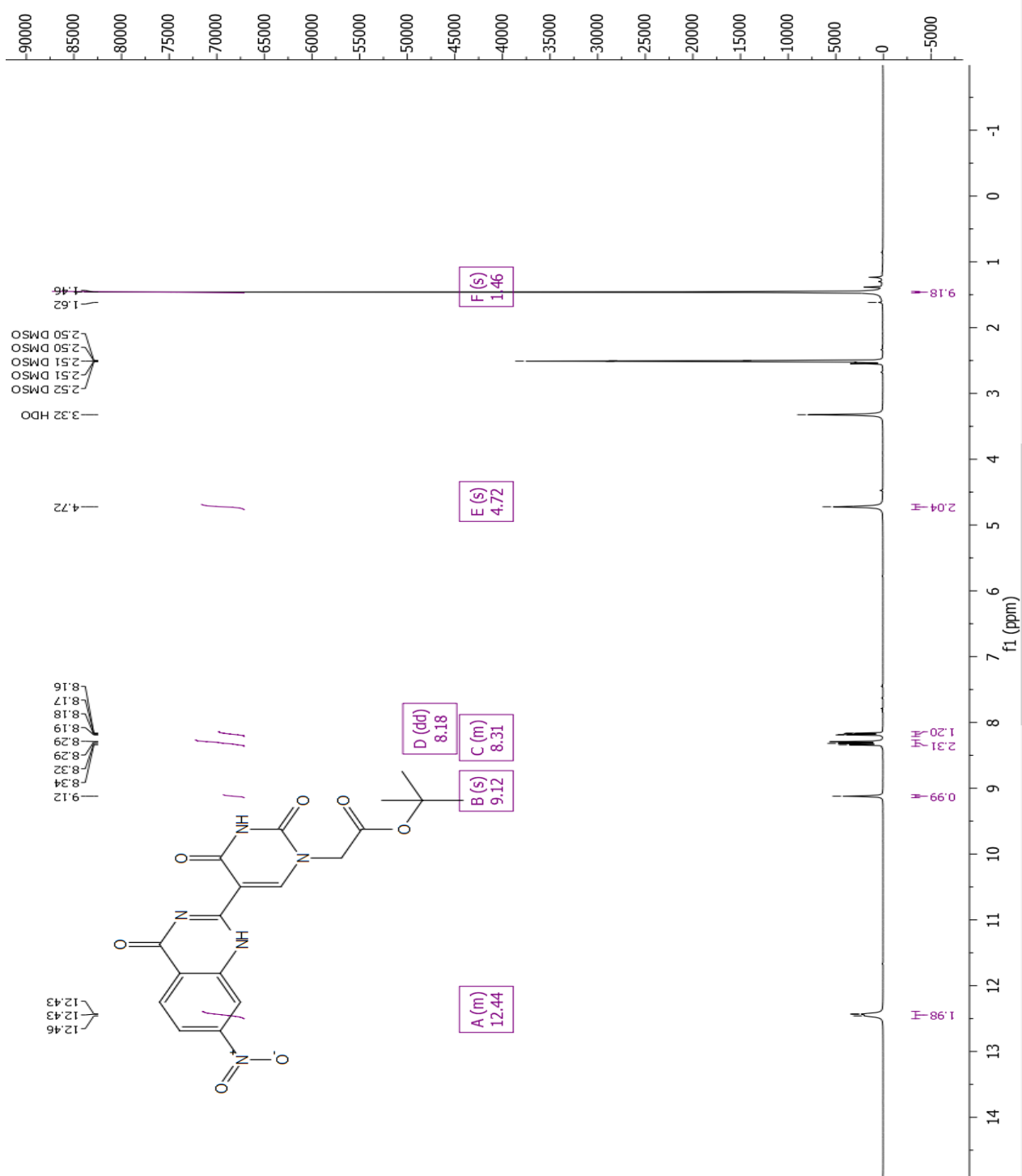
¹H NMR spectrum of tert-butyl 2-(5-(6-nitro-4-oxo-1,4-dihydroquinazolin-2-yl)-2,4-dioxo-3,4-dihydropyrimidin-1(2H)-yl) acetate (37)



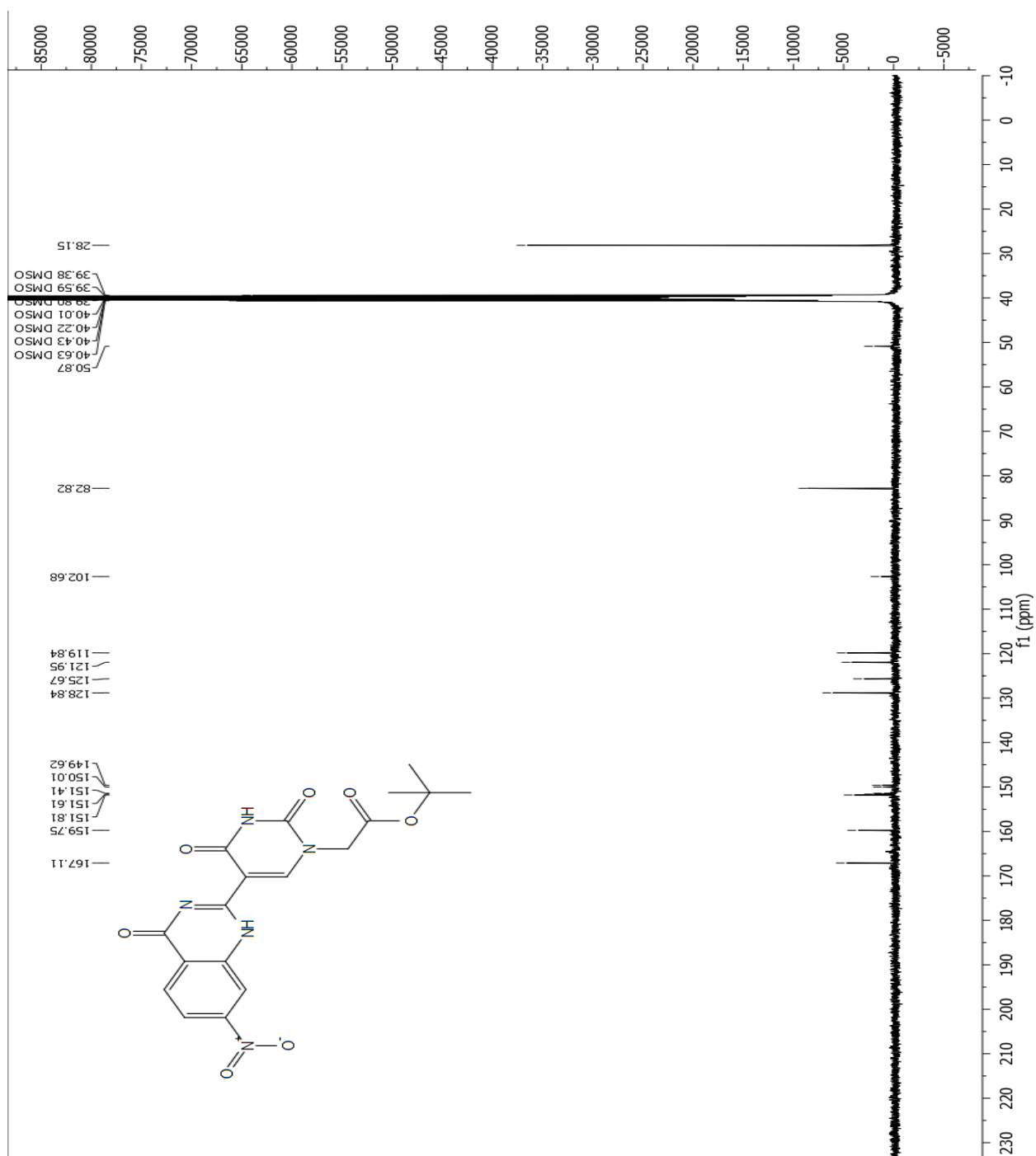
^{13}C NMR spectrum of tert-butyl 2-(5-(6-nitro-4-oxo-1,4-dihydroquinazolin-2-yl)-2,4-dioxo-3,4-dihydropyrimidin-1(2H)-yl) acetate (37)



¹H NMR spectrum of tert-butyl 2-(5-(7-nitro-4-oxo-1,4-dihydroquinazolin-2-yl)-2,4-dioxo-3,4-dihydropyrimidin-1(2H)-yl)acetate (38)



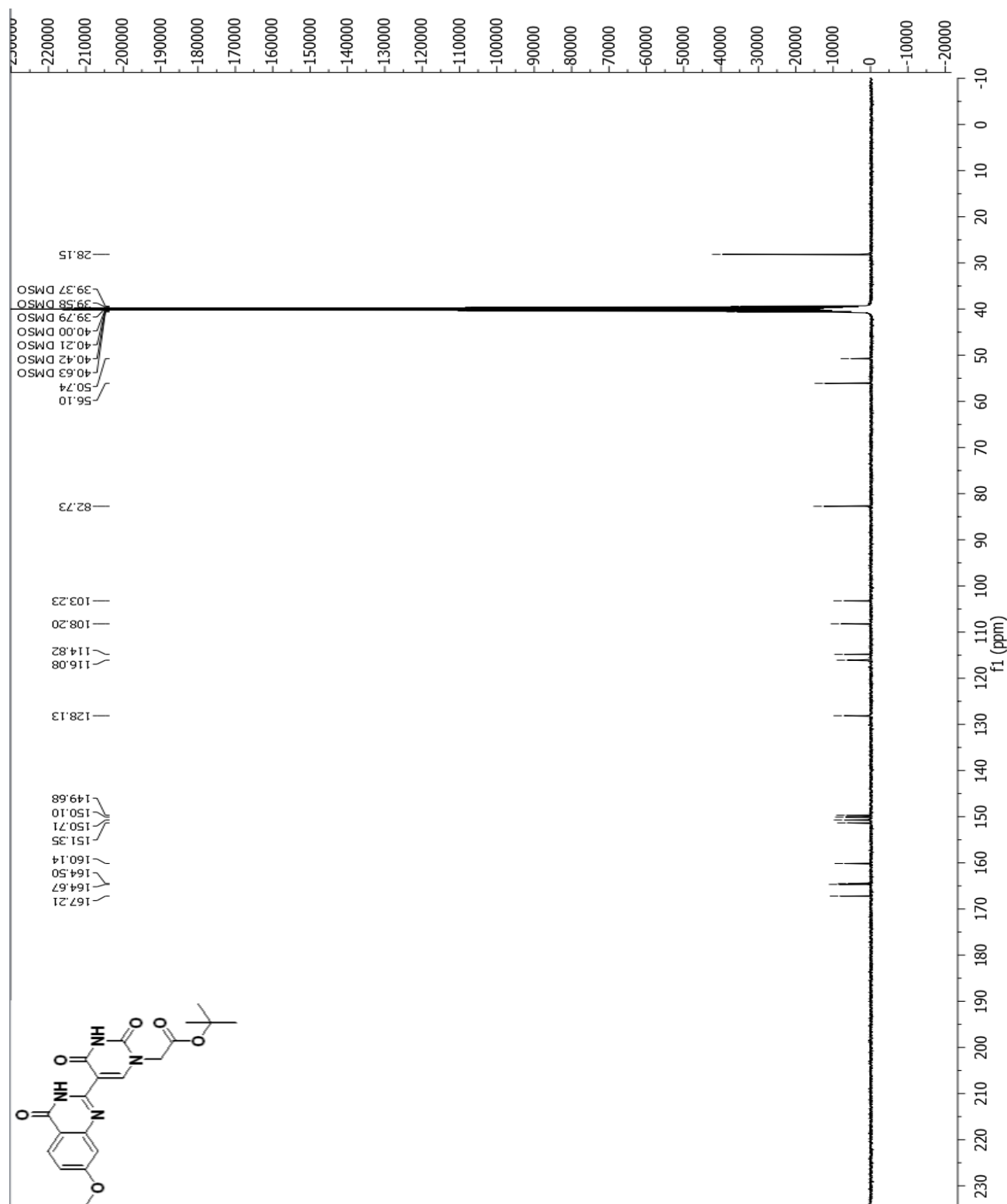
^{13}C NMR spectrum of tert-butyl 2-(5-(7-nitro-4-oxo-1,4-dihydroquinazolin-2-yl)-2,4-dioxo-3,4-dihydropyrimidin-1(2H)-yl)acetate (38)



Chemical structure of compound 10 is shown below the spectrum:

CC(C)OC(=O)CNc1nc(=O)c2c(c1)nc(=O)c3ccc(OC)cc3n2

^{13}C NMR spectrum of tert-butyl 2-(5-(7-methoxy-4-oxo-1,4-dihydroquinazolin-2-yl)-2,4-dioxo-3,4-dihydropyrimidin-1(2H)-yl) acetate (39)



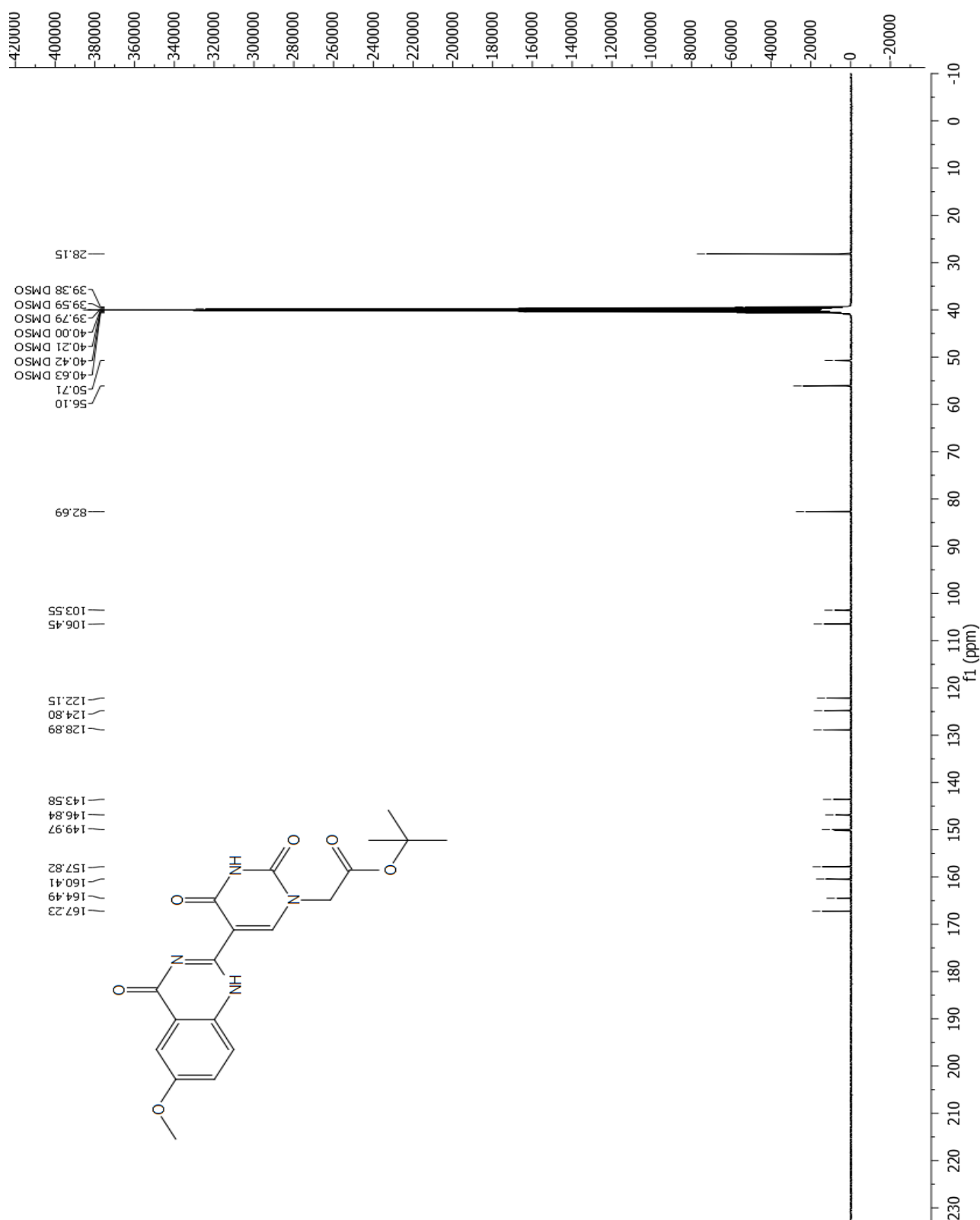
Chemical Structure of Compound 10:

COc1ccc2nc3c(nc(=O)c3c2)C(=O)Nc4ccn(CC(=O)OC(C)(C)C)c4=O

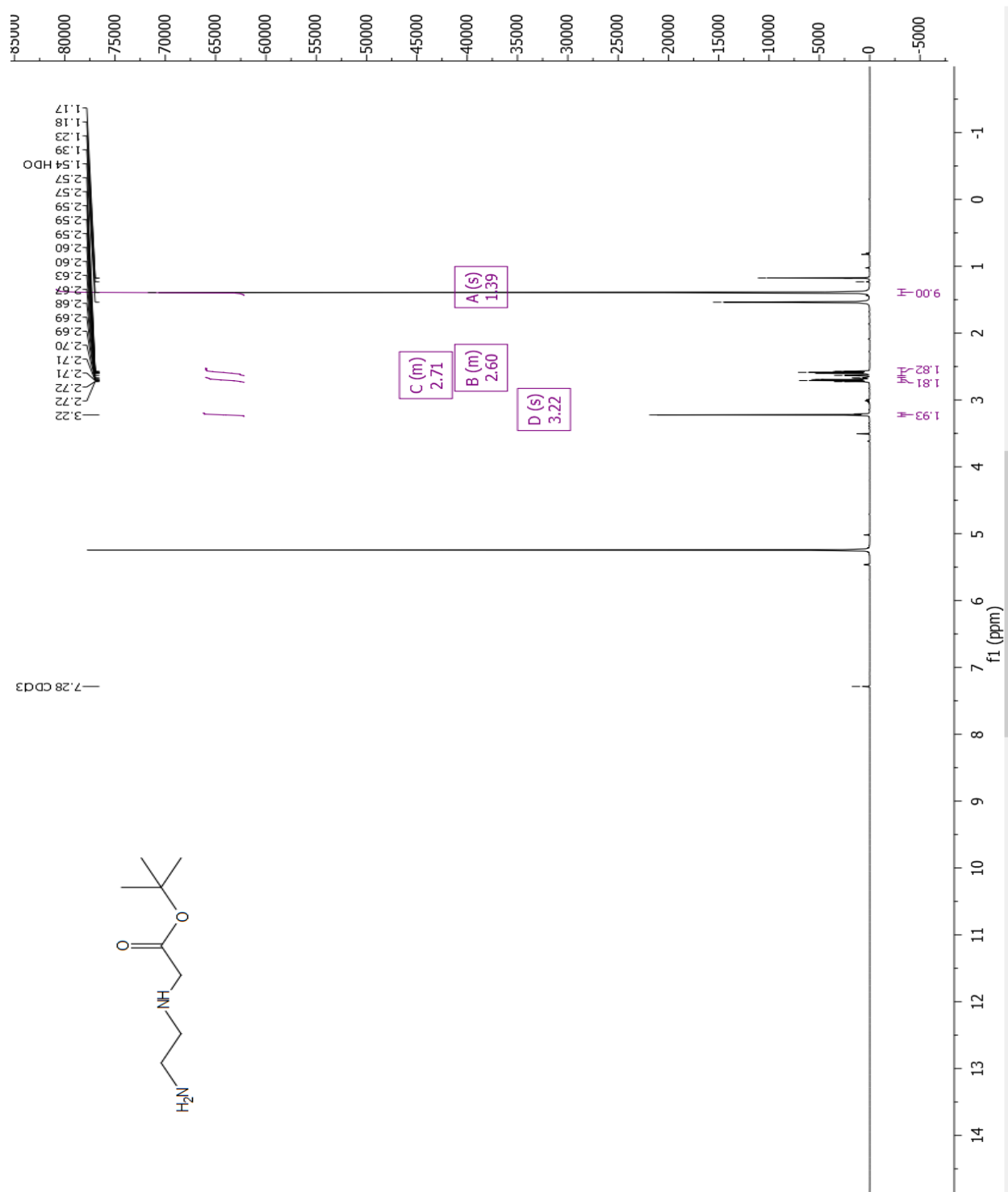
¹H NMR Data (DMSO-d₆):

Peak Label	Chemical Shift (ppm)	Multiplicity	Integration
A	12.33	s	0.90
B	12.13	s	0.98
C	8.94	s	1.03
D	7.59	d	1.05
E	7.51	d	1.92
F	7.43	dd	3.04
G	4.69	s	9.00
H	3.88	s	
J	1.45	s	

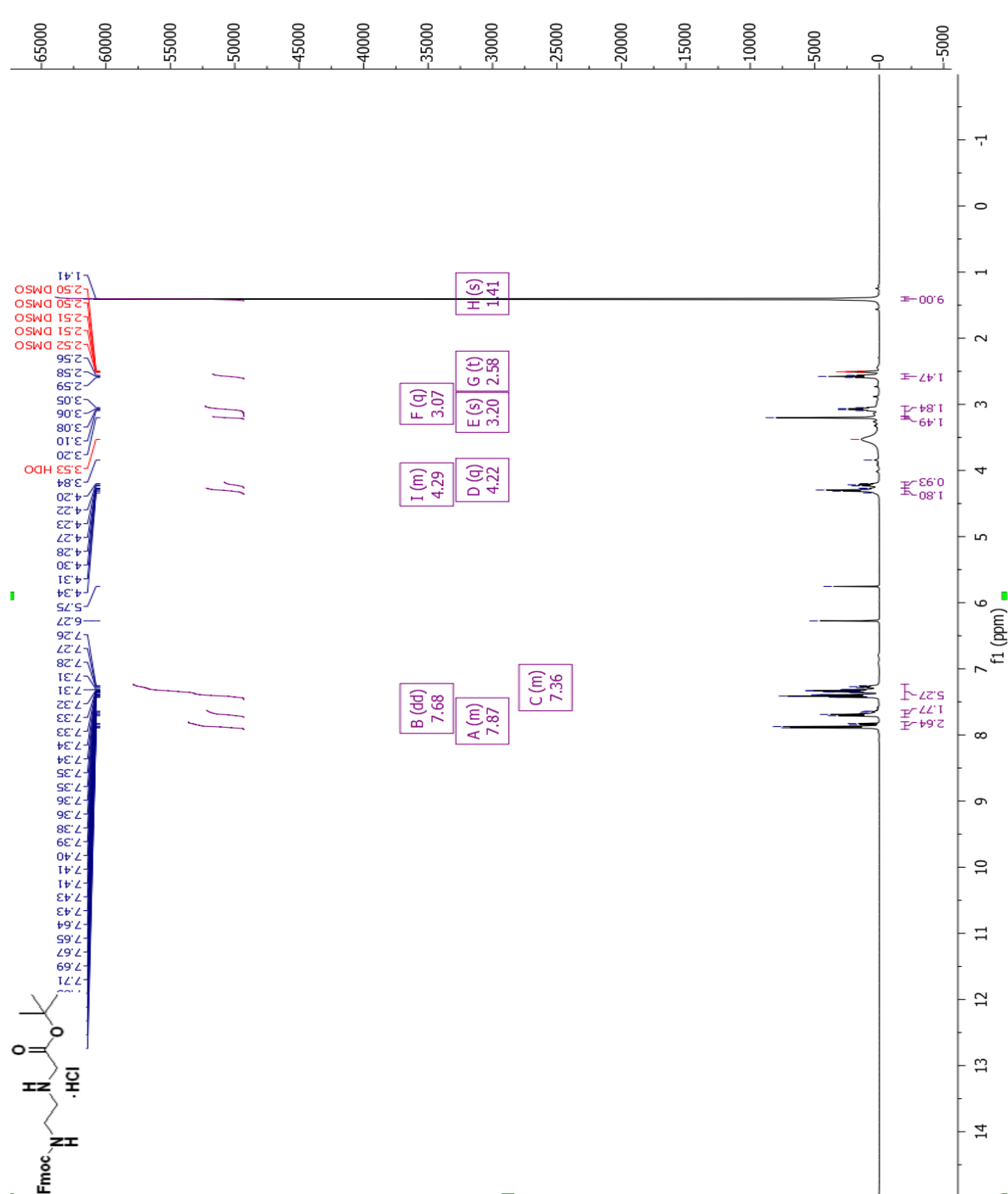
^{13}C NMR spectrum of tert-butyl 2-(5-(6-methoxy-4-oxo-3,4-dihydroquinazolin-2-yl)-2,4-dioxo-3,4-dihydropyrimidin-1(2H)-yl)acetate (40)



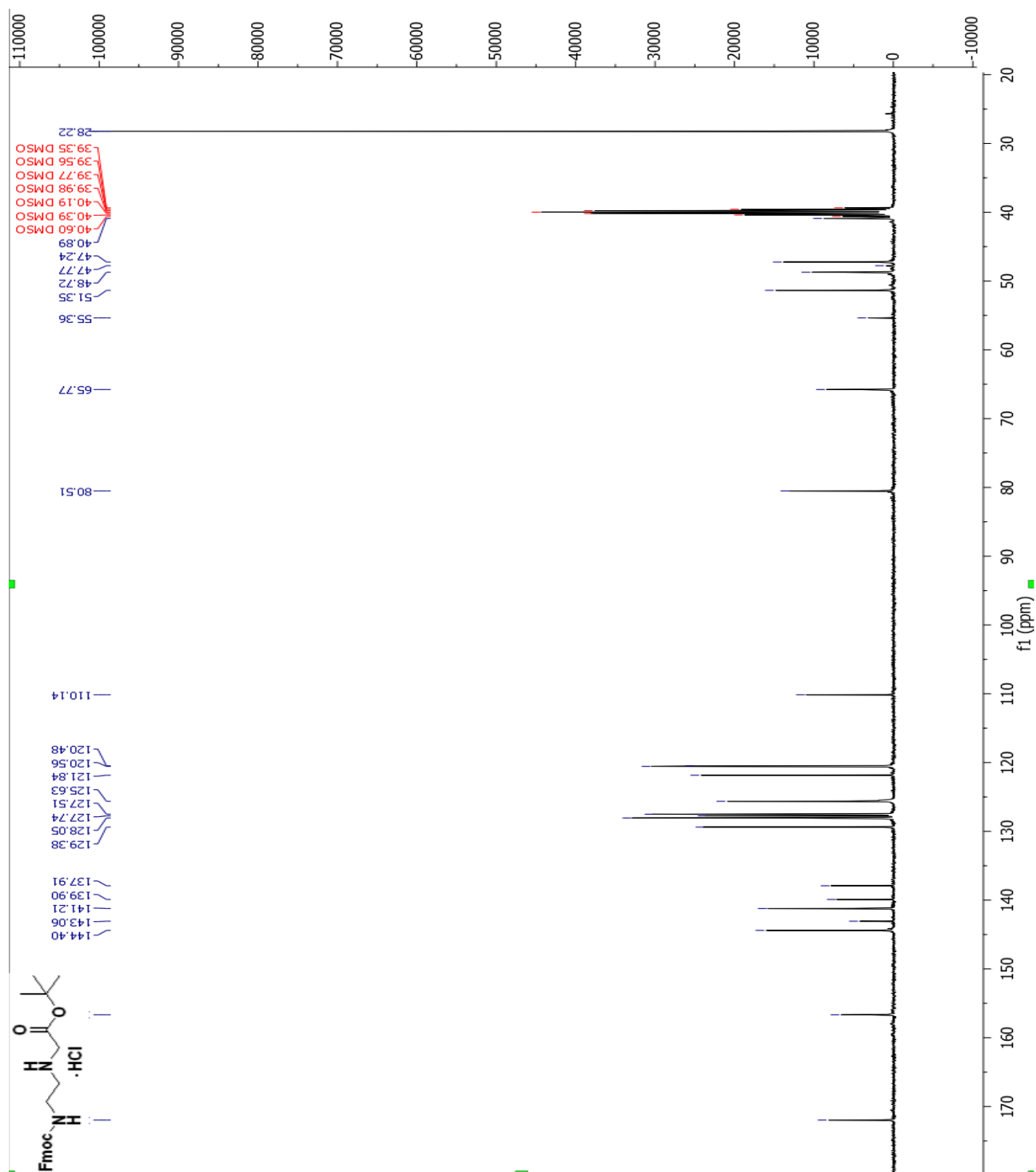
¹H NMR spectrum of tert-butyl (2-aminoethyl)glycinate (41)



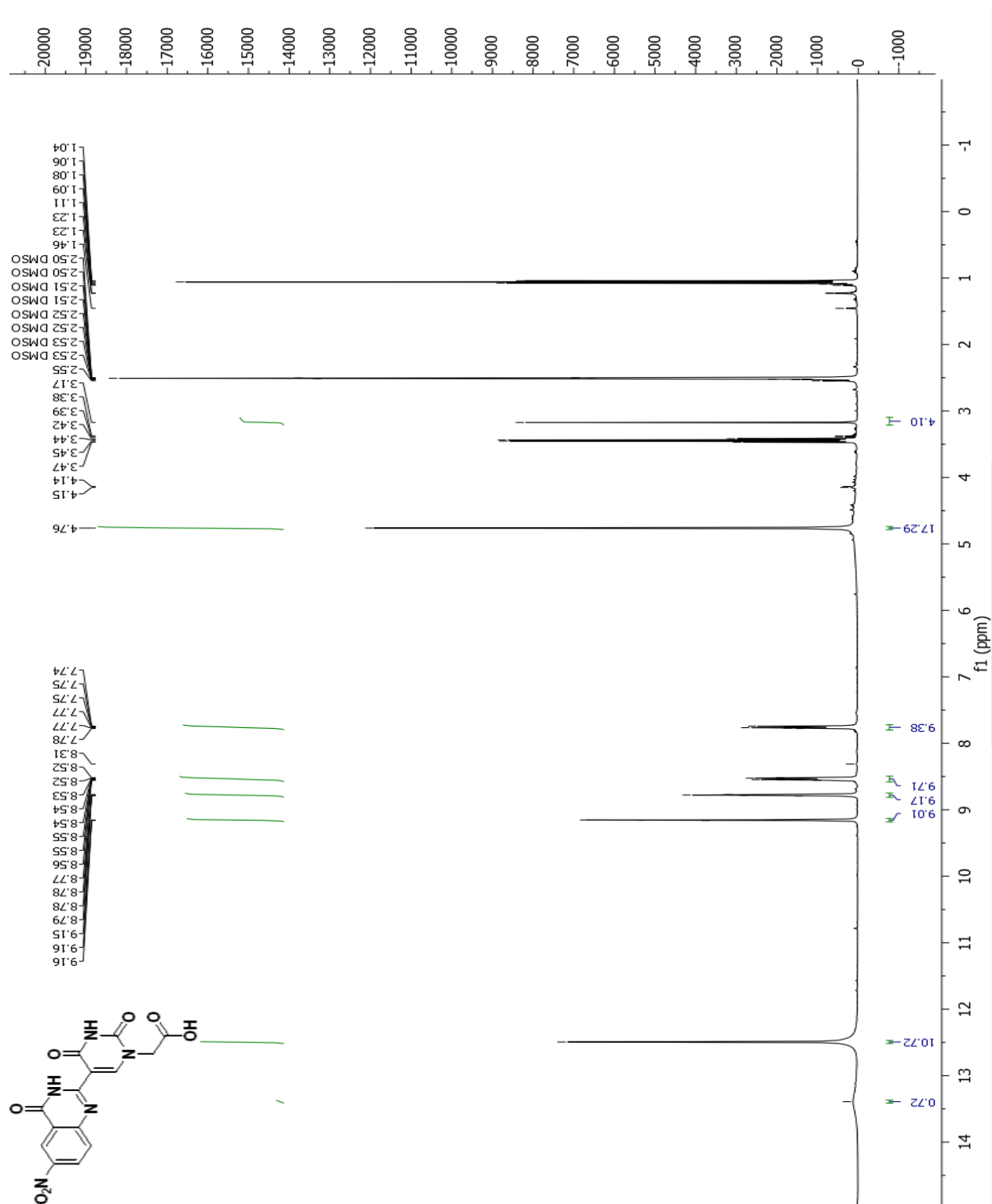
¹H NMR spectrum of tert-butyl (2-((((9H-fluoren-9-yl)methoxy)carbonyl)amino)ethyl)glycinate (42)



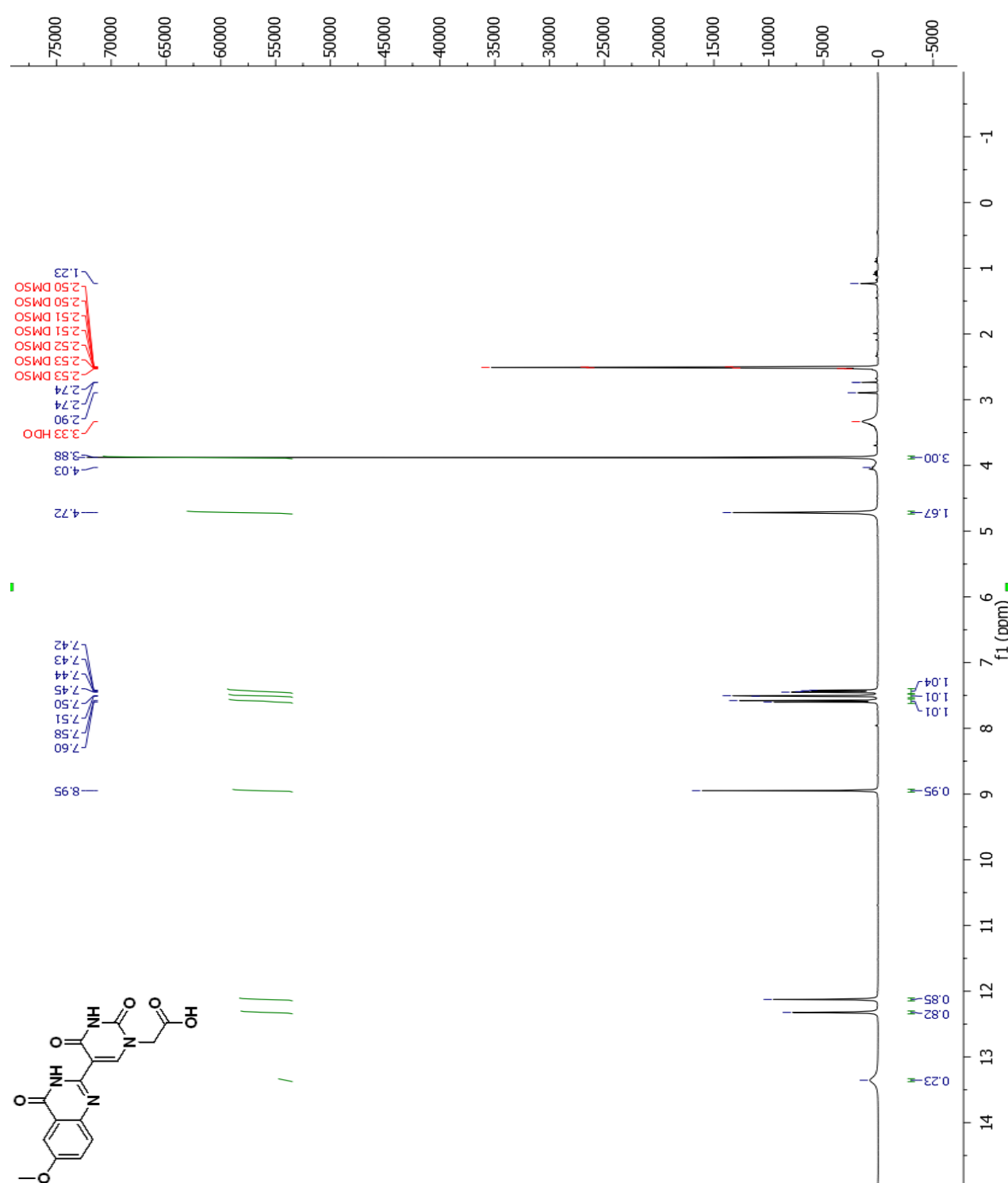
^{13}C NMR spectrum of tert-butyl (2-((((9H-fluoren-9-yl)methoxy)carbonyl)amino)ethyl)glycinate (42)



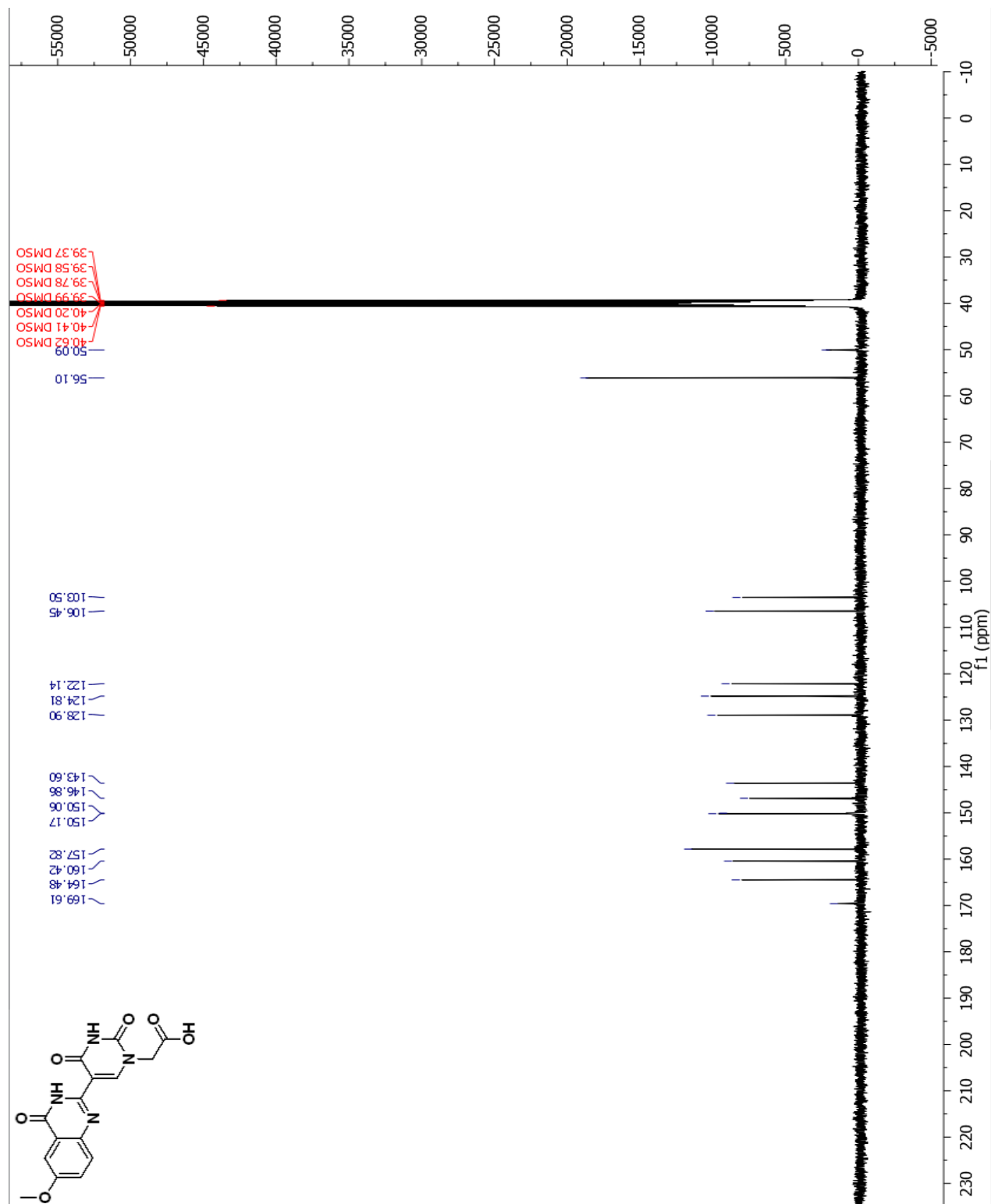
^1H NMR spectrum of 2-(5-(6-nitro-4-oxo-3,4-dihydroquinazolin-2-yl)-2,4-dioxo-3,4-dihydropyrimidin-1(2H)-yl)acetic acid(44)



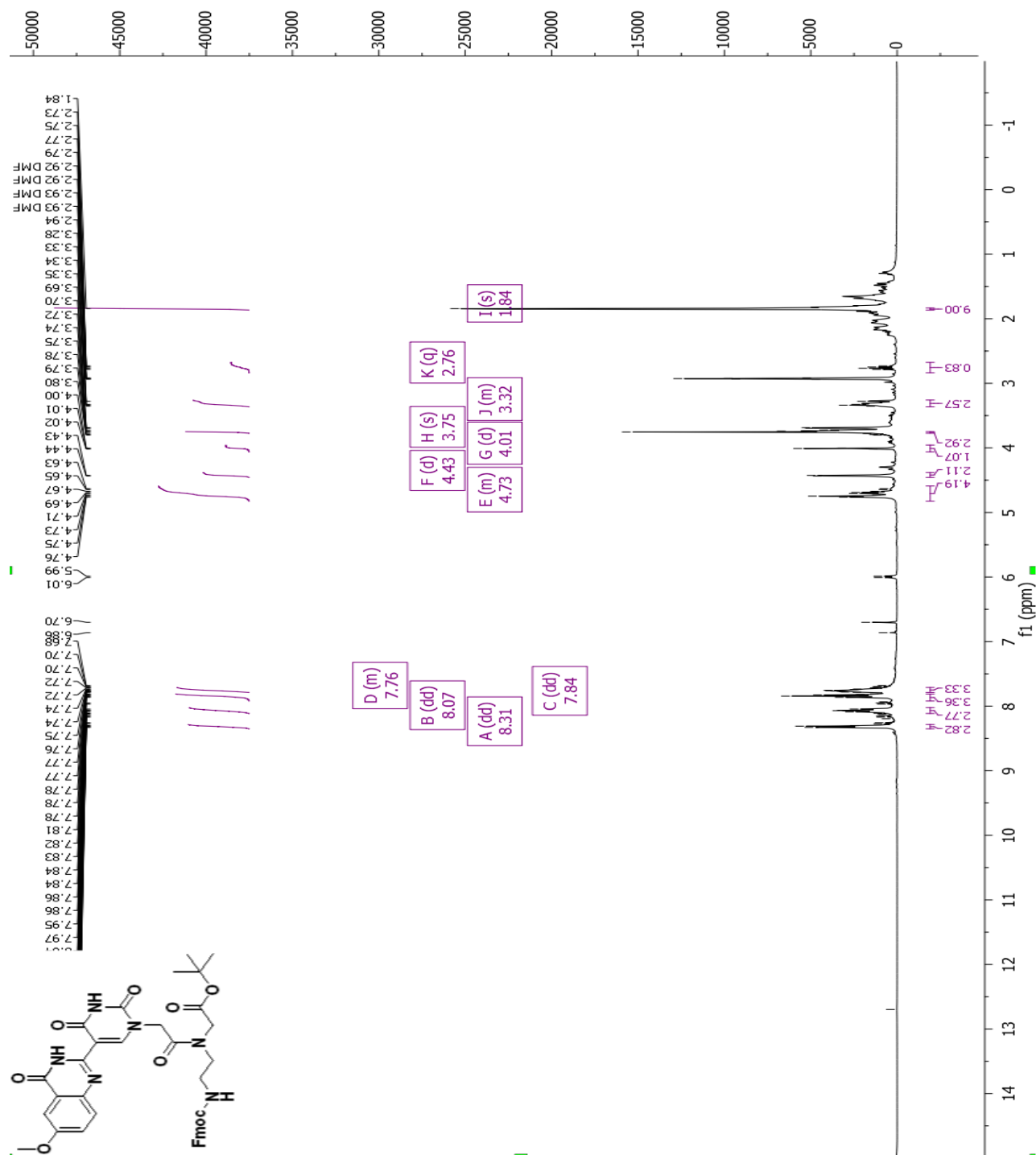
¹H NMR spectrum of 2-(5-(6-methoxy-4-oxo-3,4-dihydroquinazolin-2-yl)-2,4-dioxo-3,4-dihydropyrimidin-1(2H)-yl)acetic acid (45)



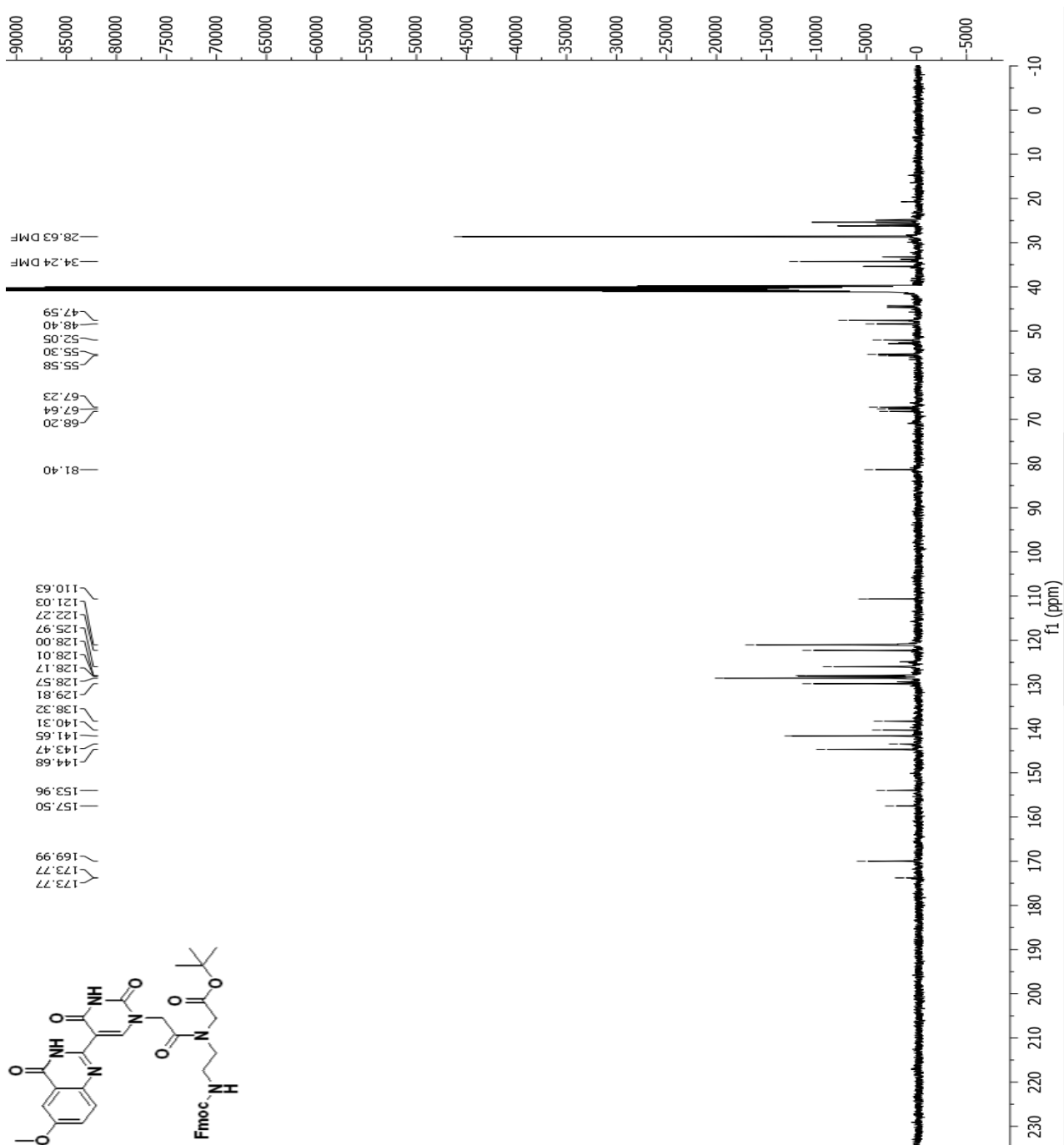
¹³C NMR spectrum of 2-(5-(6-methoxy-4-oxo-3,4-dihydroquinazolin-2-yl)-2,4-dioxo-3,4-dihydropyrimidin-1(2H)-yl)acetic acid (45)



^1H NMR spectrum of tert-butyl N-(2-((((9H-fluoren-9-yl)methoxy)carbonyl)amino)ethyl)-N-(2-(5-(6-methoxy-4-oxo-3,4-dihydroquinazolin-2-yl)-2,4-dioxo-3,4-dihydropyrimidin-1(2H)-yl)acetyl)glycinate (46)

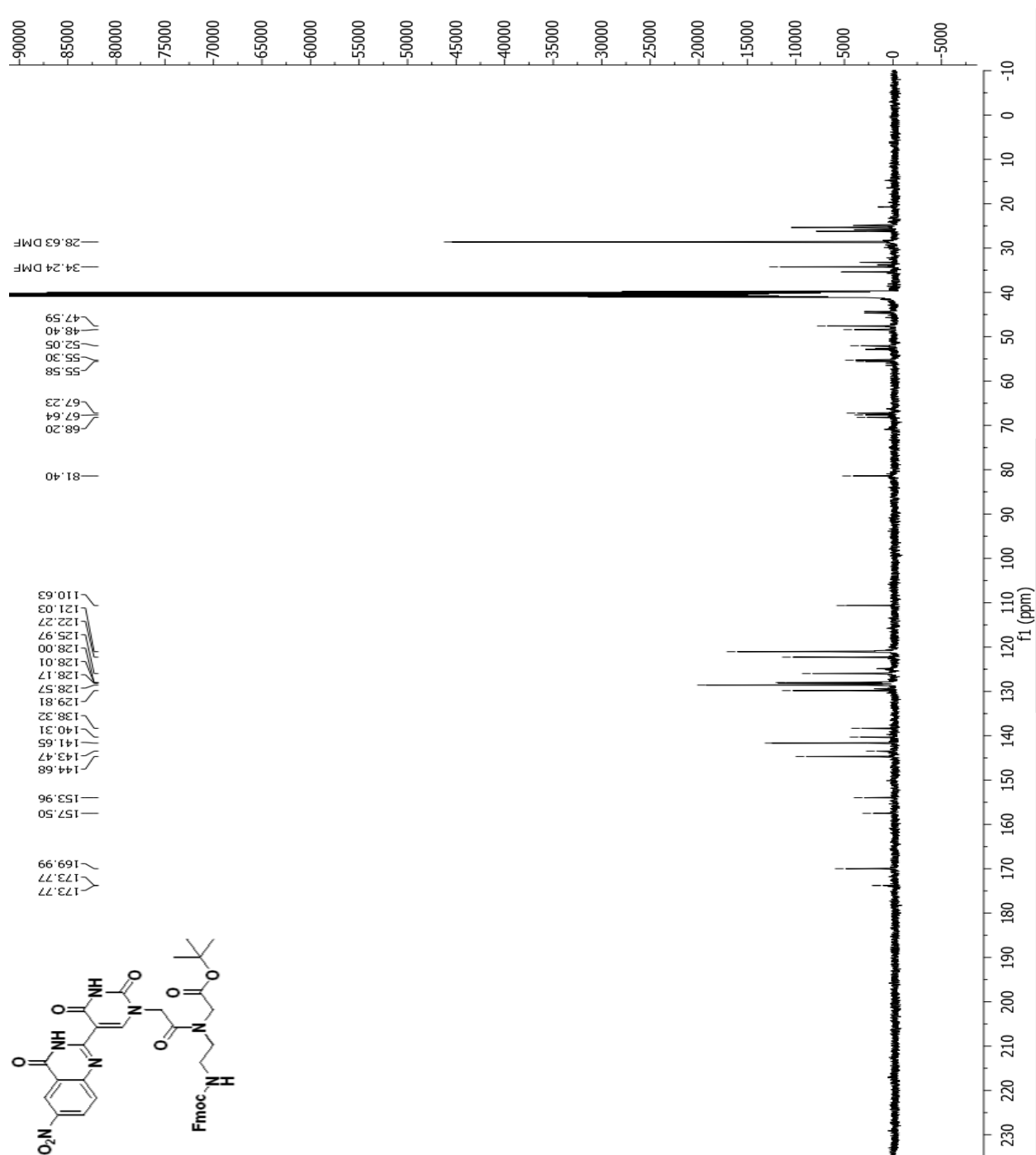


¹³C NMR spectrum of tert-butyl N-(2-((((9H-fluoren-9-yl)methoxy)carbonyl)amino)ethyl)-N-(2-(5-(6-methoxy-4-oxo-3,4-dihydroquinazolin-2-yl)-2,4-dioxo-3,4-dihydropyrimidin-1(2H)-yl)acetyl)glycinate (46)

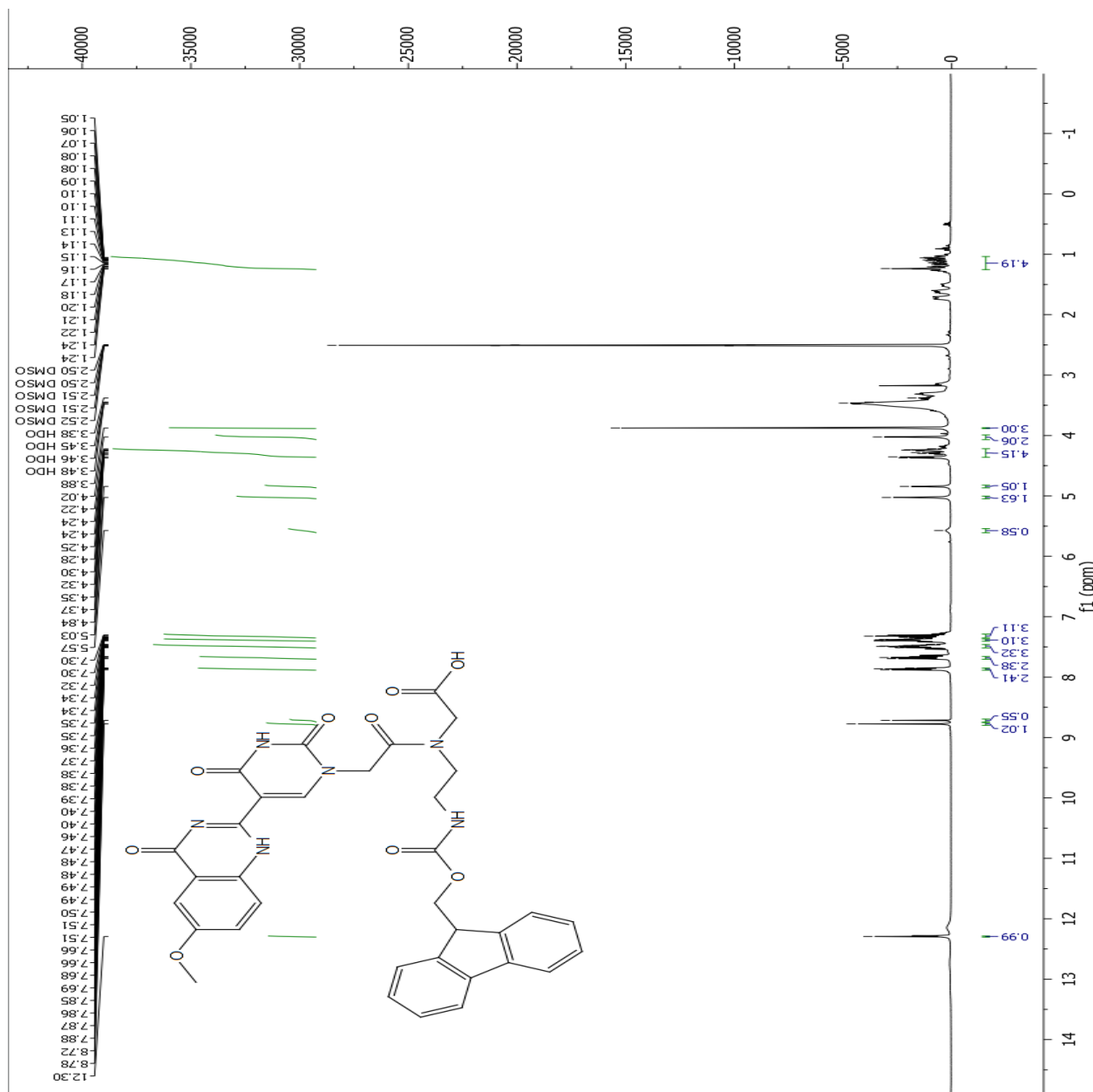


¹H NMR spectrum of compound 10 in DMSO-d₆. The spectrum shows peaks from 1.2 to 8.8 ppm. Integration values are provided for several peaks: 9.00, 7.11, 0.98, 3.64, 1.16, 0.46, 5.08, 1.85, 2.72, 0.36, and 0.69. The chemical structure of compound 10 is shown as an inset.

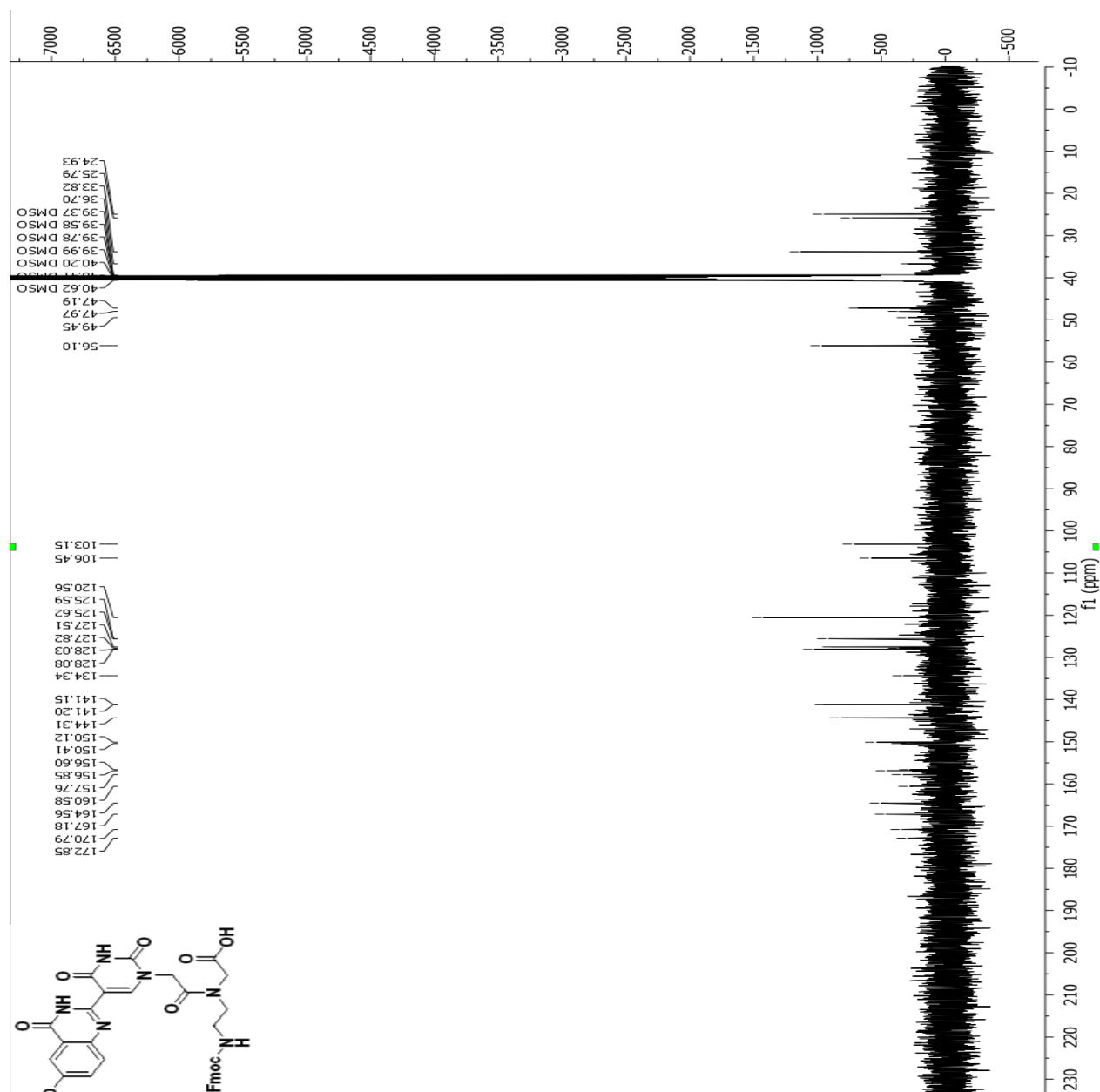
¹³C NMR spectrum of tert-butyl N-(2-((((9H-fluoren-9-yl)methoxy)carbonyl)amino)ethyl)-N-(2-(5-(6-nitro-4-oxo-3,4-dihydroquinazolin-2-yl)-2,4-dioxo-3,4-dihydropyrimidin-1(2H)-yl)acetyl)glycinate (47)



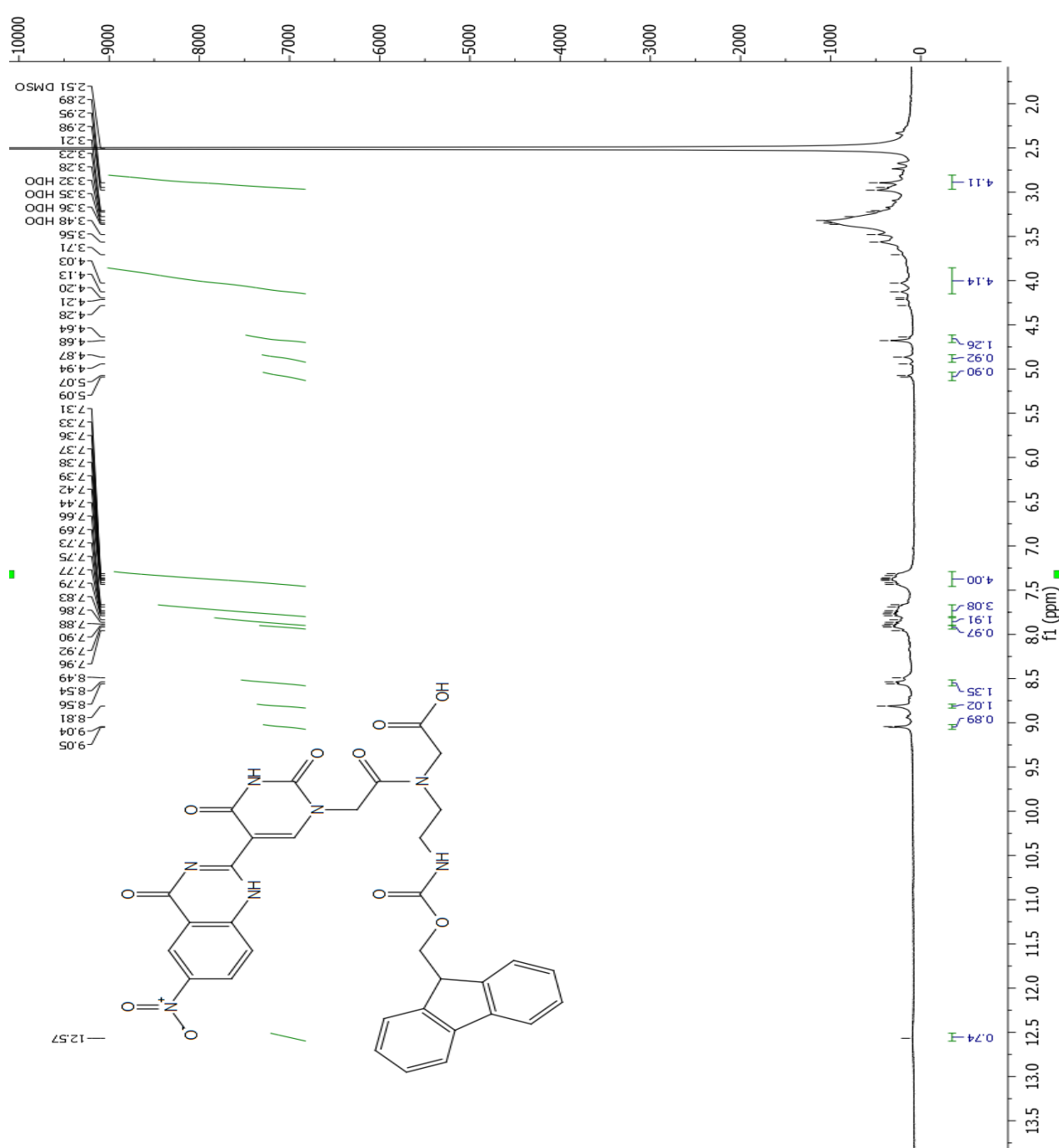
¹H NMR spectrum of N-(2-((((9H-fluoren-9-yl)methoxy)carbonyl)amino)ethyl)-N-(2-(5-(6-methoxy-4-oxo-3,4-dihydroquinazolin-2-yl)-2,4-dioxo-3,4-dihydropyrimidin-1(2H)-yl)acetyl)glycine (48)



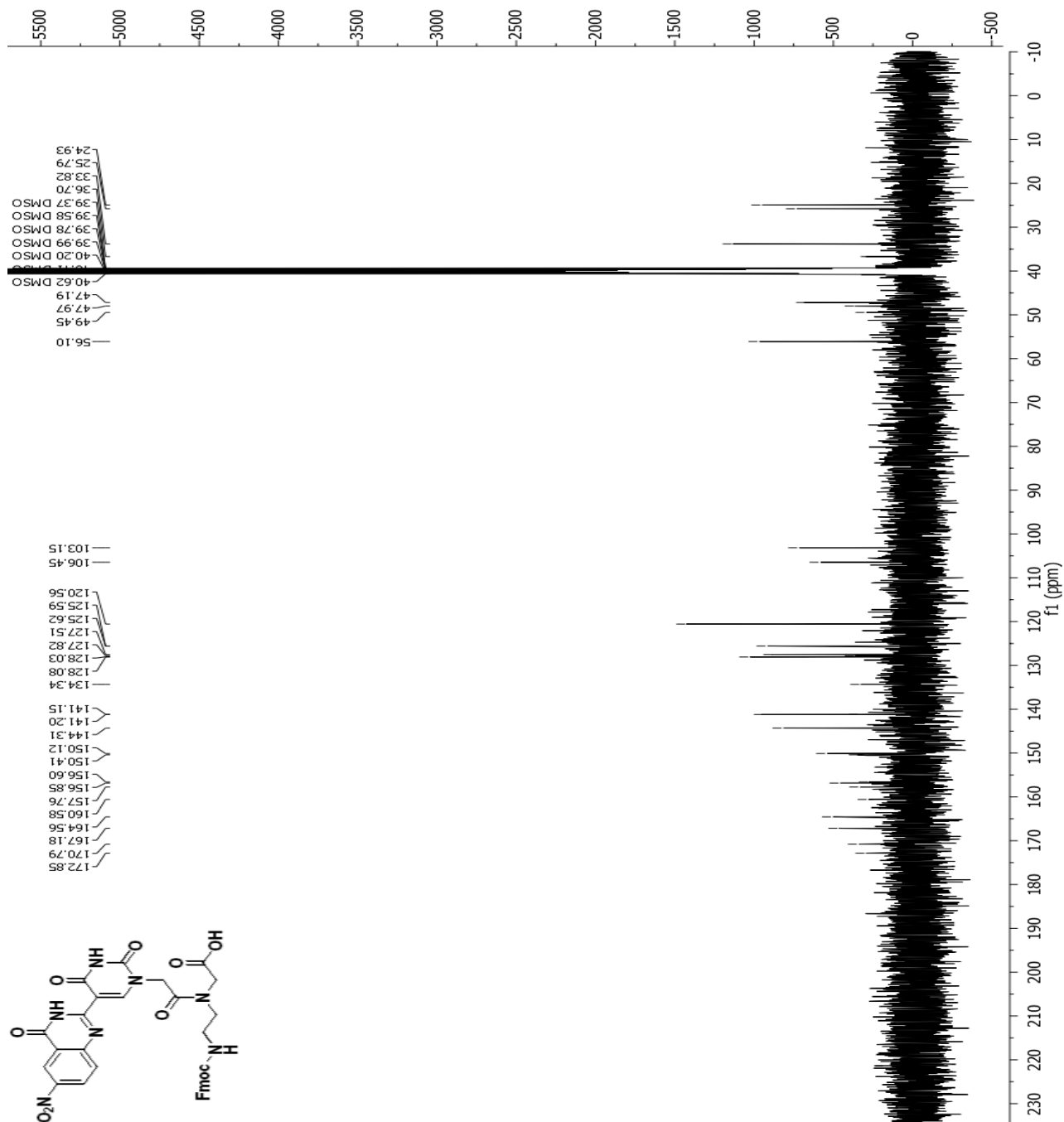
^{13}C NMR spectrum of N-(2-((((9H-fluoren-9-yl)methoxy)carbonyl)amino)ethyl)-N-(2-(5-(6-methoxy-4-oxo-3,4-dihydroquinazolin-2-yl)-2,4-dioxo-3,4-dihydropyrimidin-1(2H)-yl)acetyl)glycine (48)



¹H NMR spectrum of N-(2-((((9H-fluoren-9-yl)methoxy)carbonyl)amino)ethyl)-N-(2-(5-(6-nitro-4-oxo-3,4-dihydroquinazolin-2-yl)-2,4-dioxo-3,4-dihydropyrimidin-1(2H)-yl)acetyl)glycine (49)



^{13}C NMR spectrum of N-(2-((((9H-fluoren-9-yl)methoxy)carbonyl)amino)ethyl)-N-(2-(5-(6-nitro-4-oxo-3,4-dihydroquinazolin-2-yl)-2,4-dioxo-3,4-dihydropyrimidin-1(2H)-yl)acetyl)glycine (49)



Education

- 2017-Present Master of Science Student in Chemistry**
Western University, Ontario, Canada
(Supervisor: Prof. Robert H. E. Hudson)
- 2013-2017 Bachelor of Science Student in Chemistry**
Isfahan University of Technology, Isfahan, Iran
- 2008-2012 Graduated from High school of Exceptional Talents (NODET)**
Shahid Beheshti High School, Kermanshah, Iran

Honors and Awards

- 2018 Graduate student teaching assistant**
Selected as a distinguished teaching assistant, Western University, ON, Canada
- 2015 Distinguished Cultural Activist**
Isfahan University of Technology, Iran
- 2014 Distinguished Poet**
In the 3rd Nasim Poem Festival, Isfahan University of Technology
- 2014 Awarded as the Best Soccer Player and Top Scorer** in the 21st student sport Olympiad, Isfahan, Iran
- 2013 Ranked 73rd (Top 0.03%)**
In the “National Universities Entrance Exam” in Foreign Language, among near 400,000+ Participants, Iran
- 2011 Selected as a qualified person**

First stage of “Iranian National Biology Olympiad”, Iran

2010 Praised for “A Proposal for Security of Safes and Remote Controls of Home Appliances”

In the 11th Kharazmi Youth Festival, Tehran, Iran

2009 Praised for “A Proposal for Security of Safes and Remote Controls of Home Appliances”

In the 3rd Festival of Invention and scientific-research Innovations in the High school of Exceptional Talents, Kermanshah, Iran

Work Experiences

2017-Present Teaching Assistant (Organic Chemistry 2213B and 2223B), Western University, Canada

2017-Present Chemistry Tutor

Tutored high school, first year and second year university students in general and organic chemistry

2016-2017 (Summer) Water Quality Analyst as the internship, Kermanshah Water waste treatment, Kermanshah, Iran

2014-Present Coordinator and Chief editor of the Cultural and Scientific “Alchemist Journal”, Iranian Chemistry Student Society (ICSS), Iran

2015-2017 Chemistry and Biology Teacher, GAJ International Publication, Isfahan, Iran

2013-2016 (Summer) Assistant Coach (Kermanshah Persepolis F.C.)- Coached children ages 6 to 13
• Acquired basic medical training

Publications

2019 Hudson, R. H. E.; Heidari, A.; “On the necessity of nucleobase protection for 2-

thiouracil for Fmoc-based pseudo- complementary PNA oligomers synthesis" *J. Org. Chem.* (manuscript submitted)

- 2019** Ghorbani-choghamarani, A.; Tahmasbi, B.; Hudson, R. H. E.; Heidari, A. Microporous and Mesoporous Materials Supported Organometallic Palladium Catalyst into Mesoporous Channels of Magnetic MCM-41 Nanoparticles for Phosphine-Free C-C Coupling Reactions. *Microporous Mesoporous Mater.* **2019**, *284*, 366–377.
- 2019** Heidari, A.; Dinari, M. "Ultrasonic-assisted synthesis of novel Sucrose-modified CMC/Silver nanocomposites (in preparation)

Presentations

- 2019** **Oral Presentation: CSCC 2019**, Heidari, Ali; Hudson, R. H. "Synthesis of 2-thiouracil PNA monomer for Fmoc-based synthesis of pseudo-complementary oligomers" **102nd Annual Canadian Society for Chemistry Conference**, Laval university Quebec, Canada
- 2019** **Poster Presentation: CAMBR 2018**, Heidari, Ali; Hudson, R. H. "On the necessity of nucleobase protection for 2-thiouracil for Fmoc-based pseudo-complementary PNA oligomers synthesis" Center for advance materials and biomaterials research (**CAMBR**), Western University, ON, Canada
- 2018** **Poster Presentation: QOMSB0C 2018**, Heidari, Ali; Hudson, R. H. "Synthesis of 2-Thiouracil and 2-Thiothymine PNA for Fmoc-based Synthesis of Pseudo-

complementary Oligomers” Quebec-Ontario Mini Symposium for Synthetic and Bioorganic Chemistry (**QOMSB**OC), Toronto, ON, Canada

- 2018** **Oral Presentation: 21st annual CBGRC**, Heidari, Ali; Hudson, R. H. “Synthesis of 2-Thiouracil and 2-Thiothymine PNA for Fmoc-based Synthesis of Pseudo-complementary Oligomers” 21st annual **CBGRC** (Chemistry and Biochemistry Graduate Research Conference), Concordia University, Quebec, Canada
- 2018** **Poster Presentation: 3rd Synthetic Biology Symposium**, Heidari, Ali; Hudson, R. H. “Synthesis of 2-Thiouracil and 2-Thiothymine PNA for Fmoc-based Synthesis of Pseudo-complementary Oligomers” 3rd Synthetic Biology Symposium, Western University, ON, Canada
- 2017** **Oral Presentation: IUT Undergraduate Research Award Symposium**, Heidari, Ali; Mohammadnezhad, G. “Pure green chemical approach for synthesis of Ag₂O Nanoparticles”, Isfahan University of Technology, Isfahan, Iran
- 2016** **Oral Presentation: 8th Student Leadership Conference (SLC)**, Heidari, Ali; Jafari, M. T. “Supplemental Learning: Beyond everyday leadership” Isfahan University of Technology, Isfahan, Iran
- 2016** **Poster Presentation: 23rd Annual ISC Conference**, Heidari, Ali; Mohammadnezhad, G.; Dinari, M. “Synthesis and evaluation of bactericidal properties of Ag₂O nanoparticles against *Aeromonas hydrophila*”, 23rd Annual Iranian Society for Chemistry (ISC) Razi University, Kermanshah, Iran
- 2015** **Invited Talk: National Chemistry and Biology Olympiad: Preparation for test Takers** A Seminar for High School Students, National Organization for Development of Exceptional Talents, Kermanshah, Iran

Professional Diplomas and Certificates

July 2019 Class A2 German language

Sep 2017	Teaching Assistant Training Program or TATP (Western University)
Sep 2017	Teaching Assistant Training Program or TATP (Western University)
Sep 2016	Data Analysis- edX Online Learning (DelftX)
Sep 2016	Introduction to Forensic Science- COURSERA Online Learning- Nanyang Technological University, Singapore
Aug 2016	Basic Steps in Magnetic Resonance- edX Online Learning (EPFLx)
Jul 2016	The Science of Solar System- COURSERA Online Learning- Caltech
May 2016	Workplace Safety and Health Diploma-ALISON Free Online Learning
May 2016	Safety and Health in the Science Laboratory for Teachers- ALISON Free Online Learning
May 2016	Medicinal Chemistry: The Molecular Basis of Drug Discovery- edX Online Learning (DavidsonX)
Feb 2016	Photovoltaic Cells, Green Energy and Environmental challenges- Razi University, Kermanshah, Iran
Dec 2015	Diploma in Environmental Sciences- ALISON Free Online Learning
Nov 2015	Analyzing and Visualizing Data with Excel- edX Online Learning (MicrosoftX)
Dec 2015	Principles of Biochemistry - edX Online Learning (HarvardX)
Sep 2015	MATLAB Programing & Coding- ISIRAN institute
Jan 2014	Advanced Essay Writing-English Student's Society of Razi University (ESSR), Kermanshah, Iran
Jul 2014	Learning of Welding Inspection-Isfahan University of Technology Open Learning Center
Dec 2014	Fundamentals and Challenges of a Sustainable Chemical Industry- Isfahan University of Technology Open Learning Center

Service to the Chemistry Community

2018- 2019 Mechanism Monday Organizer

- Founded a voluntary mechanism club for chemistry graduate students at the University of Western Ontario (UWO)
- Conducted weekly meetings to discuss interesting or neat organic reaction mechanisms in a group setting, with the goal of improving problem-solving, and teaching skills for the attendees

2018- 2019 Chemistry Show Coordinator

- Responsible for preparing demonstrations, including testing new experiments to showcase
- Responsible for setup and takedown at an outdoor venue

2018 Liquid Nitrogen Ice cream

- Responsible for preparing and making ice cream with liquid nitrogen for new science Students

2017 Isfahan University of Technology Undergraduate Chemistry Conference (IUTUCC)

- Conference Chair: Coordinated, and directed the conference management committee of ten undergraduate students
- Responsible for organizing all aspects of a three-day conference with attendance of 120 chemistry students and faculty members